U.S. DEPARTMENT OF COMMERCE
National Technical Information Service

PB-278 521

Assessment of Operational Automated Guideway Systems - Jetrail

Transportation Systems Center, Cambridge, Mass

Prepared for

Urban Mass Transportation Administration, Washington, D C

Dec 77

Technical Report Documentation Page

1. Report No.	2. Government Accession No.	3. Recipient's Catalog No.
UMTA-MA-06-0067-77-1		PB278521

4. Title and Subtitle	5. Report Date
ASSESSMENT OF OPERATIONAL AUTOMATED GUIDEWAY SYSTEMS - JETRAIL	December 1977
	6. Performing Organization Code
7. Author(s): G. Anagnostopoulos et al.	8. Performing Organization Report No.: DOT-TSC-UMTA-77-55
9. Performing Organization Name and Address: U.S. Department of Transportation, Transportation Systems Center, Kendall Square, Cambridge, MA 02142	10. Work Unit No. (TRAIS): MA-06-0067
	11. Contract or Grant No.
12. Sponsoring Agency Name and Address: U.S. Department of Transportation, Urban Mass Transportation Administration, 400 Seventh Street, S.W., Washington, D. C. 20590	13. Type of Report and Period Covered: Final Report, August 1975-March 1976
	14. Sponsoring Agency Code

15. Supplementary Notes

16. Abstract

As part of the Urban Mass Transportation Administration's continuing Automated Guideway Technology (AGT) Program, the Transportation Systems Center conducted an assessment of the Braniff International Airlines Jetrail system located at Love Field in Dallas, Texas. This report is an assessment and evaluation of Jetrail, the first operational completely automated, demand-responsive, group rapid, intra-airport transportation system. It connects a parking lot at the entrance to Love Field and the Braniff terminal with three-quarters of a mile of double-lane monorail and has ten suspended vehicles, a maintenance facility, and three stations. The system was intended to retain passengers in the face of increased congestion at Love Field. Jetrail operated successfully from April 1970 to January 1974, at which time Braniff moved to the new Dallas-Ft. Worth Regional Airport. Over six million passengers were carried 1.3 million miles during this period without a fatality or major mishap. The system did this in spite of the engineering novelty and early, low reliability of the propulsion and control system.

The Jetrail system continues to be used as an engineering test-bed for a prototype linear induction motor propulsion system. This latter system, Astroglide, is being developed by PRT Systems Inc. Since the motor has no moving parts, it is more simple than the rotary motor and drive train of the Jetrail system. This report provides information on the Jetrail operational experience and the Astroglide prototype for transportation planners, designers, developers, and operators of AGT systems for intra-airport, urban, recreational, and freight applications.

17. Key Words	18. Distribution Statement
Astroglide, Evaluation, Jetrail, Automated Guideway Transit, Demand-Responsive, Intra-Airport Transportation Systems	Available to the Public through the National Technical Information Service, Springfield, Virginia 22161.

19. Security Classif. (of this report)	20. Security Classif. (of this page)	21. No. of Pages	22. Price
Unclassified	Unclassified	276	A13-A01

Form DOT F 1700.7 (8-72) Reproduction of completed page authorized

PREFACE

This report describes an assessment of the Jetrail Automated Guideway Transit system in Dallas conducted by the Transportation Systems Center (TSC). The project was sponsored by the Department of Transportation, Urban Mass Transportation Administration (UMTA) through its Office of Research and Development, Socio-Economic and Special Projects Division, as part of UMTA's Automated Guideway Technology (AGT) Assessments Program. The work reported herein was performed between August 1975 and March 1976. It consisted of a technical review of the system, on-site inspection, measurements, technical interchange with personnel from the user and system developer, analyses, and evaluation.

This assessment is the product of a team effort whose members have contributed in following areas: Raymond A. Wlodyka, power and propulsion; Iris A. Mitropoulis, system dependability; John Putukian, guideway; and Ronald D. Kangas, background. George Anagnostopoulos had overall responsibility for preparation of the report as well as contributing to the remaining subject areas.

Acknowledgement and special thanks are given: to Chauncey W. Watt and Thomas M. Dooley for their contributions; to Michael Lenard of MITRE and Anthony Yen of Stanford Research Institute (formerly of MITRE) for technical consultation; to A.J. Healey for the Ride Quality Measurements; and to Bruce F. Kingsbury for his diligence in editing the manuscript.

Preceding page blank

METRIC CONVERSION FACTORS

Approximate Conversions to Metric Measures

Symbol	When You Know	Multiply by	To Find	Symbol
		LENGTH		
in	inches	2.5	centimeters	cm
ft	feet	30	centimeters	cm
yd	yards	0.9	meters	m
mi	miles	1.6	kilometers	km
		AREA		
in^2	square inches	6.5	square centimeters	cm^2
ft^2	square feet	0.09	square meters	m^2
yd^2	square yards	0.8	square meters	m^2
mi^2	square miles	2.6	square kilometers	km^2
	acres	0.4	hectares	ha
		MASS (weight)		
oz	ounces	28	grams	g
lb	pounds	0.45	kilograms	kg
	short tons (2000 lb)	0.9	tonnes	t
		VOLUME		
tsp	teaspoons	5	milliliters	ml
Tbsp	tablespoons	15	milliliters	ml
fl oz	fluid ounces	30	milliliters	ml
c	cups	0.24	liters	l
pt	pints	0.47	liters	l
qt	quarts	0.95	liters	l
gal	gallons	3.8	liters	l
ft^3	cubic feet	0.03	cubic meters	m^3
yd^3	cubic yards	0.76	cubic meters	m^3
		TEMPERATURE (exact)		
°F	Fahrenheit temperature	5/9 (after subtracting 32)	Celsius temperature	°C

Approximate Conversions from Metric Measures

Symbol	When You Know	Multiply by	To Find	Symbol
		LENGTH		
mm	millimeters	0.04	inches	in
cm	centimeters	0.4	inches	in
m	meters	3.3	feet	ft
m	meters	1.1	yards	yd
km	kilometers	0.6	miles	mi
		AREA		
cm^2	square centimeters	0.16	square inches	in^2
m^2	square meters	1.2	square yards	yd^2
km^2	square kilometers	0.4	square miles	mi^2
ha	hectares (10,000 m^2)	2.5	acres	
		MASS (weight)		
g	grams	0.035	ounces	oz
kg	kilograms	2.2	pounds	lb
t	tonnes (1000 kg)	1.1	short tons	
		VOLUME		
ml	milliliters	0.03	fluid ounces	fl oz
l	liters	2.1	pints	pt
l	liters	1.06	quarts	qt
l	liters	0.26	gallons	gal
m^3	cubic meters	35	cubic feet	ft^3
m^3	cubic meters	1.3	cubic yards	yd^3
		TEMPERATURE (exact)		
°C	Celsius temperature	9/5 (then add 32)	Fahrenheit temperature	°F

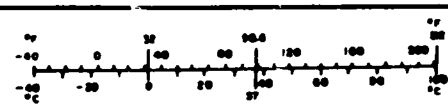

CONTENTS

CONTENTS (CONTINUED)

CONTENTS (CONTINUED)

LIST OF ILLUSTRATIONS

LIST OF ILLUSTRATIONS (CONTINUED)

LIST OF ILLUSTRATIONS (CONTINUED)

LIST OF ILLUSTRATIONS (CONTINUED)

LIST OF ILLUSTRATIONS (CONTINUED)

LIST OF TABLES

LIST OF TABLES

EXECUTIVE SUMMARY

As part of UMTA's continuing Automated Guideway Technology (AGT) Assessment program, the Transportation Systems Center (TSC) of the U.S. Department of Transportation has conducted an assessment of the Braniff Airlines Jetrail system located at Love Field in Dallas, Texas. Jetrail is an intra-airport Automated Guideway Transit (AGT) system operating in a loop between a parking lot and the airline's terminal. This assessment was sponsored by the DOT Urban Mass Transportation Administration and conducted under the auspices of the Office of Socio-Economic and Special Projects of the Office of Technology Development and Deployment.

The assessment is intended to:

a) Obtain and compile engineering, economic, and system operational performance information which could be used in planning future AGT systems.

b) Identify the problems and associated solutions, encountered during the design, development, implementation, and operation of this system.

c) Information for more effective implementation and operating strategies for future automated Guideway Transit (AGT) system programs.

This report is intended to assist policy-making officials at all levels of government, planners, and system developers in their consideration of future urban AGT system applications.

BACKGROUND

During the mid-sixties, passenger service was approaching capacity at the Braniff Airlines' terminal at Love Field. Braniff anticipated an expansion of their operations as air travel was growing rapidly. In 1967, Braniff decided to expand its facilities from 7.5 gates to 26.5 gates by constructing a new terminal. This was done in spite of the impending move to the new Dallas-Ft. Worth (DFW) Regional Airport, scheduled for operation in the mid-seventies.

The construction of a new terminal facility at Love Field would encroach on scarce parking space resulting in added congestion and inconvenience. The selected solution provided a Braniff check-in point with a 1500-car parking area near the entrance to Love Field together with the construction of a modern automated guideway transit system to transport people from this remote parking facility to the new Braniff terminal. This loop service was coordinated with valet parking and direct dispatching of checked-in baggage to the aircraft.

In April 1968, Braniff selected the Stanray Corporation's Jetrail Automated Guideway Transit System. Selection was based on low cost, its state of development, flexibility and compatibility with the existing environment, and the belief that a system primarily constructed of standard components could be easily reinstalled at a new location.

Jetrail's initial test operation began in September 1968. Braniff assumed management of the system in July 1969. The system operated in continuous service between April 1970 and January 1974. Jetrail passenger service was terminated when Braniff commenced operations at the new Dallas-Ft. Worth Regional Airport.

A significant maintenance effort has been required to keep the Jetrail System operational because of reliability problems of certain components. In addition, the short 4-5 year design life has left the system with worn-out components. In consequence, PRT Systems Corporation has modified a single Jetrail vehicle to improve performance and reliability, and provide for improved operation in ice and snow conditions. The modification involved replacing the original Jetrail power and propulsion sub-system with a linear induction motor (LIM) and associated motor controller sub-system. This improved system is named "Astroglide".

TECHNICAL DESCRIPTION

Jetrail is a fully automated elevated suspended monorail system designed as a loop, with three on-line stations (Braniff terminal building, baggage claim area, and the remote parking lot) operating over 1.6 miles (2.6 km) of guideway, including storage, maintenance, and by-pass facilities. The system has ten vehicles, each with a capacity of ten passengers. The vehicles are constructed of steel-reinforced fiberglass, and are suspended on solid rubber wheels.

The vehicles are controlled automatically by a hardwired command and control subsystem that receives speed commands from a system of relays which operates as a redundant block-control system. In addition, each vehicle is followed by a stepped-speed-command zone or tail that will stop a vehicle prior to collision. The system is demand responsive.

Some of the more important technical and operational characteristics of the system are summarized in Table ES-1.

OPERATIONAL PERFORMANCE

Jetrail was operated 24 hours per day, 7 days per week. Over the life of the system (April 1970 - January 1974), Jetrail carried an estimated six million passengers over 1.3 million vehicle miles with no fatalities or major mishaps.*

As reported by Braniff, the overall availability of the system was 99.7 percent. The calculated availability and reliability were 99.8% and 97.6%, respectively, for 24 hours of operation. This is based on failures resulting in delays greater than six minutes. The system was considered to have failed when no spares were available and system restoration could not be effected within six minutes. A key factor in achieving the high reliability and availability was a scheduled maintenance program carried out by a dedicated team.

Braniff reported the actual operating capacity of the system was approximately one half the theoretical maximum, or 600 passengers/hour. A passenger flow for a typical day was approximately

* A single accident did occur when a catering truck which was parked under the guideway raised its body into the path of an oncoming vehicle. An impact occurred and there were some injuries to passengers of unknown extent, however, the cases are still in litigation.

TABLE ES-1. SUMMARY OF SYSTEM CHARACTERISTICS

Automation	Fully automated
Type of Service	Demand-responsive point-to-point, loop
Maximum Theoretical One-Way Capacity	1358 pass/hr
Maximum Practical One-Way Capacity (80% of theoretical)	1086 pass/hr
Headway (min.)	20 sec.
Operating Speeds (discrete)	1.5 mph, 4.5 mph, 9.0 mph, 15 mph
Average Speed	11.8 mph
Average one-way (0.7 mi) transit time	3.5 min.
Vehicle Weight	6000 lbs.
Vehicle Capacity	10 pass/veh (6 seated)
Availability	24 hr., on demand
Stations	On-line, 2 principal, 1 secondary
Guideway	Mono-rail, standard I-beam, cylindrical steel column supports
Switches	Wayside, lateral transfer
Fare	No Charge
Cost (orig. installation)	$2,500,000
Estimated Operation Cost (typical urban area)	$427,000 (1976 dollars)

7,000. Jetrail service was provided free of charge.

PASSENGER OPERATION

From the passengers' point of view, the system was much like an elevator except that the system operated horizontally. The following sequence will serve as an illustration. When a passenger drove into the parking lot near the entrance to Love Field and proceeded to the station entrance, a valet parked the car and a ticketing agent forwarded the baggage to the aircraft. The passenger then entered station A, took an elevator to the second level and walked to the loading area which looked much like most elevator lobbies, but longer. A button was pushed calling for a vehicle. When it arrived, the passenger boarded and selected one of two stations. When the vehicle reached, say, station B, the Braniff terminal the doors opened automatically and the passenger walked to the waiting aircraft. The returning passenger similarly used Jetrail by calling a vehicle and proceeding to station A where baggage and automobile were picked-up.

Elderly or handicapped persons could use this system readily under normal operating conditions since the system is essentially level. There are stairs at the baggage station C but baggage can be forwarded, precluding the need to use this station.

SYSTEM COST

A $1.5 million fixed-price contract was awarded to the Jetrail Division of the Stanray Corporation in April, 1968, for the development and installation of the Jetrail system at Love Field. Because the system was the first of its kind, there was virtually no experience on which to base the design. Consequently, design difficulties were encountered which resulted in a $500 thousand overrun. Braniff undertook the operational testing, investing an additional $500 thousand for testing and engineering modifications which made the total investment $2.5 million. The capital cost was therefore approximately $1.5 million per lane-mile.

Braniff reported operating costs for one year during 1973-74 of $172,027, of which labor accounted for $112,672. This does not reflect the true labor cost of a full-time, two-man crew because one technician was called from the Braniff staff as needed. A more accurate accounting would have shown an operating cost of $345,090 ($251,536 being due to labor). In 1976 dollars, the annual operating and maintenance costs of this same system in a typical urban application would be $427,000.

The following data shows the costs per vehicle-mile in 1973 dollars, with 1976 dollars in parentheses, calculated from Braniff's data and from an estimate of a typical urban application. They are done for two passenger estimates, 6 and 10 million, over the life of the system, 3.75 years, and an estimated load factor of 33 percent. The cost per seat-mile may be found by dividing each vehicle-mile cost by ten seats.

Passenger Estimate	Braniff	Typical Urban
6×10^6 passengers	$0.51 veh-mi	$1.02/veh-mi ($1.37)
10×10^6 passengers		$0.66/veh-mi ($0.89)

CONCLUSIONS

This section summarizes some of the more significant conclusions of the assessment project. For convenience these are grouped into three principal areas:

1) The Jetrail system and its operation
2) The Astroglide modification to Jetrail
3) The design and development approach and related problems

JETRAIL SYSTEM CONCLUSIONS

1. The Jetrail, the first intra-airport operational demand responsive AGT System, successfully met its principal performance objectives, and operated satisfactorily for 45 months, safely, with acceptable system availability and with acceptable operating costs. The system, as it evolved, would be suitable for a variety of urban applications providing design modifications are made to reduce fire safety hazards, to improve all-weather operation, and to reduce materials and reliability limitations.

2. Fire safety measures should be incorporated into the vehicle, for instance, passive measures such as that provided in a memorandum entitled Guideline Specification for Flammability and Smoke Emission TSC-76-LFS-6 and active measures, such as, a Halon 1301 fire control system currently under development.

3. For general urban applicability, the capability to operate in snow and ice conditions must be developed. Guideway covering or heating are alternative methods that could be considered.

4. For cost effective urban operation, modifications should be made to improve system reliability and maintainability, e.g., modifications should be made to the vehicle control system and propulsion system, in particular, to the power collector shoes, propulsion motors, and eddy-current transmission.

5. The control system with its redundant blocking represents a well designed, innovative system that could likely be expanded to a larger activity center, to a line-haul, or to a network system, provided management aspects, including failure and empty vehicle management are implemented.

6. Initial cost and short-life considerations led to the selection of galvanized steel power and signal rails. These are worn out and require replacement. A longer life, lower maintenance power and signal collection system should be developed for typical urban applications.

7. Ride quality is acceptable as compared with the International Organization for Standardization (Document 2361) in spite of the apparent roughness caused by the expansion joints which were added after sytem installation. However, it should be pointed out that the I.S.O. has no standard for roll. Although ride quality measurements did not exceed the standards, more comfort could be achieved by improving the expansion joint design, the guideway alignment, or designing a secondary suspension system.

8. Careful guideway redesign is suggested to capitalize on the small cross-sectional area achieved in Jetrail and somewhat compromised in this development. The environmental limitation cited in (3) above should be corrected in the design process.

9. The system noise environment within the vehicle and outside is quite acceptable; 71dBA has been measured in the interior and 72dBA on the exterior.

ASTROGLIDE SYSTEM CONCLUSIONS

10. Further testing of the Astroglide System improvements which were made to enhance overall reliability should be performed to measure its dependability (combinations of reliability and availability) and maintainability. Astroglide utilizes a linear induction motor (LIM) which would eliminate drive wheel problems and permit operation during icing conditions.

11. Because the energy consumption of the Astroglide (LIM) is greater than that of the Jetrail eddy-current transmission and motor, the system should either be operated at higher speeds (35 mph) or the LIM and its propulsion control system should be redesigned for a lower velocity. Either of these will result in a more efficient operation, i.e., lower energy consumption.

DEVELOPMENT PROCESS CONCLUSIONS

12. Because the overall development approach allowed insufficient time and effort for initial design, development, and testing, the advantages and disadvantages for future AGT systems should be carefully weighed between correcting a minimal design effort in the test phase and devoting more time to engineering design and development before entering the test phase. The latter alternative will lead to less risk in the final development.

13. More time and effort should be devoted to the development of system interface specifications, component specifications, and testing before the selection and installation of off-the-shelf

hardware. Some of these components were among the principal sources of failures, particularly within the propulsion and propulsion control system. The developmental approach using of-the-shelf hardware did not permit sufficient specification and testing to insure their applicability to a specific operational environment.

1. INTRODUCTION

Changing patterns of urban spatial and social structures have created a need for examination of new transportation technologies and innovative system concepts. The pattern of increasing dispersion of origins and destinations throughout a metropolitan area leading to the gradual decline of the central city as the focal point for urban activity has generated mobility requirements that cannot be adequately served solely by existing public transportation systems. This pattern has had an adverse impact on the quality of urban life including the denial of personal mobility to large segments of the urban population.

The Automated Guideway Technology (AGT) systems represent one new transit mode, which has the potential of meeting these changing needs in a cost-effective manner. The issues raised relative to these complex, unmanned AGT systems include capital and operating costs, reliability, maintainability, safety, comfort, and security.

Since little factual data on existing AGT systems in revenue service has been gathered, the Urban Mass Transportation Administration (UMTA) of the U.S. Department of Transportation has initiated a program to assess and evaluate such systems which will assist planners, policy-makers, and technical developers in formulating realistic developments of AGT systems.

SCOPE

This report describes an assessment of the Braniff Jetrail system located at Love Field in Dallas, Texas, conducted by the Transportation Systems Center (TSC) of the U.S. Department of Transportation (DOT), in conjunction with personnel from the MITRE Corporation. The assessment project was funded by the DOT Urban Mass Transportation Administration (UMTA) and conducted under auspices of its Office of Research and Development, Office of Socio-Economics and Special Projects, as part of UMTA's Automated Guideway Technology (AGT) Assessment Program. This assessment was performed between August 1975 and March 1976. It consisted of a review of technical reports, some testing, and several on-site inspections, as well as technical interchanges with personnel from Braniff International Airlines and PRT Systems Corporation.

The assessment of the Braniff Jetrail system at Love Field was to obtain (a) a review of the design, development, and implementation of the system to determine experience gained; (b) engineering, operational, human factors, and economic data; and (c) information for more effective implementation and operating strategies for future Automated Guideway Transit (AGT) system programs.

Section 2 describes the background and events leading to the selection of the Jetrail system. Technical descriptions of system components and an assessment of operational performance are provided in Section 3 and 4 respectively. Discussion of the system costs are provided in Section 5. The System evaluation of Jetrail is contained in Section 6, and finally, recommendations are contained in Section 7.

The Background (section 2) Technical Description (section 3), and System Costs (section 5) include information provided by Braniff of the Jetrail system and by PRT Systems Inc. of the Astroglide system. Some of the capacity calculations in section 3 have been made by TSC. However, the Operational Performance (section 4) was developed from Braniff and PRT Systems Inc. data, with measurement and analysis performed by TSC. Section 6 Evaluation, and Section 7, Conclusion and Recommendations, represents the evaluation and opinions of the TSC assessment team.

2. BACKGROUND

This section provides the background for the technical and operational description of the Jetrail system. The chronological background is summarized in Table 2.1.1.

2.1 RATIONALE FOR ESTABLISHING JETRAIL

During the mid-sixties, when the new regional airport for Dallas-Ft. Worth was in the planning stage, Love Field, where Braniff Airlines had their headquarters, was approaching its peak passenger-carrying capacity. Braniff, with seven and one half gates available, was planning an expansion of their activities. U.S. air travel was growing rapidly, as was the air freight activity. Concomitantly automobile traffic congestion was continually increasing at the airport terminal. Braniff management was concerned that a probable loss of connecting traffic would occur at Dallas unless Love Field's capacity was expanded prior to the completion of the new airport. To prevent this loss, a new Braniff terminal wing at Love Field, with nineteen additional gates (six leased to other airlines) was constructed in spite of the impending move to the new Dallas-Ft. Worth regional airport scheduled for operation in the mid-seventies.

Since this new construction encroached on already scarce parking space, Braniff management realized that the resulting inconvenience, particularly for Braniff passengers, would hamper its growth capability. The solution to these problems was a Braniff check-in point and a 1500-car parking area near the entrance to Love Field in conjunction with a modern automated guideway transit system to transport passengers to their terminal. At the check-in point valet parking was provided as was checked-in baggage to the aircraft. The operation of the parking lot was contracted for on per capita basis. The land for these purposes was leased from the city of Dallas.

Braniff management interviewed thirty potential builders of transit systems and in April, 1968 selected the Jetrail Division

TABLE 2.1.1. CHRONOLOGY OF JETRAIL PROJECT

1963-65	Early design and development of Jetrail by the Jetrail Division of Stanray Pacific Corporation
1967-68	Operation of full-scale test track in California
1967	Braniff announced plans for terminal expansion at Love Field, including construction of a transit system.
1967	Dallas City Council approved Braniff plan
1968	Screening of transit system candidates
1968, April	Stanray Corporation's Jetrail system selected;
1968, September	First test operation of a vehicle on Love Field Track
1969, July	Braniff assumed management of project
1970, April 18	Revenue operation of system started at Love Field
1973, Dec. 31	Unsolicited proposal for demonstrating LIM propulsion on Jetrail, submitted to UMTA by PRT Systems, supported by the Franklin Institute Research Laboratories and Braniff.
1974, Jan. 13	End of revenue operations at Love Field; Braniff passenger service transferred to the new regional airport.
1974, September	Installation and first operation of LIM propulsion on Jetrail vehicle, system renamed Astroglide. (Stanray Corp. still retains the patents and rights to the Jetrail system.)

of Stanray Corporation's Jetrail system on the basis of low cost and adequate developmental status. Other factors in the selection were the need for an elevated system that was environmentally compatible with an established facility (Love Field), and Braniff's belief that the system should be constructed of standard structural and electrical components to permit installation at a new location within sixty days. To complete the preparations, the Dallas City Council's agreement to the project was obtained.

The fundamental approach used was to perform the least amount of design and development work and to correct oversights during the test phase. The approach seemed sensible because it was felt little development would be required. The emphasis was on initial cost savings rather than life-cycle cost considerations.

Because the system would have a limited use of 4-5 years at Love Field, consideration was given to moving Jetrail to DFW Regional Airport or selling the system to recoup some of the investment. Moving the system to the DFW airport was subsequently rejected by the DFW airport board in 1972 due to differing requirements.

Fourteen months after implementation began, it become apparent that Stanray had underestimated the cost of installing the system and that their hopes of a rapidly expanding and profitable market for Jetrail were not going to be realized. Stanray divested itself of the Jetrail division, but retained the Jetrail files in their Chicago office. Braniff then completed the Love Field project. Thus, system acceptance was made by the final developer.

During this early period, revenue operations were delayed by necessary modifications which included:

a. Guideway structure modification to (1) allow for thermal expansion at the beam joints, (2) reinforce the beam and column interface by the use of gusset plates, and (3) reinforce the beams in the curves to increase torsional stiffness.

b. Frequent failures in the vehicle electrical control equipment made it necessary to trace circuits and re-solder joints.

c. The motors were originally undersize at 5 horsepower. They were increased to 7.5 horsepower using the same frames. As a result over-heating and bearing problems occurred, which persisted over the operational life of the system.

d. The original contact shoes wore out in a few hours. Lubricating the rails every four months and using a different shoe material extended the shoe life to the present 4-5 months.

In addition to these delays revenue operations were also delayed by the lack of an appropriate public agency to certify the safe operation of the system. As a result there was a greater need for Braniff to thoroughly test every aspect of system operation. Only structures and the electrical wiring were inspected and approved by Dallas city inspectors; it was Braniff's responsibility to assure safe operation in all other aspects.

2.2 PRESENT STATUS

After movement of commercial airlines to the Dallas-Ft. Worth airport, Love Field is now devoted to general aviation. As a result there is no further need for Jetrail and it has been placed in a non-operational state. Braniff International Airlines owns the system and hopes to sell it, "as is". To effect the sale of Jetrail, Braniff has made an agreement with the PRT Systems Corporation for marketing services, wherein Braniff is held harmless for the sale of the "as is" Jetrail system. To keep it saleable, Braniff provides minimal maintenance. Two of the stations, station A and C, are currently leased to other businesses. The carousels have been removed from the baggage station (C).

After cessation of operational service some Braniff employees, who had been assigned to work with the installation from the beginning, have equipped one of the vehicles with PRT Systems Corp.

LIM propulsion system (Astroglide). The Jetrail system is being used as a test-bed for the Astroglide development. From Braniff's point of view, these expenses are a small price to pay to improve the prospects of sale for their unused equipment. This effort was begun in 1973 by PRT Systems on their own with Braniff's cooperation.

PRT Systems Corporation is an independent (from Braniff) company started by former members of the original Stanray design and Braniff operation teams. They have obtained all Jetrail drawings and specifications but not patent rights. They are licensed to sell LINTROL linear motors and controls under an agreement with Herbert Morris Ltd. of England.

Future applications of Jetrail expansion of the present vehicle fleet at a new location, would be considered by Braniff and PRT Systems preferably on the basis of LIM propulsion for all additional vehicles, i.e., conversion to the Astroglide system. The reliability due to lack of moving parts (e.g., bearings, brushes, gears); decreased weight [estimated to be 2300 pounds (1000 kg) reduction for the Jetrail vehicle that weighs 6000 (2700 kg) pounds empty and 7500 (3400 kg) pounds fully loaded]; substantial improvement in support-wheel life due to the elimination of a tractive function of these wheels and due to a partial reduction of the vertical load on the wheels (up to 90 percent of vertical load is reduced at full power by the LIM's levitating effect); less vulnerability to weather (ice and snow); and reduced cost of the LIM unit compared to the propulsion system of the original vehicles.

At present, the LIM-equipped Astroglide vehicle has an uneven ride, indicating that the development of the controls is not complete. Some preliminary performance measurements were made by the TSC team and they are covered in section 4 and the appendix. The LIMs were designed for larger vehicles and higher speeds than the 7500 (3400 kg) pound and 15-mph (24 km/hr) requirements of the Love Field installation. The vehicle at Love Field is capable of normal operation with only one of its LIM's functioning. For a short distance it was brought up to a speed of 37 mph (59 km/hr). The synchronous speed capability inherent in the LIM equipment installed in the Astroglide vehicle is 40.27 mph (64 km/hr).

Training of vehicles to increase system capacity has been considered from the vehicle control point of view. The required changes in control logic have been identified but no detailed designing or construction of the modified control equipment has taken place. No indication has been given that mechanical problems related to training suspended vehicles have been considered.

2.3 PATENT STATUS

The Jetrail system at Love Field has a number of patents associated with it and one registered trademark. The U.S. trademark registration of the mark "Jetrail" is Registration Number 915,392, issued June 22, 1971, now in the public domain. There are also several foreign registrations of this mark. The patents of the Jetrail system include the static switch, U.S. Patent Number 3,593,668; the rail car body construction, U.S. Patent Number 3,606,843; and the rail car body design, Patent Number 219,246. As of January 1976, these patents and trademarks were owned by the Stanray Corporation. However, Braniff has purchased the Jetrail system with full rights to re-apply, modify, or dispose of the system.

3. TECHNICAL DESCRIPTION

3.1 SYSTEM DESCRIPTION

The Jetrail system is a fully-automated elevated suspended monorail transportation system Fig. 3.1.1. The system is designed to transport people between the Braniff terminal building (Station B), the baggage claim area (Station C), and the outlying parking lot area (Station A). The configuration of the system is a shuttle-loop operating between the two main stations - 0.7 mile (1.1 km) separation. Storage, maintenance, and bypass facilities are also provided (see Figure 3.1.4).

The system incorporates ten vehicles each with a capacity of ten passengers, six seated and four standing. The vehicles are automatically controlled by two single-speed, three-phase electric motors. The drive motor torque is transmitted to solid-rubber drive wheels through an electro-magnetic eddy-current transmission and a differential mechanical drive. The mechanical drive mechanism holds the vehicle on the guideway positively. The eddy-current transmission controls the torque (positive or negative) provided to the wheels. The two electric motors and their drives are mounted on separate pivoted trucks that permit a 15 ft (5 m) turning radius. A separate mechanical, magnetic brake for emergency operation is used in addition to the eddy-current service brake. The primary suspension is provided by eight solid-rubber wheels.

The guideway is entirely elevated, consisting of standard steel I-beams supported by cylindrical steel columns. Switching is achieved at the wayside by lateral transfer of alternative guideway connecting elements. The eight contact rails (three power, one ground, and four signal) are mounted to the guideway and the matching contact shoes transmit the three-phase power, grounding, speed control, and presence-detection information commands related to vehicle safety and system operation.

FIGURE 3.1.1. JETRAIL VEHICLE ON THE GUIDEWAY

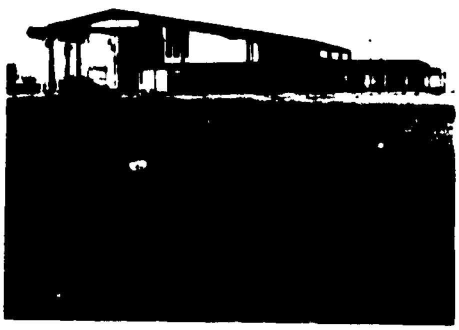

FIGURE 3.1.2. PARKING LOT STATION

FIGURE 3.1.3. BRANIFF TERMINAL STATION

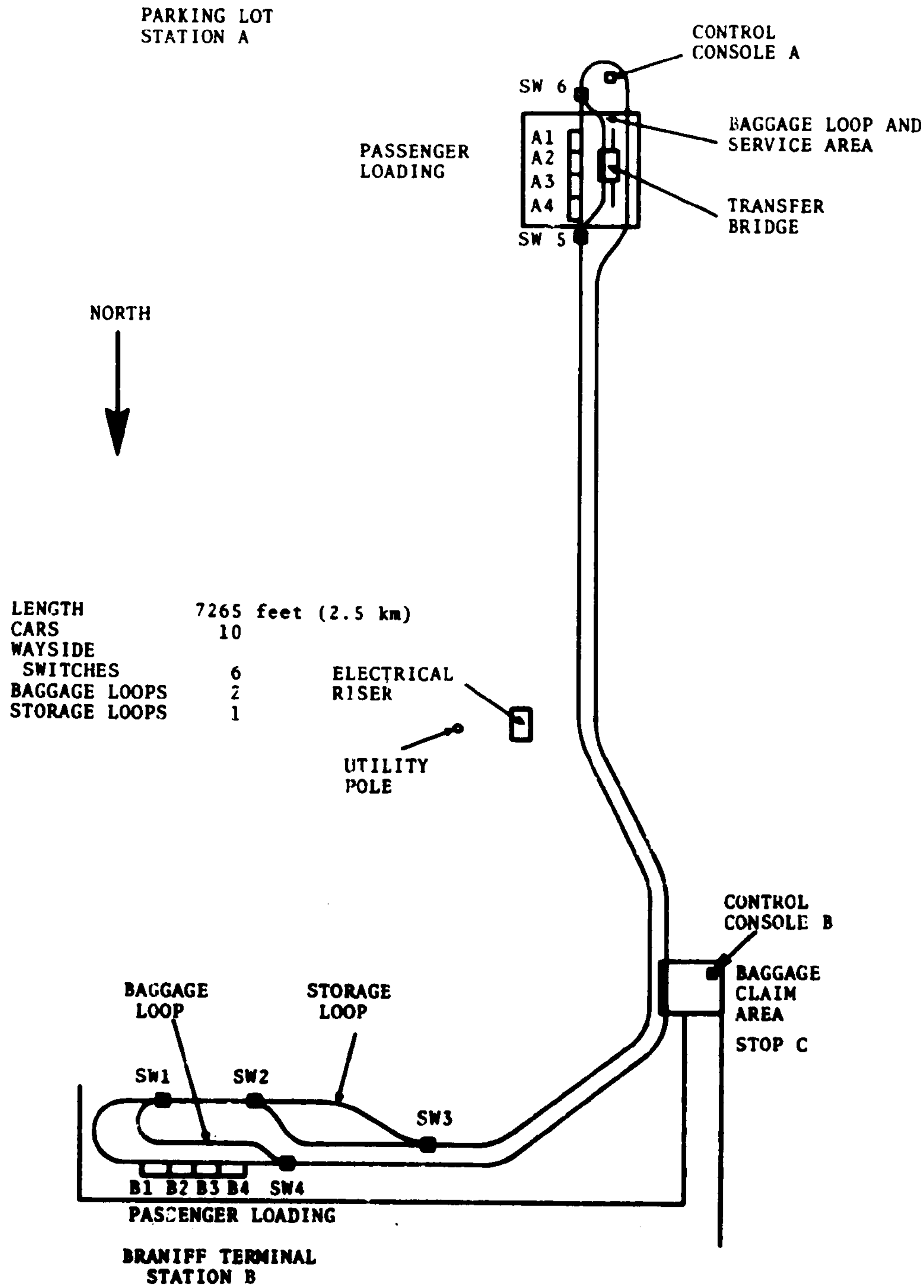

FIGURE 3.1.4. SCHEMATIC OF THE JETRAIL SYSTEM

Automatic system operation is achieved by means of a hard-wired system of relays which operates as a redundant block control system. The system is demand-operated in either a low- or high-flow mode.

Although design provisions were made for two baggage vehicles, they were never incorporated into the system. Baggage was moved between stations by automotive trucks.

3.1.1 System Characteristics

The Jetrail vehicles operate at four discrete nominal speeds.

	(mph)	(km/hr)	(ft/sec)	(m/sec)
Speed 1	1.5	2.4	2.2	0.67
Speed 2	4.5	7.2	6.6	2.0
Speed 3	9.0	14.5	13.2	4.0
Speed 4	15.0	24.0	22.0	6.7

The speed sequence over the guideway is shown in Figure 3.4.1.

The average speed is 11.8 mph (17.3 ft/sec, 19 m/sec), requiring 3.5 min. to travel the 3632 ft (0.7 mile, 1.1 km) between stations A and B, or 7.0 minutes to complete the 1.38-mile (2.2 km) loop. Assuming that the unloading of passengers at the aft-most loading bay, the relocation of the vehicle to the foremost loading bay, and the loading of passengers requires 55 seconds, the maximum theoretical one-way capacity of the system is 1358 passengers/hour. This is based on ten vehicles with a maximum design capacity of ten passenters. However, with a maximum crush-load of 14 passengers (eight seated and six standees), the system will have an increased theoretical capacity of 1902 passengers/hour. The maximum practical one-way capacity is considered to be about 80% of the theoretical maximum, or 1086 passenter/hour.

The Jetrail system could theoretically accommodate up to 21 vehicles on the guideway simultaneously (based on a 20-second headway and an average speed of 11.8 mph, 19 km/hr), indicating a further potential increase in passenger capacity. However, to accept the added vehicles loading and unloading facilities would have to be doubled.

The maximum operating capacity experienced was reported by Braniff to be approximately half the theoretical, or 600 passengers per hour. This is not based on an actual count but on a sample estimate made on the basis of 2.2 passengers per car entering parking lot A. Over the life of the system (April 1970-January 1974) it carried an estimated six million passengers with no fatalities.

The Jetrail System Operational Characteristics

System Performance:

max. theoretical one-way capacity	1358 pass./hr.
max. practical one-way capacity	600 pass./hr. (est. Braniff)
max. practical one-way capacity	1086 pass./hr (80% theor.)
min. theoretical headway	approx. 7.3. sec.
headway	20 sec.
availability	on demand, 24 hr./day
type service	point-to-point, demand-responsive collection and dist.
type network	loop
traveling unit	single vehicles
interior noise	71 dBA
exterior noise	72 dBA

Vehicle Performance:

average velocity	11.8 mph (19 km/hr)
max. velocity	15 mph (24 km/hr)
max. grade	4%
average acceleration/deceleration	3.2 ft/sec^2 (0.97 m/sec^2)
max. jerk	-
emergency deceleration	3.5 ft/sec^2 (1.1 m/sec^2)
stopping precision in station	-
degradation if guideway is wet	none
degradation for ice and snow	inoperative
vehicle design capacity	6 seated, 4 standees
vehicle crush capacity	8 seated, 6 standees
energy consumption	-

Stations:

type	on-line, 3-berth, platoon loading
type boarding	level
ticket & fare collection	free service
security	none
boarding capacity	1028 pass./berth/hr
debarking capacity	1440 pass./berth/hr
max. wait time	3.8 min.
vehicle in-station dwell time	20-55 sec.
station spacing (principal)	0.7 mile (1.1 km)

Individual Service:

privacy	multiple party
transfers	none
stops	at baggage claim (Sta. C) from Braniff terminal (Sta. B)
accommodations	seated and standing
security	none
instruction	auditory and signs
passenger articles	small packages & luggage
comfort	heating, ventilation, and air conditioning

Cargo Capability:

luggage	from parking lot (Sta. A) to aircraft by truck - 2 Jetrail baggage cars never implemented.

Reliability and Safety:

fail-safe features	two levels of control redundancy without use of vital relays
strategy for passenger evacuation	knotted rope
strategy for removal of failed vehicles	push with trailing vehicle or tow from ground
system lifetime	design goal 15 yrs.
vehicle	design goal 7 yrs.

operational life	4 years
system Mean Time Before Failure (MTBF)	113 hrs. (approx.)
system restore time after failure	variable-usually <15 minutes
system availability	99.7 - 99.9% (approx.)
vehicle MTBF (single)	52 hours (approx.)
guideway MTBF	12,000 hours (approx.)
command and control MTBF	3,000 hours (approx.)

Personnel Requirements:

Vehicles & stations are unmanned. Personnel are required at one central control facility, maintenance, and administration.

The Jetrail System Physical Description

Vehicle:

length, overall	11.25 ft (3.4 m)
height, clear inside	6.5 ft (2 m)
width, clear inside	5.25 ft (1.6 m)
weight, empty	6000 lbs (2700 kg)

Suspension:

type	Vehicle suspended by 8 solid-rubber tired wheels. 4 drivers and 4 idlers running on a steel I-beam flange
lateral guidance	16 solid-rubber tires wheels
sway (roll)	4 shock absorbers

Propulsion & Braking:

type & no. of motors	2 rotary induction
motor rating	7.5 HP each (5.6 kW)
type drive	Electromagnetic eddy-current transmission providing positive and negative torque coupled with a mechanical differential and gear train for final drive of wheels. 2 driving wheels per truck.

type power	480 Vac, 3ϕ, 60 Hz
power collection	Sliding contact shoes on galvanized steel power rails
type service brakes	eddy-current 2 per vehicle
type emergency brakes	mechanical/electro-magnetic
Switching:	
type	Lateral transfer of interconnecting guideway elements
switch time (lock-to-lock)	6 sec
speed thru switch	4.5 mph (speed 2)
Guideway:	
type	mono-rail, standard I-beam
supports	cylindrical steel columns
width (center-to-center)	12.1 ft (3.7 m)
total length including storage, turnouts, and maint.	8400 ft (2.5 km)
length, shuttle-loop	7265 ft (2.2 km)
average height of vehicle floor above ground	16 ft (4.9 m)
max. grade	4%
min. turn radius	15 ft (4.5 m)

3.2 VEHICLES

3.2.1 Body

The vehicle is a fiberglass shell attached to a steel frame, having windows in the upper half and a door on the right side. Polyurethane foam insulation lines the inside of the fiberglass. The general features of the vehicle exterior are shown in Figure 3.2.1.

The welded steel frame structure is attached to the two trucks which contain the suspension, lateral restraint, and anti-sway systems. The weight is carried by eight solid-rubber (four driving) wheels, which ride on the supper surface of the lower flange of the I-beam. The truck is inherently constrained to the guideway in a

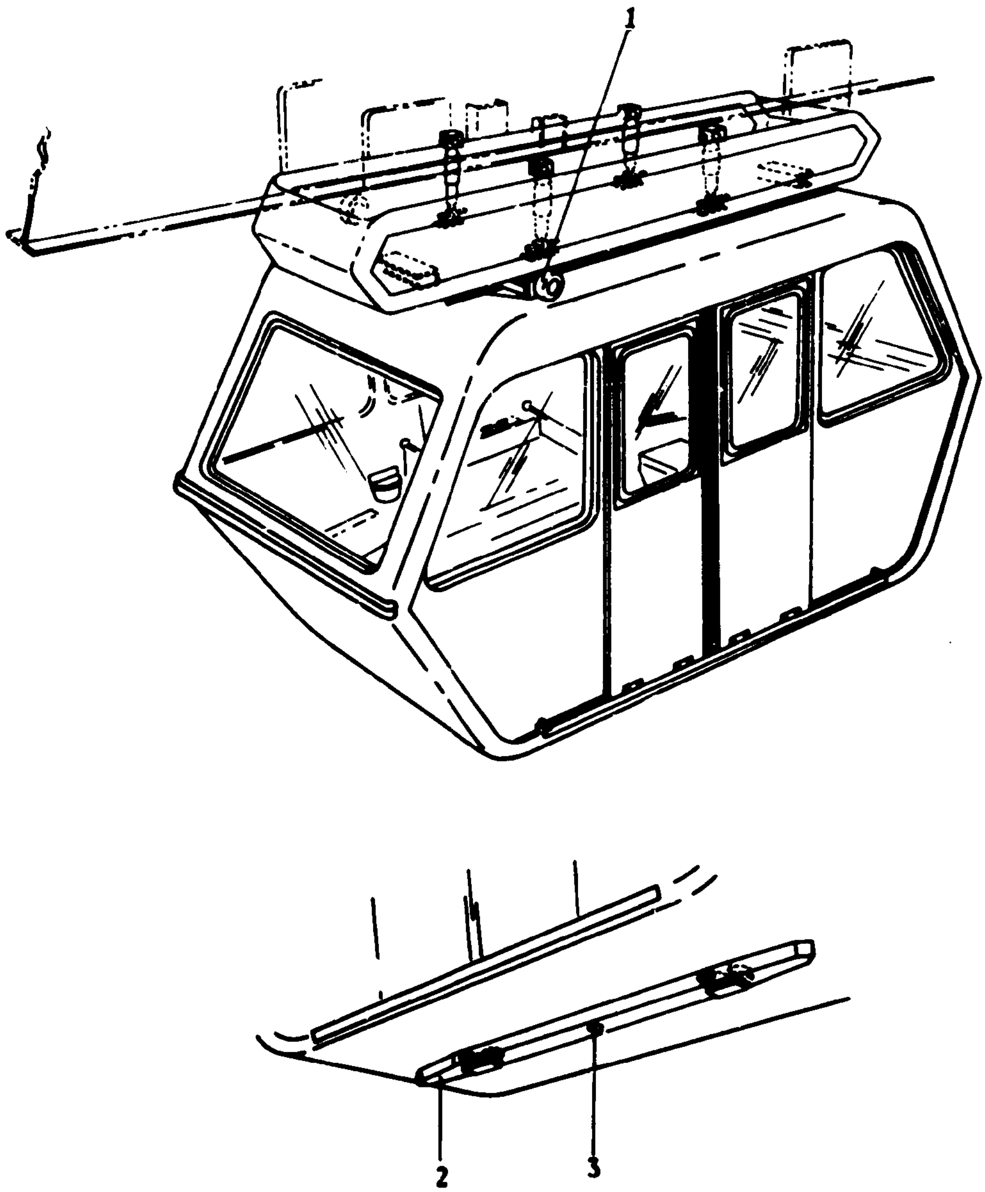

FIGURE 3.2.1. SOME DETAILS OF JETRAIL VEHICLE AND SUSPENSION

positive and safe manner (Fig. 3.2.2). The rubber of the wheels provides the only springing – no secondary suspension is provided. To properly position the vehicle during loading and unloading, a guide-arm assembly (item 1) and a wheel assembly (item 2) are used. See also Figure 3.2.1 items 1 and 2. The guide-arm assembly, mounted on the bottom of the vehicle, works in conjunction with a slot attached to the stations platform to insure that there will be no roll, or sway, during loading and unloading. The wheel assembly, in conjunction with the bottom surfaces of two trusses, attached to the guideway at the stations, insures vertical alignment of the vehicle and station platform floors. Rubber bumpers are provided, front and rear, to avoid damage during parking or pushing of the vehicles.

The vehicle is accessible from the right side through bi-parting electromechanical automatically-operated sliding doors as shown in Figure 3.2.3. Door panels are constructed of steel sheets in a sandwich construction over a steel frame. Station doors are of identical construction but are taller and wider. The station doors are electrically interlocked with vehicle position switches such that they can only be opened when the vehicle is properly positioned. Pressure-sensitive safety door-edge switches are used as is weather stripping on the outboard edges of all door panels.

The interior of the vehicle is shown in Figures 3.2.4 and 3.2.5. The seats (item 1) extend the full width of the car at the end. The baggage rack (item 2) is located opposite the vehicle extrance in the center of the vehicle and serves as a protective cover for the air conditioning unit (item 3). The structural frame supports the plywood sub-floor. A 1/8-inch (3.2 mm) thick rubber mat is bonded to the sub-floor and covered by carpeting which extends up underneath the seat cushions. Two louvers (item 4) underneath each seat permit ventilation of the electrical components (items 5, 6, 7, 8, 9, 10 and 11) housed under the seats. An exterior louver (item 7) on the left side of the vehicle interfaces with the air-conditioning unit.

The seat bottom is hinged (and normally locked) permitting access to the manual override controls see Figure 3.2.6. Removable

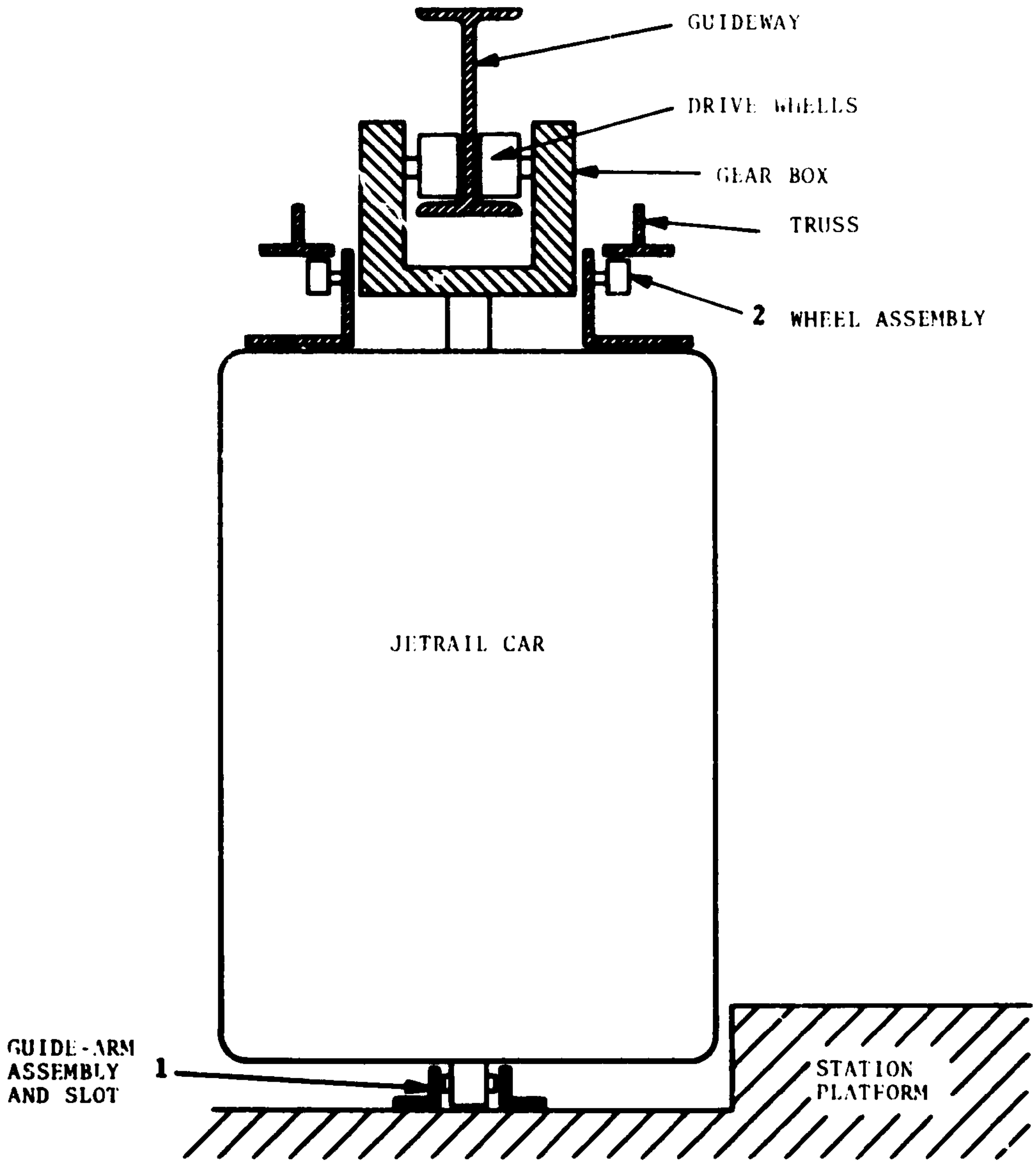

FIGURE 3.2.2. SCHEMATIC OF JETRAIL GUIDING AND SUSPENSION

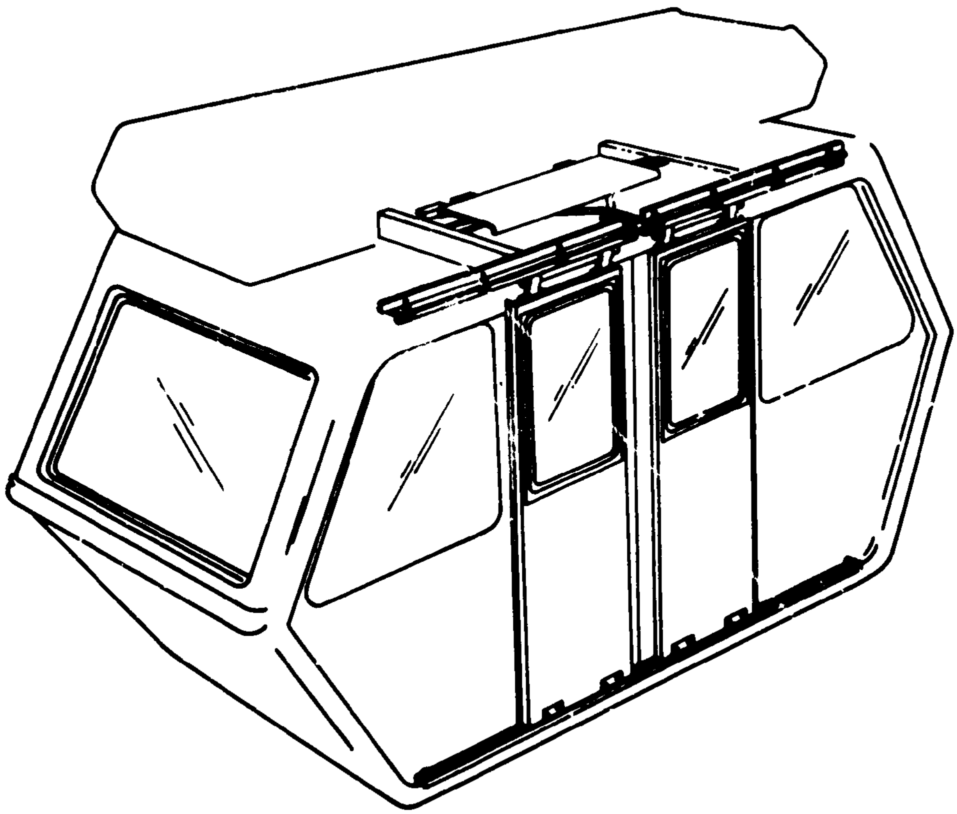

FIGURE 3.2.3. DETAILS OF JETRAIL DOORS

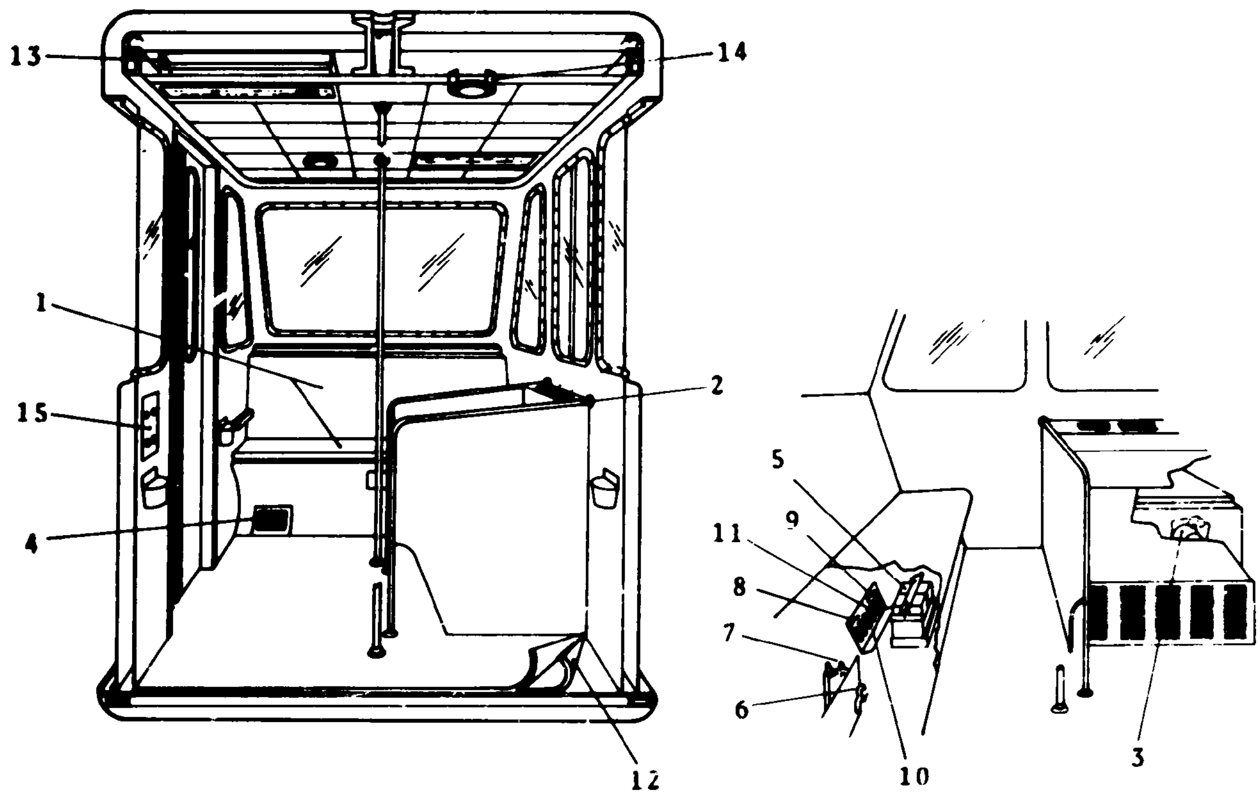

FIGURE 3.2.4. DETAILS OF JETRAIL INTERIOR

FIGURE 3.2.5. VEHICLE INTERIOR

FIGURE 3.2.6. JETRAIL VEHICLE CONTROL BOX

seat pads are attached to the seat structure. The seat structure is a fiberglass element integral with the vehicle body.

The walls are finished with 1/16-inch (1.6 mm) Wilson Art Panels bonded to 1/8-inch-thick (3.2 mm) Tempered Masonite backing. The glass is 3/16-inch tinted safety plate glass.

A mat switch (item 12) installed over the entire sub-floor under the carpeting, is connected to the vehicle control panel. A weight of 10 lbs (4.5 kg) or more on the floor signals that the vehicle is occupied (i.e., by means of a normally open relay). Each seat is provided with three pressure-sensitive micro-switches which also may indicate occupancy.

The ceiling consists of Acoustimetal aluminum ceiling panels. Recessed into the ceiling are two flat prismatic light panels (item 13) each housing two 120-V, 60 Hz, fluorescent lamps. Two recessed emergency light fixtures (item 14) are connected to two Burgess 12-volt, type TW2 batteries which provide internal vehicle lighting automatically in the event of power failure. A red emergency light located on the outside bottom center of the vehicle (item 3, Fig. 3.2.1) also indicates a power failure. Switches are provided underneath the rear seat for manually operating the lighting systems.

The automatic and manual controls and the main vehicle distribution transformers are located under the seats. The transformers are 5-kVA units, supplying 220-and 120 volts, 1-ϕ, 60 Hz power to the controls, lights, door-control power supply, convenience outlet, and air-conditioning unit. One 120-V, 1-ϕ, 60-Hz convenience outlet with a protective lock is located in each vehicle at the rear seat. The outlet is inactive when locked and maintenance personnel must unlock it prior to use. The main power disconnect switch is concealed behind a removable ceiling panel opposite the entrance. The emergency egress rope is also located behind the same panel.

The station selection buttons are just under the window near the door (item 15). A red emergency stop button is among these and when pulled out applies emergency brakes and activates a loud bell within the vehicle.

The air-conditioning (cooling and heating) unit (Frigidaire Model ARHW-1838R) has the capacity of 18,000 BTU-hr(18 MJ/hr or 5.2 kW)utilizing 3.0 and 5.2 kW for heating and cooling respectively.

3.2.2 Propulsion

The Jetrail propulsion system utilizes two eddy-current transmission drive subsystems, each mounted on separate vehicle trucks. Each drive system consists of an electric motor coupled to an eddy-current transmission, and electro/mechanical brake, a differential gear box drive unit, and finally the drive wheels. The electric motor is a 3-phase, 480-volt single-speed unit rated at 7.5 horsepower (5.6 kW). The torque transmitted to the drive wheels is governed by controlling the magnetic coupling between the drive motor and the eddy-current transmission. The eddy-current transmission, or magnetic clutch, operates on the principle that when currents are induced in a conductor moving in a magnetic field, the field associated with the induced currents tends to align itself with the inducing field. In the eddy-current type of coupling, a variable strength electromagnet is rotated by the prime mover, or constant speed motor. That is, the inducing field is a rotating dc field developed in a coil attached to the motor output shaft and connected to a dc source through slip rings. The clutch output member, positioned in the rotating field is forced to rotate due to the interactions of the rotating field and the field produced by the induced eddy-currents. As field strength is varied by changing the amount of current, the output torque is varied. Figure 3.2.7 shows the speed torque characteristics of eddy-current coupling. The torque is nearly constant until approximately 90% of the input speed is reached, at which point the torque rapidly approaches zero. This occurs, because it is a slip device, - torque depends on the difference between input and output speed. The output torque is also a function of the inducing magnetic field, which in turn is proportional to the magnetizing ampere-turns. Because the dc coil is wound with many turns, relatively high torques can be transmitted with relatively low control currents.

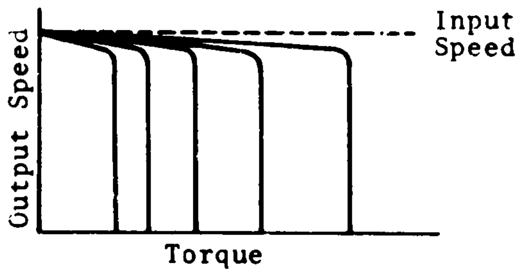

FIGURE 3.2.7 SPEED VERSUS TORQUE

In addition, normal service braking is achieved with the eddy-current transmission. A separate stationary coil around the output shaft is used for braking. As the field strength of the braking coil is varied by changing the amount of current, eddy-currents are induced in the output rotor applying a negative torque, or braking force. Braking, or negative torque, can be varied considerably by relatively small control currents.

3.2.3 Emergency Brakes

Emergency brakes are spring-operated disc brakes. These are normally held open by the action of an electromagnetic field and are applied when the magnetic field is interrupted. This field can be interrupted by either pulling the emergency stop button, action by the logic control subsystem when an emergency is imminent, or action by power relays when the vehicle or system loses power.

3.3 POWER DISTRIBUTION

The power distribution system is composed of two subsystems; 1) a power substation system, which transforms the high-voltage utility power to low-voltage ac for distribution throughout the system, and 2) a network subsystem of protective devices, interconnections, insulators, rails, and power collectors, which deliver power from the power substation to the vehicles on the guideway.

The power substation system consists of only a single substation (Figure 3.3.1). It is located approximately midway between the Braniff terminal (station B) and the parking lot (station A). The main electrical power is supplied from a power company utility pole and transformer (N8910) through the emergency switch and an electrical riser to the junction box on top of the I-beam. In the event of a power outage, emergency power is supplied automatically by a generator through the electrical riser to the same junction box. (Figure 3.3.1 and 3.3.2.)

The substation is rated for 300 kVA, which at 3-phase, 480 volts, and 60 Hz, corresponds to 360 amperes. It is backed up by a 150 kVA emergency generator, which allows reduced operation during power outages.

FIGURE 3.3.1. JETRAIL SUBSTATION

FIGURE 3.3.2. EMERGENCY GENERATOR

Power is delivered from the substation to the vehicle by a three-rail system. Power conductor and signal collector rails of galvanized steel carry 3-phase input power as well as the electrical command signals. The function of each conductor bar (rail) is indicated in Figure 3.3.3. The T-bar, located primarily in station areas, is a flat conductor bar carrying dc special function channels 1 and 2. A channel 1 signal transmitted from the vehicle indicates to the system logic that a door is open or closed, a door safety edge is activated, or an emergency run or stop condition exists. A channel 2 signal indicates that the vehicle is empty or occupied and that a station has been selected.

The galvanized steel rails are attached to the I-beam web. A series of jumper cables, consisting of AWG #0000 (0.46 in.,11.5 mm) aluminum conductor, tie into the rails at 300-foot (91 m) intervals – joining the individual phases in both directions of travel.

Jetrail vehicles receive input power and electrical command signals from the conductor rails through sliding-shoe-type collectors. The collector shoes (brushes), made of brass with carbon inserts, are mounted on pivoting arms and a snubber mechanism, which maintains shoe pressure and correct alignment with the conductor bar (Figure 3.3.4). Each truck has one set of power and signal collector shoes.

3.4 COMMAND, CONTROL, AND COMMUNICATIONS

The Jetrail automatic command and control system is an innovative feature of the system. The automatic control function is accomplished by a vehicle control subsystem that receives speed commands from a hardwired, double-redundant electrical block-control circuit. It does not employ any computers or software. The system represents a significant improvement over existing hardwired block-control logic circuitry due principally to the application of redundant logic.

The Jetrail control system can be divided into three subsystems: speed control, block control, and safety and redundant blocking. The system can also be operated in a degraded mode.

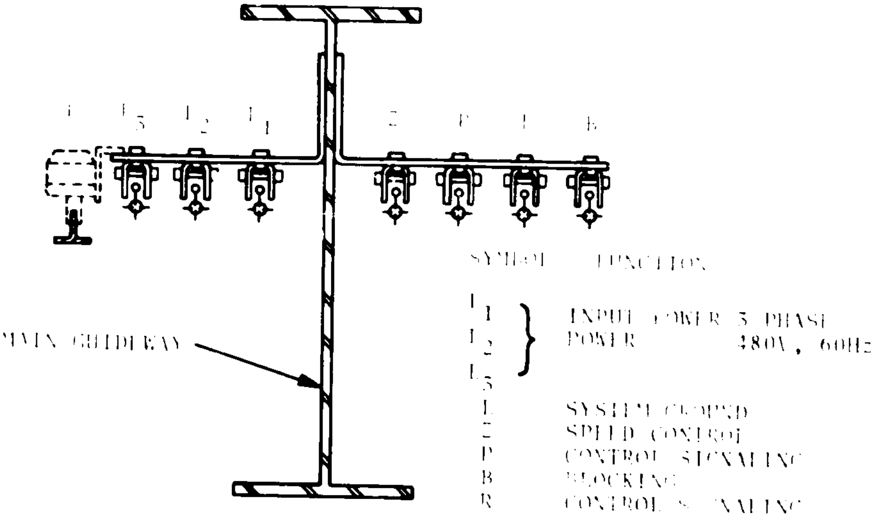

FIGURE 3.3.3. CONDUCTOR BAR FUNCTIONS

FIGURE 3.3.4. PROPULSION UNIT

3.4.1 Speed Control

The speed control system logic divides the entire guideway into speed segments by dividing the Z-bar conductors into short lengths and establishing a dc potential on each bar segment proportional to speed. The vehicle speeds corresponding to commanded speeds and Z-bar voltages are given in Table 3-4-1. The entire 1.38 miles of single-lane guideway are divided into 208 speed segments of different lengths – Z-bar segments as long as 100 feet are in the straight portions of the guideway and segments as short as 2 feet are in and near the station areas. These speed segments are in turn combined into the speed zones shown in Figure 3.4.1.

For vehicle drive to occur, normal dc potential of the Z-bar must be nominally at 20, 50, 80, or 110 volts dc depending on the speed command code. Therefore, the vehicle will change speed to the command speed that has been hardwired into the guideway logic.

TABLE 3-4-1. VEHICLE SPEEDS VS. COMMANDED SPEEDS

Vehicle Command Code	Nominal Vehicle Speed (mph)	(km/hr)	Z-bar Voltage (Volts dc nominal)	Resistance (ohms)
0	0	0	0	
1	1.5	2.4	20	2500
2	4.5	7.2	50	250
3	9.0	14.5	80	75
4	15.0	24.0	110	~0

Vehicle Controller

As previously stated, vehicle propulsion is provided by two single-speed, 3-phase electric drive motors, each mounted on a vehicle truck. Output drive-motor torque is transmitted to the drive wheels through an eddy-current transmission. A Spicer differential and two gear boxes one on each side of the guiderail complete the power train. The drive wheels are mounted on the gear

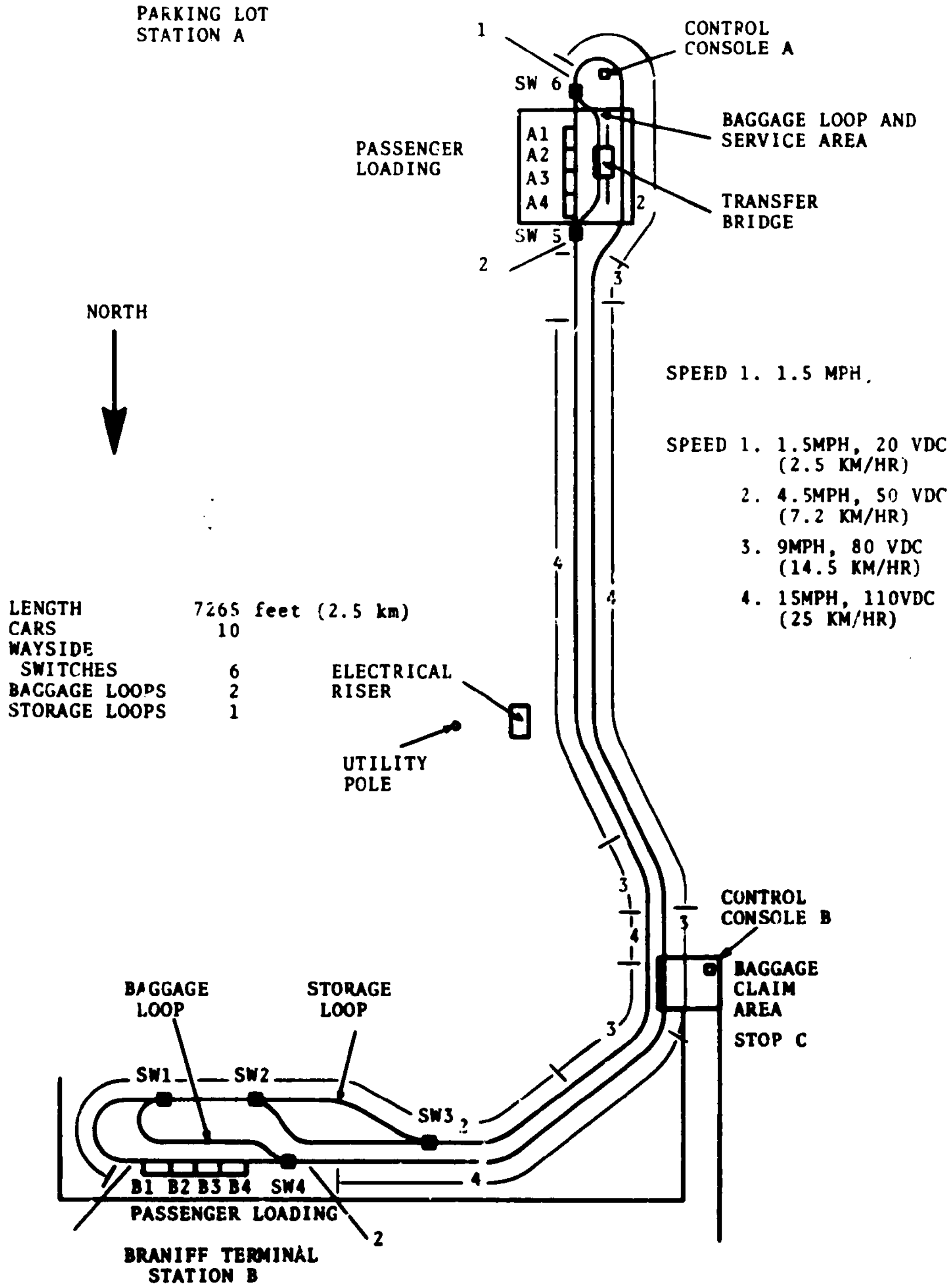

FIGURE 3.4.1. SCHEMATIC OF SPEED ZONES

box output shafts. The emergency brake is mechanically applied and held off electrically, i.e., by a solenoid.

Drive speed is controlled by a dual-channel eddy-current transmission speed-control circuit. The eddy-current transmission incorporates both a clutch-drive and a service-brake function. The dual-channel speed control circuit is a solid-state closed-loop control circuit used to regulate vehicle speed.

The eddy-current transmission output rotor provides a feed-back signal to the speed control circuit. This is accomplished by inducing a current in a magnetic pickup as the 90-tooth gear on the drive shaft (tachometer) is rotated. The induced current flow is the output of the magnetic pickup that is an ac signal having a frequency directly proportional to the output rotor (or drive output) speed. The output of the magnetic pickup is then fed to an ac-to-dc converter.

This positive dc feed-back voltage is summed with a negative dc Z-bar signal reference voltage to obtain an error signal. Adjustment of the speed potentiometer permits fine tuning of the error signal, hence the commanded speed. If negative, the error signal advances the firing angle of the eddy-current clutch SCR (silicon controlled rectifier) which increases drive speed. If positive, the error signal advances the firing angle of the eddy-current brake SCR, decreasing the drive speed. In either case (positive or negative) the greater the amplitude of the error signal, the greater the increase or decrease of vehicle speed. The vehicle controller is schematically shown in Figure 3.4.2. By varying the gain on the clutch or brake SCR the rate of accleration or braking may be controlled.

Over-Speed Sensing

The overspeed device is designed to sense overspeed relative to the Z-bar voltage independent of the remaining systems. The overspeed sensing system uses the secondary tachometer that is on the rear drive unit to compare with the primary tachometer on the front unit to detect an over-speed condition, (Figure 3.4.3). If

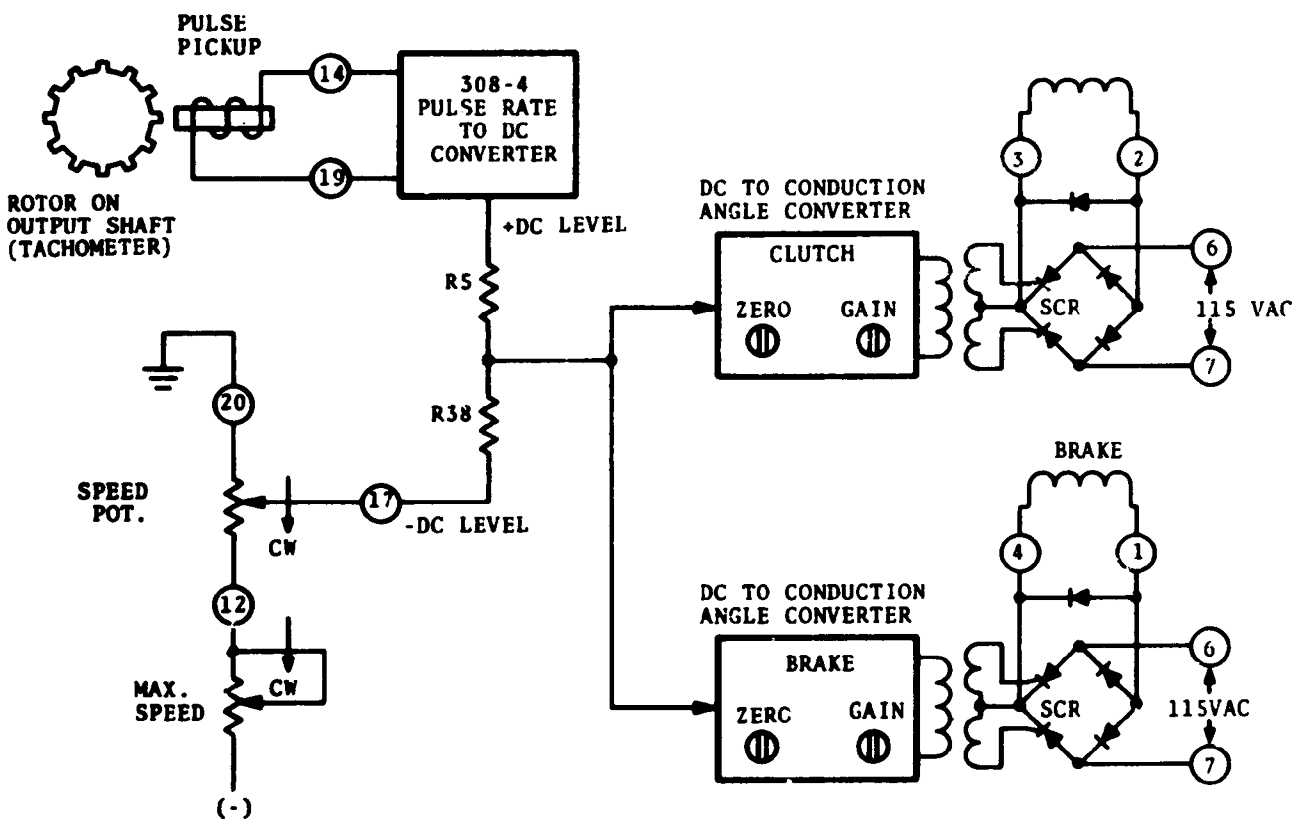

FIGURE 3.4.2. SCHEMATIC OF CONTROL CIRCUITS

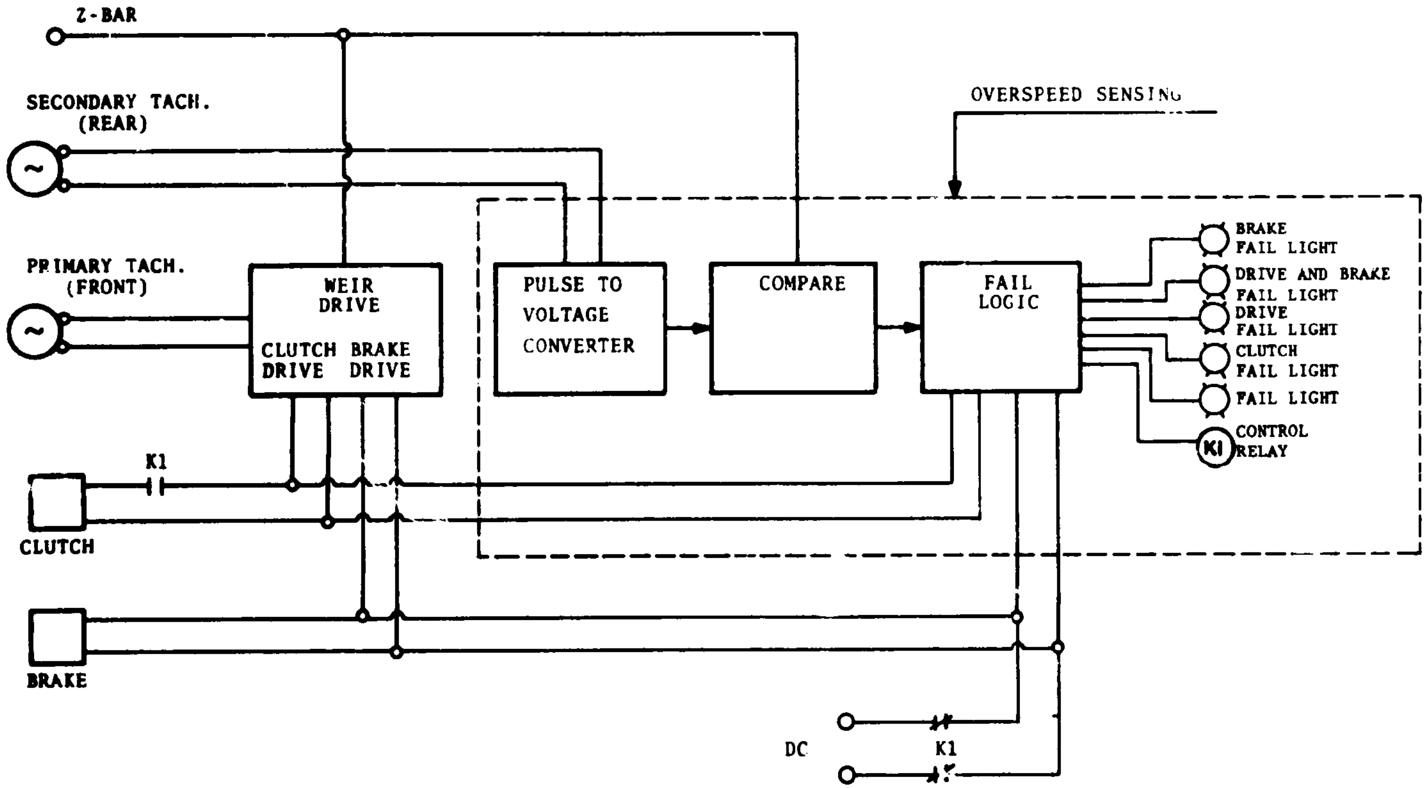

FIGURE 3.4.3. SCHEMATIC OF OVERSPEED CONTROL

the sensed speed is greater that the speed command of the Z-bar voltage, an over-speed signal is sent to a delay circuit, set for 5 to 10 seconds. After the delay period, if the over-speed condition still exists, the clutch circuit is opened and power is applied to the brake.

The braking action will probably reduce the speed of the vehicle below the speed commanded by the Z-bar voltage. At this time the delay circuit will reset and remove the brake power. If the overspeed condition recurs the clutch will reopen, and the brake will be energized. This allows the vehicle to "jog" into the station even though a drive failure has occurred.

In addition, lights are provided to indicate proper operation of the clutch, clutch drive, brake, and brake drive. Proper interpretation of the fail lights also discloses over-speed sensing failure.

3.4.2 Block Control

A series of relays at central control maintains a four-Z-bar restricted speed zone behind each vehicle. The Z-bar immediately in back of a traveling vehicle is at speed-0 command (dead stop). The second Z-bar in back is at speed-2 command. The third Z-bar is at speed-3 command. Hence, the vehicle is followed by a stepped speed zone that will stop a following vehicle prior to collision. Figure 3.4.4 shows a schematic of the control system. A vehicle is schematically shown in this figure with appropriate speed commands on each Z-bar segment. In a slightly different manner Figure 3.4.5 shows the speed commands on each Z-bar segment relative to the vehicle. If a lead vehicle at speed-3 (9 mph, 14.5 km/hr) is being approached by a vehicle at speed-4, (15 mph, 24 km/hr) the following vehicle will receive a speed-3 command when it reaches the 3rd trailing Z-bar segment, slowing the vehicle to 9.0 mph (14.5 km/hr). If at this time the lead vehicle stops, the following vehicle upon reaching the 2nd trailing Z-bar segment will receive a speed-2 command and slow to 4.5 mph. Upon reaching the 1st trailing Z-bar segment the vehicle receives a speed-0 command

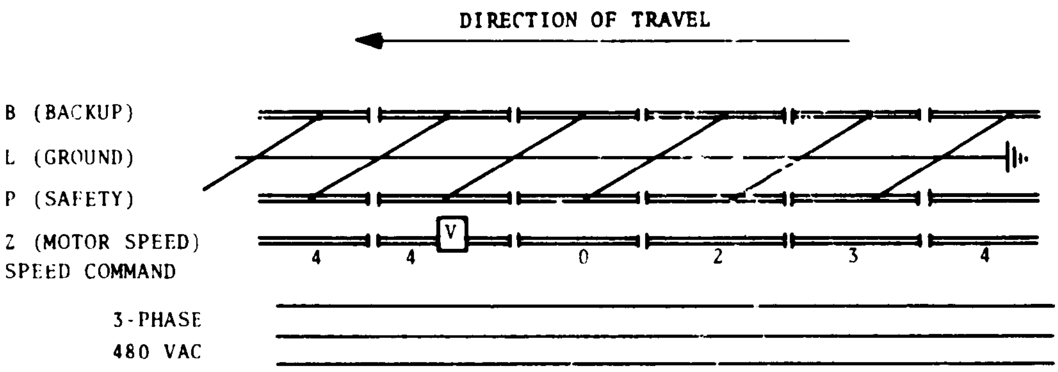

FIGURE 3.4.4. SCHEMATIC OF REDUNDANT SIGNAL WIRING

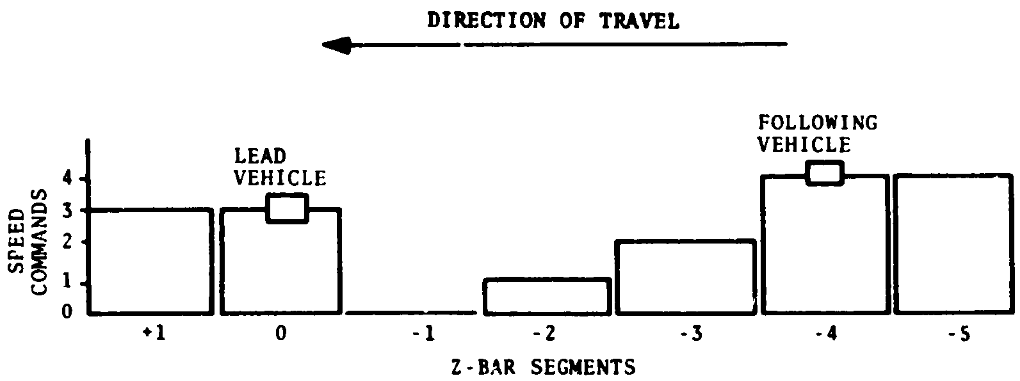

FIGURE 3.4.5. SPEED ZONES IN VICINITY OF VEHICLE

and comes to a stop. When the lead vehicle moves on down the guideway, it will be followed by its stepped-speed-command "tail". The segment where the following vehicle was brought to a stop [Z-bar segment (-1)] is restored to speeds 2, 3, and 4 sequentially and that vehicle will be allowed to proceed.

The control of the speed is accomplished by regulating the voltages to the Z-bars. Voltage is transmitted to the Z-bars from the central control through a series-cascade circuit. There is one such cascade control circuit for each Z-bar segment. Each circuit is itself composed of cascaded stages of resistors across relay contacts. When all the relay contacts are closed the Z-bar receives the full voltage (110 V dc). As additional resistance is added, the voltage is decreased in accordance with the values given in Table 3.4.1. That is, when all but one relay contact is closed a 75-ohm resistance will be introduced dropping the voltage to 80 V dc. When all but two relays are closed, 250 ohms of resistance will be in series, dropping the voltage still further to 50 V dc. Finally, when only the last relay is closed, 2500 ohms of resistance will be in series resulting in a voltage of 20 V dc.

Emergency and degraded operating modes are incorporated into the control system by not permitting the entire speed command sequence to function, hence reducing the Z-bar voltage appropriately. Degraded operating modes are used during unfavorable environmental conditions.

3.4.3 Safety and Redundant Blocking

To insure operation of the block-control system a redundant system has been incorporated in the P-bar segments (Fig. 3.4.4). These segments are totally redundant to the Z-bar control segments. If a vehicle does not receive a comparable signal from both of these segments a relay will be activated opening the line to voltage and reducing Z-bar potential to zero.

The B-bar shown in Figure 3.4.4 is physically wired to the P-bar of the next segment to provide the next speed command signal a vehicle will receive. This operates a redundant blocking system in a vehicle which may be approaching another vehicle during failure of normal speed control blocking. The B-bar under this condition will cause a relay on the redundant blocking panel of the following vehicle to de-energize, opening the wiring to eddy-current clutch and causing the following vehicle to stop.

3.5 SWITCHING

Six automatically actuated wayside rail switches are incorporated in the Jetrail guideway to switch vehicles into and out of by-pass spurs. The switches consist of motor-driven frames which support two rail sections, one curved and one straight as shown schematically in Figure 3.5.1. Switching is achieved by lateral transfer of alternative (straight or curved) guideway sections to mate them with the appropriate stationary guideway rail segment.

The switch segments receive power and command signals from the power distribution and block-control networks. The curved and straight guideway segments are electrically fed in parallel. The power and signal distribution rails do not make mechanical contact with adjacent fixed segment rails when in position. Rather, the rails have a small gap between them, but the collector shoes are large enough to span this gap to permit continuous operation through the switch.

Figure 3.5.2 shows an entire switch assembly with vehicles in the wash and storage area adjacent to station B. A closer view of the switch frame with a curved guideway segment in place is shown in Figure 3.5.3. The metal housing protects against the weather – the doorway allows access for maintenance. Figure 3.5.4 shows switch details with a straight guideway segment in position.

The time required to effect switching is 6 seconds, lock-to-lock. This is well below the 20-second headway of the vehicles and somewhat below the minimum theoretical headway of 7.3 seconds. In all cases switches are traversed by the vehicles at speed 2 (4.5) mph, 7.2 km/hr).

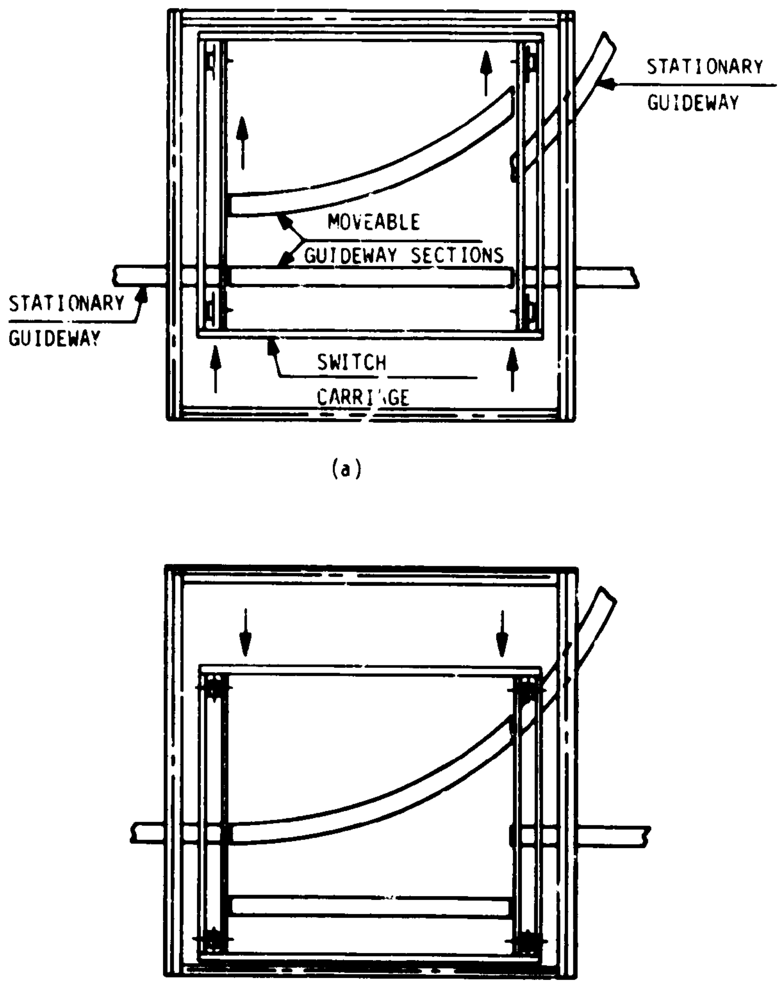

FIGURE 3.5.1. SCHEMATIC OF A SWITCH FRAME

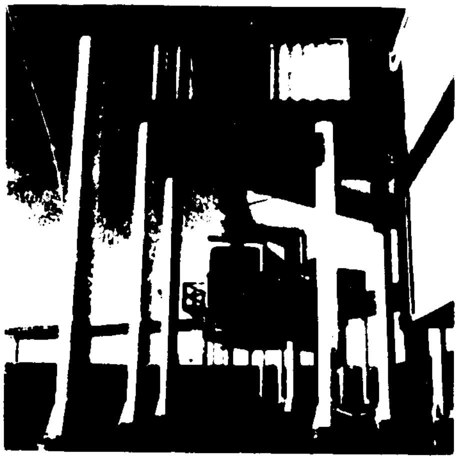

FIGURE 3.5.2. VIEW OF A SWITCH HOUSING

FIGURE 3.5.3. SWITCH DETAIL - CURVED SEGMENT IN PLACE

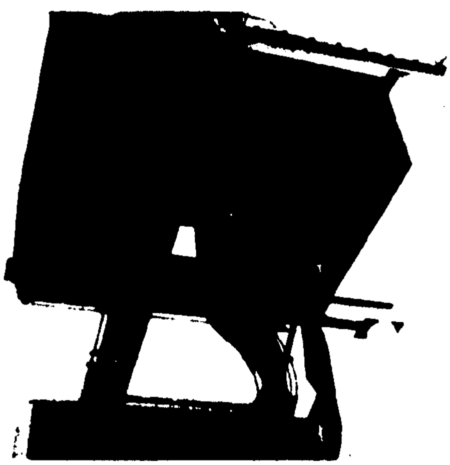

FIGURE 3.5.4. SWITCH DETAIL - STRAIGHT SEGMENT IN PHASE

3.6 GUIDEWAY

Jetrail was intended to preclude the need for Braniff patrons to fight for the existing congested terminal access road and parking facilities. Hence, the Jetrail system was devised to provide transportation from a parking lot just inside the entrance of Love Field to the Braniff passenger terminal. The system was designed as a loop system connecting the parking lot area (station A) to the Braniff terminal (station B) both of which are on line stations (Figure 3.1.4).

3.6.1 Layout

In order to connect the principal stations A and B, 7265 feet (1.38 mi, 2.4 km) of guideway loop was needed. The guideway was elevated to fit the system into the existing environment without excessive intrusion. It essentially runs north to south along the edge of an existing road, crossing it at an oblique angle near the Braniff terminal. Jetrail also crosses a street and a brook (Figure 3.6.1) at a right angle in the vicinity of the parking lot (station A). The topography is essentially level. The average clearance height above the ground is 16 feet (4.8 m) to provide clearance for surface transportation.

The Jetrail guideway consists of an I-beam rail arranged in a continuous loop for travel between stations, with bypass spurs or loops for supplemental functions of storage and maintenance. The guideway layout is shown in Figure 3.1.4. A third on-line station C (Figure 3.6.2) was added in the baggage claim area permitting passengers to obtain their luggage from the carousels, enter the vehicle, and proceed to the parking lot (station A). Located near station B, the system has a baggage loop and a storage spur which also serves as a wash area. A maintenance area is at station A. Six wayside guideway switches are included in the system to transfer vehicles to and from these loops. These additional loops make the total length of single track guideway 8460 feet (2.56 km). The center-to-center width of guideway is 12'-1" (3.6 m).

FIGURE 3.6.1. GUIDEWAY CROSSING THE BROOK

FIGURE 3.6.2. BAGGAGE STATION

FIGURE 3.6.3. GUIDEWAY SHOWING CROSS-BRACING

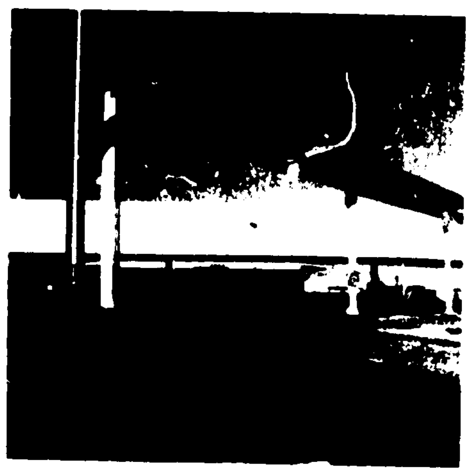

FIGURE 3.6.4. GUIDEWAY SHOWING STIFFENERS

The guideway is basically tangent with large radius curves (about 600 feet, 180 m) and small (15 feet, 4.5 m) radius curves in the stations which complete the loop. None of the curved sections are superelevated. In negotiating the 15 foot (4.5 m) radius of guideway, the vehicle speed is reduced to speed 2 (4.5 mph, 7.2 km/hr).

The maximum grade is about 4 percent between stations B and C. Note that for the AGRT and Dual Mode Programs, the DOT specifications call for a maximum grade of 6 percent with a dwell time of about 5 seconds at the cruise speed of 40 mph (64 km/hr). The Jetrail system had a dwell time on the order of 10-15 seconds on a 4 percent grade as it was accelerated from a stop between stations B and C.

The sub-soil of the area was reported by the Jetrail personnel to consist of a layer of about 20-25 (6-7.5 m) feet of medium strength clay on top of shale. This foundation condition dictated the design criteria for the foundations of the elevated guideway which in conjunction with vehicle/guideway loading conditions permitted the use of spread footings.

3.6.2 Guideway Structure

The basic guideway element consists of a 27-inch (70 cm) deep overhead structural steel I-beam spanning about 50 feet and designed to carry a ten passenger-6000 lb (2700 kg) empty and 7500 lb (3400 kg) gross weight-vehicle (Figure 3.6.3). Each guideway beam is supported at the columns by cantilevered, tapered-steel I-beam girders. They tapered from a 12-inch (30 cm) depth at the guideway to a 24-inch (60 cm) depth at the column. The girders are welded to the column caps. The bottom of the guideway is nominally 25 feet (7.5 m) above the ground. Additional girders and truss elements are used between column supports to increase torsional rigidity (Figures 3.6.3 and 3.3.2). Furthermore, in the curved section of the guideway where it is subject to additional torsion, I-beam stiffeners have been attached to the top of the guideway elements. This technique has also been employed to permit an increase span length (Figure 3.6.4). That is, doubled beams are used to cross the street and the brook near station A (Figures 3.6.4 and 3.6.1). Expansion joints have been incorporated into the ends of the guideway elements.

The guideway support structure consists of 18-inch (45-cm) diameter steel pipe columns 0.312 inches (8 mm) in thickness. The vertical columns are bolted to spread footings.

Guides are installed, in the form of overhead trusses, on each side of the guide rail in the station loading and unloading areas. These mate with caster wheels on the top of the vehicles to insure the correct floor height in the station area and help prevent sway.

3.7 STATIONS

Three on-line stations are provided; station A at the outer parking lot, station B at the Braniff terminal, and station C for passengers desiring to carry their own baggage near the Braniff terminal.

Station A has several functions; passenger handling, service, maintenance, and shelter. Valet-parking and baggage check-in for the intended flight are available at curbside. An elevator or stairs takes passengers to the Jetrail vehicle loading level. This level is carpeted and resembles a typical building elevator boarding area. The boarding doors are steel and have call buttons near by. Three doors are for boarding and one for disembarking Jetrail passengers.

Service and maintenance functions are primarily performed in a maintenance area integral with station A. Maintenance is discussed in Section 3.8.

Station B was attached to the Braniff terminal with its boarding level the same as the terminal arrival floor. It is approximately 14x60 feet (4.2 x 18 m), carpeted, with windows in each end and has four Jetrail doors as in station A.

Station C although originally intended to be a baggage stop was used as a station for passengers desiring to pick up their own luggage at flight termination. It was attached to the Braniff terminal carousel baggage area. Passengers must walk from the carousels up a flight of stairs to get to the station C disembarking area. This station is similar to that of station A but has only one loading door.

A passenger arriving on Braniff can check his luggage through to Jetrail station A. If so, the luggage is transported by truck to that station. When the passenger arrives he picks up his luggage and automobile at the curbside. If the luggage is not checked through to Jetrail it must be claimed at the regular carousel. At which time the passenger walks the short distance to station C up the stairs to the boarding level and calls for a Jetrail vehicle.

3.8 MAINTENANCE

Maintenance facilities are provided within station A for the general service and repair of vehicles and in the storage loop for cleaning and washing vehicles (Figure 3.1.1). The cleaning facility is a steel frame wash rack with an open steel grill floor for washing. It is located on the storage loop (Figure 3.1.4). It has an electrical power outlet for vacuum cleaning operations and a water supply for washing. The cleaning operation is essentially manual. Cleaning operations are performed by a single individual working one shift, seven days a week, whereas maintenance is available 24 hours a day.

The maintenance service area consists of two bays and a parts and storage area. The service area is entered via an off-line guideway segment. Switch SW6 is thrown to enter this off-line segment (Figure 3.1.4). The vehicle is stopped on the transfer bridge and the bridge carrying the vehicle is then moved laterally by electrical drive into the service area. Because this leaves an open guideway segment on the off-line segment, the transfer bridge is interlocked with switch SW6 to prevent entry by another vehicle. Once the vehicle is in the service area it is pushed manually onto a guiderail either into the forward bay or aft into the rear bay. The forward bay is used for heavy work on the propulsion and propulsion drive system since it has hoisting equipment. The rear bay is used for light maintenance work.

Control console A, one of the two redundant control consoles is also located within the maintenance service area. This affords capability for quick operating changes from this console during the time when maintenance is being performed. Normally the technician is at control console B. At the same time any control console failures such as relay malfunctions can be quickly corrected due to the proximity of spare parts. The colocation of control and service functions permits almost single-handed operation and maintenance of the system. As will be discussed later in section 4.3 Braniff utilized one full-time Jetrail maintenance technician available 24 hours a day and one Braniff aircraft technician available on-call. In this way operating and maintenance costs were minimized. The two technicians were in two-way radio contact and therefore could react quickly to system emergencies and unusual air passenger arrival situations.

3.9 RELIABILITY

Reliability of operation and system availability were extremely important to Braniff because if the Jetrail system did not perform to some high standard, patronage would be reduced. The original intent of the system was to increase patronage by offering convenience and easier access to Braniff Airlines than that afforded to other airlines at Love Field. In spite of the importance of reliability and availability, a realiability specification for the system was not included in the original contract. Such a specification would have significantly raised the price, considering that at the time of development no completely automated systems of this type were in daily operational service anywhere. Although there were monorails and semi-automatic systems in park and recreation areas.

The approach adopted was to select a system requiring little or no development and employing commercially available equipment with proven capability. Of course, this approach does not indicate the conditions under which this capability has been proven or how it might relate to an urban transportation system and its associated operational environment. The developmental approach and available capital did not permit any reliability testing of components or subsystems, but only to build, test, and debug the operational system. A six-month test program was allowed for debugging the system prior to operation. Changes in operational procedures and maintenance also contributed to achieving the high reliability required.

3.10 ASTROGLIDE

The Jetrail vehicle operational experience resulted in a relatively large number of propulsion and vehicle control system failures which required a significant maintenance effort to keep the system operational (see Section 4.3.3). In order to eliminate these failures and minimize the required maintenance, PRT Systems Inc., made modifications to the Jetrail vehicle Number 10 by removing the eddy-current transmission propulsion system and incorporating a mechanically simpler linear-induction-motor (LIM) propulsion and control system.

The LIM system consists of two single-sided motors, one mounted on each vehicle truck and a control system currently mounted in the vehicle (see Figures 3.10.1, -2, and -3). The HVAC system was removed and the motor control system was mounted in a vertical cabinet to facilitate maintenance during the prototype development test phase. This is shown in Figure 3.10.4. This equipment is expected to be repackaged and mounted on top of the vehicle in the production model.

The differentials and gear boxes were eliminated reducing the vehicle weight by 2600 pounds (1200 kg) to 4400 pounds (2200 kg). The original drive and support which rolled on the upper surface of the lower flange are no longer used for traction but are only used as idler support wheels. The lower face of the I-beam flange is used as a reaction rail by the LIM.

The linear induction motor is the basic electrical machine used to provide the propulsion for the vehicle. The linear induction motor is analogous to the rotary induction motor in that they both produce output, thrust (linear) or torque (rotary), through the interaction of an exciting magnetic field and an induced

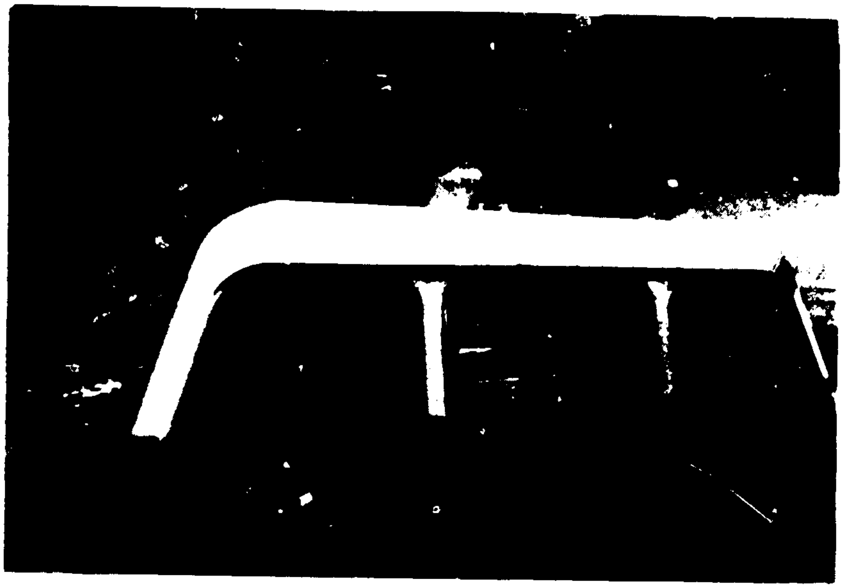

FIGURE 3.10.1. DETAIL OF LIM MOTOR AND SUSPENSION

FIGURE 3.10.2. DETAIL OF LIM AND GUIDE WHEELS

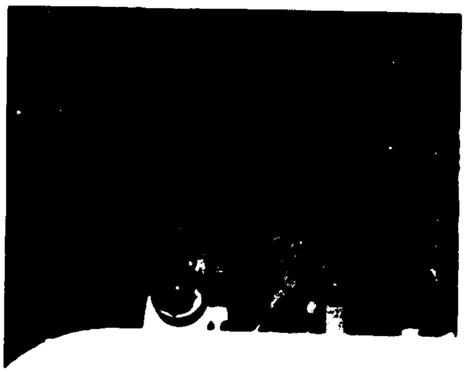

FIGURE 3.10.3. DETAIL OF LIM COLLECTOR SHOES

FICURE 3.10.4. TEMPORARY LIM CONTROL BOX

secondary magnetic field. In each case the excitation is produced by multi-phase windings which are located in the stator. For the linear induction motor the induced secondary magnetic field occurs in the reaction rail which for the Astroglide system is the guide rail. In a linear machine the synchronous speed of the traveling magnetic field is related to the operating frequency and pole spacing, p. For a machine operating at 60 Hz with a given pole spacing, the velocity of the moving field is 2 x 60 x p. For the Astroglide system, with a 15-cm pole spacing, the synchronous velocity is 64.5 km/hr.

The difference in relative velocity between the primary magnetic field and the reaction surface is called the slip velocity and is generally expressed a percentage of the synchronous velocity. In the Astroglide system, the slip velocity is the difference between vehicle synchronous velocity, 64.5 km/hr, and actual vehicle velocity. Slip velocity has a direct influence on operating efficiency because the fraction of input power available for propulsion is proportional to the ratio of vehicle velocity to synchronous velocity. In the Astroglide system, where maximum operating velocity is 24 km/hr, maximum efficiency is 24/64.5=38%. Linear motors used for transit applications must operate with relatively large air gaps between the stator and reaction rail and thus operate at lower power factors compared to rotary machines. The non-laminated reaction rail results in higher eddy current losses than in laminated structures and thus efficiency is further reduced.

The absence of a conductive layer between the stator and the reaction rail results in lower thrust for a given excitation level and in high attractive forces between the stator and reaction rail. This attractive force in the Astroglide system is greater than five times the thrust force and tends to lift the vehicle toward the guideway structure,thus, decreasing the rolling friction of the idler wheels. When the lift force exceeds the weight of the vehicle, the vehicle levitates, rising toward the secondary reaction rail. This is an unstable condition because attraction increases as the air gap gets smaller. To maintain an air gap of approximately 0.375 inches (9.5 mm), a set of idler wheels have been mounted to the LIM support to prevent the LIM from contacting the secondary steel I-beam (Figure 3.10.2).

The degree of levitation and propulsive thrust is proportional to the magnetic field strength. Since field strength is the parameter used to control vehicle speed, the levitation forces are not specifically controlled. But rather, whatever vehicle levitation force is obtained is a helpful result of propulsion control.

Each LIM was designed to deliver 350 lbs (1580 newtons) of thrust at a standstill. It has the characteristics of a high slip induction motor where thrust decreases from the maximum at standstill to zero at synchronous speed. This is shown in Figure 3.10.5. The synchronous speed of the Astroglide LIM is about 40 mph (64 km/hr). The design cruise speed of the Jetrail system is 15 mph (24 km/hr) indicating that the available thrust of the Astroglide system when operating at this speed is in excess of 300 lbs (1350 newtons). The characteristics shown in this figure are for a single motor connected directly across the three-phase input line (i.e., 3-phase, 480 volts, 60 Hz). A motor connected in this manner will accelerate to an equilibrium speed when the thrust developed by the motor equals the thrust required to drive the load and overcome losses.

The Astroglide propulsion system was not designed to meet any specific set of performance criteria, such as, velocity, wind, grade, weight, and acceleration. Rather, a break-away thrust measurement of the Jetrail system was made using a pull force sensor between two vehicles. This force was determined to be 350 lbs (1580 newtons). Since each of the two motors was designed to supply 350 lbs (1580 newtons) of thrust, the two motors provide a total capability of 700 lbs (3160 newtons). This redundant design feature allows a fault to occur in one of the motors without degradation in performance.

Although the Jetrail operational speed was 15 mph (24 km/hr), the LIM system was designed with a synchronous speed of about 40 mph (64 km/hr) to permit higher speeds (approximately 35 mph (56

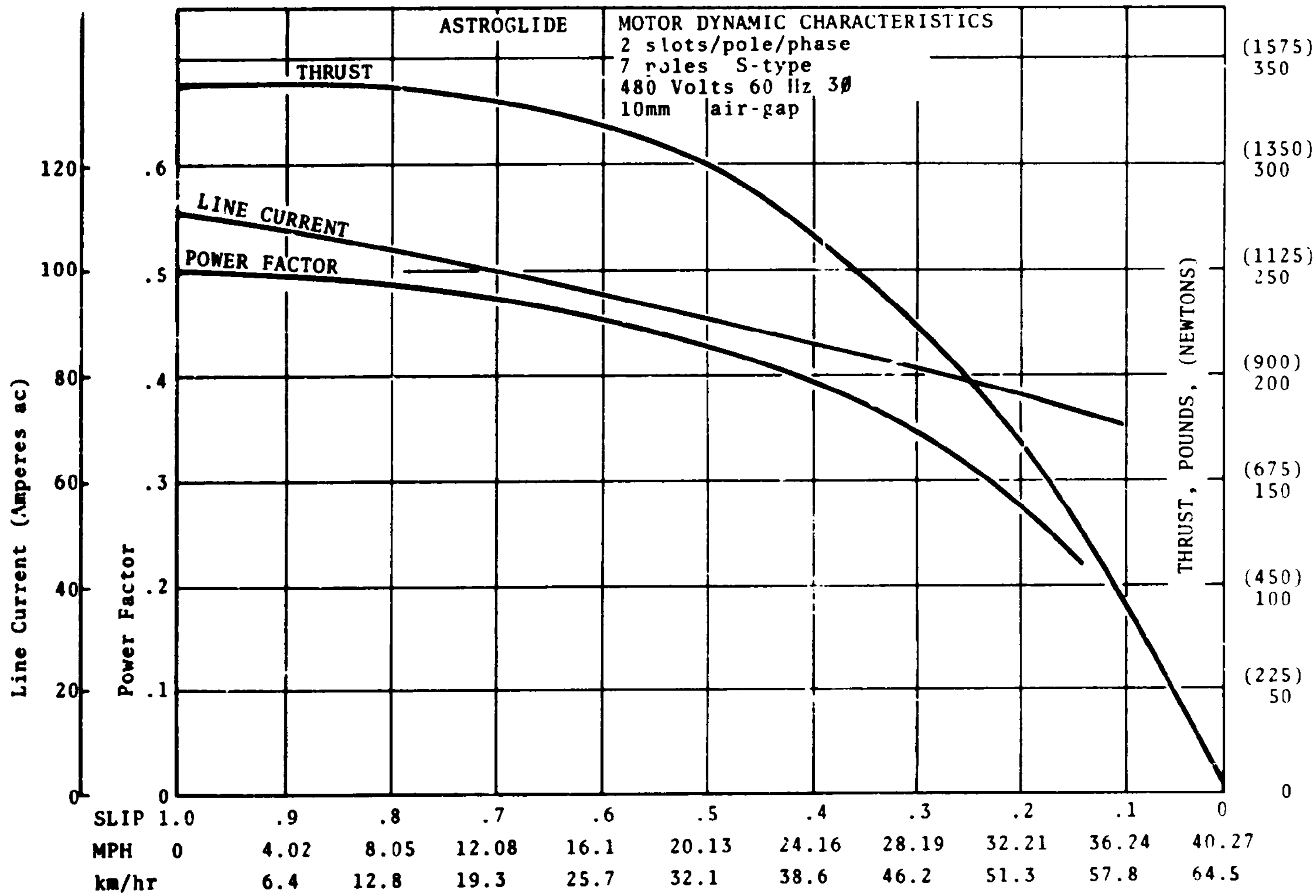

FIGURE 3.10.5 ASTROGLIDE LIM CHARACTERISTICS

km/hr)) on future applications. Thus in the Jetrail test system the prototype LIM Astroglide system operates between a slip of 0.63 (63%) and 1.0 (100%). This is a rather high slip factor leading to significant inefficiency.

It is important to note that the characteristics shown in the Figure 3.10.6 are for a single motor connected directly across the 3-phase input line. A motor connected this way will accelerate to an equilibrium speed at which point the thrust developed by the motor equals the thrust required to drive the load and to overcome losses. Motor speed will vary with loads. Even slight variations due to positive grade will result in reduced speed. Motor speed fluctuates slightly as the load varies.

Developed thrust is proportional to the square of the applied voltage, thus thrust may be regulated by controlling voltage, whereas motor speed may be regulated by controlling frequency. Motor saturation effects at low frequencies make simple constant-voltage variable-frequency control impractical. An efficient method of control is to vary both voltage and frequency thereby effecting control of the two parameters which govern system performance. Motor characteristics with a variable-voltage, variable-frequency inverter drive are shown in Figure 3.10.6. Peak thrust can be controlled over the entire speed range, and the motor can be operated at an efficient point on its characteristic curve. A drive system using frequency and voltage control exhibits higher efficiency and power factor than the voltage controlled system.

Inverter drives for ac motors are presently used in industrial applications, but are not common in transportation systems. The favored transit control scheme is the one used on Astroglide where applied voltage is the only controlled parameter. It is considerably simpler.

Voltage control is achieved with thyristors used in a phase delay switch to vary the amplitude of the applied motor voltage. The thyristors (SCR) are connected in series with the motor windings (Figure 3.10.7(a)). Figure 3.10.7(b) shows the sinusoidal outputs when the SCR's are full on. Figure 3.10.7(c) shows the output voltage when SCR turn-on is delayed by some phase angle α.

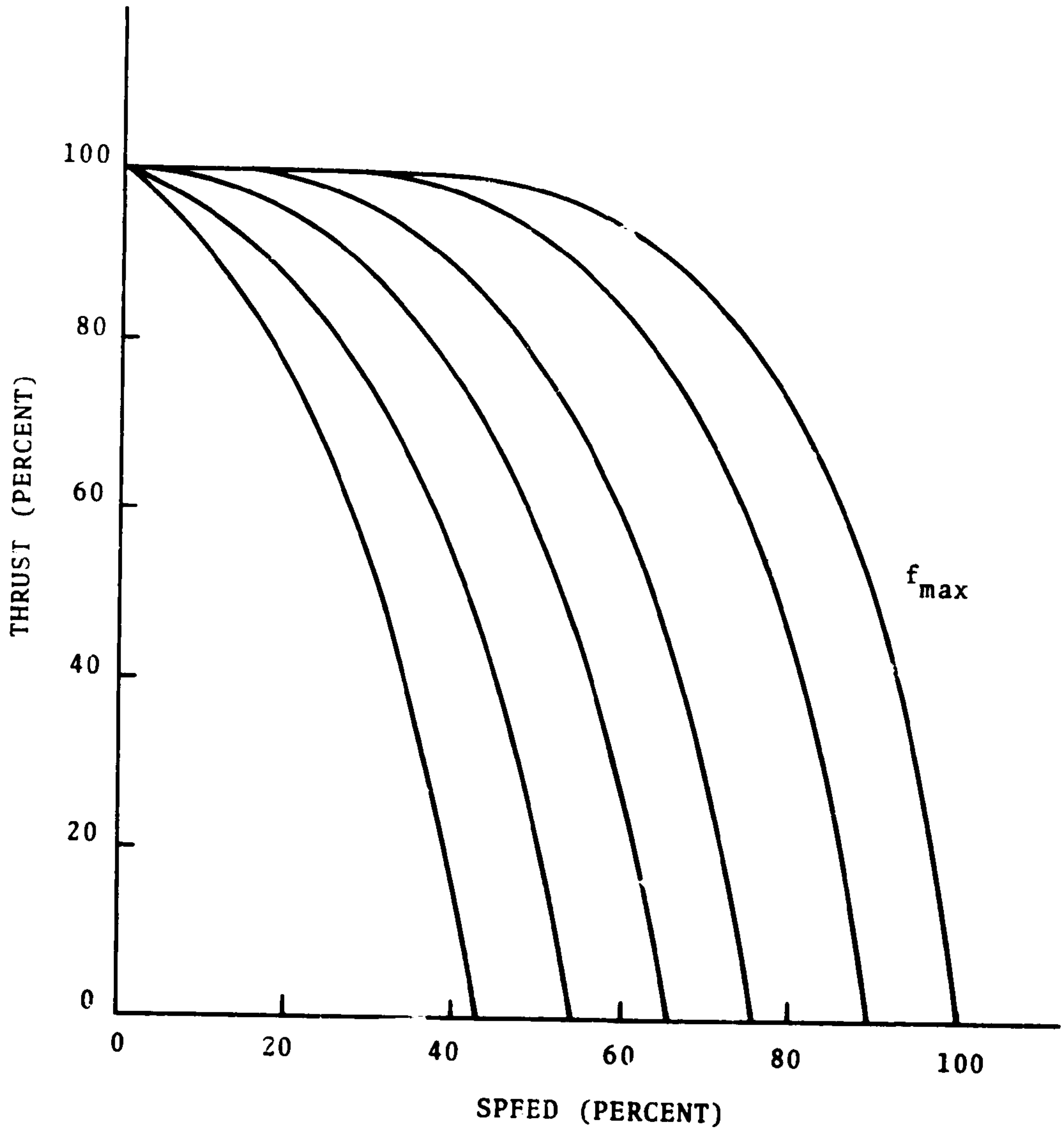

FIGURE 3.10.6 TYPICAL INDUCTION MOTOR CHARACTERISTICS WITH VARIABLE FREQUENCY AND VARIABLE VOLTAGE WITH CONSTANT VOLTS/HERTZ

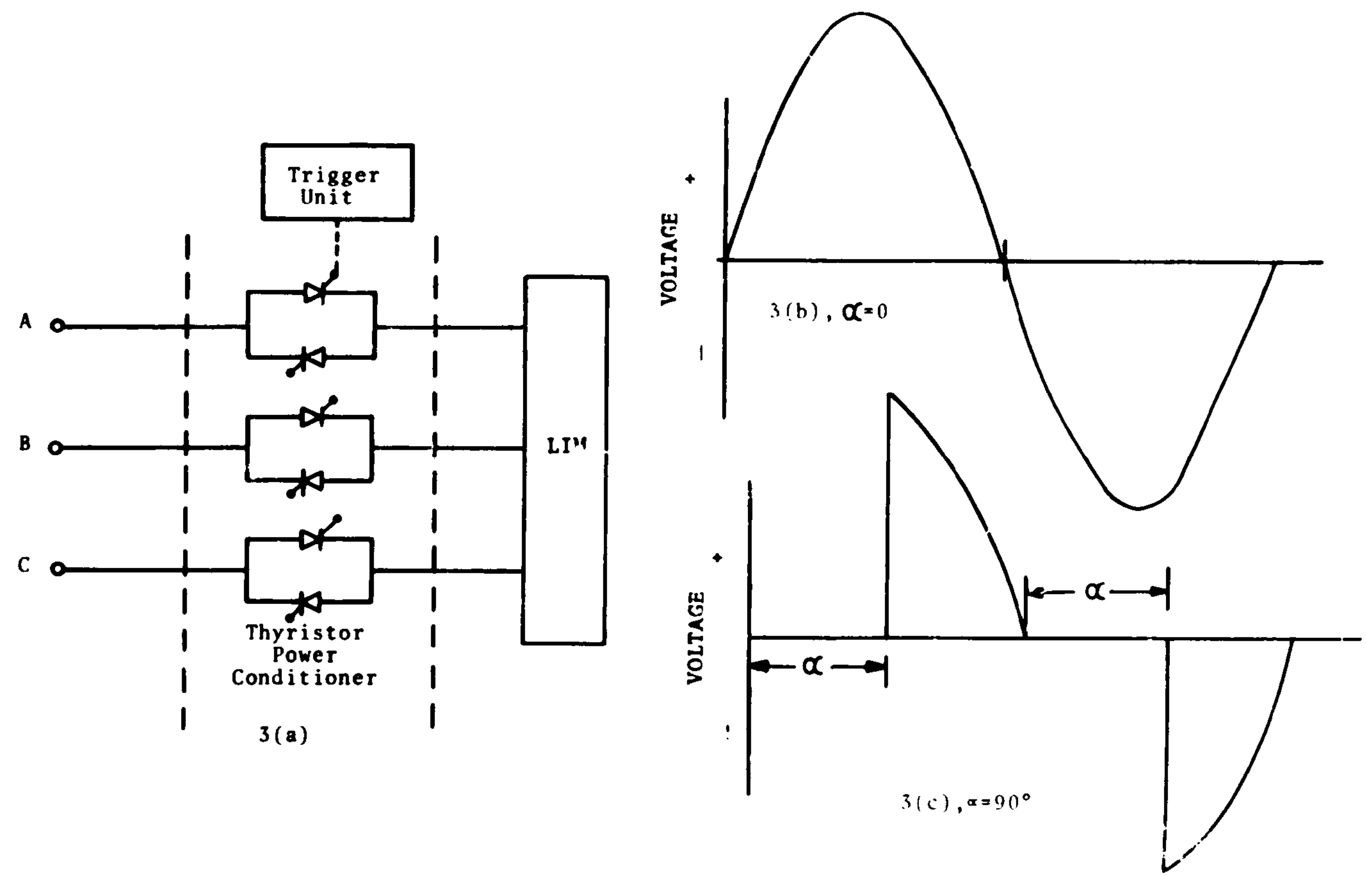

FIGURE 3.10.7 SCHEMATIC OF THYRISTOR POWER CONDITIONER

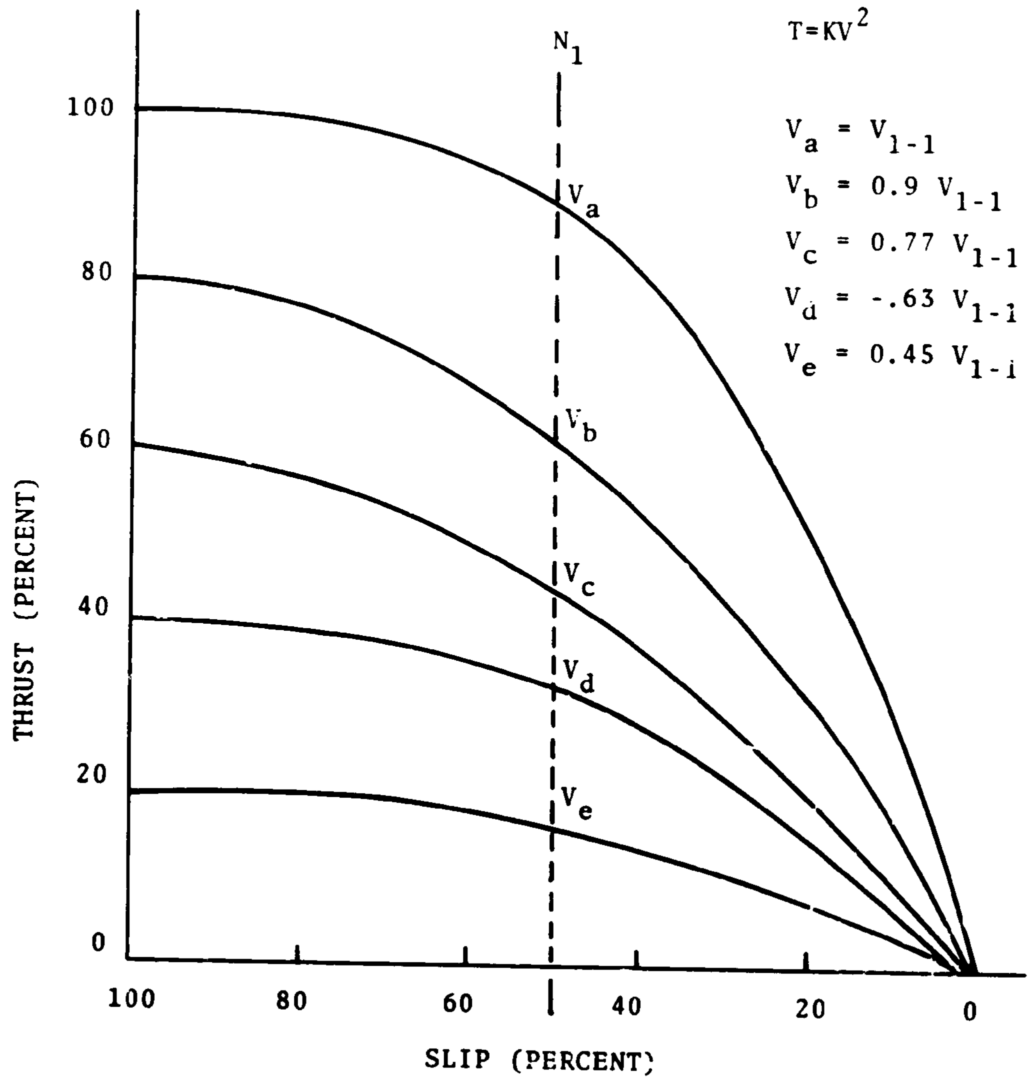

FIGURE 3.10.8 TYPICAL INDUCTION MOTOR CHARACTERISTICS WITH VARIABLE **VOLTAGE** CONTROL

Motor characteristics for a primary voltage control system are shown in Figure 3.10.8. These typical characteristics are shown as an example (ref. 2) and are not for the particular motors used on Astroglide. To maintain a constant speed, such as N_1, the SCR firing point would be advanced or delayed until the thrust developed by the motor equalled the thrust required to overcome the losses to operate at the controlled speed.

Phase-delayed thyristor turn-on and the wide air gap both contribute to a low power factor in the LIM system. Capacitors have been connected across the input lines to provide a source of leading reactive power to balance the system and thus improve the operating power factor. The motor excitation current is a lagging current and the capacitor current is a leading current; the resultant current circulates between the capacitors and the motor, but not through the input lines. The result is a lower system power factor.

LIM system braking is accomplished by reversing the motor connections at the drive thus providing a reverse thrust. The system at Jetrail uses contactors to accomplish the motor connection reversal, but solid state switches are being investigated. Solid state switches are both faster and quieter.

Emergency braking utilizes the same electromagnetic disc brakes as the Jetrail eddy-current clutch drive system and are actuated by the same functions. That is, they may be applied by depressing an emergency stop switch, or automatically by logic control or loss of power.

4. OPERATIONAL PERFORMANCE

The operational performance assessment of the Jetrail and Astroglide systems was based on observations, measurements, and analyses performed by the TSC assessment team as well as on data from Braniff and PRT Systems Inc. Because Jetrail was not in operational service at the time of this assessment, some kinds of performance data could not be collected, e.g., those relating to passenger capacity and system availability. Therefore, it was necessary to estimate some of the performance characteristics by analytical techniques.

Measurements of the propulsion systems of both Jetrail and Astroglide systems were made. The Jetrail propulsion performance characteristics are discussed in Section 4.2. Comparisons between the two systems are discussed in Section 4.9, Astroglide Operation. Measurement of noise as well as human factor parameters were also made. Ride quality measurements were made and the results are discussed in Section 4.4. The ride data and analysis are in Appendix E.

4.1 OPERATING DESCRIPTION

In order to conveniently describe the operation of the Jetrail system, a sequence of events during a trip will be analyzed for both low- and high-flow operation. A number of different scenarios each with specific initial conditions are described. Figure 4.1.1 is a schematic of the system depicting the four loading and unloading berths at stations A and B. The six wayside guideway switches providing access to the storage, baggage, and service loops are also shown.

4.1.1 Low-Flow Operation

When operating the system under low-flow conditions, the number of vehicles positioned at station A may be varied from one to four vehicles. The number of vehicles stored in the station B

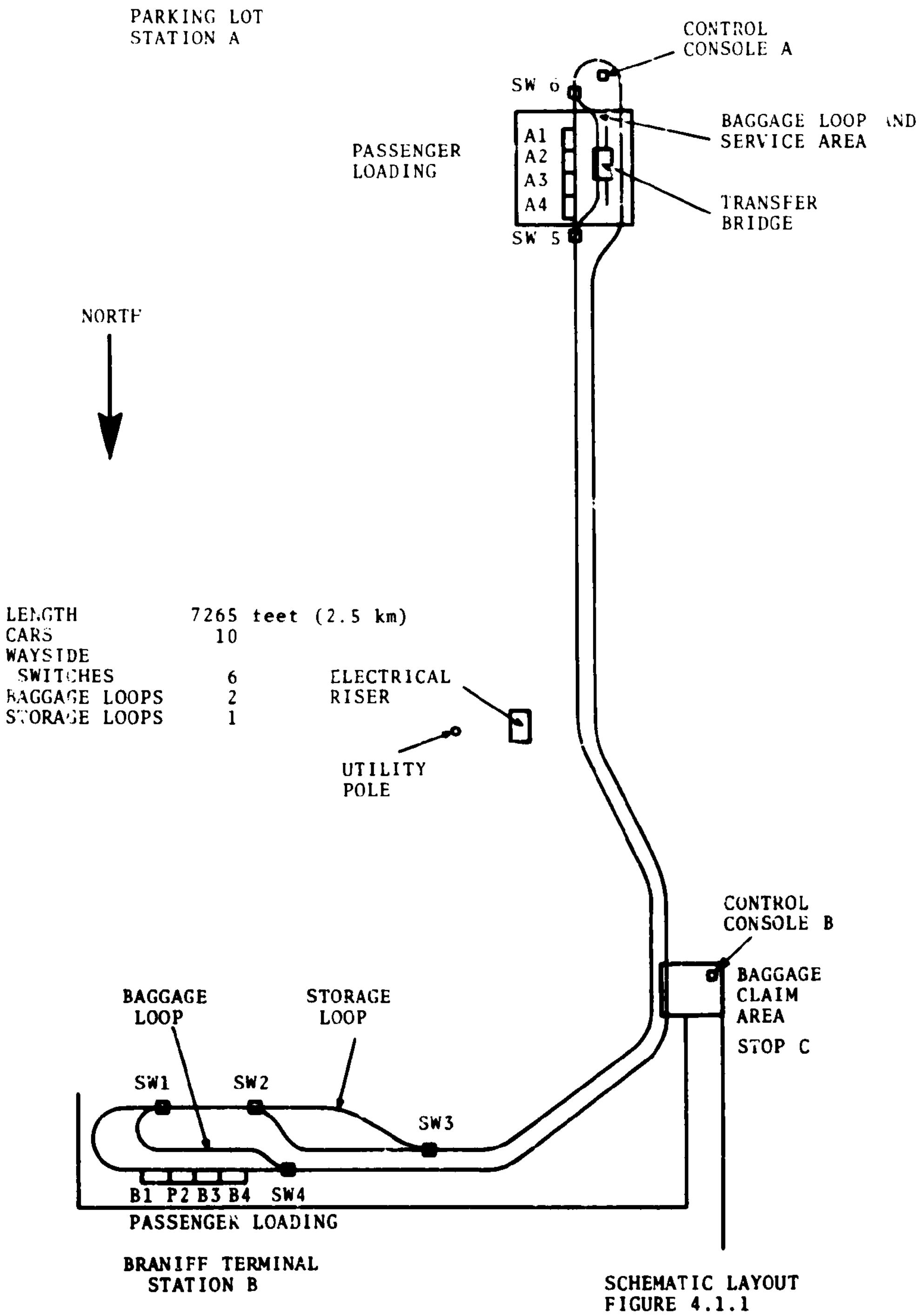

FIGURE 4.1.1. SCHEMATIC SHOWING LOADING BERTHS

storage loop may be varied from one to five. However, the number of vehicles in station B cannot be varied, i.e., one vehicle is maintained at station B. Specifically, the static conditions for low-flow operation locate four vehicles at station A, positioned at berths A1, A2, A3, and A4 and one vehicle at station B positioned at berth B4. Up to five vehicles are stored in the station B storage loop.

Scenario 1

At time t=0 seconds, the vehicle call button located at berth B4 is pressed by passenger "X". Station doors and vehicle doors at B4 open, allowing passenger "X" to enter the vehicle. Inside the vehicle passenger "X" presses a destination button (in this case, station A, the parking lot) and sits down.

At time t=20 seconds, station and vehicle doors at B4 close at which time the vehicle will be dispatched to station "A".

If a potential passenger "Y" had called for a vehicle at station "C", the vehicle with passenger "X" would slow to speed 1 and stop, admitting passenger "Y". The doors would remain open for twenty seconds - after which the vehicle would be dispatched to station "A".

Had there been no call for a vehicle at station "C", the vehicle would have slowed to speed 2, proceeded by station "C" and resumed speed 4 continuing to station "A'.

As the vehicle enters a track section approximately midway between stations C and A, the vehicle at berth A4 is dispatched, causing the vehicles at berths A3, A2, and A1 to move up one berth sequentially. This provides an empty berth (A1) for the vehicle arriving from B4. This action is timed to assure that berth A1 is clear to permit the arriving vehicle to enter berth A1 without delay.

Returning now to station "B" at time t=20 seconds, the instant the vehicle was dispatched from berth B4, a vehicle in the storage loop will be moved to berth B4.

The vehicle which was dispatched from berth A4, to allow the passenger to exit is enroute to station "B". When this vehicle's "T"-signal collector contacts the T-bar located prior to switch SW3 it will result in movement of the switch to the turnout position, routing the vehicle into the fifth position of the storage loop returning the system to the initial static condition.

The dispatching times noted, nominally 20 seconds, are all adjustable at the control consoles. It is of interest to note at this time that, under dynamic operating conditions, had a vehicle been downstream (beyond) switch SW3 when the vehicle at berth B4 was dispatched, no vehicle would have been called out of storage. Rather, the vehicle in motion downstream of switch SW4 would have moved toward berth B4 to fill the vacancy, stopping first at berth B1 if there was an indication of a party or a parcel in the vehicle.

Scenario 2

Assume the static operating conditions as outlined at the beginning of Scenario 1.

Passenger "Y" depresses the vehicle call button at station "C". A vehicle will be dispatched from berth B4 to station "C" (baggage claim). The vehicle will slow to speed 1, and stop at the station berth. Both vehicle and station doors will open to admit passenger "Y". After a timed delay (nominally 20 seconds), the vehicle and station doors will close and the vehicle will proceed to station "A". The system operations will then continue as outlined under Scenario 1.

Under dynamic operating conditions, had a vehicle already departed berth B4 when passenger "Y" depressed the vehicle call button at station "C", the vehicle in motion would still stop at station "C", provided it has not passed the track decision point. If the vehicle has passed this track decision point, the next vehicle at berth B4 would be dispatched to station "C".

Scenario 3

At time t=0 seconds, assume the static operating conditions as indicated in Scenario 1.

Passenger "Z" at station "A" desires to go to station "B".

The passenger depresses the vehicle call button located beside door A4. The vehicle and station doors will open allowing the passenger to enter the vehicle. Inside the vehicle, passenger "Z" will press the destination button for the "Braniff Terminal" (station B).

At time t=0 seconds, the vehicle will be dispatched from berth A4 to station "B".

The vehicle arriving at station "B", with either a preselected destination or an indication of a party or a parcel in the vehicle (sensed by the floor mat switch or seat switches), will slow through speed 2 to speed 1 and stop at berth B1. The vehicle and station doors will open, allowing passenger "Z" to exit the vehicle. When the vehicle stops at B1, dispatching of the car at berth B4 will be initiated as the system begins to re-establish the static condition.

Returning to station "A" (Scenario 3) at t=20 seconds, when passenger "Z" caused the vehicle at berth A4 to be dispatched, the vehicles at berths A3, A2, and A1 will move up one berth each, sequentially. This action will leave berth A1 free to accept the vehicle dispatched from B4. After passenger "Z" had debarked at door B1, the vehicle which carried him from A4 would move up to berth B4 and stop with vehicle and station doors closed.

4.1.2 High-Flow Operation

A key switch located at station "A" is used to select either the low-flow or high-flow mode of operation. Operation of the system in the high-flow mode will dispatch any vehicles located in the "B" storage loop to station B. The vehicles will position themselves at berths B4, B3, B2, and B1. Any other vehicles in the "B" station area will be blocked out upstream at intervals of one track section.

Vehicle and station doors at berths B4, B3, and B2 will be opened, permitting passengers to enter any of the three vehicles docked at these berths. After a nominal timed delay of twenty seconds the vehicle and station doors at berth B4 will close, and the vehicle will be dispatched to station "A". Twenty seconds later the vehicle at berth B3 will be dispatched, followed by the dispatching of the vehicle at berth B2 in another twenty seconds. An elapsed time of sixty seconds permits dispatching of three vehicles.

At this time, any vehicles positioned at B1 or blocked upstream will move forward, docking at all four doors (provided four or more cars were available) with door B4 being always utilized first. Of course, any vehicle with a preselected destination or indication of a party or a parcel in the vehicle will stop at berth B1 for offloading prior to moving forward to berths B4, B3, and B2.

The operation at station "A" in high-flow mode is identical to that described for station "B". Station "C" stops may be eliminated in the high-flow mode at the control console.

After the high-flow mode has been established, 12 minutes are required to re-establish the low-flow condition. The flow mode key switch at station "A" of course would have to be manually switched to the low-flow position to commence this re-establishment.

4.1.3 Sequential Starting

If the Jetrail system were operating in the high-flow mode when the main power (480 V) was interrupted, a large transient overload would occur when power was restored. This transient is caused by the in-rush of exciting current to the motors, transformers, and clutch-brake coils and could involve all 8 cars simultaneously.

By delaying the application of power to the main loads in each vehicle the peak starting transient load would be reduced to a value which would not overload the power source. A timer is included in each vehicle control circuit, so that only the main power transformer currents would initially load the power source.

The timer, set to a different value in each vehicle, completes its delay and closes the circuit to the other vehicles' loads, including the motors. Thus, the start-up of each vehicle would occur in a sequence over a period ranging from 2 to 20 seconds.

4.2 PERFORMANCE CHARACTERISTICS

4.2.1 Velocity Characteristics

The velocity profile for a single Jetrail vehicle trip around the 1.38 miles (2.2 km) of guideway is shown in Figure 4.2.1. The relation of each point on the velocity profile to the guideway layout is shown in Figure 4.2.2. This velocity differs from a normal operational revenue service profile in two respects:

1. The vehicle experienced an intentional emergency stop at point C of the profile to evaluate the vehicle deceleration characteristics.
2. The vehicle experienced a normal service-brake stop at point F, midway between the baggage station C and the parking lot station A due to a short across the Z-bar.

The shorted Z-bar is interpreted by the control system as an occupied block (quasi-occupied) and hence brings the vehicle to a normal stop. As this fault was present throughout our testing period, it served as a test of the collision avoidance control system, and it worked successfully for some 40 test cycles. The manual mode of operation was used to by-pass the blocked section. It should be noted that, since the system was not operational, maintenance and repair were minimal - bar shorts were not corrected, trolley grease was not applied, and power and signal rails were not replaced. This resulted in unprogrammed stops and intermittent power losses appearing as downward spikes in Figure 4.2.1 corresponding to rapid decreases in velocity. Furthermore, the galvanized power and signal rails have reached their useful life and need to be replaced.

To show how the velocity profile varied along the guideway refer to Figures 4.2.1 and 4.2.2. From the Braniff terminal, station B (point A) the vehicle accelerated to speed 2 followed by a power drop-out and continuing to speed 4. It then slowed to

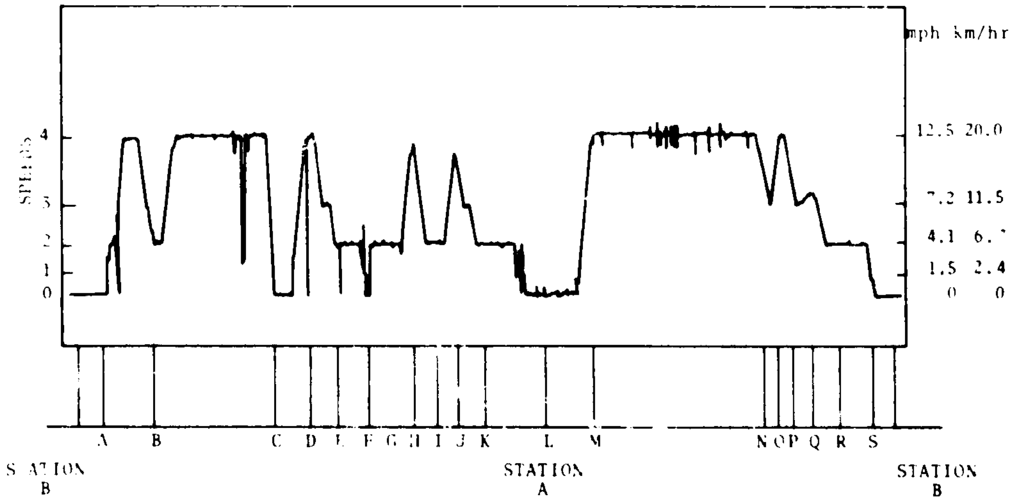

FIGURE 4.2.1. VELOCITY PROFILE (FROM A RECORDING)

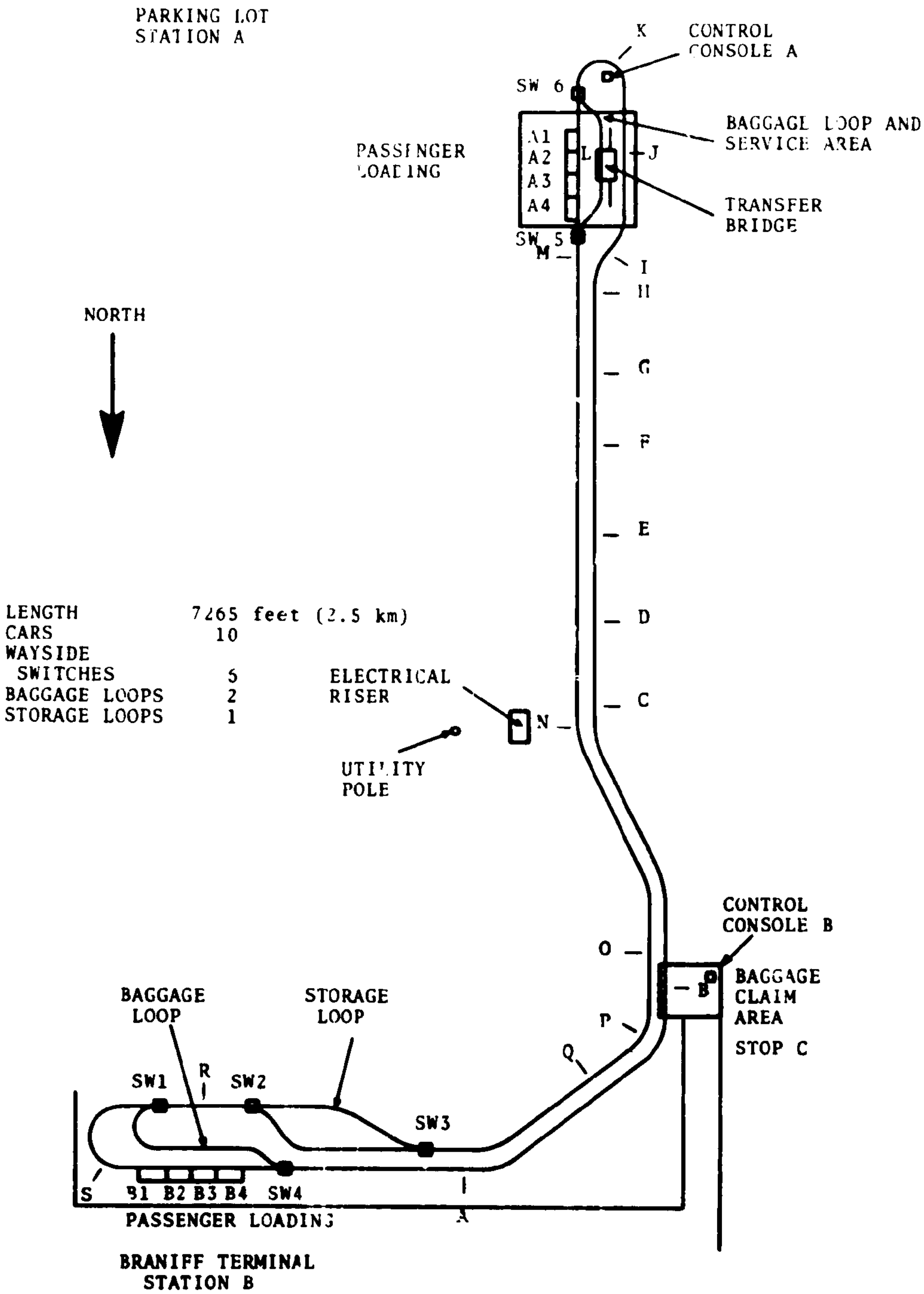

FIGURE 4.2.2. SCHEMATIC SHOWING VELOCITY PROFILE

speed 2 while passing by the baggage station C (point B) and then back up to speed 4. This was followed by a power drop-out and a deliberate emergency stop (point C). The vehicle was again accelerated to speed 4. It then encountered the quasi-occupied block where it came to a programmed stop (points D through F). The remaining points can now be followed to complete the loop to station B. This represents an operational run with the exceptions noted.

To relate the commanded vehicle velocity profile to actual vehicle velocity, time-distance measurements were made. These are shown in Table 4.2.1 for both the Number 4 Jetrail eddy-current transmission (ECT) vehicle and the LIM powered Astroglide vehicle (converted Jetrail No. 10). The eddy-current transmission vehicle velocity varied from 11.0 to 12.5 mph (17.5 to 20 km) on the 4% upgrade and downgrade slopes respectively. Velocities in the other speed commands did not vary. The LIM vehicle, on the other hand, did not measurably vary on up or down grades.

TABLE 4.2.1. ACTUAL VELOCITY AS A FUNCTION OF COMMAND SPEED

Command Speed	ECT Up-Grade (mph), (km/hr)	ECT Down-Grade (mph), (km/hr)	LIM Up/Down-Grade (mph) (km/hr)
1	—*	—*	2.1(3.4)
2	4.1(6.6)	4.1(6.6)	4.7(7.5)
3	7.2(11.5)	7.2(11.5)	7.5(12.0)
4	11.0(12.1)	12.5(20.0)	15.5(25.0)

*Not available.

Velocity in each speed mode was commanded from the wayside and was regulated by an on-board controller. Velocity was not the measured parameter, rather tachometer voltage was. Therefore, velocity in any speed mode varied from vehicle to vehicle. In the case of the Jetrail-ECT-test vehicle, there is a significant difference (26%) from the command speed 4 (15 mph)(24 km/hr).

4.2.2 Acceleration Characteristics

The acceleration characteristics for the eddy-current-transmission (ECT) and LIM vehicles are shown in Figure 4.2.3. These accelerations were obtained from an analysis of voltage vs. time measurements of both the Jetrail ECT and Astroglide LIM vehicles. Voltage vs. time histories as well as the details of the derivation of these accelerations and decelerations can be found in Appendix A. The initial acceleration of the LIM and Jetrail ECT vehicles were 0.37 g's (11.8 ft/sec^2, 3.2 m/sec^2) and 0.12 g's (3.88 ft/sec^2, 1.18 m/sec^2), respectively.

These accelerations are normal service accelerations. The Jetrail ECT vehicle accelerations are comparable to Rapid Transit vehicles with standing passengers (0.1 to 0.15 g's). The LIM vehicle on the other hand, exceeds even the specifications for the Advanced Group Rapid Transit System (0.2-0.25 g's sustained). However, the 0.37 g's acceleration has a duration of approximately 0.35 seconds and therefore should not be classed as a sustained acceleration. It is within the 16-minute boundary for Fatigue Reduced Proficiency (working environment) Level as specified in ISO 2631. Beyond this point the acceleration is approximately 0.1 g and well within sustained acceleration limits. Interestingly enough, this high-acceleration, short-duration pulse was perceptible to the test team, but did not result in any appreciable body acceleration.

It is hypothesized that this high-acceleration pulse is a result of the LIM vehicle transition from a top supported position to a levitated position. That is, when the vehicle is attracted to the guideway rail, it partially unloads the upper suspension wheels, prior to its making contact with the gap-maintaining lower guide wheels. During this interval the vehicle is without rolling-friction forces thereby resulting in a higher acceleration for a short duration. When the lower guide wheels come in contact with the bottom of the guideway rail, a rolling-friction force is again developed which lowers the acceleration.

Emergency and service braking decelerations were also obtained

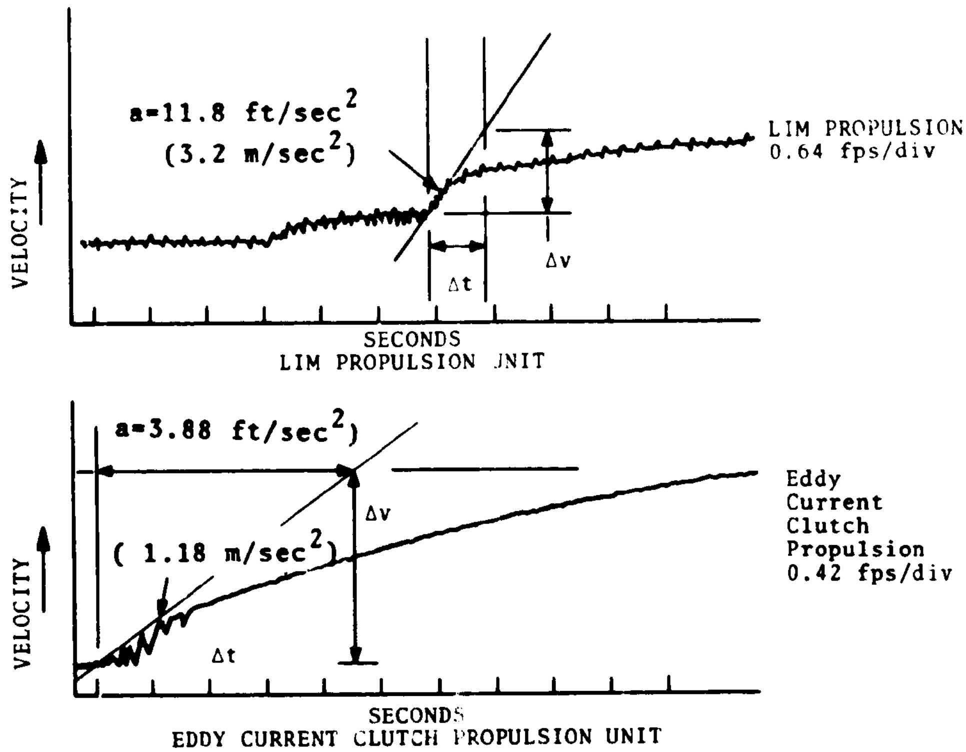

FIGURE 4.2.3. COMPARATIVE ACCELERATIONS (FROM A RECORDING)

from the measured voltage vs. time data. Normal service braking produced a deceleration of 0.03 g's (0.94 ft/sec^2, 0.31 m/sec^2) in the Jetrail ECT vehicle Emergency braking resulted in 0.081 g's (2.62 ft/sec^2, 0.87 m/sec^2). These are well within acceptable limits for standing passengers (0.15 g's longitudinal).

The sustained emergency deceleration for the LIM-propelled vehicle was determined to be 0.035 g's (1.17 ft/sec^2, 0.39 m/sec^2). Initially, the deceleration rose to a value of 0.35 g's (11.2 ft/sec^2, 3.7 m/sec^2) for a duration of approximately 0.4 seconds and then dropped back to the sustained 0.035 g value. This initial deceleration which occurs at the beginning of each deceleration phase is not a function of brake application alone but is also due to the phase-off of the power conditioner resulting in a momentarily high-loss of kinetic energy.

Since only velocity data was measured, it was not possible to resolve jerk (da/dt).

4.2.3 Propulsion System Characteristics

The Jetrail eddy-current transmission vehicle power characteristics are similar to those of any induction motor operating directly across power input lines. Voltage and current at the motor remain sinusoidal, therefore, there is no distortion reactive power. The system operating power factor is reasonably high, near 0.7, for all running load conditions.

Measurements were made of the Jetrail ECT system. Detailed data are shown in Appendix A. The instrumentation and measurement procedure is discussed in detail in Appendix A. A summary of this data is presented in Table 4.2.2. This data was obtained from a vehicle moving on the up-grade section of guideway between the Braniff terminal, station B, and the baggage station, C. Power levels for the downhill return trip are slightly lower.

TABLE 4.2.2. JETRAIL EDDY-CURRENT TRANSMISSION VEHICLE POWER CHARACTERISTICS

State	Current (ARMS)	Apparent Power (kVA)	Active Power (kW)	Reactive Power (kVAR)	Power Factor
Standby	4.18	3.5	0.57	1.2	0.16
Acceleration (1)	67.0	55.5	42.2	29.5	0.76
Speed 2 (4.1 mph)	25.1	20.8	13.7	10.6	0.66
Speed 3 (7.0 mph)	27.2	22.6	16.0	11.8	0.71
Speed 4 (12.3 mph)	29.3	24.3	17.1	11.8	0.70
Brake (2)	15.7	13.0	2.3	11.2	0.17

NOTE:
(1) Peak value levels decrease linearly to cruise levels.
(2) Continuous during braking.

Current waveforms were observed for one complete trip around the guideway and were found to be sinusoidal for all operating conditions. This is indicative of a system without harmonics and distortion power. Because there is no waveform distortion, all reactive power is displacement-reactive power. Therefore, the VAR transducer output is a true indicator of the total system reactive power.

The standby state exists when the motor is off and power is drawn only for the vehicle control and auxiliary power systems. The measured current is single phase. Although the power factor is low (0.16), the input levels are also low thereby resulting in a negligible impact on system power characteristics.

Peak active power is drawn during acceleration from a standstill at which time the vehicle requires 42.2 kW. At this time reactive power is also at a peak (25.5 kVAR), as well as apparent input power (55.5 kVA) and the power factor (0.76). As the speed increases from speed 2 to 3 and then to 4, the active power increases from 13.7 to 16.0 to 17.1 kW. This is an approximate increase in active power of about 3.4 kW. Apparent power increased similarly, ranging from 20.8 to 24.3 kVA. However, the reactive power and the power factor for each of these states remain nearly constant. The reactive power and power factor range between 10.6 to 11.8 kVA and 0.66 to 0.71 respectively.

Profiles of RMS current and reactive power are similar to active power profile except during deceleration when the eddy-current brake is applied. In this state the vehicle's kinetic energy is absorbed by the eddy-current brake while the motor is idling in standby. The active power consumed is divided into approximately 0.5 kW of auxiliary power and 1.7 kW of eddy-current brake power. The 11.2 kVAR of reactive power is supplied for motor excitation. Power factor under this condition is less than 0.2. Measurement of input feed voltage characteristics, operating power consumption, operating power demand, and operating power profiles, and analysis of over-voltage and over-current protection were not made since the system was not in operational use. These characteristics are design specified to a given application.

4.3 SYSTEM DEPENDABILITY AND MAINTAINABILITY

The Jetrail operational data used in the calculation of reliability, maintainability, and availability were not recorded in a manner which would facilitate measure of these performance parameters. These reliability, maintainability, availability, and dependability measures were estimated from maintenance service sheet data on four of the ten cars in the Jetrail fleet over two one-year periods (1970-71, 1972-73). The maintenance sheets used report the vehicle brought in for service, the problem, repairs made, and disposition of the vehicle. The vehicle repair time was not recorded nor was the time of failure or the vehicle and system restoration times. Further, guideway and central control system failures were reported on a maintenance sheet with the specific vehicle experiencing a delay. To further complicate this, vehicle mileage or operating hours at the time of failure were not recorded. Therefore, a number of assumptions were necessary in order to estimate the system dependability. The assumptions were based on the best available information supplied by Braniff. Due to these assumptions and the availability of only limited data these calculations are presented here only as possible indicators of system performance and should not be taken as a definitive reliability and maintainability study based on adequate statistical samples.

The data, from the maintenance service sheets, was first classified according to the type and number of failures occurring, a failure being any occurrence causing a system or vehicle breakdown that would prevent the system from completing its function - transporting passengers between stations in a timely manner. Only failures of operational equipment contributed to failure rates. Because repair and restoration times were not available, and because spare vehicles were used for replacement, failures were not further classified. This classification of failures by car is presented in Appendix B.

The information was then used to determine a failure rate, λ (failures/hour) and a Mean Time Between Failures, MTBF (hours/failure) for each car. The latter is summarized in Figure 4.3.1

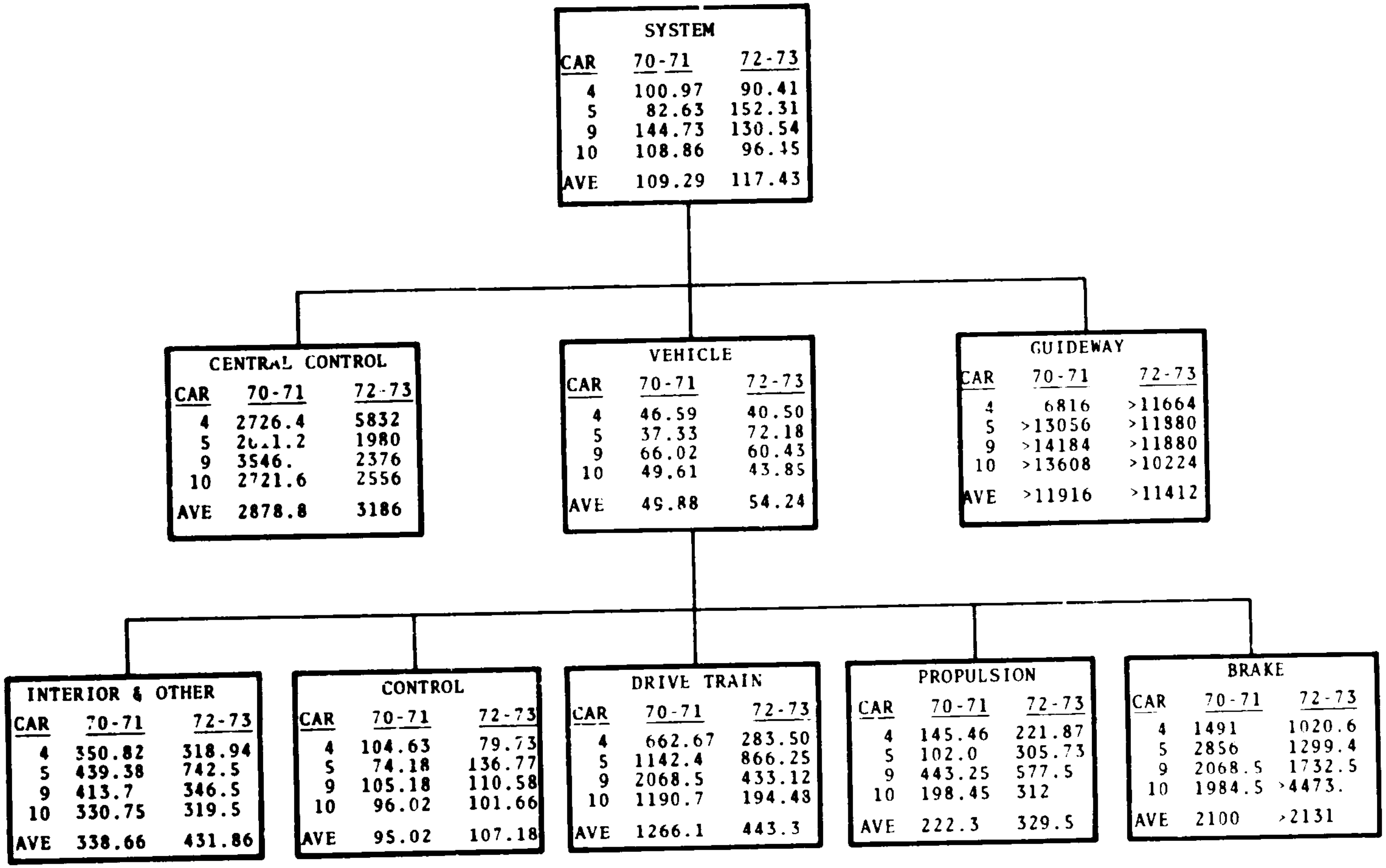

FIGURE 4.3.1. ACTUAL MEAN TIME BETWEEN FAILURES

for each one-year interval. The MTBF of each of the four cars as well as the average MTBF of these four is presented in the system level block. A breakdown of the MTBF's for the three major subsystems, central control, vehicle, and guideway are shown at the next level down. A breakdown of the vehicle subsystem is also included to indicate the relative failure rate of these components. The average MTBF's of system are 109.3 and 117.4 (hours/failure) for the 1970-1971 and 1972-1973 time spans. The overall average is 113.3 (hours/failure). These MTBF's are based on a system with a single central control and guideway subsystem and a single vehicle. Although it is perhaps unusual to relate the failures of a single vehicle to guideway and central command and control system failures, all failure data was reported relative to the vehicle in operation at the time of the failure.

In determining the Mean Time Between Failure, it was assumed that each vehicle operated 10.5 hours a day, whereas the guideway and central control subsystems were based upon 24 hours a day. The number of hours each vehicle operated daily was arrived at by first taking into account the distribution of arrival and departure of Braniff flights. This provided an estimate of passenger flow during the day. Second, the number of vehicle trips necessary to transport this number of passengers including the passenger loading was determined. Finally, the individual vehicle trip time was determined and multiplied by the number of trips to obtain the total vehicle operating time for the day. Estimates for empty vehicle movement were also included. The demand responsive nature of the Jetrail system as well as the existence of spare vehicles was taken into account in determining average individual vehicle operating time per day. A detailed explanation is provided in Appendix C.

The Mean Time Between Failures for central control and guideway is quite large compared to the mean time between failures of an individual vehicle system. Within the vehicle subsystem, control and propulsion failures occurred most frequently. Figure 4.3.2 shows the reliability of the system based on 24 hours of operation. The central control and guideway operations continuously

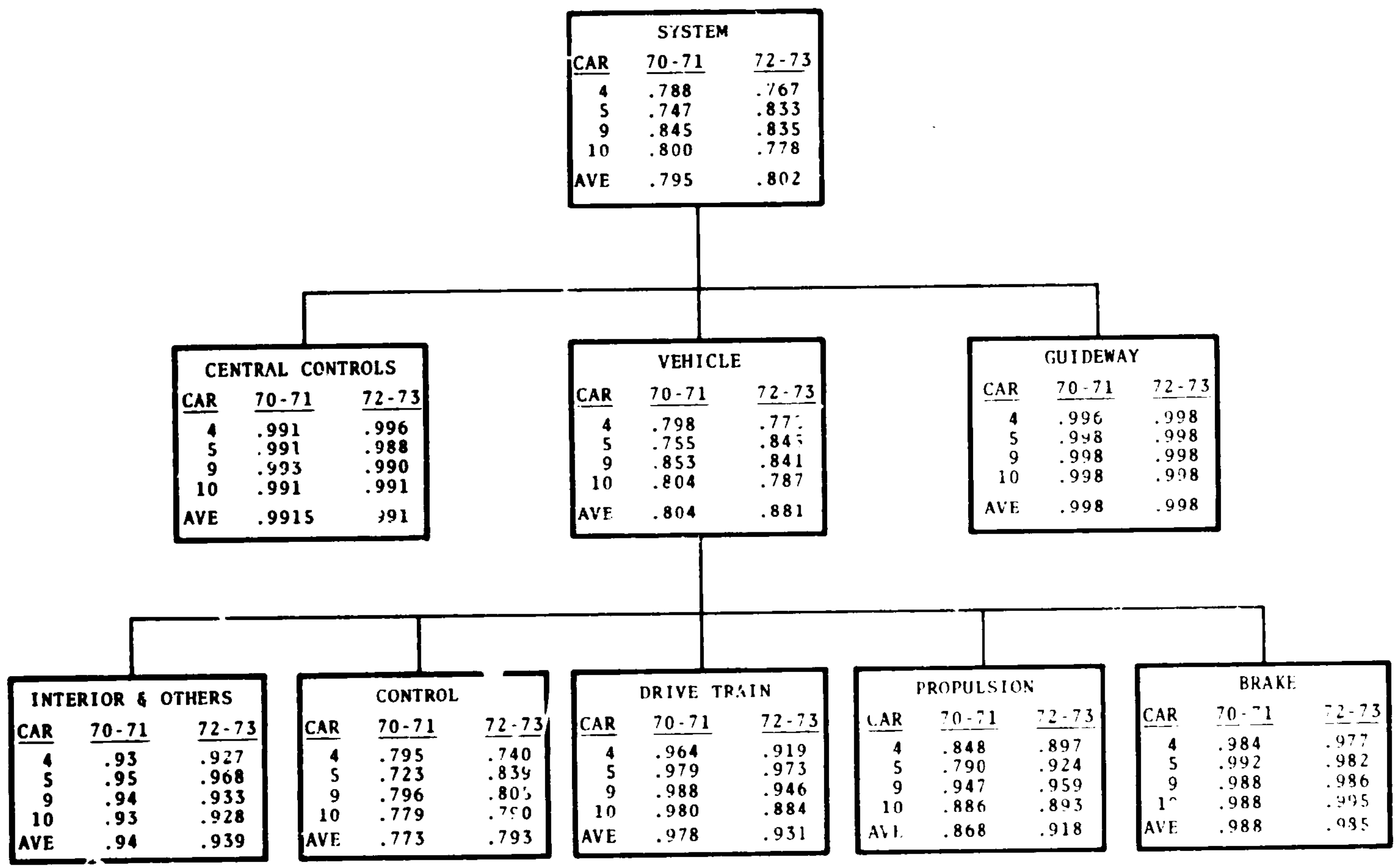

FIGURE 4.3.2. JETRAIL RELIABILITY

(24 hours per day) whereas each vehicle has been estimated to operate only 10.5 [illegible] of the 24 hours. These figures are also based on a single vehicle operating in the system. The guideway, central control, and individual vehicle reliabilities were based on an exponential distribution and determined by the equation $R = e^{-\lambda t}$. Although the analysis was made with very little data, it nonetheless provides an indication that the Jetrail system has very reliable central control and guideway subsystems, and considerably lower vehicle subsystem reliability.

4.3.1 Reliability

The three major subsystems of the Jetrail system are the central control (wayside vehicle velocity control), guideway, and vehicles. By calculating the reliabilities of these three components for a specified period of time and taking the product, Jetrail system reliability can be determined. The individual major subsystem reliabilities can be found by using the equation $F = e^{-\lambda t}$, λ being the failure rate (reciprocal of MTBF). The failure rate (λ) may be obtained from Figure 4.3.1 for the central control and guideway. However, the vehicle system MTBF must be determined in a different manner due to the number of vehicles in the system.

The vehicle subsystem consists of ten vehicles, 8 active and 2 spares. The system is considered to be performing satisfactorily when the allowable maximum of 8-vehicles are available for operation. Since quick replacement of vehicles is possible, two vehicle failures can occur without vehicle system degradation. Thus, when less than eight vehicles are operational the system is degraded, i.e., it carries fewer passengers. Vehicle subsystem degradation (a failure) occurs when a spare is not available to replace a failed vehicle. That is, when a third vehicle fails before one of the first two failed vehicles is repaired, it is considered a failure. It therefore follows that although the average individual vehicle MTBF is approximately 52 hours (based on 10.5 vehicle operating hours per day), vehicle subsystem MTBF is much higher due to the operational policy of having spares available.

A GPSS (General Purpose Simulation System) Model was developed to approximate the vehicle subsystem performance characteristics, MTBF. The model randomly selects failures in accordance with given failure distributions. The model assumes a system where 3 vehicles are in demand at all times with 2 spares available at the start (the cases of 1 and 3 spares were also considered for comparative purposes). This corresponds to the high-flow case during rush hours.

The mean time between failures for individual vehicles is assumed to be normally distributed with a mean of approximately 52 vehicle-operating hours (refer to Figure 4.3.1 for vehicle MTBF) and standard deviation of approximately 12 vehicle-operating hours (based on the sample of 8 sets of data). It is also assumed that the time to remove a failed vehicle and replace it with a spare is exceedingly small and constant (Braniff estimates 6 minutes for this function). The Mean Time To Repair (MTTR) a vehicle is considered to be exponentially distributed with a mean of 1 hour. This will return repaired vehicles to the system with times ranging from 1 minute for small repairs to 8 hours for large jobs. The simulation output includes the total number of individual vehicle failures that occurred during the simulation run as well as the number of times the vehicle subsystem was degraded. The simulation was run twice - once for 1.0 million vehicle-operating minutes (16,666 vehicle-operating hours of 3.5 years), and once for 500 thousand vehicle-operating minutes (8,333 vehicle-operating hours or 1.75 years). Using the results, the average MTBF for the vehicle subsystem was found to be 610 vehicle-operating hours. It is important to remember that each of the ten vehicles operates only 10.5 hours per day. This gives a total of 105 vehicle-operating hours per day. Since the maximum number of vehicles allowed on the guideway at any time is 8, the simulation must run for approximately 13 hours to achieve the desired 105 vehicle-hours of operation (8 vehicles x 13 hours) and simulate a day.

Table 4.3.1 shows the number of vehicle subsystem failures based on the number of spare vehicles available. As indicated, the number of spares greatly influences the number of failures observed. The case with 8 vehicles and 2 spares is representative of Jetrail. This case, with 25% spares, constitutes a relatively high spares-to-equipment ratio compared with more common ratios of 5-10%.

TABLE 4.3.1. VEHICLE SUBSYSTEM FAILURES AS A FUNCTION OF SPARES

t (min)	8 Vehicles 0 Spares	8 Vehicles 1 Spare	8 Vehicles 2 Spares	8 Vehicles 3 Spares
500,000	1265	145	13	0
1,000,000	2561	321	29	0

There is a dramatic decrease in the number of failures as a function of increasing spares, indicating the success of this operational policy. In the 500-thousand-minute case with 1 spare (12.5% spares-to-equipment ratio) the failures decreased by about a factor of nine from the case with no spares. With 2 spares the decrease is greater than an order of magnitude as compared to the one-spare case or about two orders of magnitude with respect to the case with no spares. Similar reductions are realized for the 1 million-minute case. (Figure 4.3.3.)

The Jetrail system reliability was obtained by determining the reliabilities of the three subsystems comprising the system and taking the product. Table 4-3-2 shows the total system reliability for T days using the equation $R = e^{-\lambda t}$. The failure rates for the central control and guideway are determined by averaging the respective MTBF's shown in Figure 4-3-1 and taking the reciprocal (λ = 0.00032 for central control and λ = 0.0000857 for guideway, based on a 24-hour day). Using the MTBF of 610 hours obtained from the simulation, the failure rate for the total vehicle subsystem of 8 vehicles and 2 spares is 0.00163, based on a 10.5-hour day.

Table 4.3.2 indicates that Jetrail system reliability is relatively high (at least 97% reliable after 24 hours). In reality, at some times of day not all 8 vehicles are in demand (e.g., early morning hours) therefore, these reliability measures are "worst case" estimates. Furthermore when failures do occur, less than 8

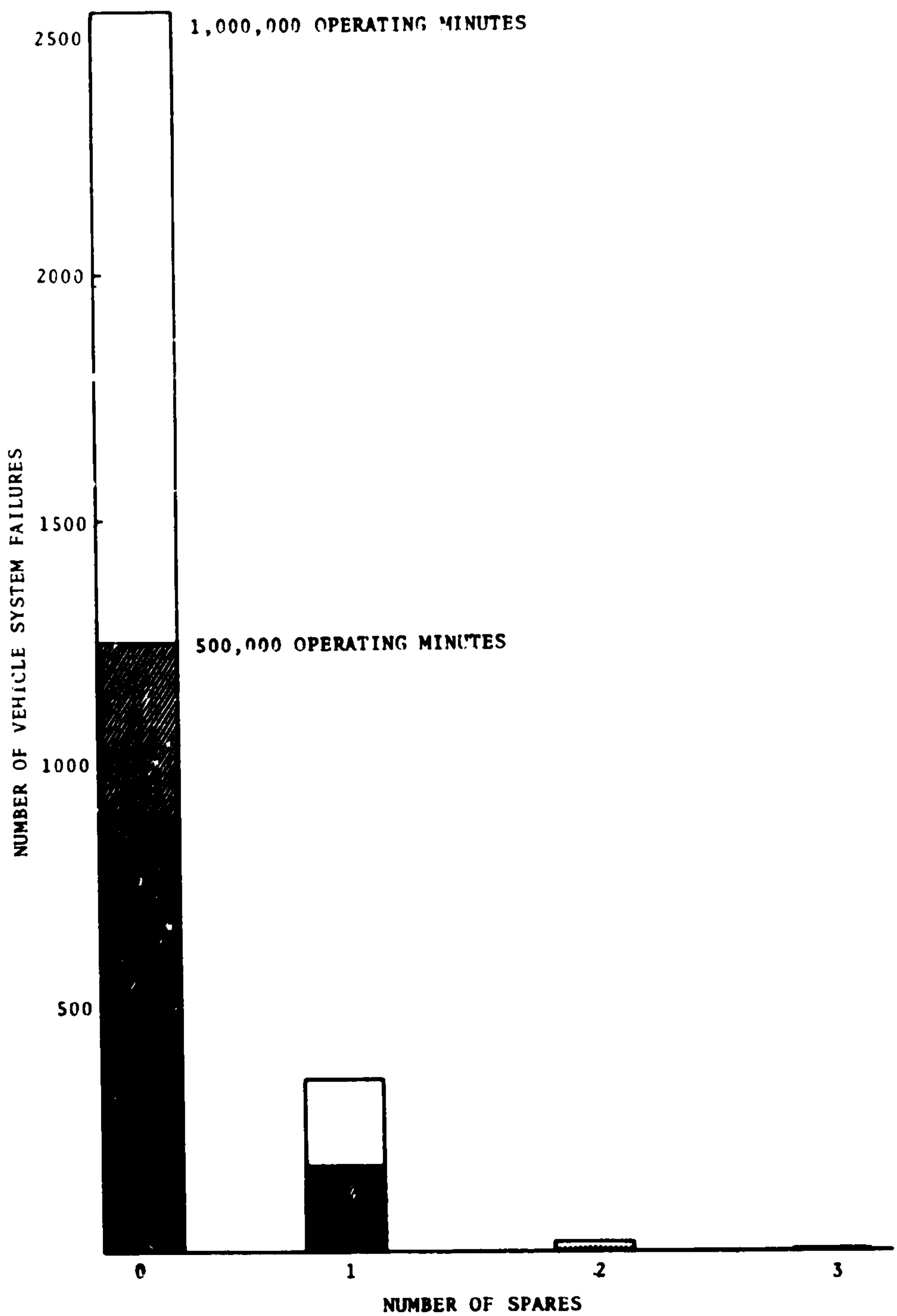

FIGURE 4.3.3. FAILURES VERSUS SPARES (SIMULATION)

TABLE 4.3.2. SYSTEM RELIABILITY

T (day)	Central Control	Vehicle System	Guideway	System
1	0.992	0.983	0.998	0.973
2	0.984	0.966	0.996	0.939
3	0.976	0.950	0.994	0.921
4	0.968	0.933	0.992	0.896
5	0.961	0.917	0.989	0.872

vehicles will be available for operation, thus the system would remain operational but in a degraded state (i.e., without the ability to carry the high-flow load). During non-rush hours reliability will be even higher. Once again, these reliabilities were determined on a very limited sample of data and are only "ballpark" estimates of actual system performance.

4.3.2 Availability

System availability is defined as the ratio of total uptime to total uptime plus downtime. For both simulations, system availability was approximately 0.9982. These measures agree with Braniff estimates of 0.997 availability. From the data, therefore, there is an indication that the system will be available when called upon about 99.7% of the time.

For the simulation lasting 500-thousand minutes, the system was in a "failed" status 13 times. Each failure lasted 56.3 minutes. Availability, therefore, is calculated to be 0.9985 for this case.

For the simulation lasting 1 million minutes, 29 failures were encountered lasting 68.2 minutes on the average. Total downtime for this case, therefore is approximately 1977.8 minutes. Availability for this case was determined to be 0.9980. The average availability of the system as determined through the simulation is 0.9982.

4.3.3 Maintainability

Operationally it was determined that the vehicle control system and propulsion experienced the greatest number of failures (Figure 4.3.1). Appendix B provides a detailed discussion of the classification of failures. A great many of the vehicle control system failures simply required adjustments. For instance, adjustments were made to vehicle speed and braking rate. Further discussion of these adjustments are provided in Section 3.4 Command, Control, and Communications. Replacement of Weir control boards (the control system for the eddy-current transmission) and power and signal collector shoes were frequently necessary.

The majority of the propulsion system failures occurred with power collector shoes, propulsion motors, and the eddy-current transmission (indicated as Weir unit and clutch). Although many of these failures did not take long to correct, others, such as, motors and ECT unit replacements took considerable time. Hence, an exponential distribution of these failures was assumed for simulation purposes using a mean-time-to-repair ECT units of 1.0 hour. This provides us with repair times ranging from a few minutes (accounting for restarts, a result of phantom and intermittent undetected failures), at the low end, to eight hours, (accounting for replacement of motors and ECT units) at the upper extreme.

The motor and eddy-current transmission (ECT) failures resulted primarily from bearing failures which in turn caused secondary failures of the motor or ECT units. Because of this, it has been hypothesized that the cantilevered support of the motor, eddy-current transmission, emergency brake, and differential drive units from the trucks produces significant shaft flexure and, hence, dynamic load imbalance. This cantilevered support design with its associated failures is what prompted the PRT Systems (Astroglide) to make the LIM modification. This design deficiency, which might be considered normal for such a system under development, resulted in an inordinately large amount of maintenance. A redesign of the cantilevered support design of the motor and ECT system was not attempted during Jetrail operation because: 1) a year or two of operation was necessary before sufficient failure data could be gathered to confirm the difficulty; 2) the system was intended to be short-lived because of the impending move of Braniff facilities to the new Dallas-Ft. Worth regional airport; 3) the operational policy of implementing two spares resulted in very few system degradations (see Table 4.3.1) that caused passenger delays resulting in loss of Braniff customers; and 4) a highly motivated, well-trained maintenance team was developed simultaneously with the discovery of these problems. Keeping the system operational to Braniff's high standards was unquestionably a challenge that the maintenance team was barely able to cope with. Therefore, PRT Systems Inc., using members of the original design and operations team is attempting to alleviate these maintenance problems by eliminating the workable, but complex eddy-current propulsion system and replacing it with a mechanically simpler, linear induction motor, which has no moving parts. Idler wheels and the emergency brake are the only moving parts of the LIM propulsion system. However, it should be noted that LIM propulsion controllers are more complex electrically than the eddy-current propulsion system, thereby trading off electrical complexity for mechanical simplicity. This may well be a good trade-off since the state-of-the-art of electrical control equipment appears to be well advanced for industrial applications. However, the application of this concept to a transportation system has yet to be proven.

4.4 COMFORT FACTORS

Ride Quality Measurements Ride quality measurements were made on both a Jetrail vehicle and an Astroglide vehicle. These measurements included vibrations along three mutually perpendicular axes as well as rotations about these axes. Computations were made to obtain the spectral density functions as well as root mean square values for one-third octave bands in order to compare the ride quality with the guidelines developed by the International Organization for Standardization (Document 2631).

The data was taken during travel in four different situations, i.e., 1. in a curve, 2. during deceleration into a station, 3. on a straight guideway section, and 4. during acceleration to full speed after a station stop.

The following conclusions were drawn:

1. Both the Jetrail and the Astroglide vehicles have acceptable overall ride quality compared with that of other systems and the I.S.O. guide. In no cases do the accelerations exceed the one-hour fatigue decreased proficiency boundary. Only a few RMS accelerations of the one-third octave bands exceed the eight-hour boundary.

2. Vehicle acceleration and deceleration cause reductions in most of the ride quality motions, however, the curve section increases these motions, i.e., when each of the three cases is compared with the ride quality motions on the straight section.

3. The ride of the Astroglide (LIM) vehicle has slightly lower R.M.S. accelerations than the Jetrail vehcile.

a. For all four measurement conditions, the vertical motions (R.M.S. accelerations) of the Astroglide (LIM) vehicle were less than those for the Jetrail vehicle.

b. In the curve and straight sections, the lateral motions of the Astroglide were less than those of the Jetrail vehicle, however, during acceleration and deceleration Astroglide had greater motions.

c. In the curve and during deceleration, the longitudinal motions of Astroglide were more favorable, however they were slightly poorer than Jetrail in the straight section and during acceleration.

d. In pitch the Astroglide vehicle was significantly better than Jetrail, however Astroglide was poorer in roll and only modestly better in yaw.

4. Overall, both vehicles had an acceptable ride quality, however the Astroglide was slightly better than the Jetrail vehicle.

Table 4.4-1 is a comparison of the measurements for each vehicle in each of the four operating situations.

The appendix should be consulted for the experimental details and technical results.

TABLE 4.4-1. RMS TO 200 HZ, CONVENTIONAL AND LIM VEHICLES COMPARED

CONDITION		a_x g's	a_y g's	a_z g's	a_θ	a_ϕ	a_ψ	RATING
SWAY	CONVENTIONAL	.0642	.0200	.0555	9.729	2.410	1.200	6
	L.I.M.	.0370	.0110	.0350	8.730	.9230	.684	3
DECELERATION	CONVENTIONAL	.0528	.0073	.0312	4.342	1.096	.4673	3
	L.I.M.	.0370	.0260	.0180	6.940	.6760	.3870	4
LONG STRAIGHT	CONVENTIONAL	.0344	.0092	.0464	5.447	1.575	.6162	5
	L.I.M.	.0380	.0080	.0320	6.640	.8810	.5590	3
ACCELERATION	CONVENTIONAL	.0463	.0064	.0456	4.488	1.262	.4562	4
	L.I.M.	.0560	.0080	.0270	6.580	.9110	.5130	4

The ride quality of the Jetrail system was, in the team's opinion, somewhat rough with respect to other automated systems but not objectionable. It was significantly smoother than the ride of some rapid rail systems. The roll and roll rate on the straight sections and on the turns were not excessive. The Astroglide system exhibited slightly higher jerk (derivative of acceleration) than the Jetrail vehicle during speed transitions. This was perhaps attributable to single motor operation during most of the test period and to changes in the rolling friction.

4.5 HUMAN INTERFACE

4.5.1 Passenger Operation

From the passenger's point of view the system is operationally much like an elevator except that the system operates horizontally. The following sequence will serve as an illustration. When a passenger drives into the parking lot near the entrance to Love Field and proceeds to the station entrance, a valet will park the car and a ticketing agent will forward the baggage to the aircraft. Tickets are presented to the passenger for both automobile and baggage.

The station entrance has six parallel, covered unloading bays where baggage could be dropped off at the curbside (Fig. 3.1.2). Baggage is hand loaded into a small truck which is driven directly to the aircraft. This eliminates double handling that would have been experienced when two Jetrail baggage cars were planned. These baggage vehicles were never implemented.

After alighting from the car, the passenger will then enter station A (Figures 3.1.2 and 3.1.4) take an elevator to the second level and walk a short distance (about 30 feet) to the vehicle loading area. The loading area looks much like an elevator lobby with four doors on a single side corresponding to loading and unloading berths - A1 to A4 shown in Figure 3.1.4. The loading area is somewhat longer (about 60 feet) than an equivalent number of doors for an elevator. Passengers are directed to the first sequential loading berth by means of a sign. The walk in terms of time is short (5-15 sec.). Because the system is demand-responsive, the time to walk to loading bays is not as critical as in a scheduled system with an open platform where passengers need to walk to the appropriate berth to enter their vehicle.

A single button on the wall will be pushed calling for a vehicle. When it arrives, the biparting steel station doors and coupled vehicle doors will automatically open allowing the passengers to enter the vehicle. The doors normally remain open for 20 seconds. If a vehicle were in the station ready for departure, it would be in the first sequential loading berth, A4, with its doors open. In the high-flow mode the doors of all three loading berths A2, A3, and A4 would be open ready for passenger loading.

Once the passenger is on board, one of two stations can be selected by pressing a button on a panel located to the right of the door (item 32 - Figure 3.2.4). However, if no button is pressed the vehicle occupancy switches in the floor or seats will initiate the starting sequence. Since stations are on-line the vehicle will automatically stop at berth B1 of station B, the Braniff terminal. As previously mentioned only a ten pound weight is necessary to actuate the occupancy switches. This permits a package to be transported between stations A and B. This feature on occasion has proved somewhat troublesome in that cement blocks were found in the vehicles causing the vehicles to remain in berth B1 and A1.

When the vehicle has reached station B, the biparting doors will open automatically and the passenger will walk to the waiting aircraft. The returning passengers will similarly use Jetrail by calling a vehicle and proceeding to station A. The vehicle will proceed automatically to station A stopping at unloading berth A1. If it were desired to step at station C, the baggage claim area, it would be necessary to press the station selection button in the vehicle.

Upon presentation of a baggage and automobile claim check both car and baggage will be picked up. Baggage is delivered to curbside where assistance can be obtained to load it into the car.

4.5.2 Vehicle Design Features

Vehicle design features to facilitate safety, passenger use, and comfort will be described. The ceiling height is 78 inches (1.9 m) permitting adequate head clearance for entry and standing passengers. The location of the airconditioning unit on the left side of the vehicle (Figure 3.2.4) does constrain movement somewhat. The limited floor space encourages passengers to sit down. The top of the airconditioning unit serves as handy storage area for baggage. The airconditioning unit is flanked by vertical stanchions for the convenience of standing passengers.

The interior of the passenger compartment is insulated and all partitions and seats are permanently fastened in place. Velcro fasteners were used to maintain the seat cushions in place. All sharp edges are rounded. Fasteners are either recessed or rounded with the exception of the fire extinguisher container and the ash trays. However, both are mounted out of the way on the left side of the vehicle, i.e., the side with the airconditioning unit. In general, safety related to sharp edges was designed into the vehicle.

Smoking was permitted in the vehicles. This was an unnecessary risk. Especially since the vehicle body and interior covering materials are not designed for fire safety. This hazard is particularly important in these vehicles where egress is difficult for the major portion of the traveling public and virtually impossible for children, the handicapped, and elderly. The use of a fire extinguisher is not dependable especially in panic situations. Therefore, it is recommended that smoking not be permitted.

4.5.3 Noise

Sound measurements were made on both the exterior and interior of the vehicle. The objective was to obtain the noise contribution that the Jetrail would make on the passengers and on the environment. Exterior measurements were made directly underneath the guideway and at 25 and 50 foot perpendicular distances away from the guideway. The measurements were made during the passage of a vehicle and in the vicinity of the electrical riser (the emergency generator). The average exterior noise was found to be 72 dbA.

Measurements were made at various locations throughout the vehicle, with the majority at seating and standing head level for a 5-foot 8-inch person. The average of these measurements on the interior of the vehicle was 71 dbA.

By comparison the exterior noise level was considerably quieter than cars passing by on the adjacent roadway (75-85 dbA), or aircraft taking off (92-115 dbA). The roadway was close to the centerline of the guideway, i.e., approximately 35 feet to the centerline of the roadway. The interior was somewhat noisier (71 dbA) than a typical office (70 dbA). Exterior noises, such as cars passing near the guideway, were clearly audible inside the vehicle.

4.6 SAFETY

4.6.1 Fire Safety

As can be inferred from the vehicle description of section 3.2, most of the materials of construction are flammable, some highly so. The vehicle itself, being made of fiberglass and resin will burn readily as will the carpeting and sponge padding. Seat pads are made of polyurethane cushions, vinyl covered and would give off toxic fumes. Replacement with a low burning-index neoprene foam is currently underway.

Vehicle electrical control equipment is enclosed by fiberglass and resin materials and is not separately vented to the outside. An electrical fire from overheating or a short circuit would give off fumes and smoke into the passenger compartment.

Fire control was provided by a single hand held fire extinguisher. A fire extinguisher on board is not considered satisfactory due to the undependable performance of passengers in panic situations. However, this was frequently stolen during fishing season and of course not available for some period of time.

4.6.2 Evacuation

For evacuation of the vehicle in the event of fire or other emergency a single knotted hemp rope was stored in an overhead panel. This must be released and the doors must be opened with a manual switch. No instructions were provided in the vehicle but are given by the operator over the two-way radio. The basic emergency strategy was to keep the passengers in the vehicle for every emergency except fire until a more reliable evacuation could be supervised using ladder trucks. Entrance by technicians or egress by passengers can be made through either the door or a window.

The knotted rope would be ineffective for children, elderly, and handicapped persons. Even otherwise healthy normal adults would have great difficulty using the rope. If the emergency occurred over the brook the hazards would have been multiplied.

In the event of fire, passengers must be evacuated within one minute otherwise they will be incapacitated. The ladder trucks cannot rescue passengers within this time since their deployment time averaged three and one-half minutes.

4.6.3 Other Safety Aspects

All door edges had safety switches, as in an elevator, to prevent the doors' closing on a person or object. Safety plate glass was used for the windows. Stanchions were provided for standing passengers.

4.6.4 Accident Report

Only one emergency was reported during the three years and nine months of operation. Apparently an airline catering truck elevated its body under the guideway. A vehicle carrying passengers ran into the elevated body. The vehicle emergency button was apparently not activated by the passengers, nor apparently did the technician at the control console take any emergency action. Injuries of unknown extent occurred to the passengers and their cases are still before the courts.

Nevertheless some six million passengers were carried, without a fatality or major mishap.

4.7 SECURITY

Little if any vandalism was experienced; some torn seats, which could have been accidently done; no significant amount of graffiti, and the occasional theft of the fire extinguisher.

Personal security was not a problem since there were no reported acts of violence or robbery.

4.8 ADVERSE WEATHER OPERATIONS

The Jetrail system was unable to operate during some ice and snow conditions because the upper surface of the lower flange accumulated ice and therefore interfered with the driving and braking functions. In the Dallas environment this amounted to about one and one-half days per year.

Rain has no known effect on the system although measurements of stopping distances were not made. During very heavy rain and wind storms the system was operated in a degraded mode, i.e., speed 2.

The Astroglide system was not greatly affected by ice and snow since it utilizes the protected lower surface of the guideway for LIM propulsion and LIM braking. Emergency braking utilizes the idler wheels on upper surface of the lower flange. Therefore a degraded mode of operation (speed 2) would be employed if this surface becomes iced. Operation would be conducted with only the service brake functioning. However if ice should build up on the upper surface of the lower flange to a thickness approaching the motor gap dimension (0.375 in., 10 mm) there would be some interference.

In addition severe icing on power rails can cause power drop-outs. Heating of power rails and the wheel riding surface or the addition of a covering could eliminate the icing problems. These solutions are also applicable to Jetrail and in fact would permit the operation of both Jetrail and Astroglide vehicles simultaneously in adverse weather. Emergency stopping distances in adverse weather conditions have not been measured.

4.9 ASTROGLIDE OPERATION

The Astroglide as previously indicated is identical to the Jetrail system with the exception of the LIM propulsion system which replaces the eddy-current transmission propulsion system. Therefore, operation of Astroglide will be limited to a discussion of the LIM performance.

The LIM vehicle power characteristics are different than the eddy-current transmission because of distortion effects and power factor correction by capacitance. Measurements of the LIM vehicle performance characteristics were made. Detailed discussion and data are presented in Appendix A.4. A summary of the LIM vehicle power characteristics is presented in Table A-3. Four conditions are identified; coast (A), low speed cruise (B), acceleration (C), and high speed cruise (D).

The first of the four identified conditions, "A", vehicle coast is where the power conditioner is phased "off". At this time the power factor correction capacitors comprise the major load. The vehicle draws 2 kW of standby power while 103 VAR of leading reactive power is supplied to the capacitors. The systems apparent power is 93 kVA at a power factor of 0.02. The current level of 111 amps (RMS) is exceeded only during vehicle acceleration. This current level is also the standby level.

The second operating condition, "B", is a low-speed cruise (speed 2). The vehicle required 27 kW of power at a system power factor of 0.5. The displacement reactive power measured is about zero, indicating a power factor of 1.0. However, there is 48 kVAR of distortion reactive power which reduces the system power factor to 0.5. At this low speed cruise point the power factor correction capacitors supply just enough leading reactive power to compensate the lagging displacement reactive power. Input current is 67 amperes (RMS), and the system total apparent power is 54 kVA.

The third operating condition, "C", is acceleration. At this point, the power, current, and reactive power are at their maxima. The vehicle requires 70 kW of power at a corrected lagging power factor of 0.75, with an input current of 130 amps (RMS) and a total apparent power of 105 kVA. The system reactive power is 78 kVAR with 62 kVAR of displacement reactive power and 47 kVAR of distortion reactive power.

The final identified operating condition "D", is high speed cruise. The power required is 39 kW at a power factor of 0.66. An input current of 74 amperes (RMS) yields an apparent power demand of 60 kVA. Total reactive power is 45 kVAR, which consists of 19 kVAR of displacement reactive power and 40 kVAR of distortion reactive power. The power factor correction capacitors correct the displacement power factor to 0.9 under these cruise conditions, but the distortion levels reduce the total corrected power factor to 0.66.

For the three power conditions, low speed and high speed cruise and acceleration, there is a distortion power component of 40 to 47 kVAR. In the standby and coasting conditions the power conditioner is phased off and distortion is a minimum. The improvement in displacement components which is indicated by displacement power factors greater than 0.75 for powered conditions is apparent, but the particular design results in high reactive power and hence high apparent power demand.

COMPARATIVE MEASUREMENTS

The LIM vehicle control system did not hold the vehicle at constant speed on all guideway sections. In addition, accelerations and decelerations were too slow for the vehicle to stabilize at new speeds in the relatively short, slow-speed segments of guideway. The comparative power levels, therefore, are not as stable or repeatable as they were with the ECT vehicle. The typical measurements listed in Table A-2, illustrate the marked differences in power levels, current levels, reactive power, and power factor between the two vehicles. The measurements indicate that the LIM power levels are approximately twice the power levels of the eddy-current transmission system, and that current and apparent power are almost three times those of the ECT vehicle.

These high levels were measured not withstanding the fact that the LIM vehicle is lighter than the eddy-current clutch vehicle. The LIM system power factor at low speed cruise was 0.5 whereas at high speed cruise it was 0.66.

For most cruise conditions and for all downhill cruise conditions, the VAR transducer indicated a leading reactive power. The distortion reactive power, however, made the net reactive power lagging and forced the system power factor to lower levels than indicated by the VAR transducer outputs. The values of the power factor correction capacitors installed on the vehicle may be correct for the application, however, they cause wide excursions in the phase angles of current and of the reactive power components. Without distortion components the vehicle would operate near a unity power factor or a slightly leading power factor for the downhill segments of the trip profile.

The LIM power characteristics reflect distortion to displacement reactive power ratios greater than 100%. Stickler, Ploetz and Raposa (2) have reported distortion to displacement ratios of 33% for a rotary induction motor operating with phase control at approximately 50% of synchronous speed. The Jetrail calculations are comparable when uncorrected displacement reactive power is used in the computations. The reactive power indicated by the VAR transducer is net displacement reactive power as corrected by the capacitors, but actual displacement reactive power flowing in the LIM's exceeds the indicated value by 100 kVAR. The degree of improvement in the power factor and reduction in total apparent power can be determined from analysis of the system phasor diagrams, shown in Appendix A.

The eddy-current clutch and the variable voltage LIM system fall into a class of system referred to as "induction motor drive with slip coupling". These systems are inherently high-loss systems when operating at low speeds because slip energy is lost. The eddy-current system dissipates the slip energy in the clutch, and the LIM system dissipates slip energy in the reaction rail. The lost energy in both cases is the difference between the energy delivered by the motor and that delivered to the load. It is proportional to the difference between motor synchronous speed and output speed. At low speeds the lost energy is greater than the energy delivered as thrust.

Previous studies on an eddy-current transmission propulsion system similar to the Jetrail system indicate a maximum efficiency of 63%, ref. (3)(4). Calculations using induction motor theory indicate that the LIM system, as used on the Jetrail vehicle, has a maximum theoretical efficiency of 24/64 = 38.5% at its maximum velocity of 24 km/hr. Efficiency could be significantly improved if the system used motors with shorter pole pitches. The motor would then operate closer to synchronous speed thereby improving efficiency. Alternatively, the LIM was designed for high speed applications (approximately 35 mph). Operating closer to the synchronous speed would significantly improve the efficiency. Because of the low efficiencies when operated at maximum speeds and the reduction of inefficiencies as speed is reduced, these types of drives are best suited for applications where required power output decreases as speed decreases, such as fans and pumps. Transportation propulsion systems require peak outputs during acceleration when speed is at or near zero; therefore, these induction motor drives are not used in systems which take best advantage of their characteristics.

Implementation of a linear induction motor system in place of the eddy-current transmission system has resulted in a weight reduction of approximately 2600 pounds. The LIM vehicle weight is reported as weighing 4400 pounds (2200 kg). Notwithstanding the fact that the LIM vehicle weighs less than the eddy-current clutch vehicle, the LIM vehicle underperforms the eddy-current clutch vehicle in all operating conditions. Again this is due primarily to the linear-induction motors being designed for higher speed applications.

During standby or coasting conditions the LIM vehicle draws over 100 amperes to supply the power factor correction capacitors with 100 kVAR of leading reactive power. In the same condition, the eddy-current system requires 11.5 kVAR of lagging reactive power for motor excitation. The LIM power factor and the eddy-current clutch power factor are very low, but the demand levels differ by a factor of 10. Active power for both vehicles is approximately 2 kW during the standby condition.

When accelerating, the LIM requires 70 kW of power compared to 42 kW for the eddy-current transmission vehicle. System power factors for the two vehicles are comparable, approximately 0.7.

Under cruise conditions, the LIM power range is of the order of 25 to 40 kW, the ECT power range is between 10 and 20 kW.

Line currents for the LIM are appreciably higher than for the eddy-current transmission vehicle. The LIM uses 130 amperes during acceleration, 111 amperes during standby, and 60 to 70 amperes during cruise. The ECT vehicle draws 67 amperes during acceleration, 4 amperes during standby and 25 to 30 amperes during cruise.

Both vehicles operate at similar power factors, but the LIM system utilizes power factor correction capacitors to improve its power factor. These capacitors supply enough leading reactive power to maintain the displacement component of power factor above 0.75. The power conditioner generates 40 to 47 kVAR of distortion reactive power whenever it is phased "on", and the system power factor is reduced.

For correction of power factor oil-filled ac capacitors are used. However, there are problems in the system attributable to their use. These are:

1. The capacitors are used over their manufacturer's ratings. They are rated for 440-volts ac, but they are used in a 480-volt, ac circuit. This over-voltage operation impairs their reliability. A failure (power factor correction capacitor has shorted) was experienced during the test program.

2. They are connected between the circuit breakers and the LIM power conditioners on the load side of the thyristor protection fuses. The fuses must pass the capacitor surge current which is often high enough to blow the fuses. Chronic fuse problems caused frequent delays of the test program.

3. Because they are connected in the lines before the power conditioners, they comprise an uncompensated load when the power conditioner is phased "off' and are the cause of the high system demand.

Based on these power measurements made on the Jetrail system, the LIM system does not appear to be an improvement over the eddy-current clutch system. The results of these measurements are limited to comparisons of the Astroglide-LIM and ECT vehicle systems investigated. They can not be extended directly to apply to other vehicles systems, or anticipated improvements in the present systems. Rather, careful analysis is necessary to obtain an indication of this system's performance in another application.

It should be borne in mind that the Astroglide-LIM system is a prototype system requiring repackaging of the motor controller and the preproduction system. Therefore, further measurements in performance and particularly in reliability are necessary to determine the performance characteristics of an Astroglide system suitable for urban use.

5. SYSTEM ECONOMICS

The capital cost of the system is discussed briefly in section 5.1. Actual operating cost to Braniff for a single year is discussed in section 5.2. In addition estimates are made and discussed in section 5.3 to provide a more accurate representation of operating costs in the location where Braniff's maintenance staff would not be available. Further, system economic effectiveness, e.g., cost per vehicle-mile and cost per/seat-mile, is considered in section 6.2.

5.1 CAPITAL COSTS

The capital costs were dictated by the criteria set by Braniff for their needs. The rationale and background covering these needs for a low-cost, intra-airport transportation system has been covered earlier in this report (Section 2). Essentially they involved: 1) early rapid operational capability, hence the use of existing components; 2) low initial cost, hence, the use of existing components; 3) short life, hence, minimal useful life of components; 4) re-sale potential, hence transportability; and 5) high availability, hence aggressive maintenance.

A fixed-price contract for the development and installation of the Jetrail system at Love Field was awarded to the Jetrail Division of the Stanray Corporation in April 1968 for $1.5 million. Stanray experienced a $500 thousand overrun because of design difficulties. Note that this system was the first of its kind and there was almost no experience base upon which to build. Braniff assumed the operational testing of the system and invested an additional $500 thousand. Therefore, the total capital cost of the Jetrail system was $2.5 million.

Fixed-price contract	$1,500,000
Stanray overrun	500,000
Braniff additional invest.	500,000
	$2,500,000

Breakdown

The fixed-price contract expenditures were reported as follows:

Guideway, footings, and foundations	$ 361,000
Stations	292,000
Switches	40,000
Power, electrification, command and control	284,000
Vehicles	220,000
Spare parts	90,000
	$1,287,000
Engineering, overhead, and profit	213,000
	$1,500,000
Overrun	1,000,000
	$2,500,000

The $1 million overrun was attributed to engineering and development costs.

5.2 OPERATING COST

5.2.1 Braniff's Estimates

The operating costs as reported by Braniff for the 1973-74 year are as follows:

Labor	
Regular time	$ 91,322
Overtime	21,350
	$112,672
Material	
Purchased parts	$ 40,669
Parts from inventory[1]	8,342
	$ 59,355
Summary	
Labor	$112,672
Material	59,355
	$172,027

[1] Start-up parts inventory was approximately $90,000.

Due to an unusual labor agreement between Braniff and its union, a full-time technician dedicated to Jetrail was used with a back-up, or assistant technician from among the regular Braniff aircraft technicians. This unusual agreement was advantageous for two reasons; 1) a full-time dedicated (exclusive) group of Jetrail technicians was developed which had knowledge of and experience on the Jetrail system and 2) the assistant technicians were used only as required thereby improving the manpower utilization.

The labor costs of the assistant technicians were not included in the Jetrail accounting. In addition, the cost of land rental is not included in these and subsequent calculations.

Braniff contracted for the operation of the parking lot, including valet parking and paid the operator $0.25 per Jetrail passenger. The total cost for this was based on an estimated 6 million passengers and is also not included in these and subsequent calculations.

5.2.2 TSC Estimates

For the use of Jetrail at another location, of course, the cost of this standby technician would have to be taken into account. The following analysis is the TSC team's estimate of these operating costs.

Labor

Two-man crew to cover a three-shift operation, seven days per week

17,472 man-hours/year
13.50 per hour (Braniff rate)
$235,872 1 year

Time-scheduled additional labor — power rail inspection

832 man-hours/year
16.88 per hour (Braniff O.T. rate)
$14,044

Time-scheduled additional labor — conductor-bar lubrication

96 man-hours/year

$16.88 per hour

$1620

Labor Summary (estimate)

Full-time crew	$235,872
Power rail inspection	14,044
Lubrication	1,620
	$251,536

Materials (per year)

Cars

Wheels and bearings	530
Shoes	$17,500
Weir Units	32,000
Motors	2,400
Couplings	400
Controls	14,560
Doors	9,700
Vandalism	2,000
	$75,130
Other materials	8,080
Power	10,344
	$93,544

Summary

Labor	$251,536
Material	93,554
	$345,090

This total of approximately $345,000 per year represents a more realistic estimate of operating and maintenance costs of the Jet-rail system that includes two full-time maintenance technicians, 24 hours per day. These costs are based on 1973 dollars. Adjusting this to 1976 dollars, the annual operating and maintenance costs would be approximately $427,000.

System effectiveness parameters are discussed in the evaluation section (section 6).

6. EVALUATION

This evaluation section contains a Performance Summary, providing a brief description of the system; System Effectiveness Parameters, providing the salient operating measures; and Technical Findings. It is based on the analyses and opinions of the TSC team.

6.1 PERFORMANCE SUMMARY

Jetrail was the first completely automated, demand, responsive intra-airport transportation system and is classed as a group-rapid transit system. It was operational for three years and nine months from April, 1970 to January, 1974. During this time, it carried an estimated 6 million people over an estimated 1.2 million miles without a fatality or major mishap. One accident reportedly occurred when a catering truck body was raised underneath the guideway obstructing the guideway-resulting in a vehicle collision. It resulted in injuries of unknown extent. This case is currently in litigation.

Due to the employment of good operational procedures and diligent maintenance this first-of-its-kind system achieved high system reliability and availability--approximately 97.6 percent and 99.9 percent respectively. This was for seven days per week, 24 hours per day of operation. Failures were defined as functional failures which required six minutes or more to correct or to replace the failed vehicle.

Because of the short anticipated life of the system a conservative philosophy was used in the design approach. That is, Jetrail was selected from the competing designs because it required the least development, hence the least risk, and because it was the lowest cost system. Available off-the-shelf components were employed as much as possible. The central command and control system incorporating a dual redundant block control system was the most innovative development of the system. It was made from off-the-shelf components incorporating a great deal of redundancy of relatively inexpensive components and features permitting ease of maintenance. Standard structural steel I-beams and columns were used to minimize guideway costs. Drive motors, eddy current transmissions, and motor controllers were also among the off-the-shelf items selected.

Some development difficulties were encountered. Many off-the-shelf items, while time tested in commercial applications, were among the principal sources of failures and did not prove suitable for this transportation application and environment. Insufficient time and effort was allowed for initial design development and testing.

The fundamental approach used was to perform the least amount of design and development and to correct oversights during the test phase. This approach appeared sensible because it was thought that little development effort was required. In addition, the constraints of limited system life and low cost supplemented this approach. Clearly, the emphasis was on initial cost savings rather than life-cycle cost considerations. Hindsight indicates that this led to design choices that were not necessarily optimum. The most innovative part of the system, the command and control subsystem, however, received considerable design attention with the result that it operated reliably and required little maintenance.

It was not realized that when reliable off-the-shelf components are used in a new system with a different operating environment the components may not function well together as a system. A greater initial system design effort including specification of the system and interface requirements in conjunction with component testing would have precluded many difficulties. Sufficient time and effort was not afforded to thoroughly investigate the use of components and to determine their suitability in this specific transportation environment.

Astroglide is a modification of Jetrail potentially providing a solution to the major problems encountered. The LIM system is intended to improve reliability and maintenance by virtue of the reduction in number of parts. The Astroglide simplification is a prototype system representing a major development which will require testing prior to achieving operational capability. The LIM is also expected to improve the operational capability in snow and ice environments due to the absence of tractive wheels.

6.2 SYSTEM EFFECTIVENESS PARAMETERS

In order to compare the effectiveness of one alternative within a system or to compare one system with another some quantitative measures are very useful. To this end, a number of effectiveness parameters have been derived which are based upon the available data from section 5 concerning operating, capital, and life cycle costs. An overall system effectiveness parameter is also determined. It should be emphasized that these effectiveness parameters should be considered only as relative measures of effectiveness to assist in making comparisons.

Operating costs - The operating costs in dollars/seat mile are presented for two cases:

1) Using Braniff's estimate of 6 million passengers over the life of the system and

2) Using an estimate of 10 million passengers over the life of the system.

Case 1 Using 6,000,000 passengers over the operational life of the system (3.75 years), the number of passengers per year, trips per year, vehicle miles per year, and cost per passenger (section 4.3) are given by the following calculations.

$$\frac{6 \times 10^6 \text{ passengers}}{3.75 \text{ years}} = 1.6 \times 10^6 \text{ passenger/year}$$

$$\frac{1.6 \times 10^6 \text{ passengers/year}}{3.26 \text{ passengers/vehicle-trip (see table C-1)}} = 4.9 \times 10^5 \text{ vehicle-trips/year}$$

4.9×10^5 vehicle-trips/year x 0.69 miles/trip = 3.4×10^5 vehicle-miles/year

The cost per vehicle-mile based on operating and maintenance cost as reported by Braniff is

$$\frac{\$1.7 \times 10^5/\text{year}}{3.4 \times 10^5 \text{ miles/year}} = \$0.51/\text{ vehicle-mile.}$$

Now using the more realistic estimate of total cost, the cost per vehicle mile based on estimated operating and maintenance for another application of Jetrail is

$$\frac{\$3.5 \times 10^5/\text{year}}{3.4 \times 10^5 \text{ vehicle-miles/year}} = \$1.02/\text{vehicle-mile.}$$

Given the vehicle capacity of ten passengers (8 seated and 2 standing), the operating cost per seat mile is \$0.051/seat-mile and \$0.102/seat-mile, respectively.

The total cost per passenger is calculated by dividing the total operating and maintenance cost per year by the total number of passengers.

$$\frac{\$3.5 \times 10^5/\text{year}}{1.6 \times 10^6 \text{ passengers/year}} = \$0.216/\text{passenger}$$

Case 2 Assuming 10,000,000 passengers over the operational life of the system (3.75 years), the number of passengers/year, vehicle-trips per year, vehicle-miles/year, and cost per passenger are as follows (Appendix C).

$$\frac{10 \times 10^6 \text{ passengers}}{3.75 \text{ years}} = 2.7 \times 10^6 \text{ passengers/year}$$

$$\frac{2.7 \times 10^6 \text{ passengers/year}}{3.54 \text{ passengers/vehicle-trip}} = 7.5 \times 10^5 \text{ vehicle-trips/year}$$

7.5×10^5 vehicle-trips/year x 0.69 miles/trip = 5.2×10^5 vehicle-miles/year

The cost per vehicle-mile based on the operating and maintenance cost reported by Braniff (see Section 5.2) is

$$\frac{\$1.7 \times 10^5/\text{year}}{5.2 \times 10^5 \text{ vehicle-miles/year}} = \$0.66/\text{ vehicle-mile}$$

For a vehicle capacity of ten passengers (8 seated and 2 standing) the operating cost is $0.066/seat-mile.

The total cost per passenger is calculated by dividing the total operating and maintenance cost per year by the total number of passengers per year.

$$\frac{\$3.5 \times 10^5/\text{year}}{2.7 \times 10^6 \text{ passenger/year}} = \$0.129/\text{passenger}$$

The above costs were based on 1973 operating costs. Relating these costs to May 1976 costs, the following changes are observed. The purchasing power of $1.00 was $0.55. (From the Monthly Business Statistics, U.S. Department of Commerce.)

$172,028/year (1973) equivalent to $231,456/year (1976)
$345,090/year (1973) equivalent to $464,303/year (1976)

$$\frac{\$231,456/\text{year}}{338,650 \text{ vehicle-mile/year}} = \$0.683/\text{vehicle-mile Case I (Braniff)}$$

$$\frac{\$464,303/\text{year}}{338,650 \text{ vehicle-mile/year}} = \$1.37/\text{vehicle-mile Case I (Other Applic.)}$$

The operating cost per seat-mile is equal to $0.14/seat-mile and

$$\frac{\$464,303/\text{year}}{519,774 \text{ vehicle-miles/year}} = \$0.89/\text{vehicle-mile}$$

The operating cost per seat-mile is equal to \$0.09/seat-mile.

Capital Cost

The capital cost in dollars per lane-mile includes all expenditures required to acquire the Jetrail system. The cost of constructing the Jetrail system in 1970 was \$2.5 million and its selling price in 1975 was assumed to be \$1.5 million. Converting the \$1.5 million in 1975 dollars to 1970 dollars (purchasing power of \$1.00 was \$0.86 for 1970 and \$0.58 for 1975), the comparative 1970 selling price would have been \$1.01 million. Subtracting this salvage value from the original construction cost provides an estimate of the capital costs over the useful life of the system, i.e., \$1.49 million.

The capital cost per lane-mile is

$$\frac{\$1.49 \times 10^6}{1.6 \text{ lane-miles}} = \$931{,}250\text{/lane-mile (1970 dollars).}$$

In 1976 dollars this is equivalent to \$1,456,100/lane-mile over the useful system life.

Life Cycle Cost

Life cycle costs are the total Jetrail costs including both operating and capital costs over the useful life of the system. They are a measure of the overall economic feasibility of the system.

The General Research Corporation's "Life Cycle Cost Model for Comparing AGT and Conventional Transit Alternatives" UMTA-CA-06-0090-76-1 was used to determine the life cycle costs of the Jetrail system. The model determines life cycle costs using present-worth techniques accounting for the time value of money and general inflation.

The results of Jetrail present value (life cycle costs) calculations are presented in Figure 6.2.1 which show the present value as a function of two interest rates 8 and 10% and three values

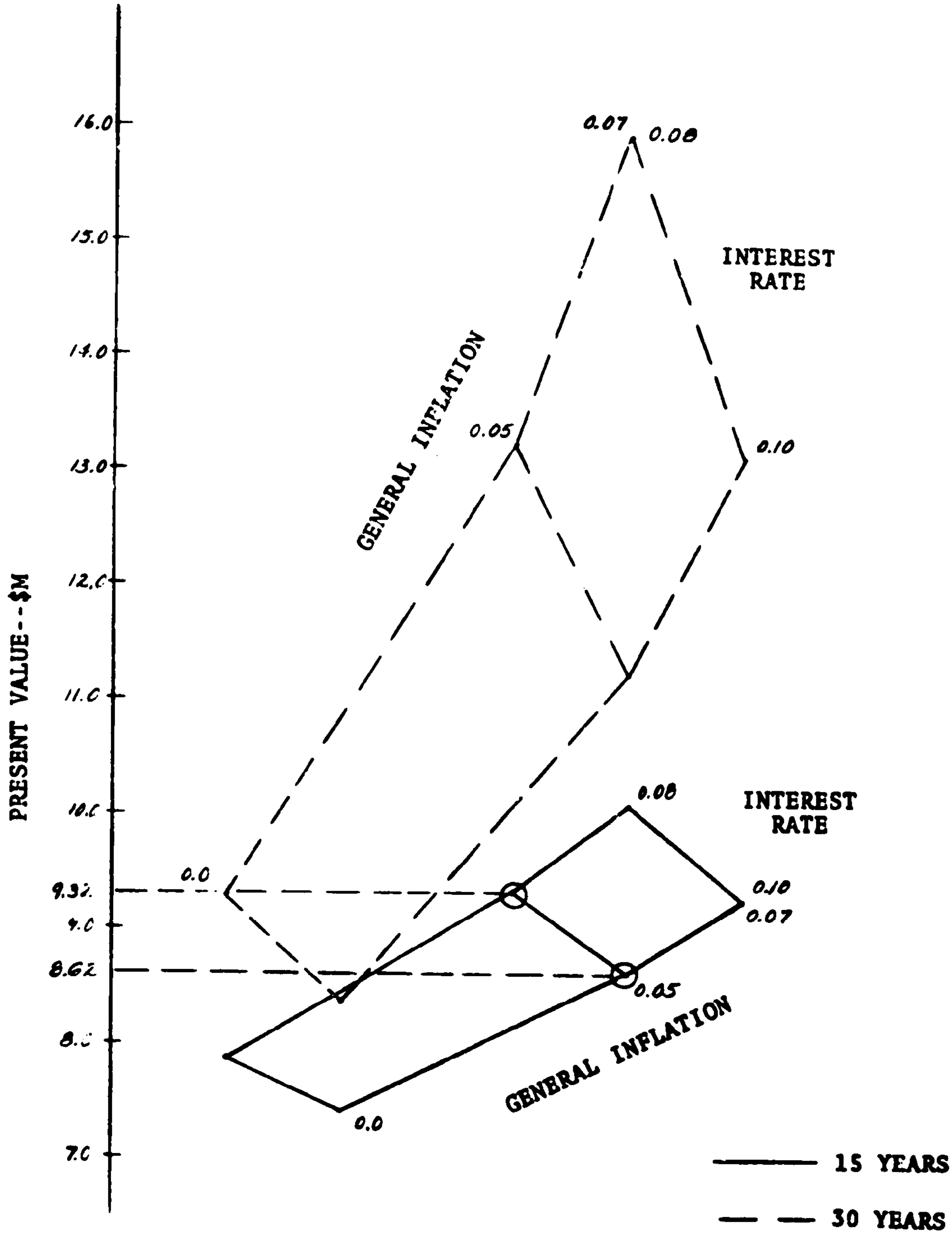

FIGURE 6.2.1. JETRAIL PRESENT VALUE

(0, 5 and 7%) of general inflation. These are done for two cases of system life, 15 and 30 years. The vehicle life was seven years, implying the purchase of new vehicles every seventh year for use in the eighth year.

The figure is used in the following manner. If it is desired to determine the present value of Jetrail with a 15 year life, a 10% interest rate, and a 5% inflation rate the lower figure would be used. At the intersection of the 5% inflation and 10% interest lines read $8.62 million to the left on the present value scale. With an 8% interest rate the present value is $9.32 million. Appendix D shows typical input values and cash flows for two cases each with a system life of 15 years and 10% interest one at a 0% and the other at 7% inflation rate.

System Effectiveness

The worth of a system is determined primarily by the effectiveness with which it functions. Operational requirements expressed in terms of single valued design adequacy requirements, such as capacity or travel time do not present a sufficiently clear analysis of the overall performance of the system, especially when considering reliability and maintainability. This interdependence makes the measurement of system performance complex.

System effectiveness can be defined as a quantitative measure of the extent to which the system performance can be expected to meet a set of specific requirements. The system effectiveness parameter includes consideration of three general areas of operational use: 1) the use, maintenance, storage, and logistics to which the system is exposed while awaiting the beginning of operation; 2) those factors associated with the actual operation; and 3) performance of the specified functions for which the system was designed.

The approach used to model system effectiveness is that shown in the Weapons System Effectiveness Industry Committee (WSEIAC) report sponsored by the U.S. Air Force System Command.

System effectiveness is defined as

SE = [A] [D] [C].

[A] is the availability vector matrix and is the probability that the system will be in condition state i at a random beginning time.

[D] is the dependability vector matrix and is the probability that the system will be in condition state j at the time of required output if it is in state i at the beginning.

Formation of the d, i, and j values will require consideration of all variables during the mission which can either degrade or improve the mission condition. If there are only two states of system condition (failed or operating), dependability becomes synonymous with reliability. This is the basis for this Jetrail discussion.

[C] is the capability matrix vector and provides a description of the system's capability of performance while in any of n condition states. This matrix will be a one-column and n-row configuration if only one figure of merit, or index, of system effectiveness measurement is used.

A simple two-state system is used to define the Jetrail system effectiveness. The purpose of the system is to transport passengers from the parking lot to the Braniff terminal, or the reverse, within 3.5 minutes or with some additional delay not to exceed 6 minutes. A delay greater than 6 minutes is considered a failure. The two system states are:

1) a successful trip completion with either no delay or a delay not exceeding 6 minutes or,

2) an unsuccessful trip with delays greater than 6 minutes.

From the foregoing the Jetrail system effectiveness can be calculated.

$$S.E. = [A]\,[D]\,[C]$$

$$= [a_1 a_2] \begin{bmatrix} d_{11} & d_{12} \\ d_{21} & d_{22} \end{bmatrix} \begin{bmatrix} c_1 \\ c_2 \end{bmatrix}$$

$$= [0.997\ 0.003] \begin{bmatrix} 0.97 & 0.03 \\ 0 & 1.0 \end{bmatrix} \begin{bmatrix} 3.5 \\ 3.5\ x > 6 \end{bmatrix}$$

$$= 3.7 \text{ minutes}$$

In this calculation

a_1 - availability of Jetrail, 0.997 (Section 4.3) (probability of the system being available for use)

a_2 - complement of availability, 0.003 (probability that the system will not be available for use)

d_{11} - probability of a vehicle starting out in State 1 (operative) and completing the trip in State 1.

d_{12} - probability of a vehicle starting out in State 1 but completing the trip (inoperative) in State 2.

d_{21} - probability of a vehicle starting out in State 2 (inoperative) and completing the trip in State 1 (operative).

d_{22} - probability of a vehicle starting out in State 2 (inoperative) and completing the trip in State 2 (inoperative)

c_1 - average trip time for State 1

c_2 - average trip time for State 2

The preceding values for availability and dependability are taken from Section 4.3. Although more than one figure of merit may be used in the capability matrix, only a single figure for schedule adherence was used.

It should be pointed out that this particular formulation of the problem using schedule adherence as the capability parameter is dependent on the specific terrain and layout of this system. Therefore, in order to compare another system to Jetrail the same terrain and layout constraints must be used.

Thus, given the requirements for Jetrail and the operating data, an indicator of this system's effectiveness has been calculated, namely, 3.7 minutes. It is the expected trip time at any random instant of time. This can be used to compare the effectiveness of changes in the operational procedure or, more important perhaps, to compare the effectiveness of another system relative to Jetrail. It should be emphasized that this measure of system effectiveness can only be used in a relative sense, i.e., comparing one system with another.

6.3 TECHNICAL FINDINGS

The following technical findings are intended to identify problems encountered and solutions devised during the design, development, implementation, and operation phases. As previously indicated the overall development philosophy was conservative, utilizing off-the-shelf hardware and permitting very little development.

The amount of analytical design effort permitted under the fixed-price contract should have been greater to prevent many of the development problems encountered.

Finding 1

Overall the Jetrail system represents the first automated Group Rapid Transit (GRT) system in intra-airport operational service. It carried over six million passengers approximately 1.3 million miles during a four year period without a fatality or major mishap while at the same time providing a high level of service.

Jetrail has been demonstrated suitable for a demand responsive AGT system in intra-airport service. A single accident occurred in the system during the three years and nine months of operations. This occurred when an aircraft catering service truck stopped under the guideway and raised the truck body. A vehicle carrying passengers ran into the truck body causing some injuries to the occupants. The extent of those injuries is unknown and the disposition of this accident is still in litigation. This accident occurred because the system does not have an obstacle detection system that could have detected the presence of the raised truck and take appropriate emergency action. However, the vehicle does have an emergency stop button, but it was not actuated by any of the passengers. It does not seem reasonable philosophically, to attempt to design a system that can automatically handle every possible contingency. Such design criteria would unnecessarily burden the automated system, penalizing it beyond reasonable safety criteria employed by other mass transportation systems. Because this accident was an unusual and unlikely occurrence, this is not felt to be a failure of the design. The vehicles could, however, be made safer by the incorporation of a crushable structure to attenuate some of the accelerations produced. Warning signs now exist in the area where the accident occurred. The area along the guideway has no objects that could fall on or block the guideway, with the exception of street lamp posts or power-carrying posts. It should be noted that the normal safety functions that stop one vehicle behind another have not experienced any failures.

Finding 2

(a) The method of emergency egress, using a knotted rope stored in the ceiling of the vehicle, can not be used by the great majority of the traveling public - especially children, elderly, and handicapped. The safety philosophy employed was to keep the passengers in the vehicle at all times and to push the vehicle or manually override the control system in order to proceed to the next station. This philosophy is sound except in the event of fire on board the vehicle, at which time it is essential to rapidly evacuate the passengers or rapidly extinguish the fire without any harmful effects to the passengers. Incapacitation of passengers will occur within one minute. The ladder trucks cannot rescue passengers within this time period (expected deployment time is 3.5 minutes), hence, other measures are necessary.

Work underway at TSC with active, Halon 1301, fire extinguishing systems has produced positive results that could minimize or eliminate the egress problem. Fires could be extinguished with no harm to passengers in a closed cabin thus obviating evacuation.

(b) Fire safety has not been designed into Jetrail. The vehicles are not fabricated with fire-retardant materials and do not conform to recent "Guideline Specifications for Flammability and Smoke Emission TSC-76-LFS-6."

The guideline indicates that passive fire-retardant materials should be employed throughout the vehicle to minimize the chances of fire hazards. A fire extinguisher on board is not considered satisfactory due to the undependable performance of the passengers in panic situations. Active fire control systems may also be employed in conjunction with the passive technique.

The equipment compartment under each seat is cooled through ventilation louvers into the passenger compartment. In the event of fire in the equipment compartment, the passenger compartment will be filled with smoke, possibly incapacitating the passengers. Thus, the equipment ventilation system should be separated from that of the passenger compartment.

Finding 3

(a) Jetrail cannot be operated in an ice and snow environment due to the wheel traction limitations. Severe icing of the power and command rails will result in power and signal dropouts. Approximately one and one-half days per year of operation have been suspended due to ice at Love Field in Dallas. Heating the guideway or covering it could permit operation but at an increase in operating or capital cost.

(b) The Astroglide LIM drive would permit better operation in ice and snow environments. It can operate unaffected over iced surfaces. Therefore, thrust and service braking will be unaffected. Ice will accumulate on the upper surface of the lower flange on which the support wheels ride. If the ice is allowed to build up in excess of the normal LIM air-gap, it can cause binding. However, prior to this condition, icing of the flange will cause the emergency brakes to become less effective, necessitating degraded (low-speed) operation. Icing of the power and command rails will result in power and signal dropouts. Therefore, although the Astroglide LIM system is not traction limited, it nonetheless suffers from some of the icing problems of Jetrail.

Finding 4

The overall development philosophy allowed insufficient time and effort for initial design, development, and testing. That philosophy was to perform the least amount of design and development and to correct oversights during the test phase.

Finding 5

(a) The development approach which used off-the-shelf hardware was generally found inadequate. Some of these components were among the principal sources of failures, particularly within the propulsion and propulsion control system. This approach did not permit sufficient specification and testing of components to insure their applicability to a specific transportation environment. Sufficiently detailed analysis is necessary to determine component compatibility with any new application.

(b) The initial propulsion motor was rated at five horsepower. This was found to be insufficient and resulted in overheating. The motor was changed to a seven and one half horsepower motor, but was fitted in the five horsepower motor frame to minimize redesign.

(c) Overheating was also experienced in the eddy-current transmission. A sealed bearing in the center of the eddy-current clutch failed frequently. Cooling louvers were cut into the eddy-current transmission, and the bearing was changed to one which could be greased. These changes in conjunction with the hand fitting of keys to correct a keyway problem resulted in half as many drive line failures.

(d) The principal maintenance, however, was still associated with the power and propulsion system even after the previously mentioned changes. Many of these failures are secondary failures resulting from primary bearing failures. Based on failure data, it is likely that the great majority of these failures were a result of the cantilevered support of the eddy-current transmission and motor. That is, there is a considerable mass suspended on the cantilevered motor and transmission frame beam producing a sizeable deflection. This deflection in conjunction with imbalance dynamics produced excessive loads in the bearings resulting in primary failures - ultimately leading to secondary failures of either the motor or the eddy-current transmission. Improvement in support, i.e., a tension support member from the saddle gear boxes to the motor, would eliminate a great deal of the deflection and the associated number of failures.

(e) The vehicle control system which regulated vehicle velocity and acceleration and brake deceleration was a commercially available item that is part of the eddy-current transmission. This needed considerable adjustment.

(f) Many collector shoe malfunctions and wear problems were initially experienced. Many different collector shoe designs and collector brushes were tried. However, the number of miles of operation obtained from a set of power collectors is not known since the mileage of each vehicle was not recorded. With the addition of trolley grease to the power rails and the latest collector design, the life is measured in months (3 to 5) as opposed to weeks when testing was initiated.

Trolley grease is applied to the power rails every three months. The Jetrail system was down for two days to apply this grease and to perform general preventive maintenance on the control and power distribution systems.

(g) Considering the torque from a seven and one-half horsepower electric motor, the gear box design appears to be considerably heavier than necessary, thus contributing significantly to the drive train intertia and weight of the vehicle. Whitworth gears are used to transmit the loads. These are non-standard items in the United States and have been changed on some vehicles to American standard gears.

(h) The rubber wheels selected were commercially available wheels designed for a fork lift truck. Although these exhibit reasonable life with heavy loads on smooth floors, they did not perform well on Jetrail. Wheel deflection is the only means of accounting for misalignments of the saddle gear boxes in the lateral plane. The addition of expansion joints in the guideway presented an environment to the wheels which they were not designed to take. Proper implementation of continuously welded rail construction would increase the wheel life

(i) The air conditioning system was undersized for the extremely hot summer temperatures encountered in Dallas. Either more reflective windows or properly accounting for the solar heat load with a larger unit should provide adequate cooling.

Finding 6

(a) Jetrail suffered initial reliability problems. This improved rapidly through a program of scheduled maintenance by a dedicated team of technicians to the point where availability and dependability were 99.9 percent and 97.6 percent, respectively. Although these are based on a limited amount of maintenance data and cannot be considered definitive, they nonetheless represent a reasonable indication of system reliability and dependability of a single vehicle.

The Jetrail operational data used in the calculation of reliability, maintainability, and availability was not recorded in a manner which would facilitate measure of these performance parameters.

(b) Initially Braniff aircraft technicians were used to maintain Jetrail. This did not work well since there was no formal training program and the system maintenance relied on on-the-job training. Technicians were not skilled enough to maintain the system rapidly and effectively. The Braniff operations manager was able to institute a dedicated, exclusive, team of Jetrail technicians at which time a major positive change in reliability was realized.

(c) To buttress this, a further operational change was instituted which put aside two of the ten vehicles as spares. Thus, when a vehicle experienced a malfunction it was quickly taken off-line and replaced with a spare.

The Meantime Time Between Failures (MTBF's) of individual vehicles was found to be approximately 52 hours. The MTBF of all vehicles (eight vehicles and two spares) considered as a subsystem was about 610 vehicle operating hours. The central control and guideway MTBF's were of the order of 3000 and 11,000 hours, respectively, indicating that the vehicles represented the principal source of failures. The majority of the vehicle failures occurred in the propulsion system and vehicle control system, in particular, power collector shoes, propulsion motors, and eddy-current transmissions.

The system with a single vehicle in it has a reliability of about 0.8. When considering a failure to be a delay greater than six minutes and eight vehicles with two spares in the system, the reliability (based on simulation results for a 24-hour period) is 0.97. A key feature of the Jetrail system at Love Field is that if a vehicle experiences a failure on the guideway there is a great deal of redundancy and manual override capability designed into the vehicle which can be used to bring it into the next station. If normal redundancy does not work, the operator can get to the vehicle within six minutes allotted and manually override the controls from within the vehicle. If this is not possible, a following vehicle can be used to push the stalled vehicle. It is not clear how the command and control safety system is disarmed to permit one vehicle to approach another. In any event it is possible to replace a failed vehicle within six minutes. In a larger network this may not be possible unless maintenance technicians and facilities are located sufficiently near to each other to permit a quick response.

Finding 7

The central control system with its redundant blocking represents a reasonably well designed innovative system. In the approximately four years of operation the safety system did not fail to stop a vehicle safely, has required little maintenance, and achieved good operational reliability (estimated MTBF of the order of 3000 hours). This was achieved without the use of expensive, vital relays. Instead it uses smaller MIL-specification aircraft relays. It is capable of being expanded into a larger activity or line-haul system. Off-line stations could be incorporated into the system with the addition of some type of merge logic. The applicability to a network warrants further investigation. A method for system management as well as failure and empty vehicle management are necessary functions that would probably require some degree of computer and software capability.

Finding 8

Due to the short life of the system and initial cost considerations, galvanized-steel power and signal rails were selected. These currently are worn out and require replacement. As previously mentioned, power collector shoes represent a significant number of failures. Hence, a compatible well designed power rail and collector shoe system would enhance operational reliability and maintainability. Such modifications are currently being developed for Astroglide. The latest development indicates that an aluminum rail with carbon and bronze brushes would provide a significantly longer life of the order of fifteen years for the rails.

Finding 9

(a) The guideway was originally installed as a continuous welded beam resting on steel supports. After a few months of testing, it was discovered that thermal distortion of the guideway had caused the beam and column joints to fail in the vicinity of the curved guideway segments. This was corrected by installing expansion joints. The ride quality as a result, was adversely affected as was the wear of the support wheels.

(b) Because of the low vehicle and guideway loads, spread footings were felt to be adequate. However, the foundation analysis did not address differential settling of the piers. Ride quality measurements indicated that settling did not cause comfort problems. However future applications of the system should include an analysis of differential settling.

(c) The vehicle suspension and lateral restraint consist of hard rubber wheels running on the lower flange and against the web of the I-beam. High frequency components due to irregularities of the beam flange and discontinuities at the expansion joints could be felt by the passengers. These accelerations were not excessive when compared with the I.S.O. 2631 one-hour Reduced Comfort Boundary Conditions. Although ride quality measurements did not exceed the standards, more comfort could be achieved by improving the primary suspension system or introducing a secondary suspension system that will provide vibration isolation.

ride quality.

(d) To eliminate the need for superelevation of the guideway the vehicle is suspended to permit roll. Modest roll rates were experienced in the transitions between curved and straight guideway. Vehicle damping is incorporated. The roll rate (no standards extant) did not appear to be more than that of a commercial passenger aircraft. Roll rates can be reduced by careful design of transition sections or by improved design of the suspension system.

Finding 10

(a) Beams in curved segments of the guideway are subject to torsion loads which induce excessive distortion of the beam lower flange and contribute to excessive wheel wear. This was corrected by adding I-beam stiffeners on top of the guideway and cross-bracing between guideways. As a result an aesthetic discontinuity and thicker cross-section was added to the small guideway beam. It resembles a bridge truss.

(b) Each guideway beam segment is supported by steel girders tapering from a 12-inch (30 cm) depth at the guideway to a 24-inch (60 cm) depth at the column. The girders rest on column caps and are welded to the caps. Vehicle loads are transmitted to the columns by a bending moment at these welds which are placed in tension. The welds failed in tension. Gusset plates were installed to attach the underside of the girder to the columns, thereby obtaining the needed girder and column bending continuity through the welds. Part of the load is now carried on shear along the column.

Finding 11

The system is relatively quiet; 71 dB A has been measured in the interior and 72 dB A for the exterior. Typical office noise level is 70 dB A.

Finding 12

(a) Recognizing the deficiencies of the Jetrail system, PRT Systems Inc. carefully assessed each of these areas including reliability, maintenance, and operational limitations in ice and snow environments and decided that a linear induction motor (LIM) could potentially enhance the reliability and maintenance by eliminating the large source of failures in the Jetrail vehicle. In addition, a LIM drive would permit better operations in ice and snow environments.

(b) It should, however, be borne in mind that the LIM system in itself represents a major sub-system development of a motor and motor controller. The motor represents a state-of-the-art device, but the motor controller is to be repackaged. This alone represents a major development requiring extensive testing prior to operation.

Finding 13

(a) The energy consumption of the Astroglide LIM is greater than the Jetrail motor with its eddy-current transmission. This is because the LIM is designed for higher-speed operation (synchronous speed of about 40 mph or 64 km/hr) than the 15-mph (24 km/hr) speed permitted on the Jetrail system. Operation and testing was conducted over a speed range necessitating a great deal of slip - hence an inefficient range of operation. Neither system is efficient at low speed.

((b) The LIM system experiences significant inductive losses in the structural steel guideway. PRT Systems indicates that copper-bearing steel such as, Corten can reduce these losses by 25 percent.

Finding 14

Both Jetrail and Astroglide vehicles can be operated simultaneously on the guideway. That is, they use the same power and control rails.

7. CONCLUSIONS AND RECOMMENDATIONS

Based upon the findings of the preceding section the following recommendations are necessary to make the system suitable for urban applications. They are essentially ordered on a one-to-one basis with the findings.

1. Jetrail has been demonstrated suitable for automated demand-responsive intra-airport loop-transportation with on-line stations. With only a few modifications, such as fire safety and egress, a covering for all weather operation, improvements for reliability and replacement of power rails, it can be improved for use at other airports. For urban applications the following should be considered.

2. A means for rapid emergency egress capable of being used by all members of the traveling pulbic-especially childred, elderly, and handicapped is necessary. Alternatively, an active fire control system, such as, Halon 1301, capable of rapid fire extinguishment without any harmful effects to the passengers could be incorporated thus obviating the need for evacuation. Because TSC investigations have indicated that effecting emergency egress is a particularly difficult solution-hence an active fire control system solution appears more effective.

Fire safety should be designed into the vehicle in accordance with Guideline Specification for Flammability and Smoke Emission TSC-76-LFS-6. That is, all vehicle fire hazards should be eliminated or minimized. However, since carry-on combustibles can not be controlled. It is also recommended that an active fire control system (Halon 1301) be used in conjunction with the passive fire safety technique. The equipment-bay cooling system should be separated from the passenger compartment.

3. If Jetrail is to be used in an environment where ice and snow are prevalent, either a guideway heating system to melt the ice or a cover to prevent accumulation should be used. This is also necessary for Astroglide.

4. The advantages and disadvantages should be carefully weighed between (a) correcting a minimal design effort in the test phase and (b) devoting more time to engineering design and development before entering the test phase.

Insufficient time and effort was permitted for initial design and development under the fixed price contract to preclude many of the design deficiencies encountered. Two schools of thought regarding a design and development approach are: one where a minimal design effort is undertaken and the problems are corrected during the test phase, and the second where careful and extensive design is performed prior to fabrication. The former technique is initially less expensive but has greater risk and variance that can result in higher overall costs than the latter approach. The former technique was employed in the development of Jetrail and resulted in a cost overrun of two-thirds. Careful consideration should be given to the application of these two techniques during the development process. This risk and cost associated with time is also analogous.

5. The approach using off-the-shelf hardware was found inadequate, because many of the components were designed to perform different functions in different environments. Sufficient time and effort should be devoted to a thorough investigation of the use of components as well as to testing of these components to determine their suitability in a specific transportation environment. It should of course be realized that precluding the development of hardware by use of available hardware can result in significant program economy.

If it is desired to use Jetrail rather than the improved Astroglide vehicle, modifications to the motor support would likely reduce maintenance associated with the motor and eddy current transmission. Note that Jetrail and Astroglide vehicles are compatible and can be mixed on the same guideway. In addition, as wear-out of Whitworth gears occurs they should be replaced by American standard gears. The implementation of continuous welded rail should be investigated to increase wheel life.

The HVAC (Heating, Ventilation, and Air Conditioning) system should be resized and made compatible with considered environments. The use of tinted windows may also prove to be advantageous.

6. Although the employment of spare vehicles is dependent on site-specific factors, strong consideration should be given to implementing this policy to increase system reliability.

A team of technicians dedicated exclusively to Jetrail or Astroglide maintenance should be used. To reduce maintenance and improve reliability either Jetrail vehicle modifications should be made, e.g., motor supports should be redesigned or the Astroglide system should be incorporated, given the completion of its development and operation at higher speeds.

7. Although the command and control system can likely be expanded into a larger activity center, to a linehaul system, or to a network system further investigation is necessary to implement system management aspects, including failure and empty vehicle management. The applicability to a network also warrants further investigation - the size of zone, the software required, and hand-over considerations are of particular interest.

8. The galvanized steel power and signal rails are worn out and require replacement. A compatible, well-designed, long-life, power rail and collector shoe system should be incorporated to enhance operational reliability and maintainability.

9. Although ride quality was found acceptable, more comfort could be achieved by introducing a secondary suspension system in the vehicle or in some manner smoothing out discontinuities in the guideway, i.e., by better alignment of the guideway or the incorporation of continuous welded beams.

10. An attempt should be made to redesign the guideway in an aesthetically compatible manner. Perhaps a covering would enhance the aesthetics while protecting against adverse weather and minimizing noise. It should, of course, be realized that this will probably adversely impact the low guideway cost.

11. No sound reduction modifications are necessary since the sound is already within typical urban ambient levels.

12. Astroglide, with its repackaged propulsion control system is a prototype system representing a major modification to the Jetrail vehicle that improves some deficiencies encountered. As such, it is a major development and extensive testing should be done to establish its dependability and maintainability. This should include the collection of proper reliability data including such items as system restoration time, operating hours, and number of vehicle miles on each vehicle.

13. If the operational speed of an Astroglide system is much below the synchronous motor speed of 40 mph, the motor should be redesigned to achieve more efficient operation at the lower velocity. This would likely also imply the redesign of the motor controller. Alternatively the Jetrail system could be modified for use at higher speeds. This would be useful for urban applications.

REFERENCES

1. G.J. Adams, H.L. Warner, and B.B. Crimes, "Jetrail - An Automated System for Transportation of Passengers, Baggage, and Commodities," SAE publication 680706, 1968.
2. J.J. Stickler, G.P. Ploetz, and F.L. Raposa, "Input Power Characteristics of the Thyristor Variable Voltage Power Conditioner," Report No. FRA-ORD&D-74-24, June 1973.
3. G.J. Adams, "Development and Test of an Eddy-Current Clutch Propulsion System," Report No. UMTA-MA-06-0027-73-1, October 1973.
4. G.J. Adams, "Test and Evaluation of an Eddy-Current Clutch/ Brake System," Report No. UMTA-MA-06-0027-74-2, February 1975.
5. I.L. Kosow, "Electric Machinery and Transformers," Prentice-Hall, Inc., Englewood Cliffs, N.J., 1972.
6. G. Fitzgerald, C. Kingsley, and A. Kusko, "Electric Machinery," third edition, McGraw-Hill Book Company, New York, 1971.

APPENDIX A

POWER DISTRIBUTION AND CHARACTERISTICS

A-1. POWER MEASUREMENTS INSTRUMENTATION

As part of the assessment program a team from TSC visited the Jetrail facility and made power characteristic measurements, during the week of Dec. 8, 1975. Measurements were made with instruments calibrated at TSC and shipped to Dallas for the tests. The instrumentation consisted of:

1) An instrumentation package housing watt, VAR, voltage, and current transducers.
2) A true RMS current converter.
3) A four channel instrumentation tape recorder.
4) Miscellaneous general purpose instruments (power supplies, oscilloscope, VTVM, etc.).

Data was taken by connecting the power measurement components between the input circuit breaker and the power conditioner. Since the LIM system is powered through its own circuit breaker, the LIM measurements excluded the auxiliary power. The air-conditioner and lights on the eddy current vehicle were disconnected to limit measurements to propulsion related components. With these loads removed, the standby power on each vehicle was approximately 2 kW. Figure A-1 is a block diagram of the power measurement system as installed on the vehicles. Transformers were used as required to maintain input levels within the specifications of the various transducers.

The current inputs to the watt and VAR transducers were taken from current transformer taps, which allowed their sensitivities to be varied over a 6 to 1 range. Voltage inputs were supplied from potential transformers mounted in the instrumentation package. The true RMS converter is a Hall-effect device whose output is a dc voltage proportional to the true RMS current magnitude. It also provides an output which is a replica of the input current waveform. This replica was used for oscilloscope observation and for instantaneous current waveform recording.

Velocity data was recorded directly from tachometer outputs in the vehicle control console. The eddy current clutch driven vehicle tachometer output consists of pulses from a magnetic pick-up, whose output frequency is proportional to vehicle velocity. The pulse output was recorded in the field. It was converted to a dc voltage proportional to vehicle velocity by a frequency-to-voltage converter during data reduction at TSC. The LIM vehicle velocity voltage is the output of a tachometer generator which generates a dc voltage proportional to vehicle velocity. This voltage was recorded directly and used as recorded during data reduction.

Continuous recordings of watts, VAR's and RMS current were made on three channels of the recorder, while the fourth channel was used for recording all other data: voice, voltage, velocity or instantaneous current.

The watt, VAR and voltage transducers are rated for inputs of 150 volts RMS. Potential transformers, included in the instrumentation package, step the input 480 volts down to 120 volts, and provide the input potentials for these transducers. The watt and VAR transducers are rated for input currents of 5 amperes RMS. They were supplied from tapped current-transformers with four output ranges: 6:1, 12:1, 24:1 and 36:1. Transformer taps were changed as required to adjust the sensitivity of the instrumentation when it was moved from one vehicle to the other.

The output signals of the transducers are 0 to 1.0 mA dc current signals whose magnitudes are proportional to the magnitude of the measured parameter. The watt transducer signal is 1.0 mA at an input power level of 1.0 kW, and the VAR transducer signal is 1.0 mA for an input level of 1.0 kVAR. As used in the Jetrail tests, with potential transformers and current transformers,

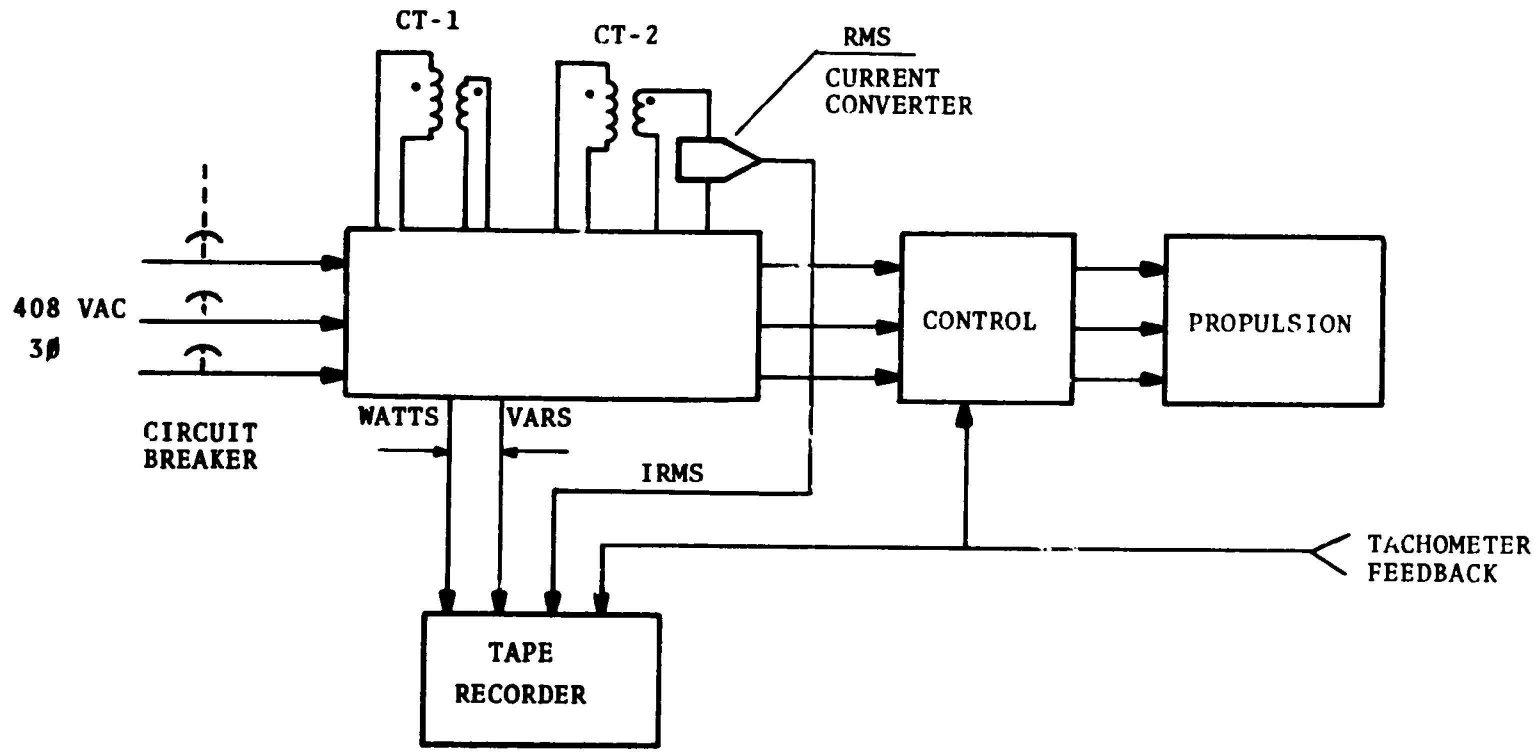

FIGURE A-1. POWER MEASUREMENT INSTRUMENTATION CONFIGURATION these instruments had the following sensitivities:

	LIM	Eddy Current
Watts:	96 kW/V	48 kW/V
VAR's:	96 kW/V	48 kVAR/V.

Connected in the proper polarity, the watt transducer output is positive when power flow is into the load and negative when power flow is from the load to the source (regeneration). The VAR transducer output is positive for a lagging power factor and negative for a leading power factor. The watt transducer, which responds to the instantaneous product of voltage and current, is valid for both sinusoidal and distorted excitation. The VAR transducer, on the other hand, relies on a phase shift network to shift the phase of the current 90°. Therefore, it is only accurate for the 60 Hz component of excitation. The reactive power components of the LIM system must be calculated from volt, ampere, and VAR measurements, but for the eddy current clutch system the VAR transducer provides total reactive power measurements.

The RMS current converter was connected to the output of a current transformer, thus its output must be corrected by the current transformer ratio. As used in the Jetrail measurements, the RMS current converter has an absolute sensitivity of

LIM = 1.4 mV/A

EEC = 2.8 mV/A

The instrument sensitivities are calibrated for each transducer. The gain settings on the instrumentation tape recorder, however, were not calibrated to reproduce a volt-for-volt output. Rather, the gain was adjusted to maintain the recorder levels within the limits indicated on the recorder level meter. Calibration voltages were recorded at the start and the end of each tape to provide a recorder calibration transfer ratio from which an absolute transfer ratio could be obtained. Sensitivities of individual strip-chart recorder traces are indicated on the individual trace records.

The power in the Jetrail system can be resolved into components according to the following criteria:

1) Apparent power is the total volt-ampere power which flows into the system. It is the sum of the products of RMS phase voltage and RMS phase current measured from the line to neutral.

$$S_t = 3(V_{1-n})(I_{1-n})$$

or in terms of RMS line voltage the RMS line current

$$S_t = 3(V_1)(I_1)$$

2) Active power, P, is that component of apparent power which is dissipated in the system as either load power or as losses. It is also known as "effective", or "real" power, and it is the time rate of energy consumed by the system.

3) Reactive power, Q, is that component of apparent power which contributes to the total volt-amperes of a system but not to active power.

4) System power factor is the ratio of the active power to the apparent power, (used power to demanded power), it is also the cosine of the angle between the apparent power and the active power.

The power factor of the system should be at a maximum, and the apparent power at a minimum. Active power and apparent power can be reduced by decreasing the load or increasing efficiency. More significant apparent power reductions and power factor improvements may be achieved by reducing the system reactive power. This can be accomplished by minimizing, or compensating for, reactive power loads (inductive and magnetic circuits) and reactive power sources (switching circuits).

There is reactive power in induction motors, rotary and linear, because they develop power by the interaction of excitation magnetic fields in their primaries (stators) and induced magnetic fields in their secondaries (rotors and rails).

The apparent power of the magnetic circuits is lagging reactive power which circulates between the magnetic circuit and the source at the supply frequency. This reactive power is not dissipated in the load, but it is part of the apparent power and is measured by demand-responsive meters.

The air-gap reduces the magnetic circuit coupling, thus a stronger excitation field is required to maintain the flux coupling, if the motor is to develop a given torque.

Rotary motors, which have small fixed air-gaps, require low excitation levels and yield operational power factors of 0.8 or higher. Linear motors in general, and those installed on the Jetrail vehicle in particular, operate at air gaps between 1/4 and 1/2 inch (6 and 12 mm) and require much more reactive excitation current to force the flux across the larger gap. The increased excitation levels result in high reactive power levels and low power factor. The LIM characteristics of Figure A-2 show a power factor of less than 0.5 with an air-gap spacing of 0.39 in. (10 mm).

To improve the system power factor of the LIM vehicle, each LIM power conditioner includes a bank of power factor correction capacitors connected in a delta configuration of 195 microfarads per leg. Each delta grouping is connected across the input lines between the circuit breakers and the power conditioner on the power conditioner side of the thyristor protection fuses. The impedance of each delta branch is

$$X_c = 1/ (377)(195 \times 10^{-6}) = 13.6 \text{ ohms},$$

The phase current in each branch is

$$I_\phi = 480/ 13.6 = 35.3 \text{ A}$$

and the line current is

$$I_1 = 3 (35.3) = 61.1 \text{ A}.$$

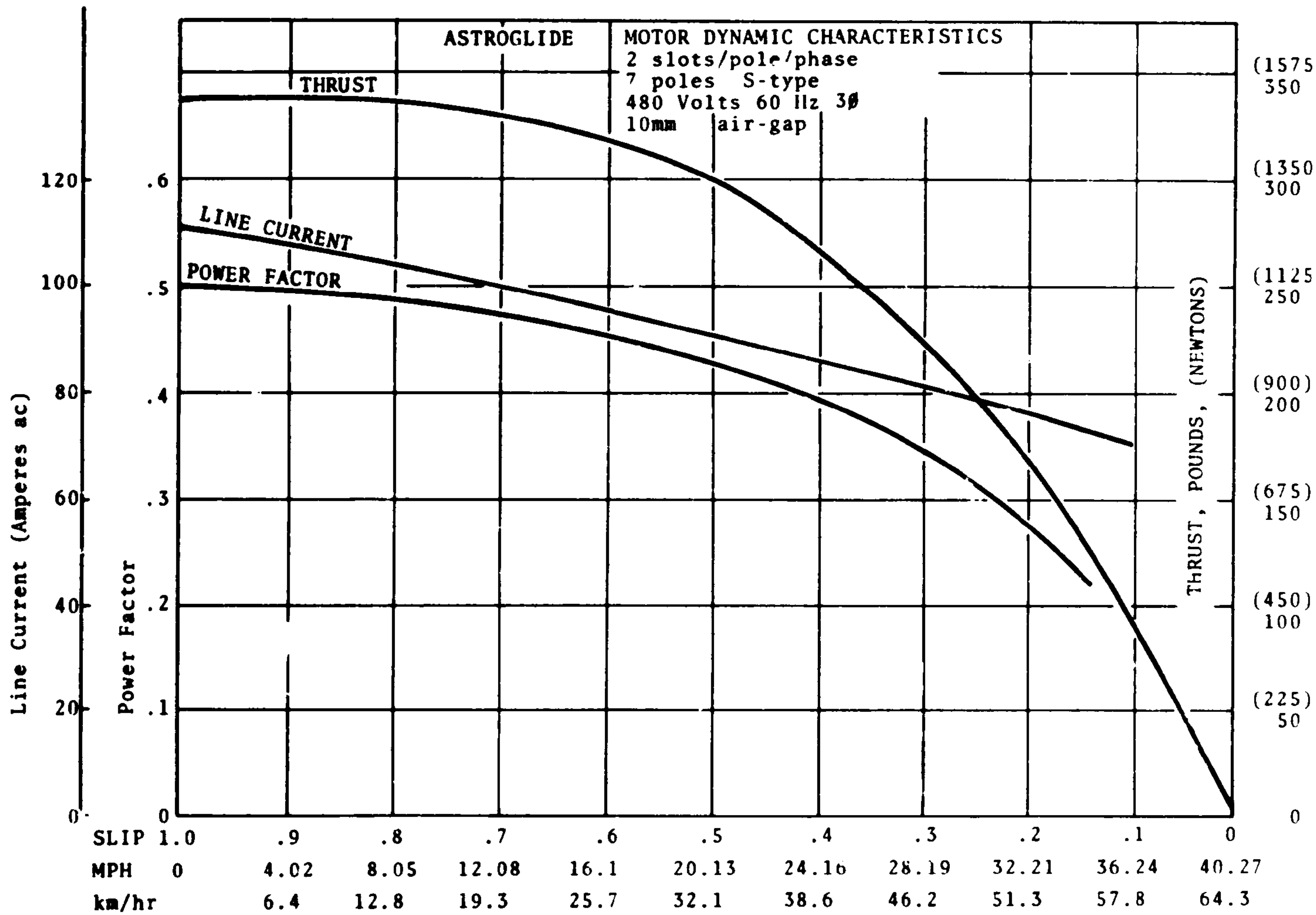

FIGURE A-2 ASTROGLIDE LIM CHARACTERISTICS

For the two motors this results in an input current of 122 amperes. The apparent power of these capacitors is

$$S = 3(480)(122) = 102 \text{ kVAR}.$$

This apparent power is leading reactive power with a power factor of zero. When the vehicle is in a coasting condition, and the power conditioners are phased back to "off", these capacitors comprise the major part of the load and draw the 100 kVAR of reactive power. For all other operating conditions, the capacitors serve as a source of reactive power and improve the power factor.

In addition to reactive power in the motor excitation there is reactive power flowing in a system with phase control, such as the LIM system. This is caused by two phenomena:

a) The delay of thyristor turn-on results in additional phase displacement of the current and voltage waveforms, and hence in a displacement component of reactive power. Displacement is introduced by reactive elements and by phase control, both of which change the phase between the current and voltage.

b) The chopping action of the phase control system generates harmonic currents which distort the waveforms and produces a distortion component of reactive power. Distortion is a component of reactive power because the harmonics do not contribute to active power, but they do contribute to total apparent power.

A-2. ACCELERATION CHARACTERISTICS

Acceleration characteristics for the two vehicles are shown in Figure A-3. The construction lines drawn over the vehicle velocity voltages show the method used to calculate acceleration for each vehicle. The initial acceleration of the LIM vehicle is

$$dv/dt = (18.5)(0.64)/(1 \text{ sec}) = 11.8 \text{ ft/sec}^2 \ (2.9 \text{ m/sec}^2)$$

$$= 0.37g$$

The eddy current transmission acceleration is:

$$dv/dt = (42.5 \text{ div})(0.42 \text{ ft/sec } (0.13 \text{ m/sec})/\text{div.})/(4.6 \text{ sec})$$

$$= 3.88 \text{ ft/sec}^2 \ (1.18 \text{ m/sec}^2) = 0.12 \text{ g}$$

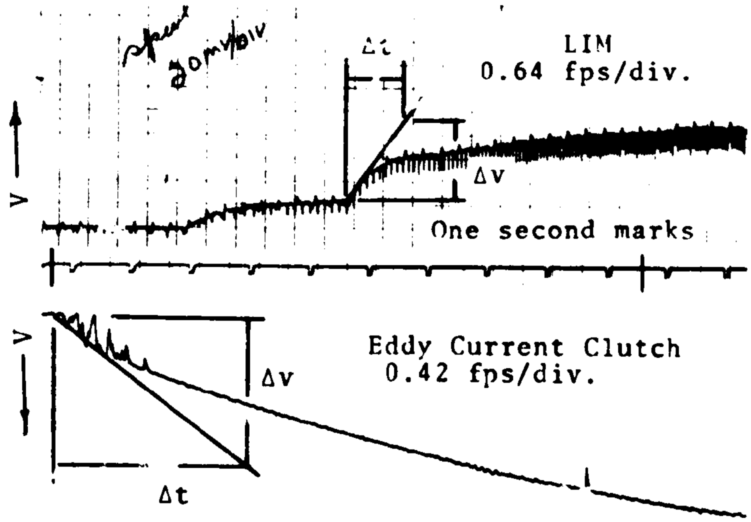

FIGURE A-3 ACCELERATION CHARACTERISTICS

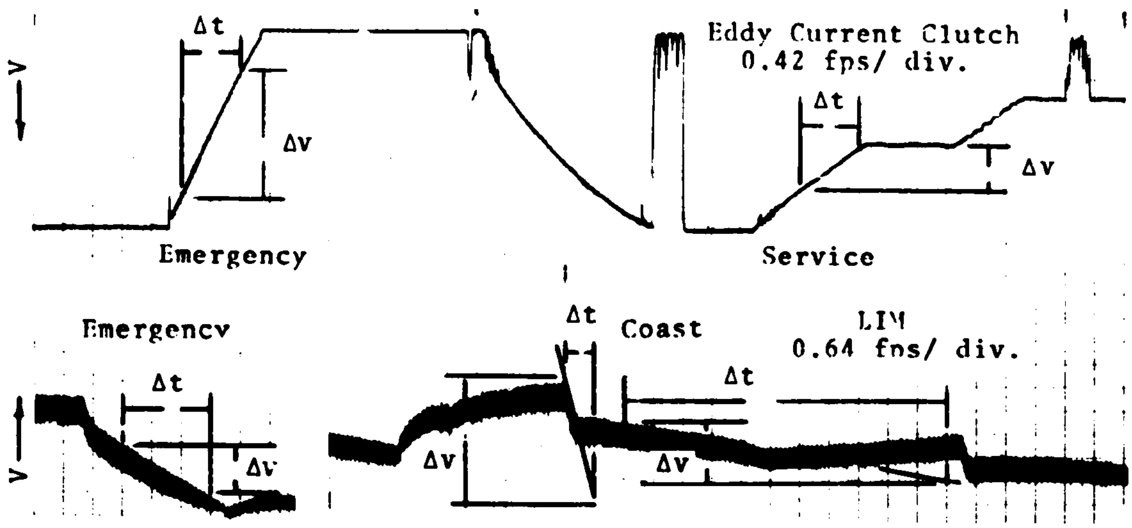

FIGURE A-4 DECELERATION CHARACTERISTICS

The eddy current transmission accelerations are comparable to published figures (1).

The LIM vehicle changes from a supported position to a levitated position, where it is attracted to the rail, and it is prevented from contacting the rail by the lower guide wheels. During the interval when the vehicle is being levitated there are no rolling friction forces, and the velocity increases suddenly until the lower wheels come in contact with the rail and frictional forces appear. The acceleration is reduced appreciably from that point as the vehicle accelerates to maximum speed.

The instrumentation did not have the capability to resolve jerk (da/dt) from the velocity data.

Decelerations, with construction lines used for calculations, are shown in Figure A-4. Two rates are shown for the eddy current transmission vehicle: emergency braking and service braking.

The emergency brake rate is:

$$\frac{dv}{dt} = \frac{(25 \text{ div.})(0.42 \text{ fps/div.})}{4 \text{ sec}} =$$

$$= 0.081 \text{ g}$$

The service brake rate is:

$$\frac{dv}{dt} = \frac{(9 \text{ div.})(0.42 \text{ fps/div.})}{4 \text{ sec}} = 0.94 \text{ ft/sec}^2 \ (0.28 \text{ m/sec}^2)$$

$$= 0.03 \text{ g.}$$

Three deceleration slopes are shown for the LIM vehicle. The first is for emergency braking, which is

$$\frac{dv}{dt} = \frac{(11 \text{ div.})(0.64 \text{ fps/div.})}{6 \text{ sec}} = 1.17 \text{ ft/sec}^2 \ (0.35 \text{ m/sec}^2)$$

$$= 0.035 \text{ g.}$$

The second slope is the initial deceleration which occurs at the beginning of each deceleration phase. The vehicle does not actually brake at this time - the power conditioner is phased off and the vehicle coasts to its new command velocity. In the transition from powered to coasting operation, a portion of the vehicle kinetic energy is lost, and the vehicle velocity decreases rapidly. This deceleration is

$$\frac{dv}{dt} = \frac{(35\text{ div.})(0.64\text{ fps/div.})}{2\text{ sec}} = 11.2\text{ ft/sec}^2\ (3.4\text{ m/sec}^2)$$

$$= 0.35\text{ g.}$$

After the initial velocity decrease, the vehicle coasts until it either reaches a lower speed or receives an acceleration command. The coasting deceleration is:

$$\frac{dv}{dt} = \frac{(5\text{ div.})(0.64\text{ fps/div.})}{10.4\text{ sec}} = 0.308\text{ ft/sec}^2\ (0.90\text{ m/sec}^2)$$

$$= 0.01\text{ g.}$$

A-3. EDDY CURRENT TRANSMISSION PERFORMANCE CHARACTERISTICS

Typical data taken for the eddy current transmission driven vehicle is shown in Figure A-5 with a set of operating points identified. Parameter values, computed from transducer outputs at those points, are listed in Table A-1. Current waveforms were observed for all operating conditions. This is indicative of a system without harmonics and distortions power. Since there is no waveform distortion, all reactive power is displacement reactive power, and the VAR transducer output is a true indicator of the total system reactive power. Power demand in kVA, as measured with the watt and VAR transducers, is comparable to the demand computed from current and voltage measurements. This correlation of measurements contrasts to the LIM vehicle measurements where harmonic distortion of the system necessitates that displacement and distortion components of reactive power be separated.

Eddy current transmission vehicle power characteristics are similar to those of any induction motor system operating directly across the input lines. Voltage and current at the motor remain sinusoidal, thus there is no distortion reactive power, and the

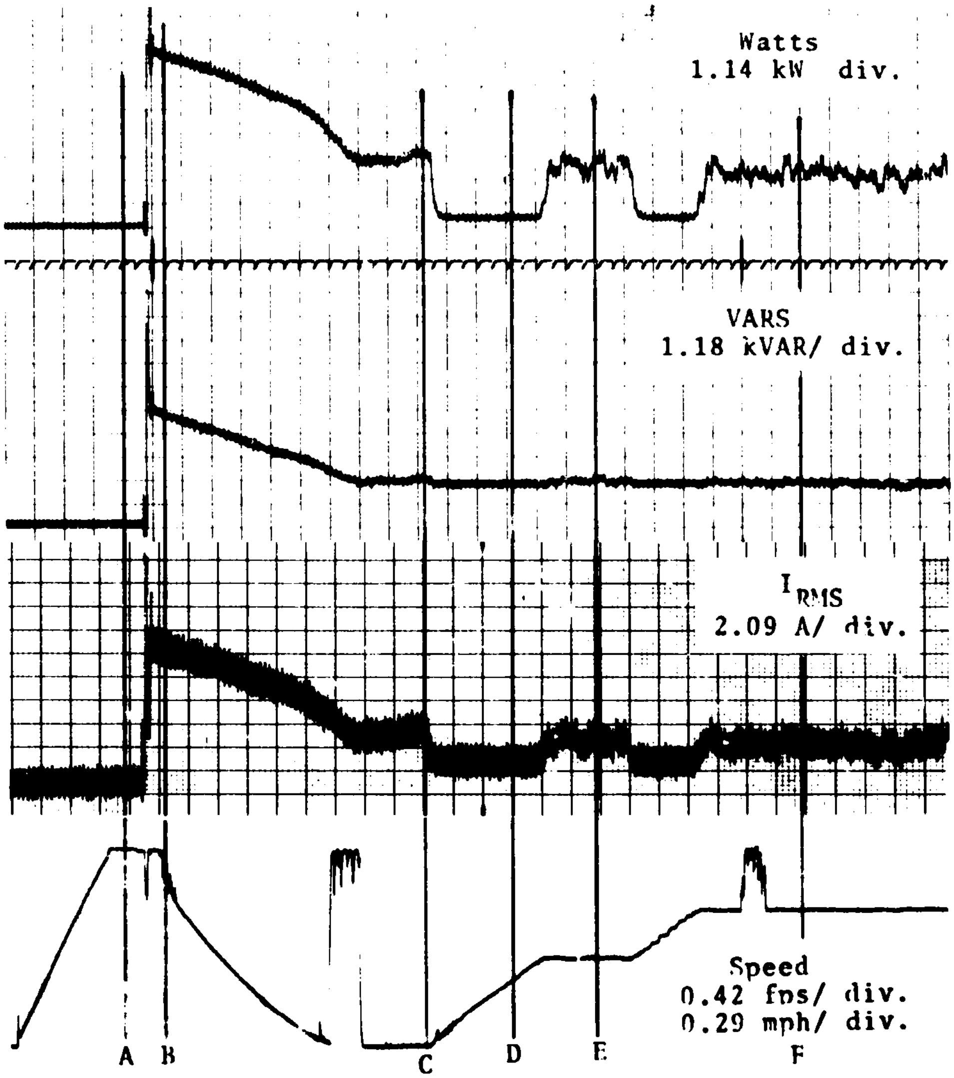

FIGURE A-5 EDDY CURRENT CLUTCH VEHICLE POWER CHARACTERISTICS

TABLE A-1. EDDY CURRENT TRANSMISSION VEHICLE POWER CHARACTERISTICS

	Condition	Active Power kW	Reactive Power kVAR	Current I_{rms}	Apparent Power kVA	Power Factor PF	Remarks
A	Standby	0.57	1.2	4.18	3.5	.16	
B	Acceleration	42.2	29.5	67	55.5	.76	Note 1
C	12.3 mph	17.1	11.8	29.3	24.3	.70	
D	Brake	2.3	11.2	15.7	13.0	.17	Note 2
E	7.0 mph	16.	11.8	27.2	22.6	.71	
F	4.1	13.7	10.6	25.1	20.8	.66	

Notes:

1. Peak Values, levels decrease linearly to cruise levels.
2. Continuous during braking

system operating power factor is reasonably high, near 0.7, for all load conditions.

Standby conditions are illustrated at point "A", where the only power drawn for the vehicle is control power. At this point the motor is off and the measured current is a single phase current supplying the energized portions of the auxiliary power systems. Although the power factor is low (0.16), the input levels are all very low, and the impact on system power characteristics is negligible.

Peak power is drawn during acceleration from a standstill, "B", where the vehicle requires 42.2 kW. At this point reactive power is also at a peak, 29.5 kVAR, and apparent input power is 55 kVA at a power factor of 0.76. Acceleration from a lower velocity to any higher velocity requires approximately 5 kW less peak power. As the vehicle speed increases, the power consumption decreases from the acceleration level to the cruise power levels.

Command	Power	Speed mpg	Speed km/hr	Point
4	17.1 kW	12.5	20	C
3	16 kW	7.2	11.5	E
2	13.7 kW	4.1	6.6	F

Reactive power, apparent power, and power factor for each of these conditions are comparable. Reactive power is between 10.6 and 11.8 kVAR, apparent power is between 20.8 and 24.3 kVA, and the power factor is between 0.66 and 0.71.

These figures are taken for a vehicle moving on the uphill section of guideway between the airline terminal building and the parking lot station. Power levels for the downhill return trip are slightly lower.

Profiles of RMS current and reactive power are similar to the real power profile except during deceleration (point "D") when the eddy current brake is applied. This point is a normal service brake operating point where vehicle kinetic energy is absorbed in the eddy current brake and the motor is idling. Power consumed is approximately 0.5 kW of auxiliary power and 1.7 kW of eddy current brake power. The 11.2 kVAR of reactive power is supplied for motor excitation. Power factor at this point is 0.17; however, the power factor rises to the 0.7 level for motor powered conditions.

A power characteristic profile for a single trip around the guideway is shown in Figure A-6. The vehicle leaves the airline terminal and follows the trip profile described in Section 4.2.1. Differences in power levels on the uphill and downhill sections are apparent, particularly in the long intervals of speed-4 operation. Comparative power component levels for the uphill and downhill segments are listed in Table A-2 of Section A-4. The tabulated values are typical cruise values for the vehicle on the Jetrail guideway. Reactive power, which is primarily motor excitation, is almost constant for all conditions; power levels increase or decrease in proportion to the torque required, as do apparent power and power factor.

A-4. LIM PERFORMANCE CHARACTERISTICS

The LIM vehicle characteristics are more complex than the eddy current transmission vehicle because of the distortion effects and power factor correction by capacitors. Measurements of the LIM vehicle characteristics were made.

A segment of a LIM vehicle power characteristic profile is shown in Figure A-7. Four operating points are identified; their parametric values are listed in Table A-3 and photographs of the instantaneous current waveforms are shown in Figure A-8.

The first of the four identified conditions, "A", is the vehicle coasting condition where the power conditioner is phased "off". At this time the power factor correction capacitors comprise the major load. The vehicle draws 2 kW of standby power, while 10^3 VAR of leading reactive power is supplied to the capacitors. The system apparent power is 93 kVA at a power factor of 0.02. The 111 amperes recorded by the current transducer is exceeded only during vehicle acceleration. This high current

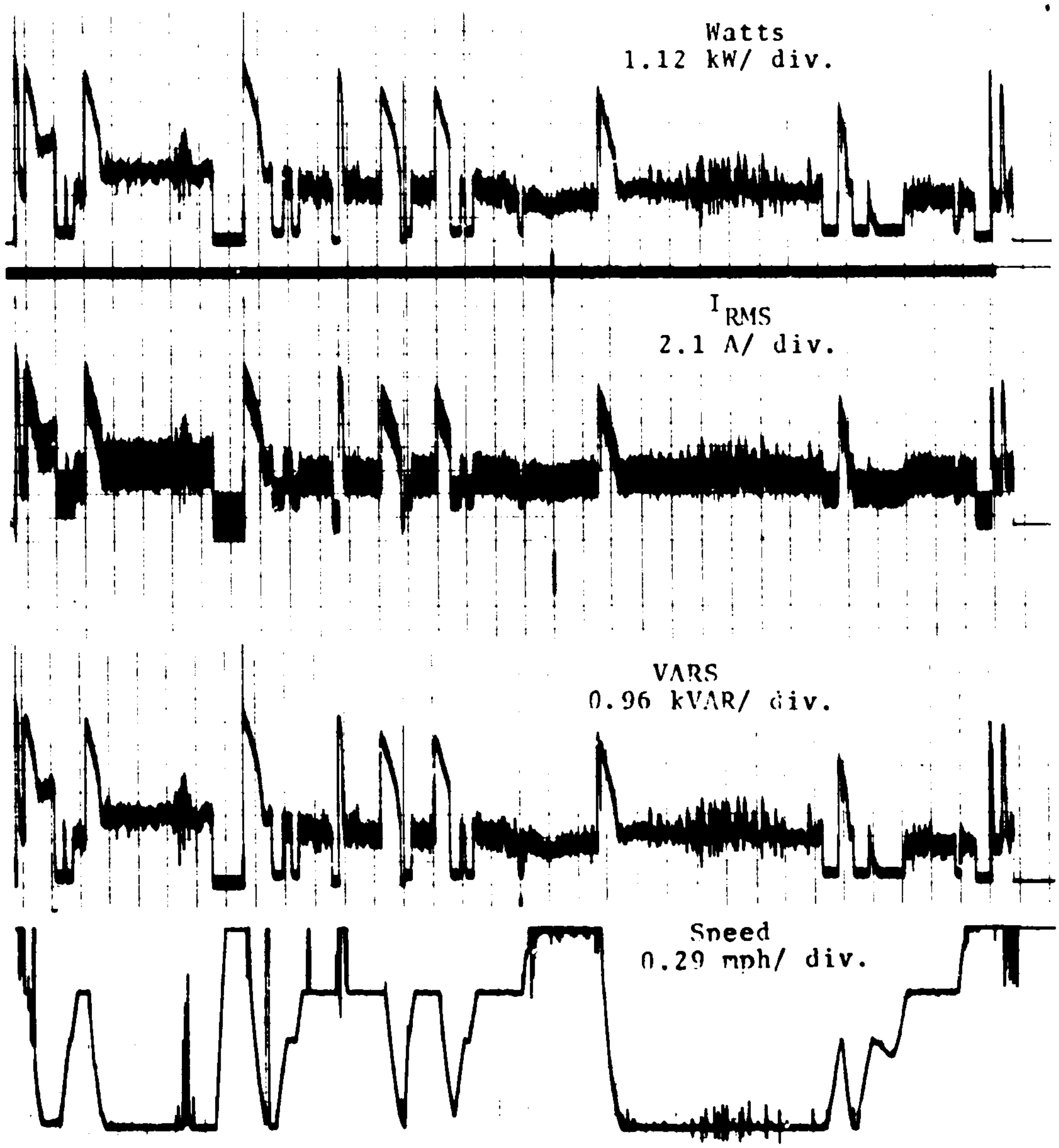

FIGURE A-6 EDDY CURRENT CLUTCH POWERED VEHICLE

TABLE A-2. COMPARATIVE POWER CHARACTERISTICS

Eddy Current Clutch

	UPHILL					DOWNHILL				
Speed	KW	KVAR	IRMS	KVA	PF	KW	KVAR	IRMS	KVA	PF
1	*	*	*	*	*	9.1	10.6	22	17.9	.51
2	12.5	10.6	23	18.7	.67	10.3	10.6	23	18.7	.55
3	14.8	11.8	25	20.4	.73	11.2	10.6	23	18.7	.60
4	17.1	11.8	28.2	23	.61	13.7	10.6	23	18.7	.73

*not available

LIM

	UPHILL					DOWNHILL				
Speed	KW	KVAR	IRMS	KVA	PF	KW	KVAR	IRMS	KVA	PF
1	29.3	62.8	69.3	56.4	.52	27	63.8	69.3	56.4	.48
2	31.5	64.1	71.4	58.1	.54	27	63.3	69.3	56.4	.48
3	31.5	64.1	71.4	58.1	.54	22.5	63.3	67.2	54.7	.41
4	40.5	61.3	73.5	59.8	.68	29.3	44.1	65.1	53.0	.55

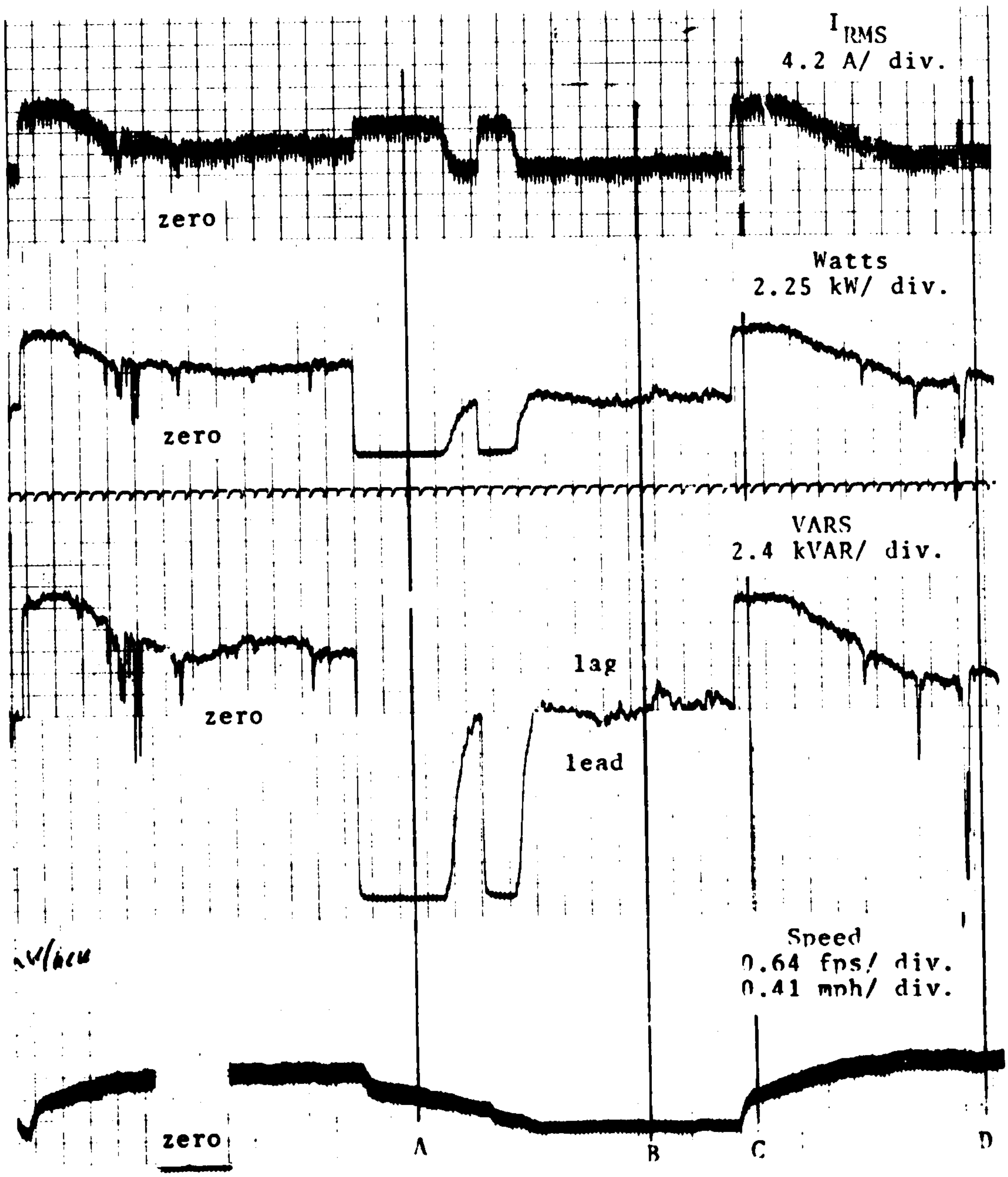

FIGURE A-7 LIM VEHICLE;TYPICAL OPERATING CHARACTERISTICS

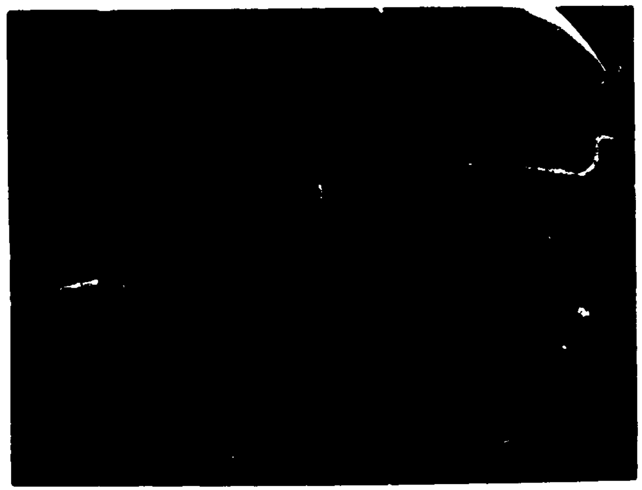

COAST

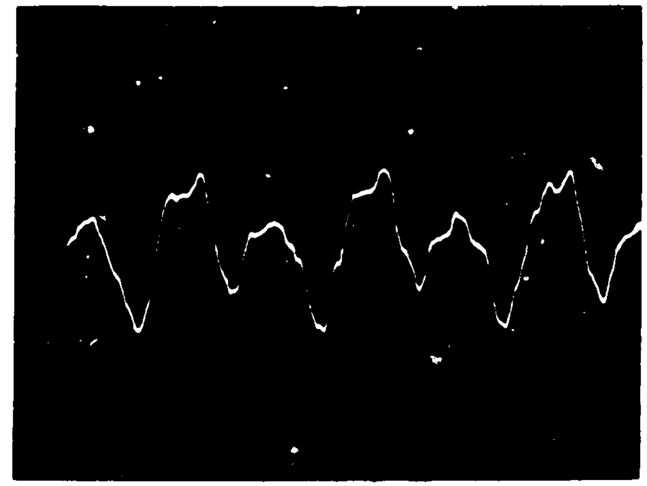

HIGH SPEED CRUISE

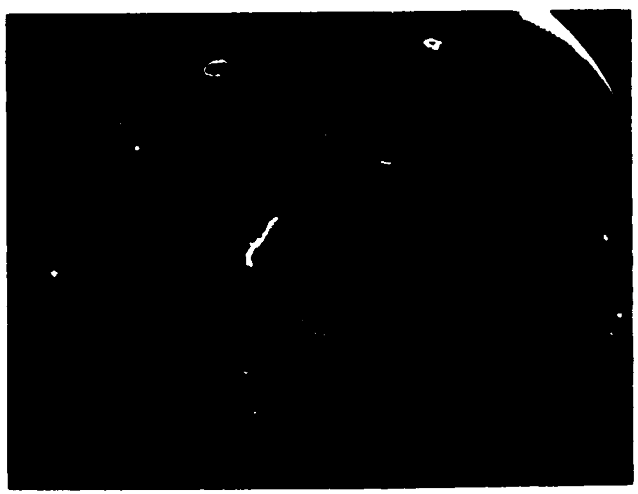

LOW SPEED CRUISE

ACCELERATION

FIGURE A-8 LIM VEHICLE CURRENT WAVEFORMS flows into the vehicle, the power conditioner circuit breakers are on, and the power conditioner is phased off. The coasting current level is also the standby current level.

The second identified condition, "B", is a low speed cruise condition. The vehicle requires 27 kW of power at a system power factor of 0.5. The reactive power measured by the VAR transducer is approximately zero, indicating a power factor of 1.0. However, there is 47 kVAR of distortion reactive power which reduces the system power factor to 0.5. At this low speed cruise point the power factor correction capacitors supply just enough leading reactive power to compensate the lagging displacement reactive power. Input current is 67 amperes (RMS), and total apparent power is 54 kVA.

The third condition, "C", is during vehicle acceleration. At this point the power, current, and reactive power are at their maxima. The vehicle requires 70 kW of power at a corrected lagging power factor of 0.75, with an input current of 130 amperes (RMS) and a total apparent power of 105 kVA. The system reactive power is 78 kVAR with 62 kVAR of displacement reactive power and 47 kVAR of distortion reactive power.

The final identified condition, "D", is high speed cruise. The power required is 39 kW at a power factor of 0.66. An input current of 74 amperes (RMS) yields an apparent power demand of 60 kVA. Total reactive power is 45 kVAR, which consists of 19 kVAR of displacement reactive power and 40 kVAR of distortion reactive power. The power factor correction capacitors correct the displacement power factor to 0.9 under these cruise conditions, but the distortion levels reduce the total corrected power factor to 0.66.

For the three powered conditions described, there is a distortion power component of 40 to 47 kVAR. The effects on the current waveforms are shown in the photographs in Figure A-8. The distortion in each case is apparent, in standby and coasting conditions the power conditioner is phased "off" and distortion is minimum. The improvement in displacement components is apparent in Table A-3, which shows displacement power factors greater than 0.75 for the powered conditions.

A power characteristic profile for a single trip around the guideway is shown in Figure A-9. The vehicle leaves the airline terminal and follows the trip profile described in section 4.2.1. Differences in power levels between the uphill and downhill sections are apparent, particularly in the long intervals of speed-4 operation. Note the wide excursions in the reactive power transducer outputs and the high input current levels during coasting intervals where the power is minimal. Comparative power levels for the uphill and downhill segments of operation are listed in Table A-2, Comparative Measurements.

The LIM vehicle control system did not hold the vehicle at constant speed on all guideway sections. In addition, accelerations and decelerations were too slow for the vehicle to stablize at new speeds in the relatively short, slow-speed segments of guideway. The comparative power levels, therefore, are not as stable or repeatable as they were with the eddy current clutch vehicle. The typical measurements listed in Table A-2 illustrate the marked differences in power levels, current levels, reactive power, and power factor between the two vehicles. The measurements indicate that the LIM power levels are approximately twice the power levels of the eddy current clutch system, and that current and apparent power are almost three times those of the eddy current clutch vehicle. These high levels were measured despite the fact that the LIM vehicle is lighter than the eddy current clutch vehicle. The LIM power factor is approximately 0.6 for all cruise conditions.

For most cruise conditions and for all downhill cruise conditions, the VAR transducer indicated a leading reactive power. The distortion reactive power, however, made the net reactive power lagging and forces the power factor to lower levels than indicated by the VAR transducer outputs. The values of the power factor correction capacitors installed on the vehicle may be correct for the application, however they cause wide excursions in the phase angles

TABLE A-3 LIM VEHICLE POWER CHARACTERISTICS

D	CONDITION	Line Current I A_{RMS}	Power P KW	System (total) Reactive power Qt KVAR	Displacement Reactive Power Qd KVAR	Distortion Reactive Power Qh KVAR	System (total) Apparent Power St KVA	Displacement Apparent Power Sd KVA	Displacement Power factor Pf_d	System Power Factor Pf_t	
A	COAST	111	2	103	103	0	93	103	.02	.02	
B	Low Speed Cruise	67	27	47	0	47	54	27	1.0	.5	
C	ACCEL	130	70	78	62	47	105	94	.75	.67	Note
D	High Speed Cruise	74	39	45	19	40	60	44	.90	.66	

Note: Sustained Values; linearly decreasing to cruise levels after 4 sec.

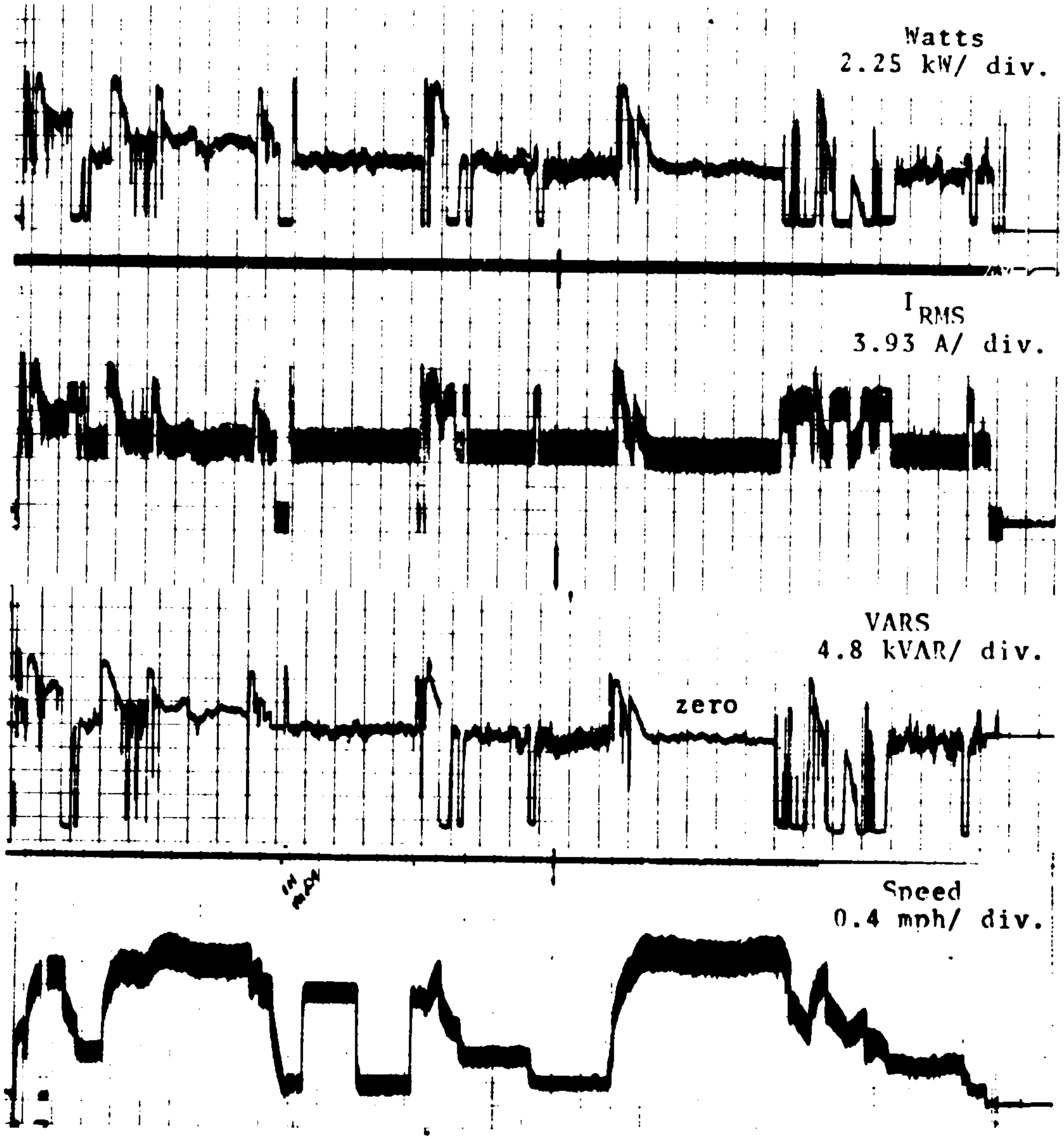

FIGURE A-9 LIM POWERED VEHICLE

of current and in the phase angles of the reactive power components. Without distortion components the vehicle would operate near a unity power factor or a slightly leading power factor for the downhill segments of the trip profile.

The LIM power characteristics reflect distortion to displacement reactive power ratios greater than 100%. Stickler, Ploetz, and Raposa (2) have reported distortion to displacement ratios of 33% for a rotary induction motor operating with phase control at approximately 50% of synchronous speed. The Jetrail calculations are comparable when uncorrected displacement reactive power is used in the computations. The reactive power indicated by the VAR transducer is net displacement reactive power as corrected by the capacitors, but actual displacement reactive power flowing in the LIMs exceeds the indicated value by 100 kVAR. The degree of improvement in the power factor and reduction in total apparent power can be determined from analysis of the system phasor diagrams, which are shown in Figures A-10 to A-12.

Figure A-10 is a phasor diagram showing the measured system power components at point "B". Phasor magnitudes and directions in this figure and in Figures A-11 and A-12 are drawn to the same scale. Phasor S_t is the system apparent power from the RMS measurements, phasor P is the power measured by the watt transducer, and phasor Q_t is the total reactive power calculated by vector subtraction of P from S_t. θ is the power factor angle.

The RMS current used to calculate total reactive power contains both fundamental and harmonic components. These components combine vectorially to produce the RMS line currents, i.e.,

$$I_1 = \sum_{n=1}^{n=\alpha} I_n^2$$

where: I_L = RMS line current

n = order of harmonic

I_n = RMS value of nth harmonic.

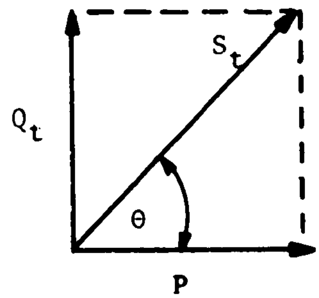

FIGURE A-10 SYSTEM POWER COMPONENTS

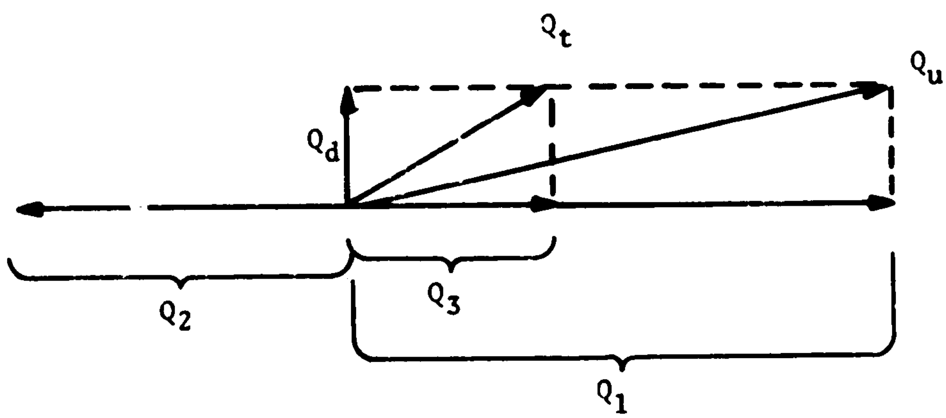

FIGURE A-11 REACTIVE POWER COMPONENTS

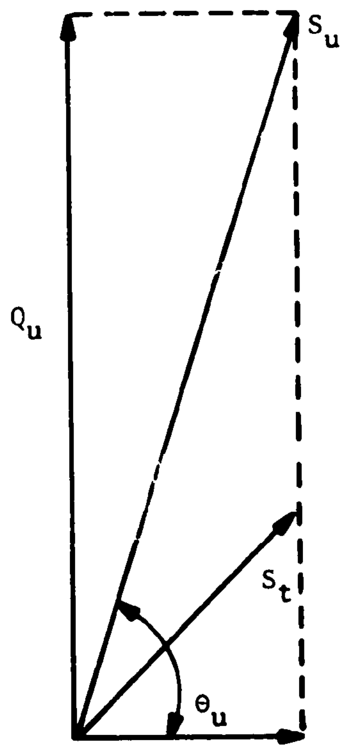

FIGURE A-12 UNCORRECTED POWER COMPONENTS

Since the harmonic distortion components contribute to the total RMS value vectorially, the distortion reactive power components also contribute vectorially to total reactive power. This is illustrated in Figure A-11, which is a phasor diagram of the displacement and distortion components of reactive power. Phasor Q_2 represents the leading 100 kVAR supplied by the power factor correction capacitors, Q_3 is the reactive power measured by the VAR transducer, and Q_1 is the uncorrected displacement reactive power computed by vector subtraction of Q_2 from Q_3. Q_d represents the distortion reactive power. It is determined by vector subtraction of Q_3 from Q_t. Vector additon of Q_1 and Q_t yields Q_u, the total uncorrected reactive power which would flow in the system if the power factor correction capacitors were removed.

The effects of the capacitors are indicated in Figure A-12, which is the system phasor diagram with the uncorrected values superimposed over the corrected parameters. The difference in apparent power and reactive power which result from the capacitors is clearly displayed.

A-5. DISTORTION

Systems which control power by interrupting current flow, as the LIM controller does, generate harmonics and distortion reactive power whose effects must be considered when evaluating power characteristics. Distortion reactive power has not been treated as an objectionable feature of phase-controlled power conditioning, and attempts to minimize it have been made only when interference problems have been traced to the power conditioner. In this report, distortion is considered as a power component which affects apparent power, reactive power, and power factor. The evaluation of possible external interference effects are not within the scope of this document.

The distortion phenomena can be isolated by performing a wave analysis of a distorted waveform, and separately evaluating the effects of the fundamental and its harmonics. A wave analysis of the instantaneous current waveform, recorded during vehicle tests, was performed at TSC using a wave analyzer as a bandpass filter.

The filter bandwidth was adjusted to pass the frequencies of interest, and the outputs are shown in Figure A-13. The figure shows the LIM vehicle power characteristics during the approach to the airline terminal building. Five traces are shown and two operating points are identified.

The first trace is the output of the analyzer adjusted for a bandwidth of 3100 Hz, which includes the fundamental and any of the first 50 harmonics. It is essentially a reproduction of the RMS input current waveform similar to the RMS converter output of Figure A-9. The principal difference between the two is that the output of the RMS converter is a linear output, but the output of the analyzer is in decibels (logarithmic).

The second trace shows the output of a wave analyzer with a bandwidth of 10 Hz centered 60 Hz. This trace is a reproduction of the fundamental component of the input current waveform. The high-amplitude oscillations apparent in the trace are due to the rapid phase changes brought about when the conditioner is phased between the coasting condition (phase angle leading 90°) and the powered condition (phase angle lagging). High amplitude oscillations also occur when the conditioner is phased between the powered and coasting condition, i.e., from a lagging phase angle to a 90° leading phase angle.

Trace 3 is a record of watts, trace 4 is a record of VAR's and trace 5 is a record of vehicle speed. The scales for these latter three are linear, and their ranges are shown in the figure.

The first operating point of interest is identified as point "A" in Figure A-13. This condition is the vehicle coasting condition when the power conditioner is phased back to "off", and the principal current is the leading current through the power factor correction capacitors. During this interval the VAR transducer indicates 100 kVAR of leading reactive power and the watt transducer indicates standby power. The apparent power indicated by the VAR transducer is essentially total apparent power input; the distortion reactive power, the real power and the power factor are all close to zero.

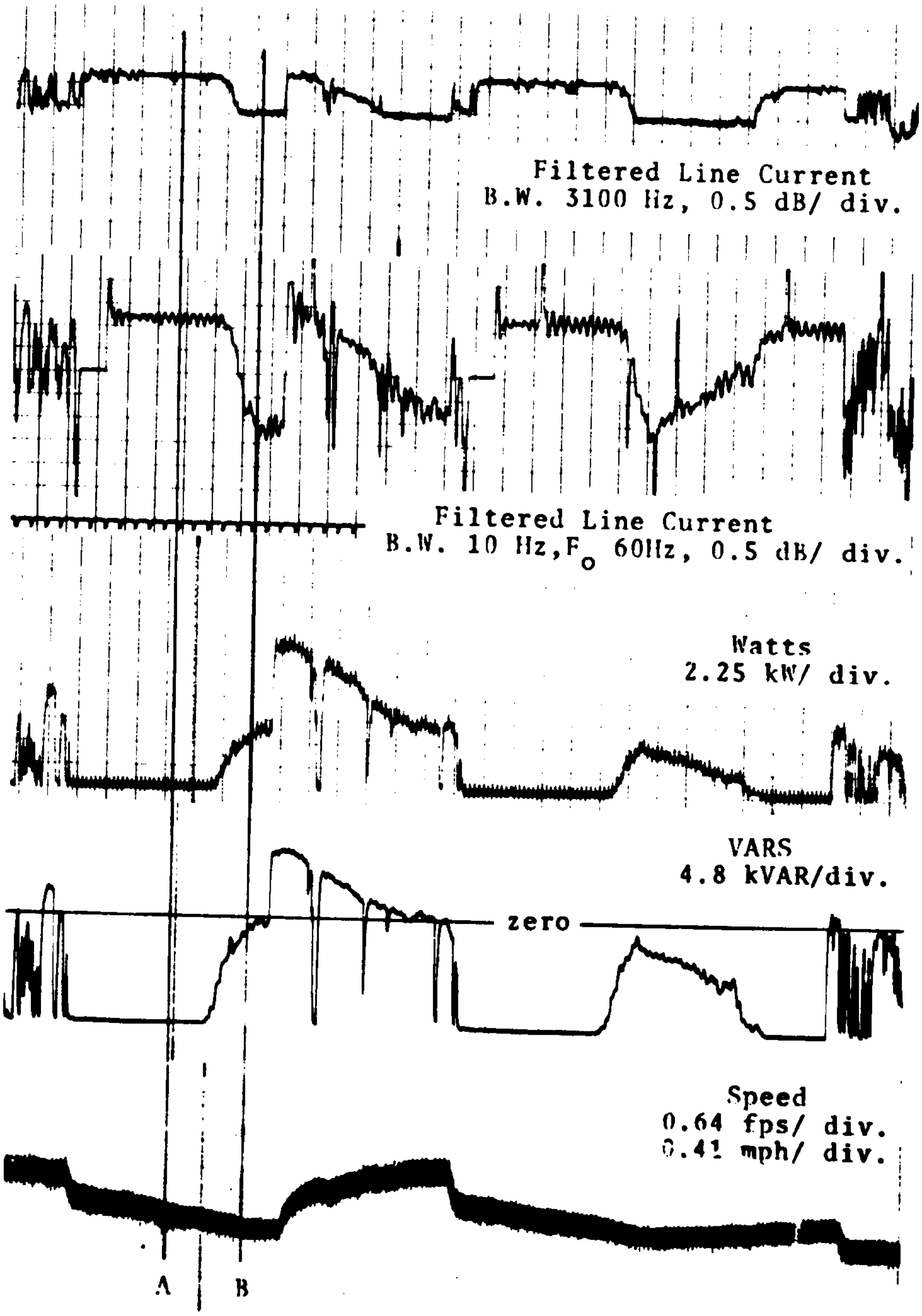

FIGURE A-13 DISTORTION EFFECTS

At point "B", the vehicle transits from a coasting to a cruising condition, and propulsion power is required. The power conditioner is phased "on" and power flows into the load. The RMS current decreases because the lagging current of the load balances some of the leading current in the power-factor-correction capacitors. The decrease in RMS current is 4 dB, (33%), but the decrease in the 60 Hz component is 12 dB, (75%). The power factor, as measured by the watt and VAR transducers, approaches unity, but the power factor calculated from RMS measurements and the watt transducer output is 0.4. The difference is due to the harmonic distortion, which is not measured by the VAR transducer.

A-6. EFFICIENCY

Although the instrumentation did not provide efficiency data, efficiency can be discussed from theoretical considerations of the system operating modes and from published data of similar systems. Both systems are high loss systems at low speeds relative to synchronous speeds. The eddy current transmission drive falls into a category of drive systems using slip coupling where slip energy is dissipated in the coupling. The LIM system relies on the increased slip of an induction motor with decreased supply voltage and slip energy is dissipated in the rail. Both systems are best suited for applications where torque required decreases as speed decreases, such as fans and pumps.

A study of an eddy current clutch drive system was conducted for DOT. The results are presented in DOT contractor reports, (3, 4). The report results show that the system efficiency is low at low speeds and that the unit tested had a maximum efficiency of 63%.

The eddy current transmission is an inefficient device at low and intermediate speeds because it is a torque, not a power, transfer device. The ac motor operates at its slip speed, N_1, close to its synchronous speed of 1800 rpm, and the clutch output shaft rotates at the controlled speed, N_2. The motor-developed torque, T_m, is transferred through the clutch to the output shaft so that the output shaft torque is also T_m, if clutch losses are neglected.

The motor horsepower is given by

$$HP_m = N_1 T_m / 5252. \qquad (A-1)$$

The output horsepower is given by

$$HP_o = N_2 T_m / 5252. \qquad (A-2)$$

The difference between the two power levels is given by

$$\Delta HP = T_m \ (N_1 - N_2)/5252. \qquad (A-3)$$

Equation 3 shows that the clutch dissipates the difference in energy of the two power levels in addition to its own losses. At low speeds the clutch dissipation exceeds the power delivered to the load and is inefficient; at mid-speed the clutch dissipation equals load power and the efficiency of power transfer is close to 50%, and at high speeds the load power is efficiently transferred. It is evident that the eddy clutch principle is most suited for speed control at relatively high output speeds. It is a good control device at all speeds, but has a low efficiency at low speeds.

In the eddy current transmission system the losses are proportional to the difference between the motor speed and the output shaft speed; similarly, the losses in the LIM system are proportional to the difference in the motor synchronous speed and the operating or "slip" speed. This fact becomes apparent from analysis of one phase of the LIM secondary equivalent circuit which is shown below:

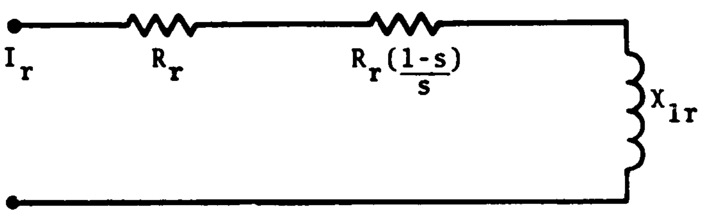

I_r = Rotor current

R_r = Rotor resistance or rail resistance

X_{1r} = Rotor reactance or rail reactance

s = slip

It can be shown (5, 6) that the rotor or rail power input consists of two components:

$$I_r^2 R_r + I_r^2 R_r (1-s/s) = P_{in}.$$

The first term represents the copper losses per phase and the second term the power developed per phase. This expression states that the power available for thrust is equal to the power supplied minus the losses. For the LIM on a Jetrail vehicle, whose maximum speed is approximately 1/2 synchronous speed, the slip is approximately 50%. The rotor power for this condition is

$$I_r^2 R_r \text{ (loss)} + I_r^2 R_2 \frac{(1-0.5)}{(0.5)} \text{ (thrust); which reduces to:}$$

$$I_r^2 R_r \text{ (loss)} + I_r^2 R_r \text{ (thrust)}.$$

At 50% slip, the power supplied to the rail is equally divided between losses and thrust.

Jetrail velocity in speed 4 was calculated to be 15.5 mph (25 km/hr) and the synchronous speed of the installed LIMs is 40.27 mph (64 km/hr); therefore, the slip at maximum speed is 0.615 and maximum efficiency of the installed system is

$$I^2 R_r + \frac{1-0.615}{0.615} (I^2 R_r) = P_m$$

$$= 1.626 (I^2 R_r),$$

$$\eta = \frac{0.626}{1.626} = 38.5\%$$

This figure represents the maximum theoretical efficiency of the installed LIM. Efficiency could be significantly improved if the system used motors with shorter pole pitches. Then the motors would operate closer to synchronous speed thereby increasing theoretical efficiency. In other words, the LIM was designed for higher applications speed (approximately 35 mph). Operating closer to synchronous speed would significantly improve the efficiency.

APPENDIX B

FAILURE CLASSIFICATION

Maintenance reports for a two- and-a-half-year period extending from June 1970 to May 1973 were analyzed for the number and types of failures occurring in the Jetrail system. To facilitate classification, the Jetrail system was divided into three major subsystems, central control, guideway, and vehicles. Since the majority of failures were vehicle related, this subsystem was subdivided into, interior and maintenance, control, drive train, propulsion, and brake subsystems. Each of these subsystems are further subdivided into components.

A failure was defined as any event that caused a functional breakdown of the system preventing it from completing its function mission - transporting passengers between stations in a timely manner. Non-functional failures such as burned-out lights and replacement of torn seat cushions were recorded as an interior-related event under the category of others, but were not counted as failures. Similarly, vehicle inspections were recorded under the category of inspection, but were not considered failures. These two categories are indicated in Fig. B-1 and Table B-1, but their numbers are not added into the total failures for interior and maintenance.

Figure B-1 and Table B-1 present Jetrail system failure data as a function of vehicle and years of operation.

Figure B-1 is a sample chart (vehicle 4) showing how failures were related to each subsystem and component. The number in the lower right-hand corner of each box is the number of failures observed during the time period. For example, the weir unit (eddy-current transmission) during the 70-71 time frame on number-4 vehicle experienced six failures. The entire propulsion related failures was 41 and altogether the vehicle experienced 128 failures - the sum of vehicle subsystem related failures. Overall the Jetrail system, as related to the number-4 vehicle, experience

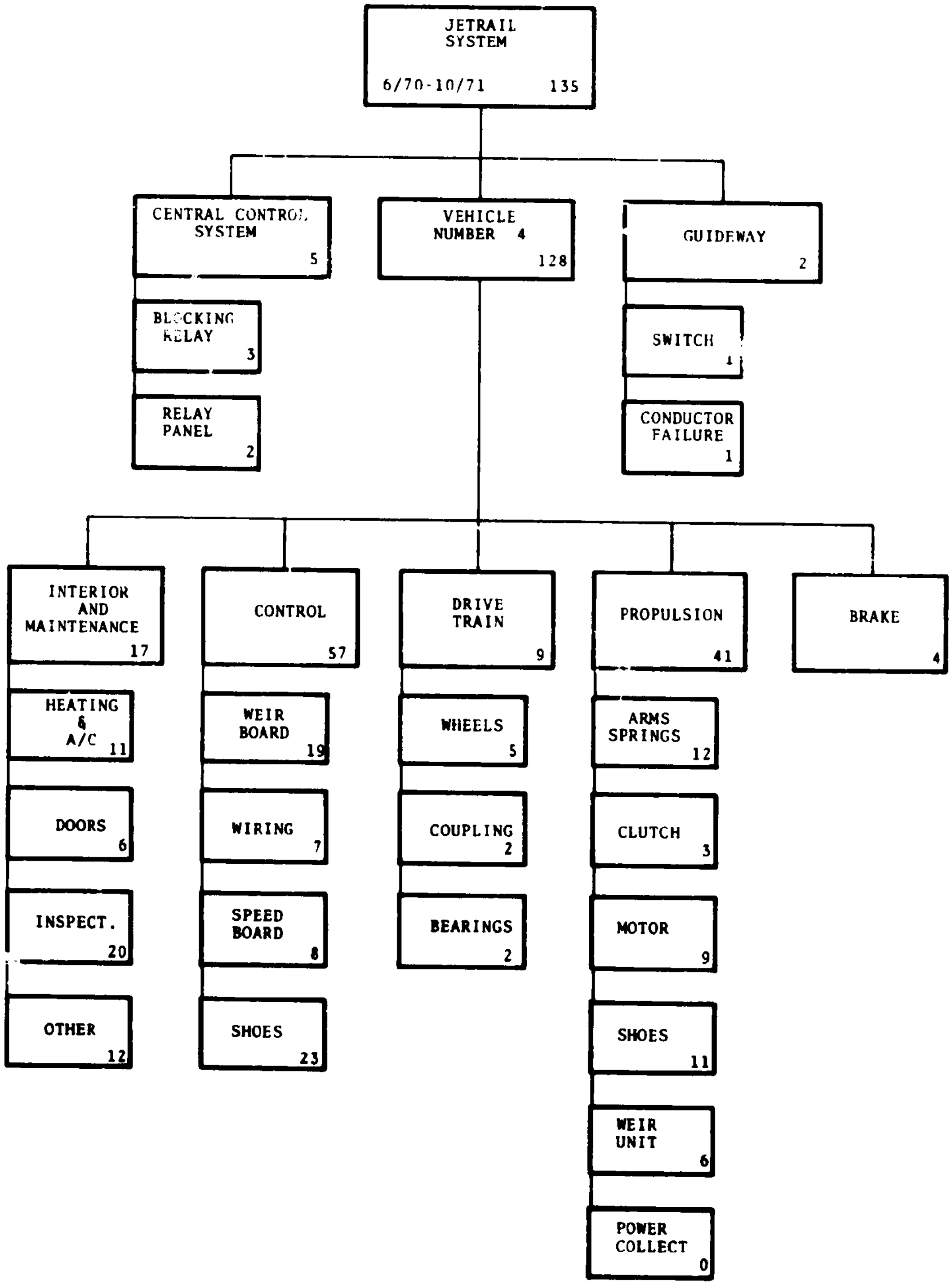

FIGURE B-1. JETRAIL SYSTEM FAILURE CHART (SAMPLE)

TABLE B-1. JETRAIL SYSTEM FAILURE SUMMARY TABLE

	6/70-12/71	1/72-4/73	6/70-12/71	1/72-5/73	5/70-12/71	1/72-5/73	5/70-12/71	4/72-5/73
SYSTEM	135	129	158	78	93	91	125	106
CENTRAL CONTROL	5	2	5	6	4	5	5	4
Blocking Relay	3	2	4	2	2	1	[illegible]	1
Relay Panel	2	2	1	1	2	4	3	3
VEHICLE	128	126	153	72	94	86	120	102
Interior	17	16	13	7	15	15	18	14
Heating&A/C	11	9	6	6	7	14	9	5
Doors	6	7	9	1	8	1	9	9
(Inspection)	20	14	10	7	10	7	11	6
(Other)	12	13	12	14	8	15	8	15
Control	57	64	77	38	59	47	62	44
Weir Board	19	36	41	25	24	28	28	22
Wiring	7	16	14	5	14	10	14	10
Speed Board	8	2	6	1	4	1	2	3
Shoes	23	10	16	7	17	8	18	9
Drive Train	9	18	5	6	3	12	5	23
Wheels		15	3	4	0	8	2	21
Coupling	[illegible]	3	1	0	3	3	1	1
Bearings	2	0	1	2	0	1	2	1
Propulsion	41	23	56	17	14	9	30	21
Arms	12	10	14	4	3	4	7	8
Clutch	3	3	4	1	2	1	1	2
Motor	9	6	14	6	1	0	10	6
Shoes	11	2	15	0	6	3	7	1
Wei. Unit	6	1	5	4	0	0	4	2
Power Collect.	0	1	4	2	2	1	1	2
Brake	4	5	2	4	3	3	3	0
GUIDEWAY	2	1	0	0	0	0	0	0
Switch	1	0	0	0	0	0	0	0
Conduct. Rail	1	0	0	0	0	0	0	0

COMPONENT SYSTEM

SUBSYSTEM

135 failures including 5 central control system and 2 guideway failures while the number-4 vehicle was in the system.

Since data for only four vehicles over two time periods was available these were aggregated and presented in Table B-1. This summary table contains information obtained from the individual vehicle charts. Each column in this table represents a vehicle. The first is the failure data for vehicle-4 shown in Figure B-1. Data for vehicles 5, 9, and 10 are also presented in Table B-1.

Individual failures of components were recorded in the lower right-hand corner of each component category.

These failures were summed to obtain the number of failures in each subsystem. In the case of the vehicle the number of interior, control, drive train, propulsion, and brake subsystem failures were summed to obtain the total number of vehicle failures. The total number of Jetrail system failures was obtained by further summation of the three major subsystems. Note that this total is for the system with a single vehicle.

As can be seen from Figure B-1 and Table B-1, the majority of system failures are vehicle-related. Of these, the vehicle control and propulsion systems have the most frequent failures. The guideway and the central control systems suffered very few failures.

APPENDIX C

METHOD OF DETERMINING DAILY VEHICLE OPERATING HOURS

The failure information presented in Appendix B is used in the determination of a failure rate and a MTBF for the vehicles and system. Since the system operated 24 hours per day, failures in the guideway and central control were based on 24 hours of operation per day. The vehicles, however, operated fewer than 24 hours a day due to the vehicle system makeup of 8 active and 2 standby vehicles and to the fact that system is demand actuated (responsive). Since data was not available on the actual hours of vehicle operation, an estimate was derived based on:

1. Braniff's estimate of 6,000,000 Jetrail passengers over the life of the system.
2. Average of 364 Braniff flights (arrivals and departures) per day at Love Field, Dallas determined from Official Airline Guide for 1972 and for 1973.
3. 1360 operating days (April 1970 to January 1974).

Using these figures, an average number of Jetrail passengers per flight was found to be approximately 12. This was obtained by multiplying the number of total flights per day by the number of Jetrail operating days and dividing the product into the total number of passengers carried. This number seemed low considering that it included airplane passengers as well as friends and relatives who have come to greet travelers or see them off.

Table C-1 shows the number of Braniff flights per day broken down into arrivals and departures by time of day. The number of Jetrail passengers associated with these flights is estimated by multiplying the number of flights by the number of Jetrail passengers per flight (approximately 12). To determine the number of minutes of vehicle operation per hour interval, it was necessary to estimate the number of roundtrips required to transport the given passengers. This number would then by multiplied by 8.83 minutes - the number of minutes necessary for a vehicle to make a roundtrip

(7.0 minutes travel time plus 55 seconds loading and 55 seconds for unloading). In order to estimate the number of roundtrips, it was necessary to determine the average number of people carried from parking lot to terminal and back to the parking lot. This roundtrip average is assumed to be dependent upon the time of day - for example, during busy hours the roundtrip total is close to 10 whereas in early morning hours the average roundtrip figure is approximately 1. Six cases are used in Table C-1 to handle fluctuations. The number of Jetrail passengers anticipated during any hour interval, therefore, is divided by the average number of roundtrip passengers (depending upon case) to get the number of roundtrips, which is then multiplied by 8.83 minutes for a roundtrip. Also calculated at the bottom of Table C-1 is the average number of passengers per round trip. This number is obtained by dividing the total Jetrail passengers (4411.7) by the total trips (total minutes/minutes per roundtrip or 5976.62 minutes/8.83 minutes = 676.85). It therefore follows that the average number of one-way passengers is assumed to be half the average number of passengers per roundtrip or 3.26.

Table C-1 indicates that on the average, each vehicle operated approximately 10 hours a day. It is important to keep in mind that this number is based on 6,000,000 passengers over the life of the system. Table C-2 performs the same calculations using 10,000,000 passengers and the result is 15 hours of operation per day for each of the ten vehicles. The 10,000,000 passenger case is used here because the estimates of the average number of Jetrail passengers per flight of 12.12 (used in arriving at the 6,000,000 passenger estimate) appeared too low. The larger estimate raised the average number of Jetrail passengers per flight to 20.2). Since these estimates do not include vehicle movement due to maintenance, an extra half hour is added on to cover this, thus making 10.5 hours/vehicle/day in Table C-1 and 15.5 hours/vehicle/day in Table C-2.

TABLE C-1 PASSENGER ESTIMATE (6,000,000)

TIME OF DAY	FLIGHTS OUTBOUND	FLIGHTS INBOUND	TOTAL (2)	JETRAIL PASSENGERS (3)	CASE (1)	TOTAL MINUTES OF VEHICLE OPERATION (4)
12A - 1A	4	3	7	84.84	4	149.88
1 - 2	0	1	1	12.12	4	21.41
2 - 3	0	0	0	-	-	-
3 - 4	0	0	0	-	-	-
4 - 5	0	0	0	-	-	-
5 - 6	2	0	2	24.24	6	214.12
6 - 7	0	5	5	60.60	5	178.43
7 - 8	13	6	19	230.28	3	339.02
8 - 9	12	11	23	278.76	2	307.79
9 - 10	8	12	20	242.40	3	356.87
10 - 11	11	9	20	242.40	3	356.87
11A - 12N	14	20	34	412.08	1	364.00
12N - 1P	10	13	23	278.76	2	307.79
1 - 2	11	9	20	242.40	3	356.87
2 - 3	9	13	22	266.65	2	294.43
3 - 4	10	8	18	218.16	4	385.42
4 - 5	11	8	19	230.28	3	339.02
5 - 6	12	11	23	278.76	2	307.79
6 - 7	12	16	28	339.36	1	299.77
7 - 8	12	10	22	266.65	2	294.43
8 - 9	8	12	20	242.40	3	356.87
9 - 10	12	7	19	230.28	3	339.02
10 - 11	7	5	12	145.44	4	256.94
11P - 12A	5	2	7	84.84	4	149.88
	(183)	(181)	(364)	(4411.7)		5976.62 MINUTES AVERAGED AMONG 10 VEHICLE = 10 HRS EACH

(1) CASES: 1 2 3 4 5 6
AVERAGE NUMBER OF ROUNDTRIP
JETRAIL PASSENGERS............. 10 8 6 5 3 1

(2) DETERMINED FROM OFFICIAL AIRLINES GUIDE

(3) DETERMINED BY MULTIPLYING TOTAL FLIGHTS BY AVERAGE NUMBER OF JETRAIL PASSENGERS PER FLIGHT (12.12 - APPENDIX C)

(4) DETERMINED BY DIVIDING TOTAL JETRAIL PASSENGERS BY THE AVERAGE NUMBER OF ROUNDTRIP PASSENGERS (DEPENDING UPON CASE) AND MULTIPLYING THE RESULTING NUMBER OF TRIPS REQUIRED BY THE NUMBER OF MINUTES FOR A ROUNDTRIP (8.83 MIN - APPENDIX C)

(5) AVERAGE NUMBER OF PASSENGERS PER ROUNDTRIP = $\frac{\text{TOTAL JETRAIL PASSENGERS}}{\text{TOTAL TRIPS} \left(= \frac{\text{TOTAL MINUTES}}{\text{MIN./ROUNDTRIP}}\right)} = \frac{4411.7}{676.85} = 6.5$

(6) AVERAGE NUMBER OF ONEWAY PASSENGERS = 3.26

TABLE C-1. PASSENGER ESTIMATE (10,000,000)

TIME OF DAY	TOTAL FLIGHTS	JETRAIL TOTAL PASSENGERS[2]	CASE[1]	TOTAL MINUTES OF VEHICLE OPERATION
12A - 1A	7	141.40	4	249.81
1 - 2	1	20.20	4	35.67
2 - 3	-	-	-	-
3 - 4	-	-	-	-
4 - 5	-	-	-	-
5 - 6	2	40.40	6	356.87
6 - 7	5	101.00	5	297.38
7 - 8	19	383.81	3	565.05
8 - 9	23	464.61	2	410.40
9 - 10	20	404.00	3	594.77
10 - 11	20	404.00	3	594.77
11A - 12N	34	686.80	1	505.56
12N - 1P	23	464.61	2	410.40
1 - 2	20	404.00	3	594.77
2 - 3	22	444.40	2	392.55
3 - 4	18	363.60	3	535.30
4 - 5	19	383.81	3	565.05
5 - 6	23	464.61	2	410.40
6 - 7	28	565.60	1	416.34
7 - 8	22	444.40	2	392.55
8 - 9	20	404.00	3	594.77
9 - 10	19	383.81	3	565.05
10 - 11	12	242.40	4	428.24
11P - 12A	7	141.40	4	249.81
	(364)	(7352.9)		9165.5 MINUTES AVERAGE AMONG 10 VEHICLES = 15 HRS EACH

(1) CASES 1 2 3 4 5 6
AVERAGE NUMBER OF ROUNDTRIP
JETRAIL PASSENGERS........... 12 10 6 5 3 1

(2) DETERMINED BY MULTIPLYING TOTAL FLIGHTS BY AVERAGE NUMBER OF JETRAIL PASSENGERS PER FLIGHT (20.20 - BASED ON 10,000,000 PASSENGERS) OVER THE LIFE OF THE SYSTEM

(3) AVERAGE NUMBER OF PASSENGERS PER ROUNDTRIP $= \frac{7352.9}{9165.5/8.83} = 7.08$

(4) AVERAGE NUMBER OF ONEWAY PASSENGERS = 3.54

APPENDIX D

JETRAIL LIFE CYCLE DATA

TABLE D-1. JETRAIL LIFE CYCLE, ASSUMPTIONS

GENERAL FACTORS

SYSTEM ECONOMIC LIFE (YEARS)	15
INTEREST RATE	0.1000
GENERAL INFLATION RATE	0.0700

SYSTEM INPUTS

	UNIT COST	NUMBER OF UNITS	RELATIVE INFLATION RATE	LIFE EXPECTANCY	SALVAGE FACTOR
AGT					
FACILITIES					
R&D	0.000	0.	0.0000	0.	0.000
GUIDEWAYS	[illegible]	2.	0.0000	15.	0.000
COMMAND/CONTROL	421.[illegible]	1.	0.0000	15.	0.000
POWER SYSTEM	0.000	0.	0.0000	0.	0.000
STATION	215.[illegible]	2.	0.0000	15.	0.000
MAINTENANCE	0.000	0.	0.0000	0.	0.000
OTHER	1932.034	1.	0.0000	15.	0.000
VEHICLES					
ACQUISITION	32.621	10.	0.0000	8.	0.000
OTHER	0.000	0.	0.0000	0.	0.000
OPERATING					
MAINTENANCE					
LABOR	19.317	42.	0.03[illegible]		
MATERIALS	3.652	64.	0.0000		
POWER	0.451	84.	0.0000		
FACILITIES UPKEEP	0.000	0.	0.0000		
OPERATING PERSONNEL	0.000	0.	0.0000		
GENERAL AND ADMIN	0.000	0.	0.0000		

EFFICIENCY ASSUMPTIONS (IF ANY)
PERCENT FACTOR FOR YEAR

TABLE D-2. JETRAIL LIFE CYCLE, RAW COSTS (MILLIONS)

	YEARS 0	1 / 11	2 / 12	3 / 13	4 / 14	5 / 15	6	7	8	9	10
AGT	3,707	0,464	0,464	0,464	0,464	0,464	0,464	0,791	0,464	0,464	0,464
		0,464	0,464	0,464	0,791	0,464					
FACILITIES	3,391	0,000	0,000	0,000	0,000	0,000	0,000	0,000	0,000	0,000	0,000
		0,000	0,000	0,000	0,000	0,000					
ROW	0,000	0,000	0,000	0,000	0,000	0,000	0,000	0,000	0,000	0,000	0,000
		0,000	0,000	0,000	0,000	0,000					
GUIDEWAYS	0,595	0,000	0,000	0,000	0,000	0,000	0,000	0,000	0,000	0,000	0,000
		0,000	0,000	0,000	0,000	0,00					
COMMAND/CONTROL	0,421	0,000	0,000	0,000	0,000	0,000	0,000	0,000	0,000	0,000	0,000
		0,000	0,000	0,000	0,000	0,000					
POWER SYSTEM	0,000	0,000	0,000	0,000	0,000	0,000	0,000	0,000	0,000	0,000	0,000
		0,000	0,000	0,000	0,000	0,000					
STATION	0,433	0,000	0,000	0,000	0,000	0,000	0,000	0,000	0,000	0,000	0,000
		0,000	0,000	0,000	0,000	0,000					
MAINTENANCE	0,000	0,000	0,000	0,000	0,000	0,000	0,000	0,000	0,000	0,000	0,000
		0,000	0,000	0,000	0,000	0,000					
OTHER	1,932	0,000	0,000	0,000	0,000	0,000	0,000	0,000	0,000	0,000	0,000
		0,000	0,000	0,000	0,000	0,000					
VEHICLES	0,326	0,000	0,000	0,000	0,000	0,000	0,000	0,326	0,000	0,000	0,000
		0,000	0,000	0,000	0,326	0,000					
ACQUISITION	0,326	0,000	0,000	0,000	0,000	0,000	0,000	0,326	0,000	0,000	0,000
		0,000	0,000	0,000	0,326	0,000					
OTHER	0,000	0,000	0,000	0,000	0,000	0,000	0,000	0,000	0,000	0,000	0,000
		0,000	0,000	0,000	0,000	0,000					
OPERATING	0,000	0,464	0,464	0,464	0,464	0,464	0,464	0,464	0,464	0,464	0,464
		0,464	0,464	0,464	0,464	0,464					
MAINTENANCE	0,000	0,450	0,450	0,450	0,450	0,450	0,450	0,450	0,450	0,450	0,450
		0,450	0,450	0,450	0,450	0,450					
LABOR	0,000	0,338	0,338	0,338	0,338	0,338	0,338	0,338	0,338	0,338	0,338
		0,338	0,338	0,338	0,338	0,338					
MATERIALS	0,000	0,112	0,112	0,112	0,112	0,112	0,112	0,112	0,112	0,112	0,112
		0,112	0,112	0,112	0,112	0,112					
POWER	0,000	0,014	0,014	0,014	0,014	0,014	0,014	0,014	0,014	0,014	0,014
		0,014	0,014	0,014	0,014	0,014					
FACILITIES UPKEEP	0,000	0,000	0,000	0,000	0,000	0,000	0,000	0,000	0,000	0,000	0,000
		0,000	0,000	0,000	0,000	0,000					
OPERATING PERSONNEL	0,000	0,000	0,000	0,000	0,000	0,000	0,000	0,000	0,000	0,000	0,000

TABLE D-3. JETRAIL SALVAGE VALUE

AGT	-0.280
FACILITIES	0.000
ROW	0.000
GUIDEWAYS	0.000
COMM AND/CONTROL	0.000
POWER SYSTEM	0.000
STATION	0.000
MAINTENANCE	0.000
OTHER	0.000
VEHICLES	-0.280
ACQUISITION	-0.280
OTHER	0.000

TABLE D-4. JETRAIL LIFE CYCLE, SUMMARY STATISTICS, RAW DATA

GENERAL FACTORS

SYSTEM ECONOMIC LIFE (YEARS)	15
INTEREST RATE	0.1000
GENERAL INFLATION RATE	0.0700

AGT

	PRESENT VALUE	7.42	7.40		PRESENT VALUE	0.98	0.97

EQUIV. ANNUAL COST

YEAR	YEARLY COST TOTAL	YEARLY COST ANNUAL	CUMULATIVE COST TOTAL	CUMULATIVE COST ANNUAL
0	3.71	0.00	3.71	0.00
1	0.46	0.97	4.17	0.97
2	0.46	0.97	4.64	1.95
3	0.46	0.97	5.10	2.92
4	0.46	0.97	5.56	3.89
5	0.46	0.97	6.03	4.86
6	0.46	0.97	6.49	5.84
7	0.79	0.97	7.28	6.81
8	0.46	0.97	7.75	7.78
9	0.46	0.97	8.21	8.75
10	0.46	0.97	8.68	9.73
11	0.46	0.97	9.14	10.70
12	0.46	0.97	9.60	11.67
13	0.46	0.97	10.07	12.64
14	0.79	0.97	10.86	13.62
15	0.18	0.99	11.04	14.60

TABLE D-5. PRESENT VALUES

CATEGORIES	AGT	BUS	TRUCK
TOTAL	7.[illegible]2	0.000	0.000
FACILITIES	3.381	0.000	0.000
ROW	0.000	0.000	0.000
GUIDEWAYS	0.595	0.000	0.000
COMMAND/CONTROL	0.421	0.000	0.000
POWER SYSTEM	0.000	0.000	0.000
STATION	0.433	0.000	0.000
MAINTENANCE	0.000	0.000	0.000
OTHER	1.932	0.000	0.000
VEHICLES	0.489	0.000	0.000
ACQUISITION	0.489	0.000	0.000
OTHER	0.000	0.000	0.000
OPERATING	3.531	0.000	0.000
MAINTENANCE	3.426	0.000	0.000
LABOR	2.574	0.000	0.000
MATERIALS	0.852	0.000	0.000
POWER	0.106	0.000	0.000
FACILITIES UPKEEP	0.000	0.000	0.000
OPERATING PERSONNL	0.000	0.000	0.000
GENERAL AND ADMIN	0.000	0.000	0.000

TABLE D-6. JETRAIL LIFE CYCLE, CASH FLOW

(INCLUDES ACTUAL INFLATION)

	YEARS 0	1	2	3	4	5	6	7	8	9	10	11	12	13	14	15
AGT	[illegible]	0,973	1,005	1,040	1,077	1,117	1,160	1,205	1,293	1,345	1,401	1,460	1,526	1,593	,656	1,846
FACILITIES	0,000	0,444	0,444	0,444	0,444	0,444	0,444	0,444	0,444	0,444	0,444	0,444	0,444	0,444	0,444	0,444
ROW	0,000	0,000	0,000	0,000	0,000	0,000	0,000	0,000	0,000	0,000	0,000	0,000	0,000	0,000	0,000	0,000
GUIDEWAYS	0,000	0,078	0,078	0,078	0,078	0,078	0,078	0,078	0,078	0,078	0,078	0,078	0,078	0,078	0,078	0,078
COMMAND/CONTROL	0,000	0,055	0,055	0,055	0,055	0,055	0,055	0,055	0,055	0,055	0,055	0,055	0,055	0,055	0,055	0,055
POWER SYSTEM	0,000	0,000	0,000	0,000	0,000	0,000	0,000	0,000	0,000	0,000	0,000	0,000	0,000	0,000	0,000	0,000
STATION	0,000	0,057	0,057	0,057	0,057	0,057	0,057	0,057	[illegible]	0,057	0,057	0,057	0,057	0,057	0,057	0,057
MAINTENANCE	0,000	0,000	0,000	0,000	0,000	0,000	0,000	0,000	0,000	0,000	0,000	0,000	0,000	0,000	0,000	0,000
OTHER	0,000	0,254	0,254	0,254	0,254	0,254	0,254	0,254	0,254	0,254	0,254	0,254	0,254	0,254	0,254	0,254
VEHICLES	0,000	0,064	0,064	0,064	0,064	0,064	0,064	0,064	0,103	0,103	0,103	0,103	0,103	0,103	0,103	0,204
ACQUISITION	0,000	0,064	0,064	0,064	0,064	0,064	0,064	0,064	0,103	0,103	0,103	0,103	0,103	0,103	0,103	0,204
OTHER	0,000	0,000	0,000	0,000	0,000	0,000	0,000	0,000	0,000	0,000	0,000	0,000	0,000	0,000	0,000	0,000
OPERATING	0,000	0,464	0,497	0,532	0,569	[illegible]	[illegible]	0,697	[illegible]	0,798	0,854	0,913	0,977	1,045	1,119	1,197
MAINTENANCE	0,000	0,450	0,482	0,516	0,552	0,590	0,632	0,676	0,723	0,774	0,828	0,886	0,948	1,014	1,085	1,161
LABOR	0,000	0,338	0,362	0,387	0,415	0,444	0,475	0,508	0,543	0,581	0,622	0,656	0,712	0,762	0,816	0,873
MATERIALS	0,000	0,112	0,120	0,128	0,137	0,147	0,157	0,168	0,180	0,192	0,206	0,220	0,236	0,252	0,270	0,289
POWER	0,000	0,014	0,015	0,016	0,017	0,018	0,019	0,021	0,022	0,024	0,026	0,027	0,029	0,031	0,033	0,036

TABLE D-7. SALVAGE VALUE

AGT	-0.721
FACILITIES	0.000
ROW	0.000
GUIDEWAYS	0.000
COMMAND/CONTROL	0.000
POWER SYSTEM	0.000
STATION	0.000
MAINTENANCE	0.000
OTHER	0.000
VEHICLES	-0.721
ACQUISITION	-0.721
OTHER	0.000

TABLE D-8. JETRAIL LIFE CYCLE, SUMMARY STATISTICS, CASH FLOW

(INCLUDES ACTUAL INFLATION)

GENERAL FACTORS

SYSTEM ECONOMIC LIFE (YEARS)	15
INTEREST RATE	0.1000
GENERAL INFLATION RATE	0.0700

ACT

PRESENT VALUE 9.28 9.25 — PRESENT VALUE 1.22 1.22

EQUIV. ANNUAL COST

YEAR	YEARLY COST TOTAL	YEARLY COST ANNUAL	CUMMULATIVE COST TOTAL	CUMMULATIVE COST ANNUAL
0	3.71	0.00	3.71	0.00
1	0.46	0.97	4.17	0.97
2	0.50	1.01	4.67	1.98
3	0.53	1.04	5.20	3.02
4	0.57	1.03	5.77	4.09
5	0.61	1.12	6.38	5.21
6	0.65	1.16	7.03	6.37
7	1.22	1.21	8.25	7.58
8	0.75	1.29	8.99	8.87
9	0.80	1.31	9.79	10.21
10	0.85	1.40	10.65	11.61
11	0.91	1.46	11.56	13.07
12	0.98	1.52	12.54	14.60
13	1.05	1.59	13.58	16.19
14	1.96	1.67	15.54	17.86
15	0.48	1.85	16.02	19.70

TABLE D-9. PRESENT VALUES

CATAGORIES	VALUES		
	AGT	BUS	TRUCK
TOTAL	9.251	0.000	0.000
FACILITIES	3.381	0.000	0.000
ROW	0.000	0.000	0.000
GUIDEWAYS	0.595	0.000	0.000
COMMAND/CONTROL	0.421	0.000	0.000
POWER SYSTEM	0.000	0.000	0.000
STATION	0.433	0.000	0.000
MAINTENANCE	0.000	0.000	0.000
OTHER	1.932	0.000	0.000
VEHICLES	0.616	0.000	0.000
ACQUISITION	0.616	0.000	0.000
OTHER	0.000	0.000	0.000
OPERATING	5.254	0.000	0.000
MAINTENANCE	5.097	0.000	0.000
LABOR	3.830	0.000	0.000
MATERIALS	1.267	0.000	0.000
POWER	0.157	0.000	0.000
FACILITIES UPKEEP	0.000	0.000	0.000
OPERATING PERSONNEL	0.000	0.000	0.000
GENERAL AND ADMIN	0.000	0.000	0.000

APPENDIX E

RIDE VIBRATIONS

INTRODUCTION.

The acceptability of the ride is one of the design considerations in new Automated Guideway Transit (A.G.T.) Systems. The design of new Systems with low cost guideways and high performance suspension and steering systems is simplified by knowing the performance of operational systems. Because of this it is important to record, characterize,and assess ride vibration levels as observed in as many current transit systems as possible. Examples of operational systems include the AIRTRANS system at the Dallas-Fort Worth Regional Airport and the Braniff Astroglide-Jetrail System at the Love Field(Dallas Airport).

One of the goals at the Transportation Systems Center is to form a data bank of measured time histories of the low frequency (0.1 Hz to 20 Hz) ride vibration as found in a number of transit systems. All six degrees of rigid body motion, namely, longtitudinal, transverse, vertical, roll, pitch and yaw, are to be considered.

Data banks of this type will permit comparative evaluations to be made during the design phase of new systems that may be somewhat comparable to one or another already in operation.

This report deals with the acquisition of the six-degree-of-freedom vibration records in the Braniff Jetrail System. Their subjective rating on behalf of the experimental staff, is discussed.

BRANIFF-ASTROGLIDE OR JETRAIL SYSTEM

This Group Rapid Transit System consists of automatically controlled vehicles suspended on a steel monorail for the purpose of moving people from the long - term parking area to the Braniff Terminal at the Love Field(Dallas Airport). The system was designed for Braniff International Airlines Inc. by Stanray Pacific Corp., initially operated in April 1970 and carried an estimated six million passengers prior to its shut-down when the new Dallas Fort Worth Airport opened.

The guideway from which the monorail vehicles hang is constructed from elevated sections of steel I-beam girders. Vehicles are suspended from front and rear sets of four solid-rubber wheels for each set and sixteen lateral guidance wheels are provided riding against the web of the I-beam guideway. Four dampers are connected between the wheels and the frame to dissipate sway motions. The series of photographs in Figure E.1 and Figure E.2 show the construction of the vehicles and the guideway and Figure E.3 gives a schematic diagram of the guideway layout. The total system is 7265 feet in length, has three stations, A, B, and C; an automatically operated storage spur; a manual service transfer table; and two automated baggage spurs. The vehicles have a four possible speeds depending on the speed code for a particular section of guideway or depending on system block control commands. The maximum speed is 15 m.p.h. and the maximum capacity is 18 passengers (10 standing, 8 seated). The system is divided conceptually into blocks or zones for control purposes. The "block control" scheme for the system is a logic control system which reduces the speed of any vehicle if another vehicle occupies any of four preceeding blocks. Electrically, in each block there are conducting rails for signal transmission to and from any vehicle in that block. Thus, each block has a signal rail and a sensing rail; power to drive the motors is transmitted through power rails around the whole network. Some blocks in the network automatically assign a slower than maximum speed when, for example, the vehicle

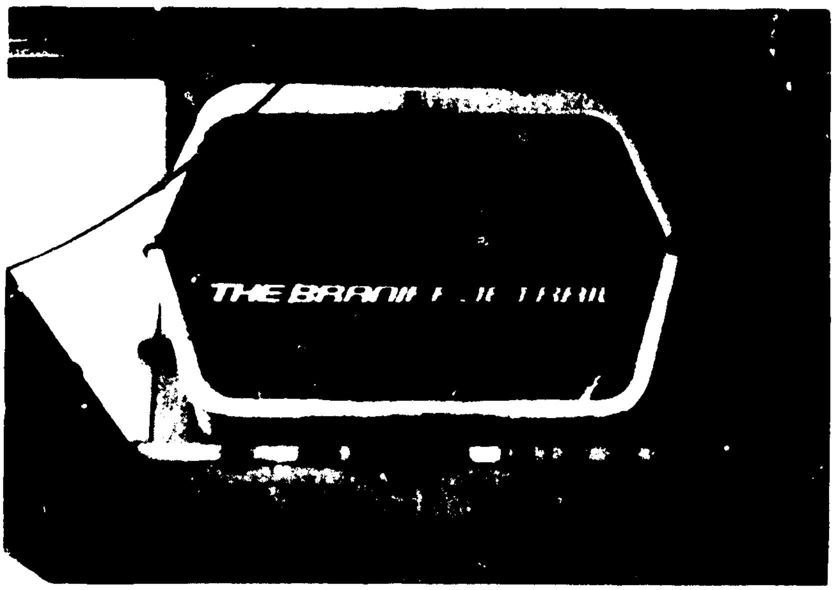

Figure E.1. Braniff Jetrail Vehicles

Figure E.2. Guideway

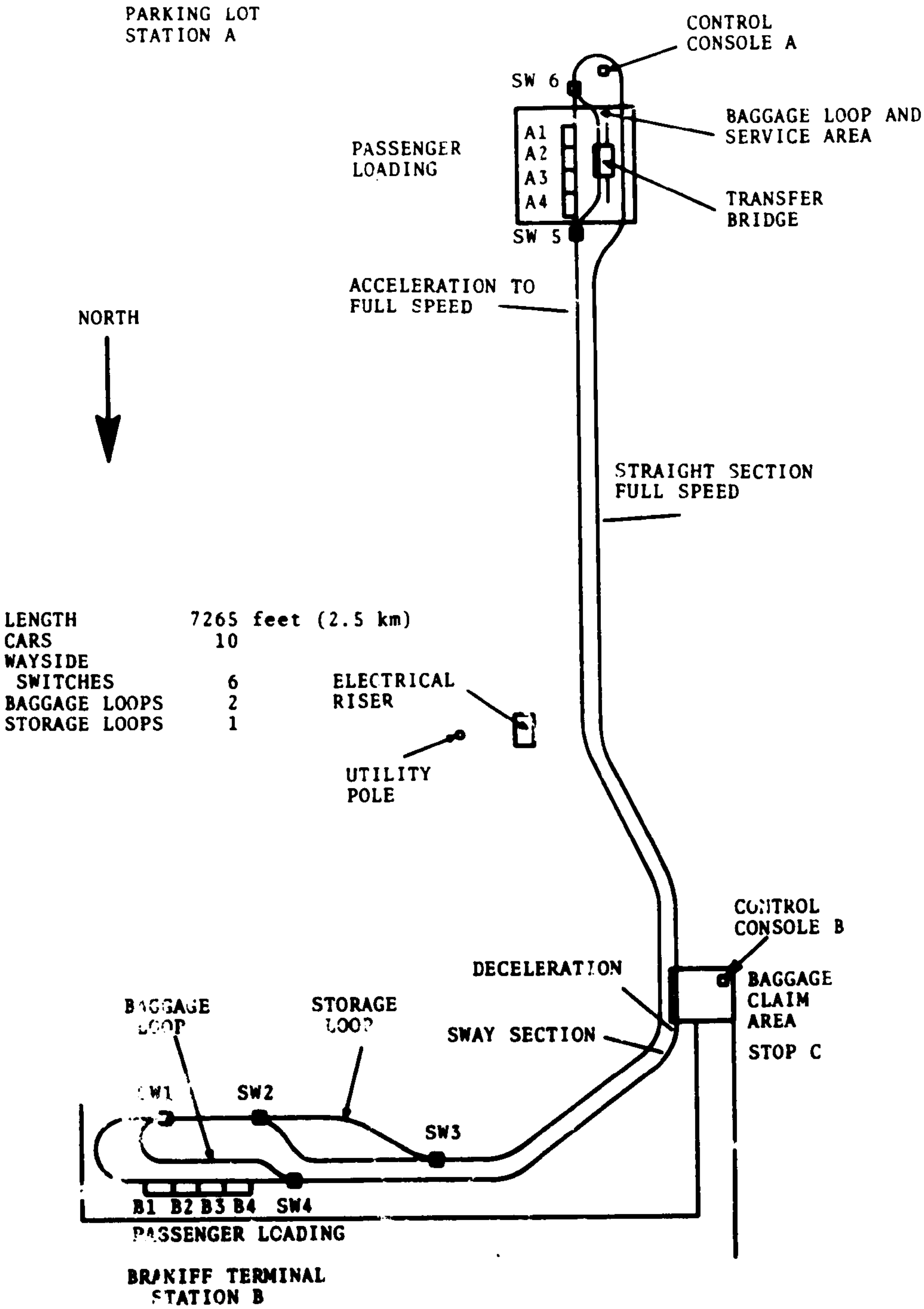

Figure E.3. Schematic of the Guideway Layout is entering a station area.

Because the vehicles hang below the guideway in pendulous fashion, there are guide rails in each station area which locate guidewheels underneath the vehicles so that sway does not occur when passengers are boarding.

Because of the lack of a secondary suspension, the ride is considerably rougher than that of an automobile. Also, because the traction forces are applied remotely from the center of gravity of the vehicle, longitudinal and pitch motions can be strong.

MEASUREMENT SYSTEM

Six-Degree-of-Freedom Acceleration Sensor.

Under the assumption that the marine plywood topped floor behaves as a rigid plate, passengers are exposed to six motions delineated in Figure 4.

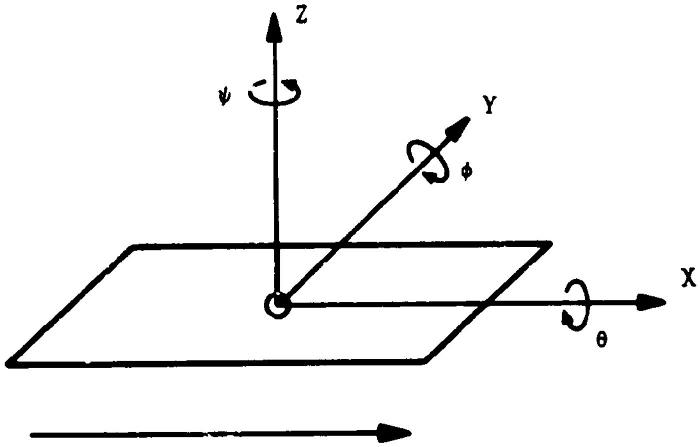

Figure E.4. Six Degrees of Motion.

These motions are:-

α_x ....longitudinal
α_y ....transverse
α_z ....vertical
α_θ ....roll
α_ϕ ....pitch
α_ψ ....yaw

It is assumed that this coordinate frame aligns with passenger orientation so that as the vehicle undergoes a sway or pitch angle, gravitational acceleration resolves along the three axis.

Accelerations come from both traction force and guideway roughness sources as well as resolution of gravity.

To measure the total acceleration with respect to the axes of Figure 4, a set of six linear accelerometers was used. The three used to measure α_x, α_y, and α_z were contained inside the 3-axis package developed by N.A.S.A. Langley Research Center and described in detail in (1)*. Basically three seismic mass accelerometers are mounted in three mutually perpendicular directions. Their ranges are ±1g. and have a sensitivity of 4.8 volts per g. and a bandwith of about 100 Hz being accurate to within 5 percent in the range 0 to 25 Hz.

The three-linear-axis unit was placed at the center of a steel frame bolted to the floor of the vehicle. Three additional accelerometers supplied by Unholtz-Dickie Corp. (Model PA1000) were deployed according to Figure 5 so that the rotational acceleration components about the origin of the N.A.S.A. unit could be extracted.

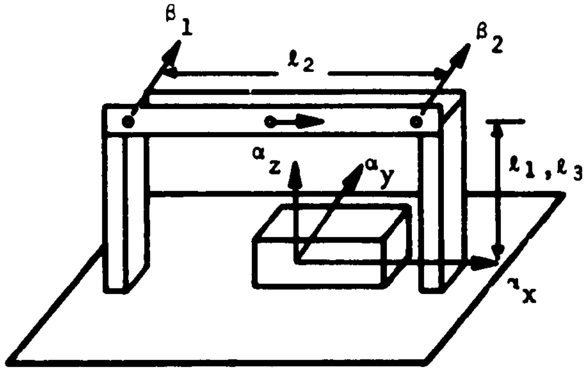

Figure E.5. Deployment of Accelerometers for Six-Degrees-of-Freedom Measurement

---

* Numbers in parentheses denote references.

$$\alpha_\theta = \alpha_y - \tfrac{1}{2}(\beta_1 + \beta_2) \; ; \; \alpha_\phi = (\beta_3 - \alpha_x)/\ell_1 ; \; \alpha_\psi = (\beta_2 - \beta_1)/\ell_2$$

The sensitivity of the Unholtz-Dickie accelerometers was set to 1 volt per g. and the separation distances ℓ_1, ℓ_2, and ℓ_3 were 21 in., 24in., and 21 in., respectively. These lengths were chosen so as to be able to sense rotational accelerations with reasonable sensitivity and accuracy.

In the construction of the frame, 3 inch steel I-beam sections were welded together on a ½ in. thick plate. The resulting structure was stiff enough to eliminate errors due to mounting flexibility. The outputs from the six accelerometers must be processed in order to extract the rotational components of acceleration. This processing takes the form of summing and subtracting some of the signals. The processing can be done a number of ways including analog processing using operational amplifiers prior to recording, using an analog computer after recording the raw accelerometer output signals, or by digital processing after the data records had been digitized. Since the digitizing of all six data channels would involve some time delays between channels, and since prior processing using operational amplifiers would require more elaborate field calibration procedures, it was decided to record the raw accelerometer output signals in the field, process the signals on an analog computer, and then re-record the processed data on tape in the laboratory.

Recording Equipment.

The output signals from each accelerometer were recorded on six channels of a Lockheed Model 417 tape recorder.

This recorder is equipped with eight channels operating in F.M. mode with a bandwidth capability of 0-2500 Hz at tape speed 7.5 in. per sec.

One of these channels is reserved at all times to playback any of the other seven which may be selected. Thus, in this work, the first six channels were used for accelerometer signals, the seventh for a signal containing vehicle speed information and the separate voice channel for vocal comment during the course of the experiment.

Other Instrumentation.

Other instrumentation, necessary for insuring the quality of the recorded signals, were an oscilloscope and digital multi-meter.

Figure 6 shows a photograph of the equipment installed inside one of the Jetrail vehicles. The acceleration sensing frame is in the foreground with the oscilloscope and tape recorder mounted on the luggage rack above and behind the frame.

Analog Post Processing

The required additions and subtractions to form α_2, α_ϕ, α_4 were done using an Applied Dynamics AD-4 analog computer. The six channels of raw data were connected to the analog computer and the processed signals were recorded on a Sango-Western 14-channel recorder and finally re-recorded on the 8-channel Lockheed recorder to provide the "permanent record" of the data. Correct time correspondence could be maintained easily by examination of the three linear acceleration channels which were unaltered during the operation. Since signal quality during reproduction would normally be of concern here, it was established that no noticeable increase in noise level occurred. This was partly due to the care taken to insure that each signal occupied as much as possible of the available voltage range, meaning that noise levels were kept as low as possible. During this last recording, a voice count was recorded every five seconds from the start so that time markers could easily identify sections to be used later for digitizing.

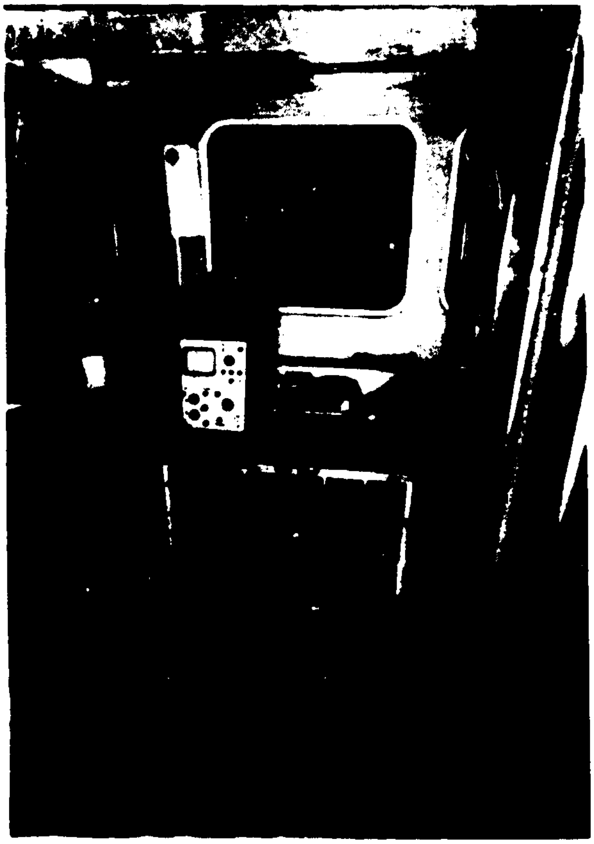

Figure E.6. Installation of Measuring Equipment.

ORGANIZATION OF THE EXPERIMENT

Re-examination of Figure E.3 will indicate that the route traveled by a Jetrail vehicle starting from Station B, takes it initially uphill followed by a left turn into Station C. There is a retardation as C is approached, followed by a jerk as the station alignment rail is contacted. Coming out of Station C the vehicle undergoes some left and right hand curves, a long straight section and then the 180-degree turn at Station A which is the half-way point. Similar routing characteristics occur on the return to Station B with the exception that Station C is not encountered.

Basically, four separate characteristics of the route were identified as:

1) Left and right hand curves in which vehicle sway occurs;
2) Deceleration into Station C;
3) Travel along the long straight section;
4) Acceleration to full speed following a station stop.

Because of the relatively short duration of one complete travel loop (approximately 9 minutes), it was decided to tape record data for more than one complete loop and, later, to isolate sections of data for detailed study. So, in the field, the six accelerometer output signals, the output from the vehicle's tacho-pulser and voice commentary were recorded during two complete loops of the system. Ratings on a seven point scale were noted corresponding to sections having the four attributes named above.

Distance landmarkers were identified by noting the passage of selected supporting columns each of which carries an identifying number. Thus later, on playback, a particular section of the record could be associated with a particular section of the system.

DATA ANALYSIS

To analyze the six-degrees-of-freedom results for spectral density and one-third octave band content, the record for one complete loop was played back into a multichannel strip-chart recorder. The sections of interest were found in particular to occur in the left-hand bend just after Station B, the deceleration as Station C is approached, the long straight section just prior to Station A and the acceleration to full speed after Station A had been passed.

Since five-second intervals were counted and recorded on the voice channel, the sections for digitizing were easily identified by particular count numbers.

The analog tape on which the post-processed analog signals (and the voice count) were recorded was then played back into a S.D.S. digitizer connected to a SIGMA 5 digital computer which produced a digital tape containing a file of digitized records.

The sample frequency was selected at 400 Hz in order to give high frequency accuracy and a record length sufficient to allow 4096 data points was taken. This means a record of at least 10.24 seconds in length (and to be safe about 15 seconds) is required. Because of the nature of the digitizing program used, a file contains an integer multiple of 750 words each having 12 binary bits. Also, only two channels are multiplexed. The procedure for handling all six channels was to treat them in three blocks of two. Although exact correspondence of starting values for each section could not therefore be made, it was determined that starting the digitizing process for each of six data channels at each characteristic section could in fact be accomplished to within a fraction of a second.

A 30-Hz bandwidth, second order Butterworth filter was used prior to digitizing so that aliasing problems could be avoided.

Spectral Density Calculation.

Having obtained a digital tape with sampled acceleration records for each of six degrees of motion for each of four characteristic sections, that data was converted to 60-bit words and the spectral density values for each section were computed using Discrete Fourier Transform Analysis together with the smoothing method described in (2). Here, frequency smoothing is used by averaging over 3, 5, and 9 adjacent frequency intervals for the frequency ranges 0.1 to 1.0 Hz; 1.0 to 10.0 Hz and 10.0 to 200.0 Hz. In this digital procedure, care was taken to double the spectral density values in the range 0 to 200 Hz so that single-sided spectra could be presented.

Root Mean Square Calculation

Integration of the spectral density over the complete frequency range (0 to 400 Hz for double-sided spectra; 0 to 200 Hz for single-sided spectra) will give the total mean square value of a signal. Its square root yields the R.M.S. value scaled in g. units for linear accelerations and in rad/sec units for rotational cases. Here, a Simpson's rule procedure is used for the numerical integration.

One-Third Octave Band Analysis.

The analysis of a record for R.M.S. content in a one-third octave frequency band where the center frequency is swept over the range 0.1 to 200 Hz is accomplished by integration of the raw power spectral values obtained by Discrete Fourier Transform Analysis. The only difference between these calculations and those for the total R.M.S. value of the signal is that the integration only takes place over a narrow range of frequency. Since the Discrete Fourier Analysis gives discrete power values at frequency intervals of approximately 0.1 Hz, an allowance is made in the numerical integration to account for the cases when the one-third octave band frequencies do not lie exactly at multiples of the frequency interval.

In the results, one-third octave R.M.S. calculated values appear and are compared where possible with the 1-hour and 8-hour tolerance levels given in the I.S.O. 2631 document (3). In the wording of (3), no mention has been made of tolerance to low frequency rotational accelerations so in these cases, no tolerance limits could be provided for comparison.

Frequency Weighted R.M.S. Measures.

According the I.S.O. document (3), broad band random vibration can also be assessed by weighting frequency values according to a function which is similar to the reciprocal of the constant comfort curve for vertical and horizontal vibration tolerance. These functions are normalized to unity values for the low range (1 to 4 Hz) for the horizontal directions.

Thus, by weighting each raw power spectral density value with the appropriate weight taken from (3) and integrating over the range 0 to 200 Hz, a single frequency weighted R.M.S. value for each record could be found.

RESULTS

The results are given in Tables E-2 and E-3 and in the Figures E.7 to E.30. They are organized to reflect spectral and one-third octave analyses in the figures and R.M.S. and W.R.M.S. values in the respective tables.

For each characteristic section, six spectral plots and six one-third octave analysis plots are given according to the Table I below.

Table E-1.
Organization of Spectral Plots in the Figures.
Conventional vehicle.

Condition	P.S.D.	1/3 Octave Analysis
Sway in curve	Figs. E.7 to E.9	Figs. E.19 to E.20
Deceleration into C	Figs. E.10 to E.12	Figs. E.21 to E.22
Long straight section	Figs. E.13 to E.15	Figs. E.23 to E.24
Acceleration to full speed from A.	Figs. E.16 to E.18	Figs. E.25 to E.26

Detailed examination yields some interesting results. Based on Figures E.13 to 15, it is seen that;

1. In the long straight section at full speed, the longitudinal ride quality is dominated by components in the 4 and 6 Hz region with additional energy around 12 Hz. Power values in these components are roughly equivalent to power values at 6 Hz and 11 Hz seen in the vertical acceleration spectrum. Strangely, the 4 Hz component was not seen in the vertical case.

2. The transverse acceleration exhibits similar power spectral density values in the 0.1 to 1 Hz region to those of the other two linear degrees of motion although its high frequency content is much lower. This is likely to arise from the fact that the vehicle is only constrained in the lateral direction when large motion excursions occur. Thus little constraining action occurs while the vehicle is traveling in a straight path.

3. With the exception of the yaw motion, the rotational motions contain high energy around 17 and 20 Hz which apparently comes from excitation of flexible structural modes. The content of the yaw motion shows lower frequencies at 2 and 6 Hz indicating that a snaking motion may be taking place. As it was definitely noticed during the test to occur at low frequency, it is suspected that the 2 Hz component of yaw caused the stronger sensation of the two components.

4. From Figures 7 to 9 it is seen that in the sway section during the negotiation of a left hand turn, the transverse acceleration has stronger power values in the 0.1 to 1.0 Hz range that any other range although the power in the longi -tudinal and vertical directions is much stronger overall. Apparently, not being constrained in the transverse direction has produced less lateral vibration while the constraint imposed by suspension on the I-beam guideway has produced sharper mid-frequency exitation for longitudinal and vertical vibration.

The data for one-third octave band analysis exhibit the same trends, of course, as that of the detailed spectral analysis figures.

Tables II and III give tabulated values of the R.M.S. from 0.1 to 200 Hz for each axis and each condition.

It is seen that if travel down the long straight is taken as a baseline condition, acceleration and deceleration cause reductions, as expected. In the curves, on the other hand, all motions are increased in intensity and this would be expected to cause the most discomfort.

As our ratings indicated (based on two ratings) the sway section was rated least comfortable. The deceleration and acceleration conditions are rated more comfortable because the vibration intensity is a strong function of speed and during the deceleration or acceleration phase, some portions of the record are still at a low speed

Table E-2.

R.M.S. to 200Hz. for 6 degree of freedom motions

	a_x	a_y	z	a_θ	a_ϕ	a_ψ	RATING
SWAY	0.0642	0.02000	0.0555	9.729	2.410	1.2000	6
DECELERATION	0.0528	0.00726	0.0312	4.342	1.096	.4673	3
LONG STRAIGHT	0.0344	0.00917	0.0464	5.447	1.575	.6162	5
ACCELERATION	0.0463	0.00642	0.0456	4.488	1.262	.4562	4

Note: RATINGS.

1. Very Comfortable
2. Comfortable
3. Somewhat Comfortable
4. Neutral
5. Somewhat Uncomfortable
6. Uncomfortable
7. Very Uncomfortable

Conventional Vehicle.

Table E-3.

I.S.O. Weighted R.M.S. Accelerations (g. units).

Conventional Vehicle.

CONDITION	X	Y	Z
SWAY	0.0247	0.0050	0.03840
DECELERATION	0.0284	0.0019	0.02526
STRAIGHT	0.0128	0.0023	0.0344
ACCELERATION	0.0224	0.0017	0.04103

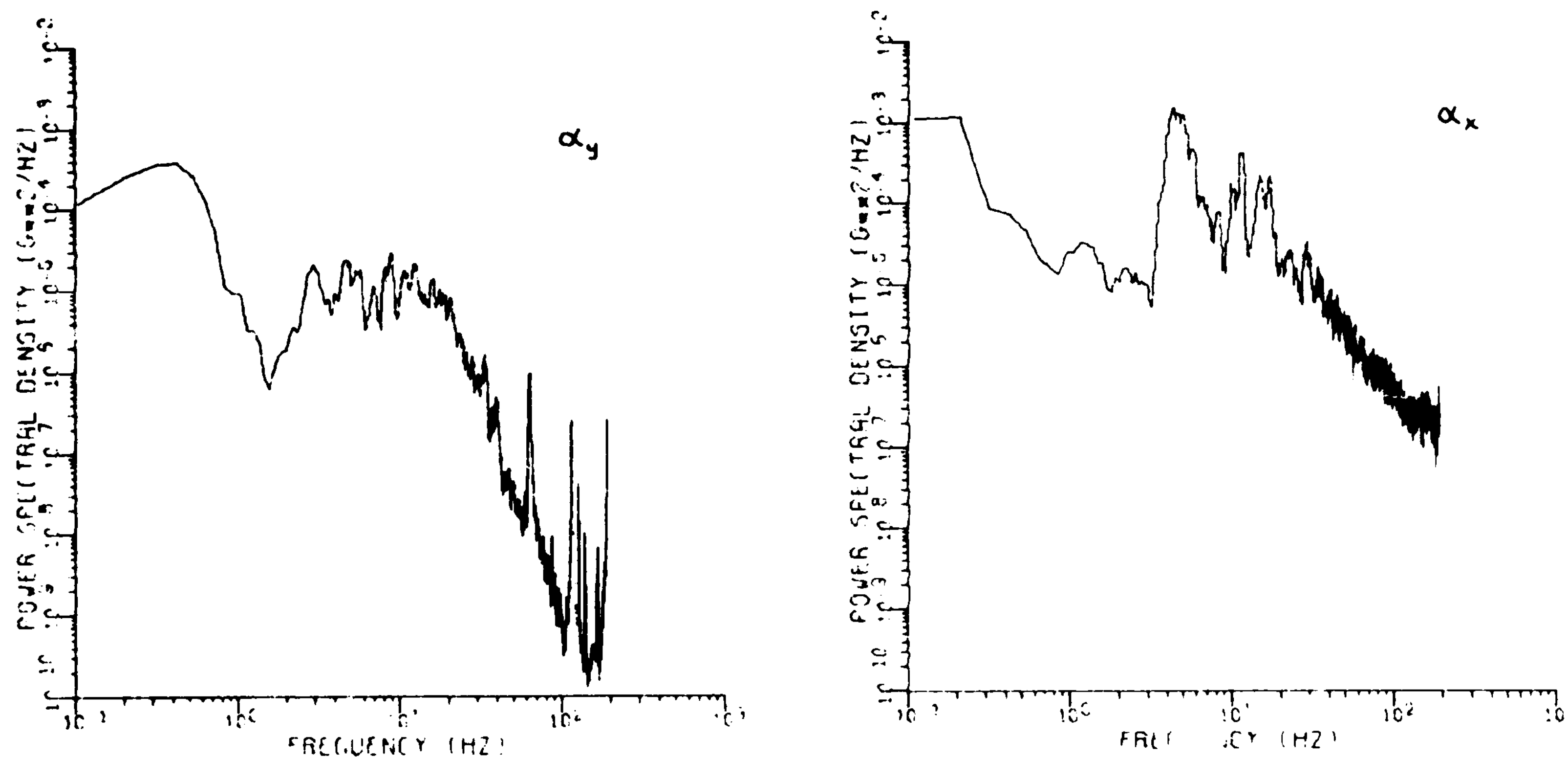

Figure E.7. Spectral Density α_y, α_x - Curve Section.

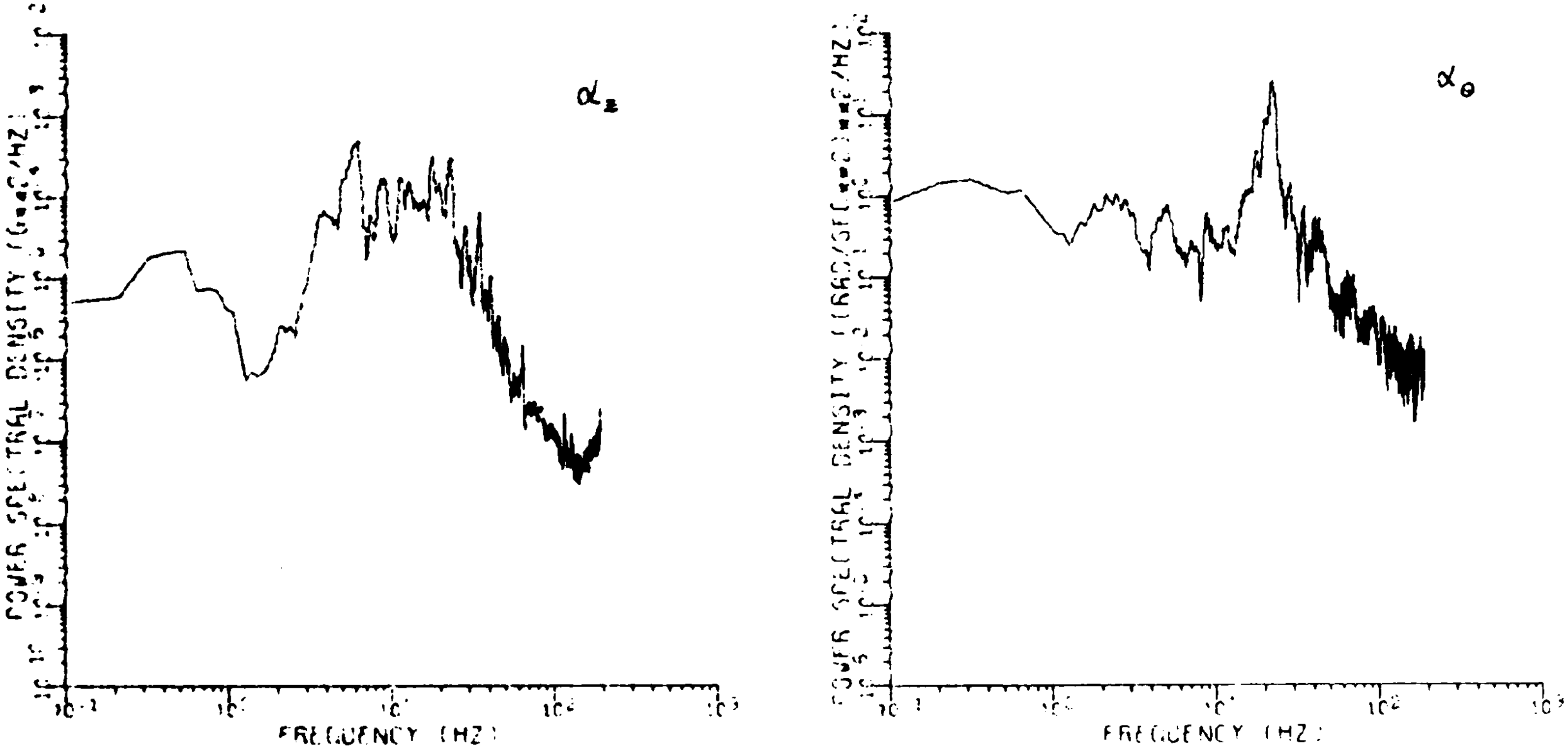

Figure E.8. Spectral Density α_z, α_θ - Curve Section

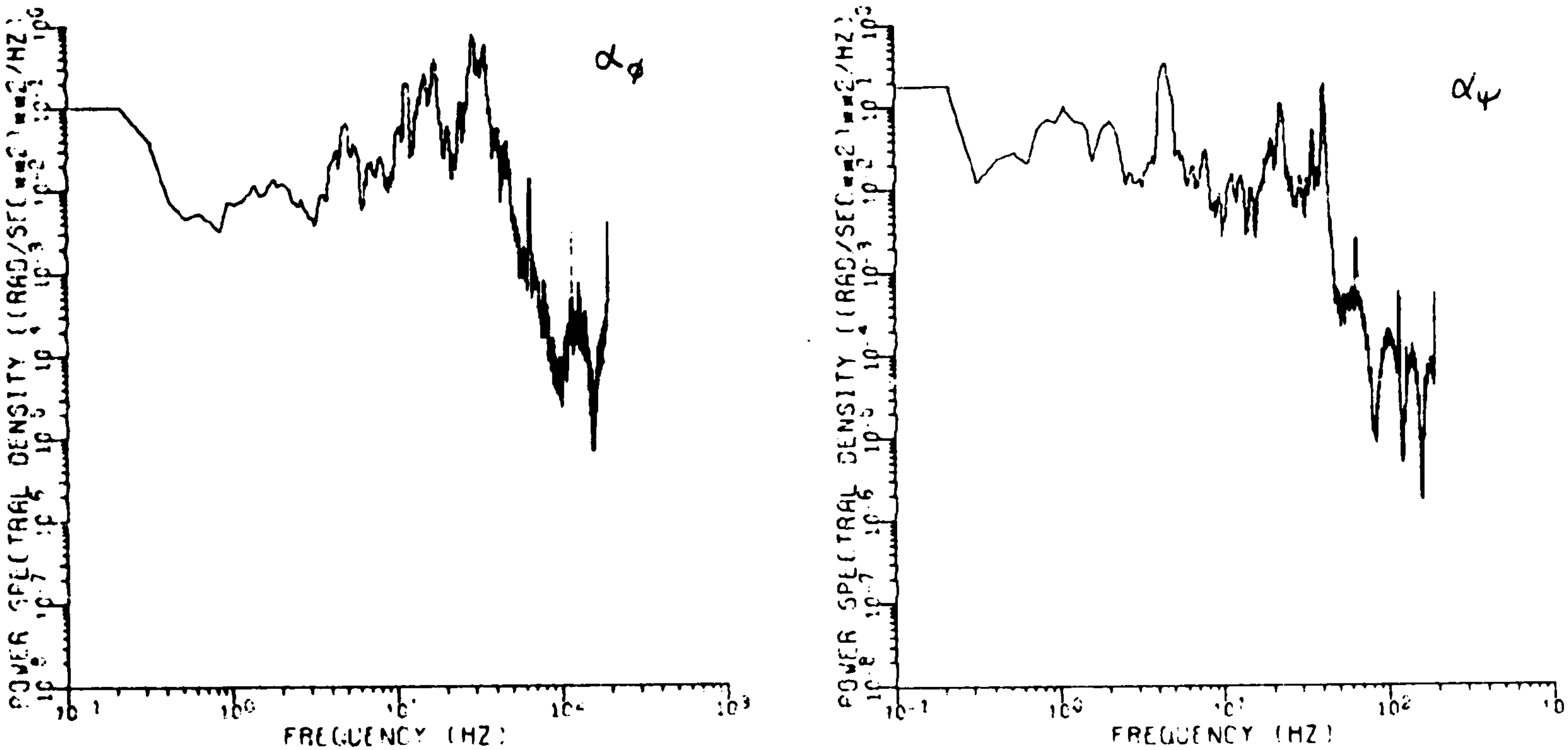

Figure E.9. Spectral Density α_ϕ, α_ψ - Curve Section

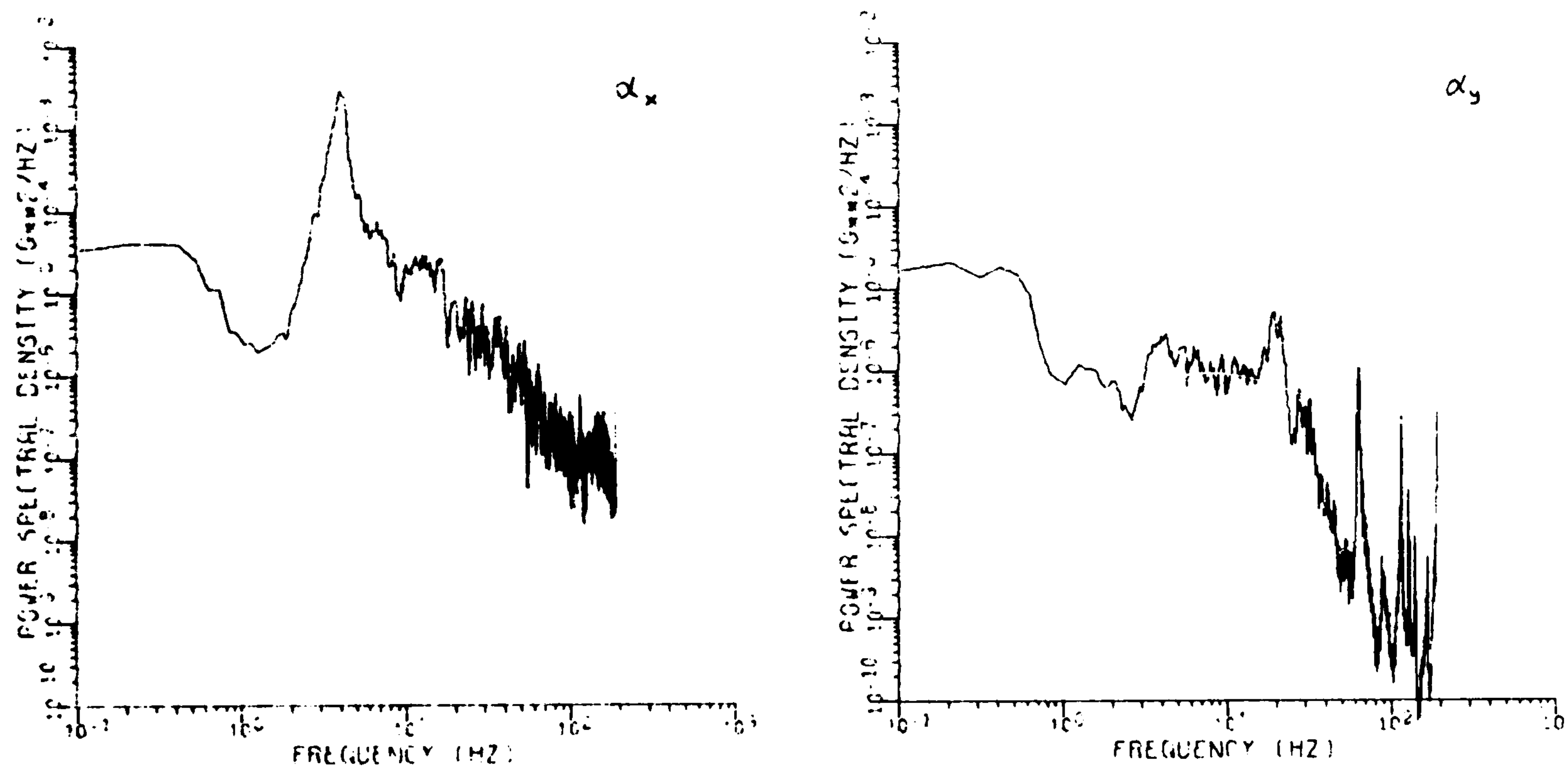

Figure E.10. Spectral Density α_x, α_y - Deceleration to Station C.

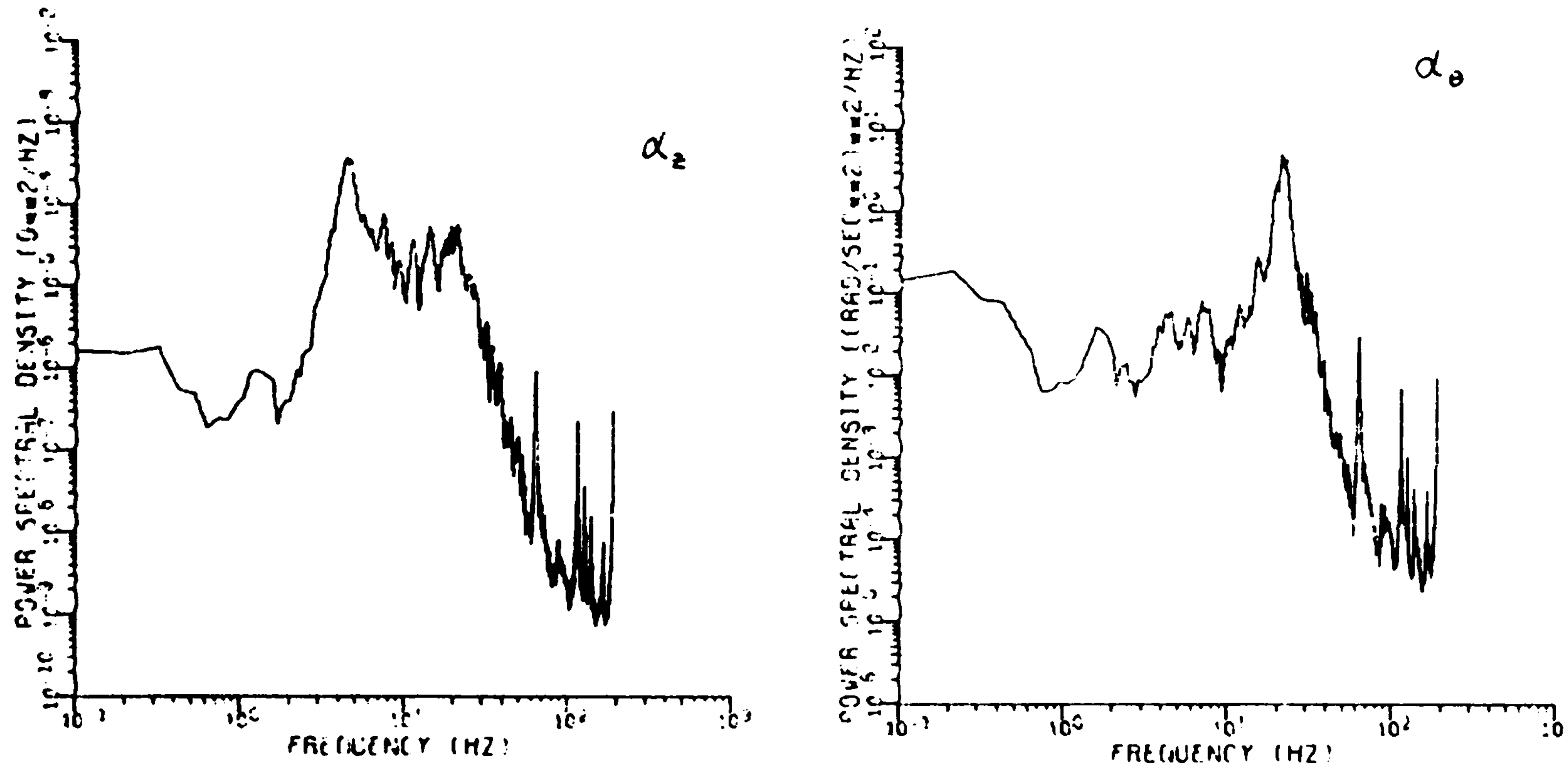

Figure E.11. Spectral Density a_z, a_θ - Deceleration to Station C.

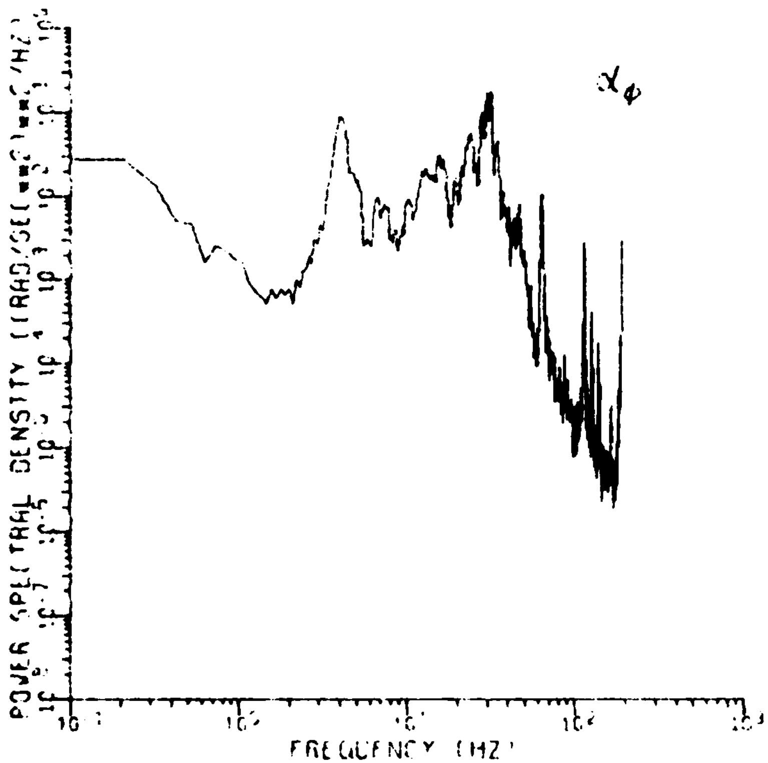

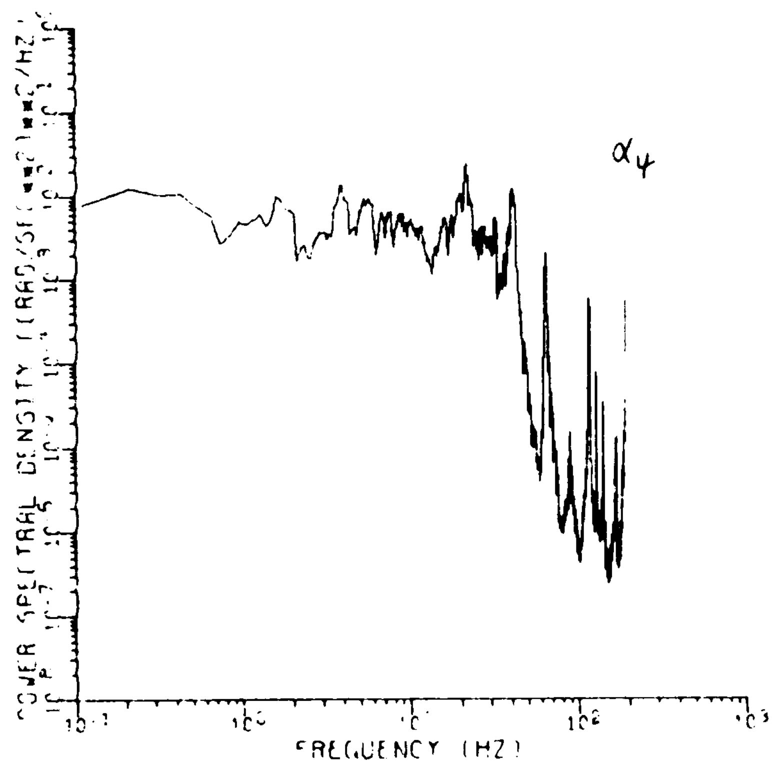

Figure E.12 Spectral Density α_ϕ, α_ψ - Deceleration to Station C.

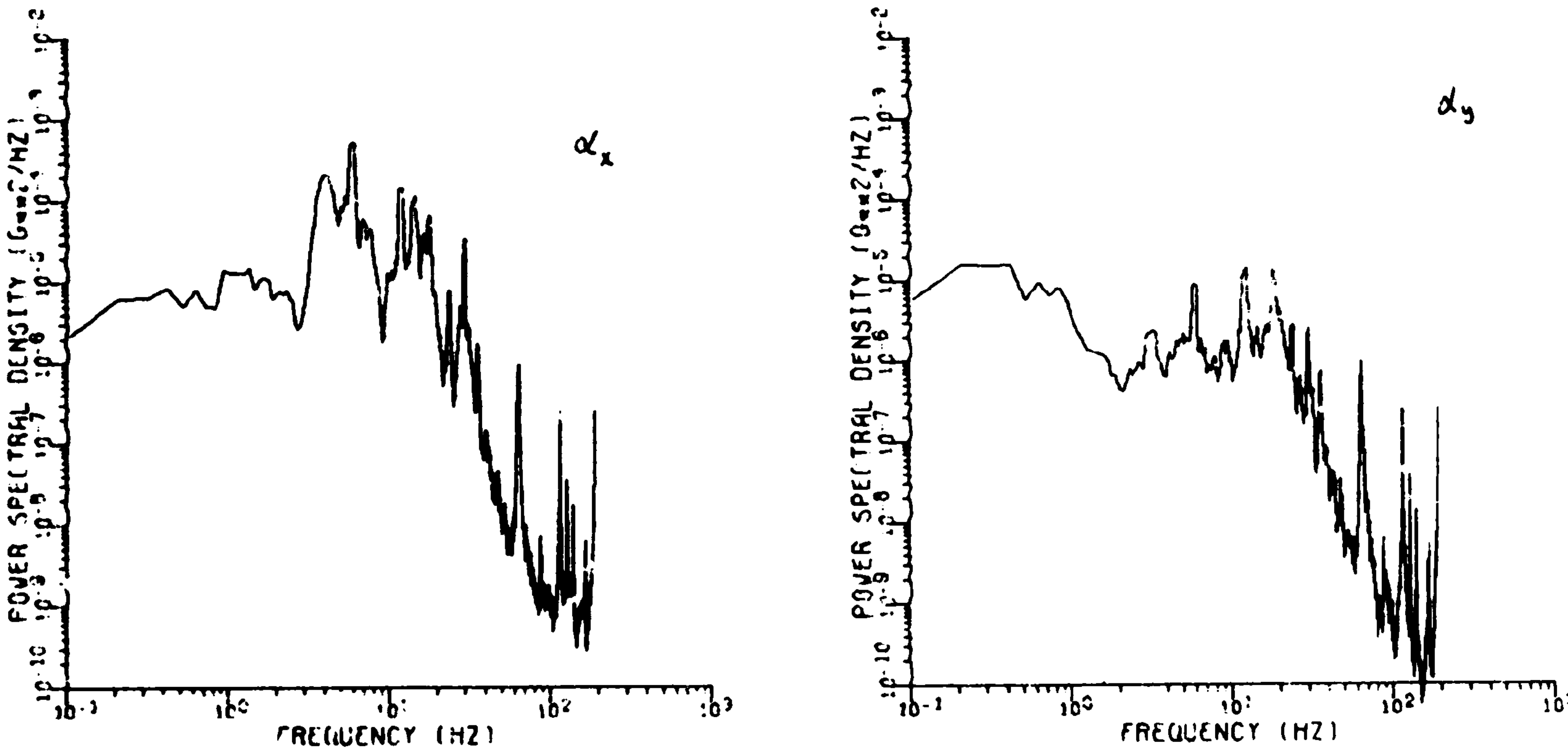

Figure E.13 Spectral Density a_x, a_y - Long Straight Section.

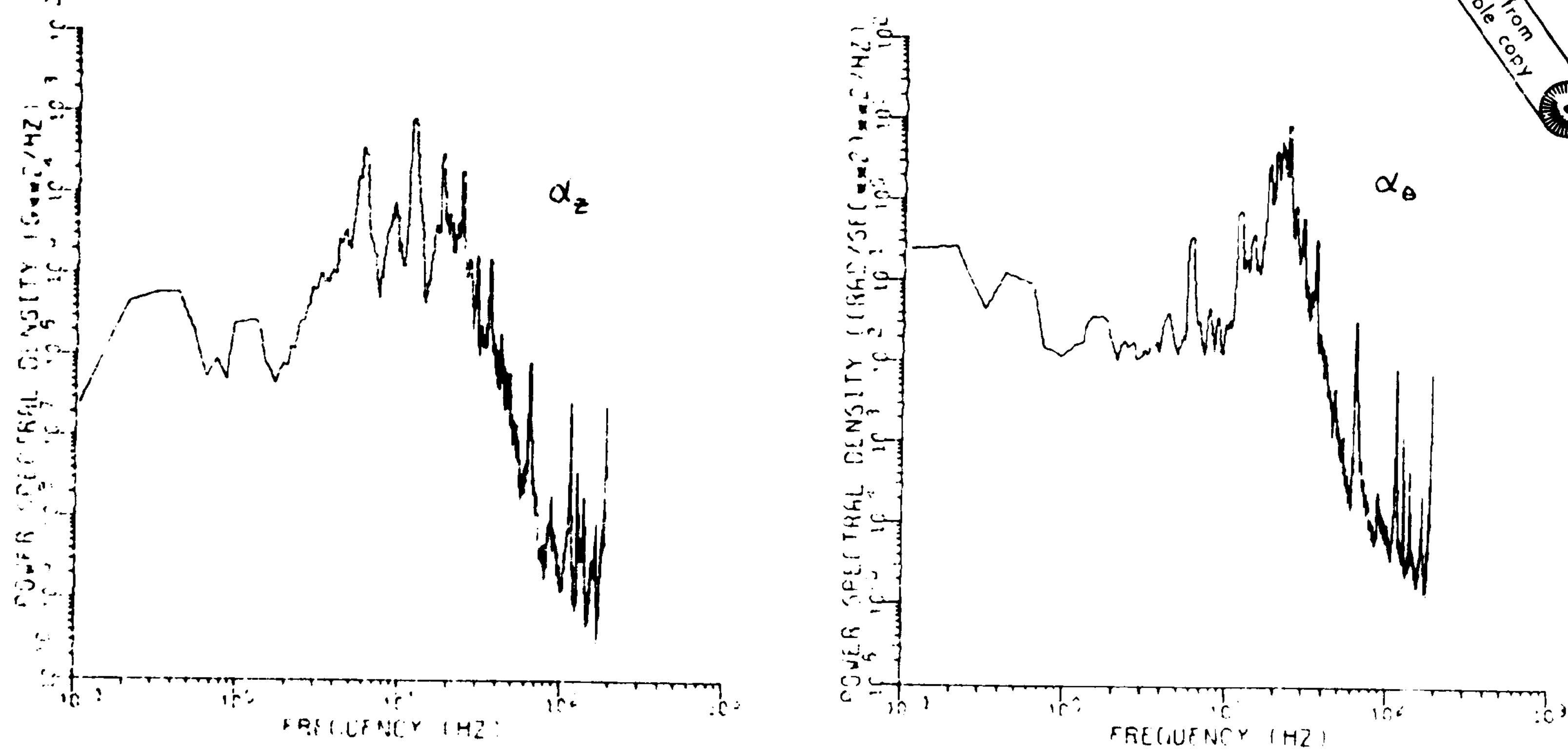

Figure E.14 Spectral Density α_z, α_θ - Long Straight Section.

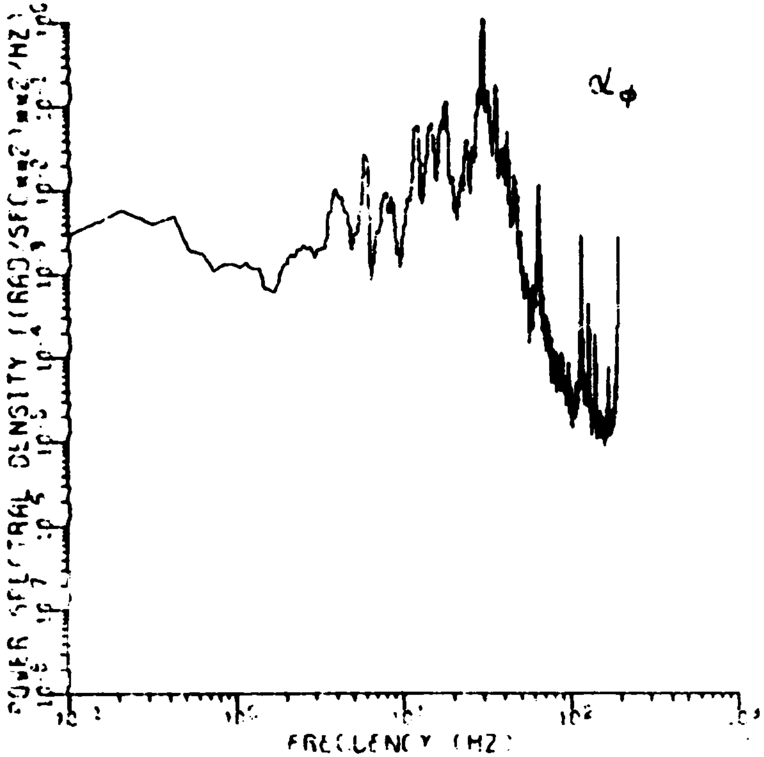

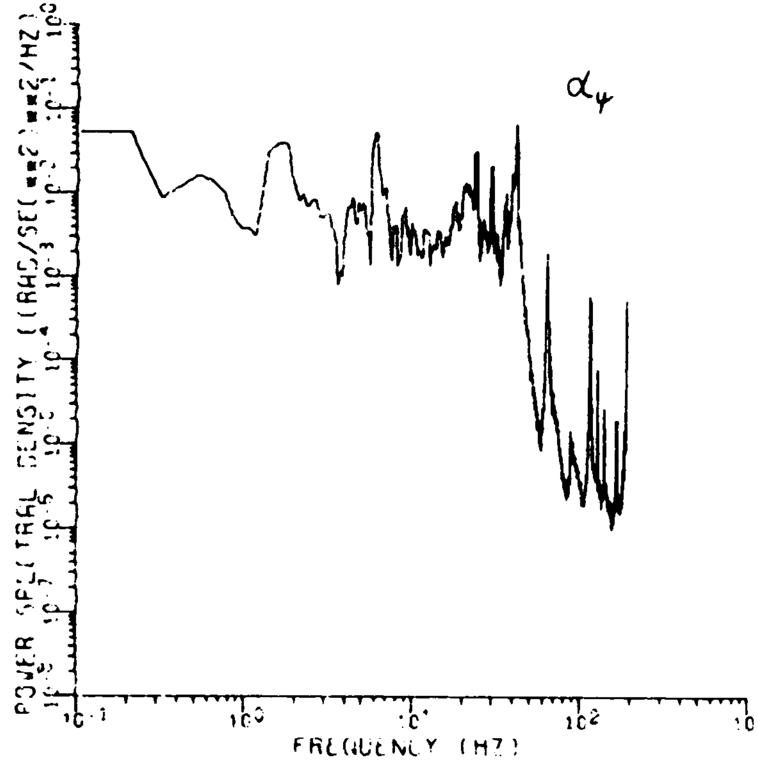

Figure E.15 Spectral Density α_ϕ, α_ψ - Long Straight Section.

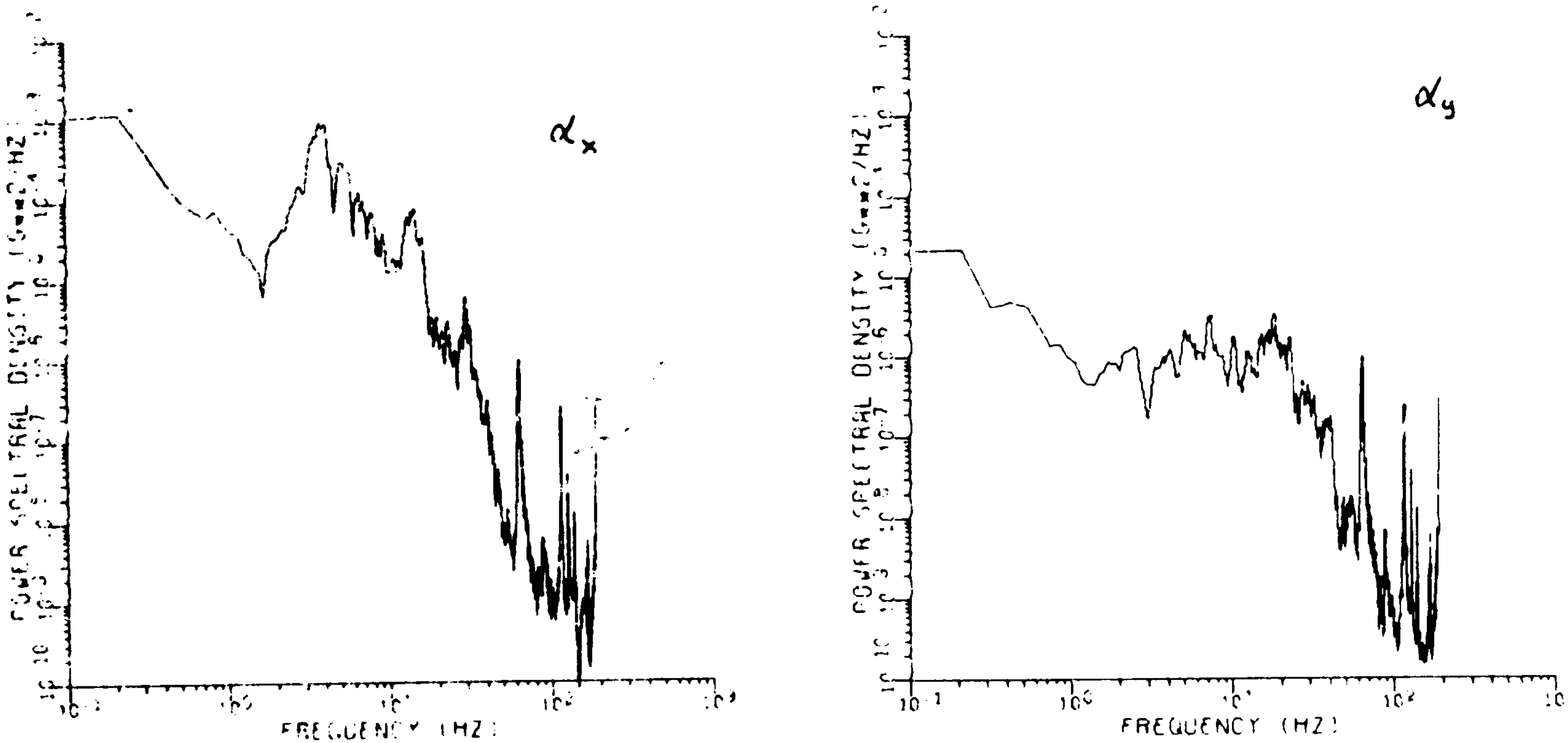

Figure E.16 Spectral Density a_x, a_y - Acceleration to Full Speed.

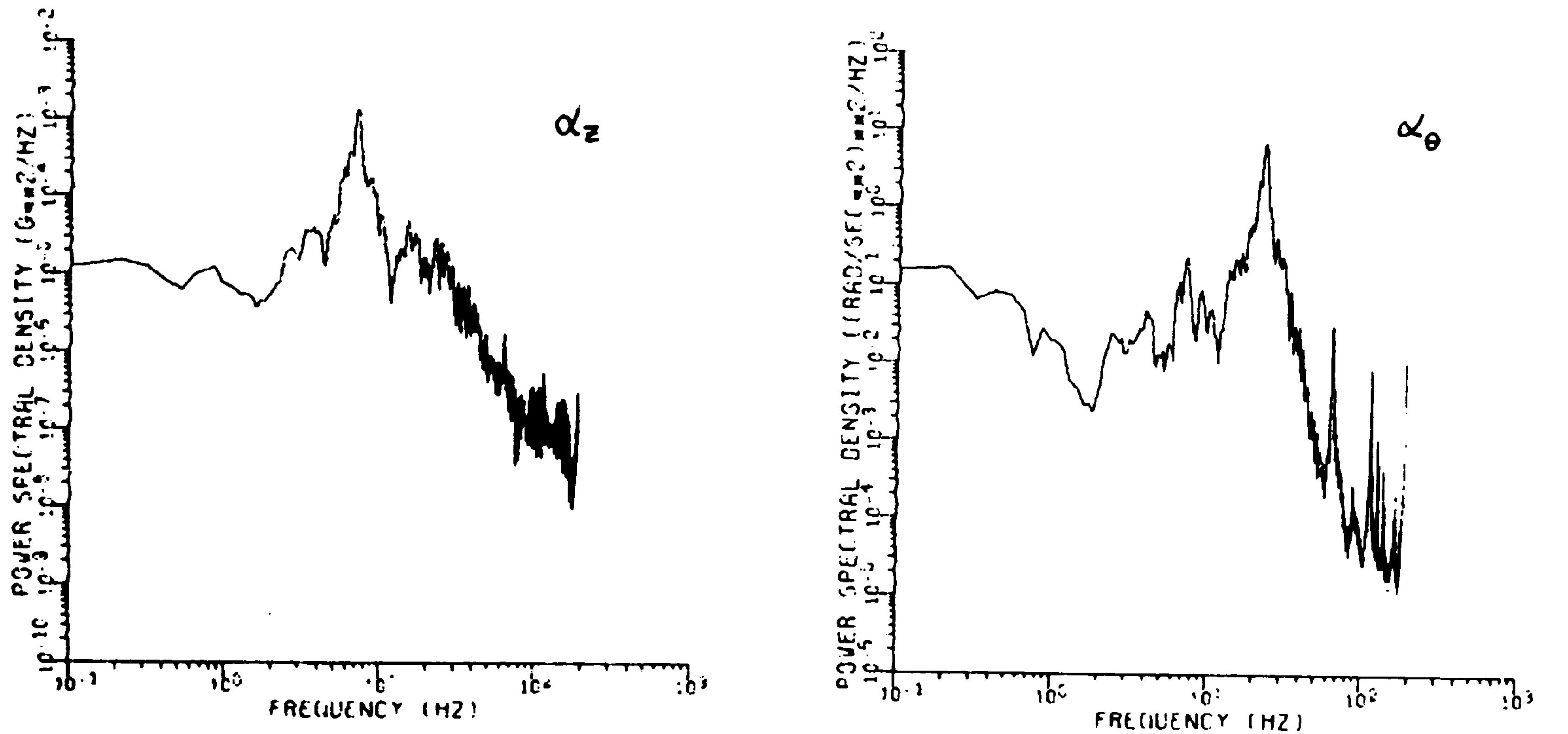

Figure E.17 Spectral Density α_z, α_θ - Acceleration to full Speed.

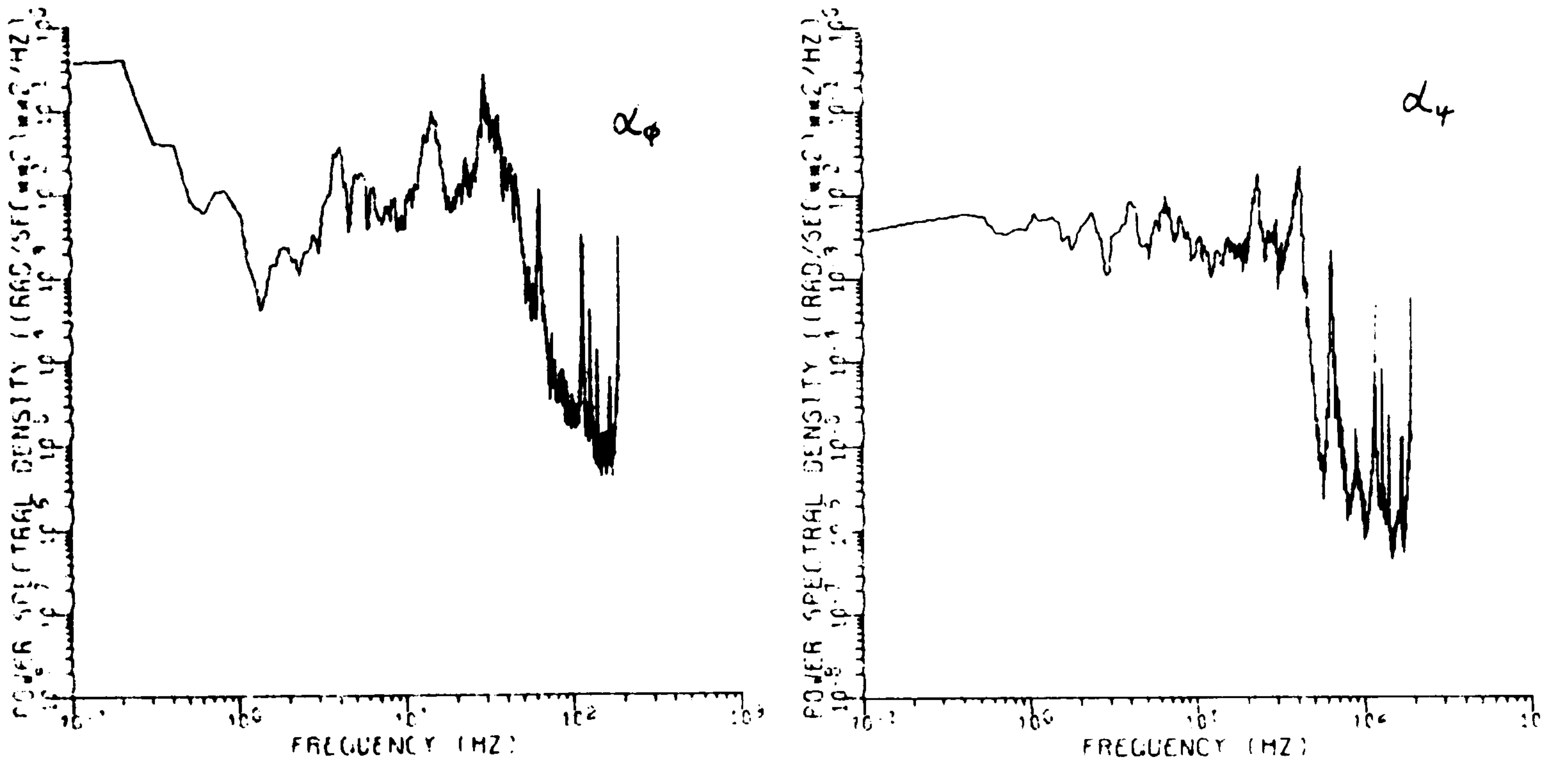

Figure E.18. Spectral Density α_ϕ, α_ψ - Acceleration to Full Speed.

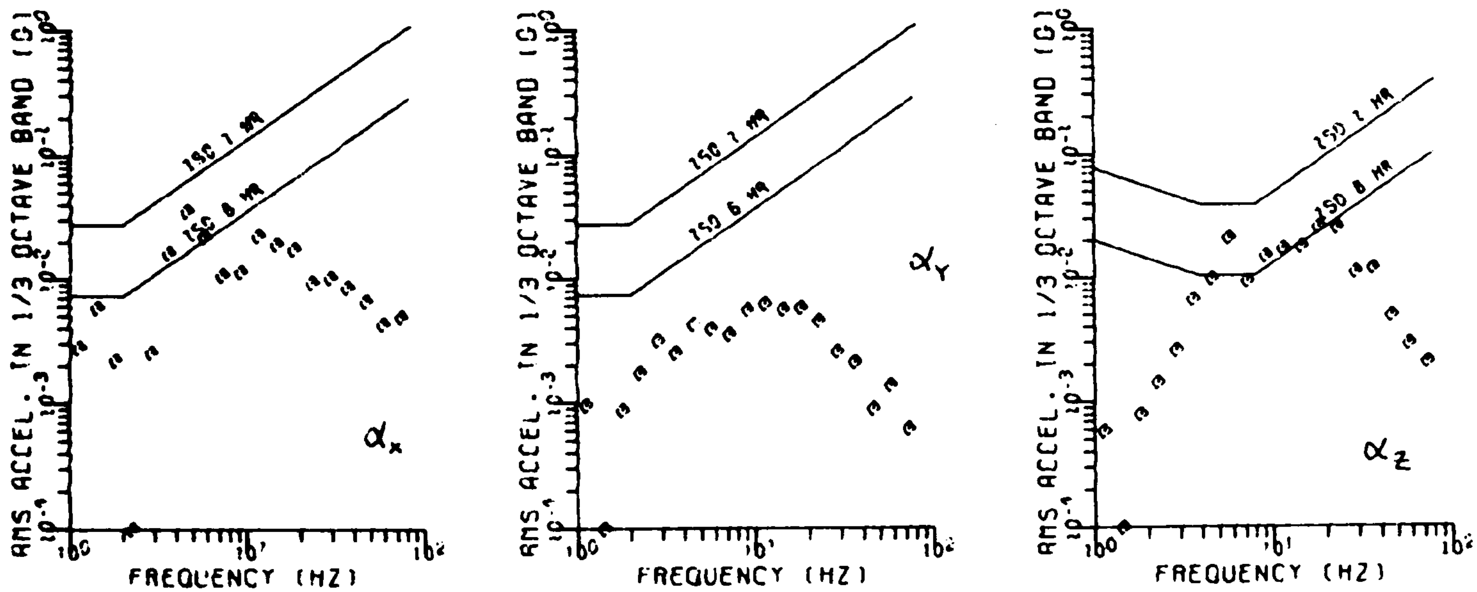

Figure E.19. 1/3 Octave Band Results a_x, a_y, a_z - Curve Section.

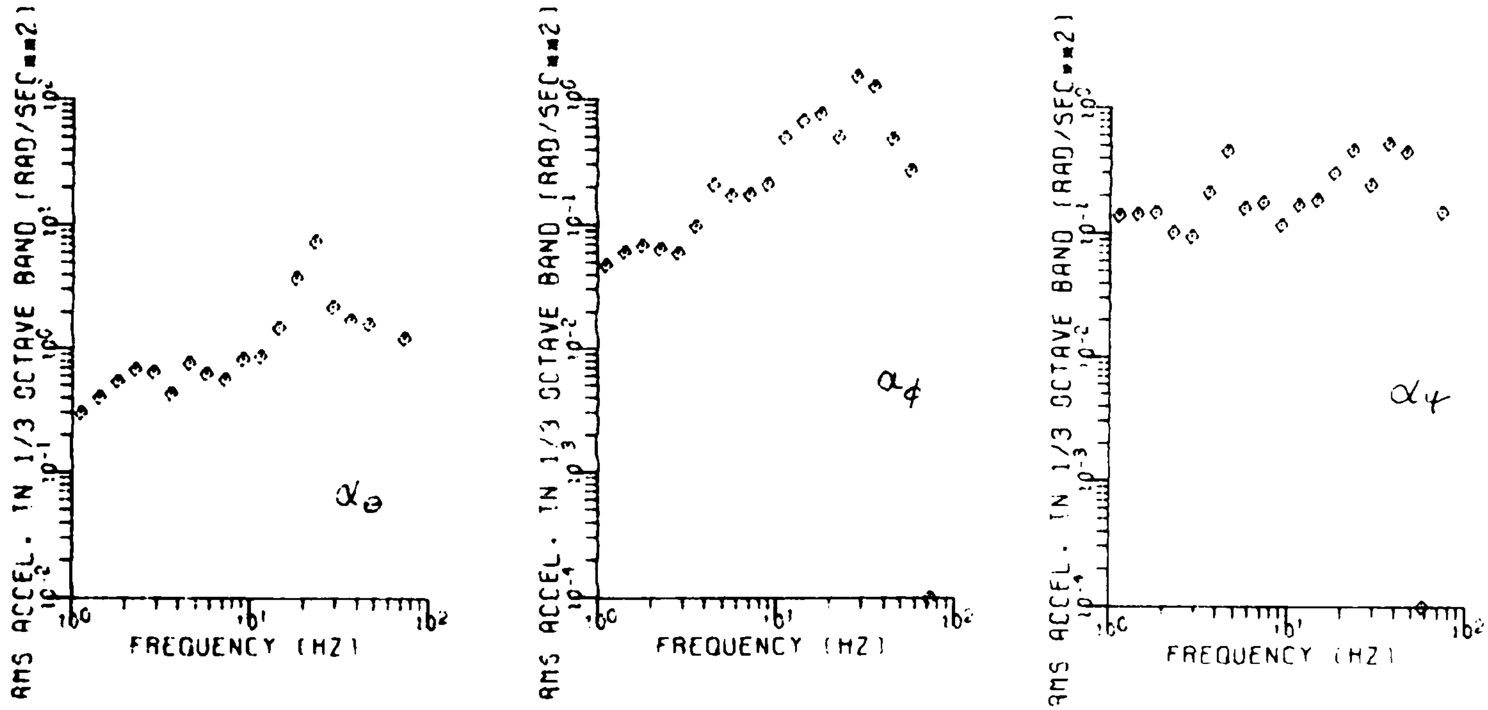

Figure E.20. 1/3 Octave Band Results α_θ, α_ϕ, α_ψ - Curve Section.

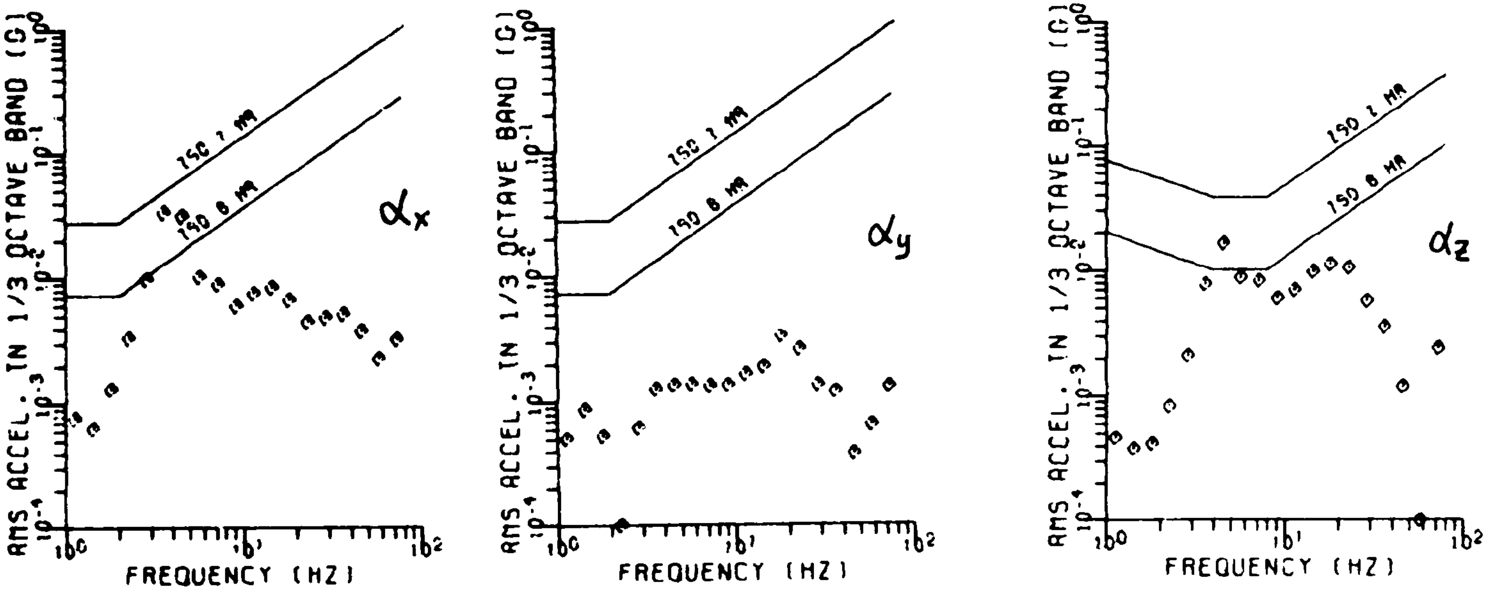

Figure E.21. 1/3 Octave Band results a_x, a_y, a_z - Deceleration into Station C.

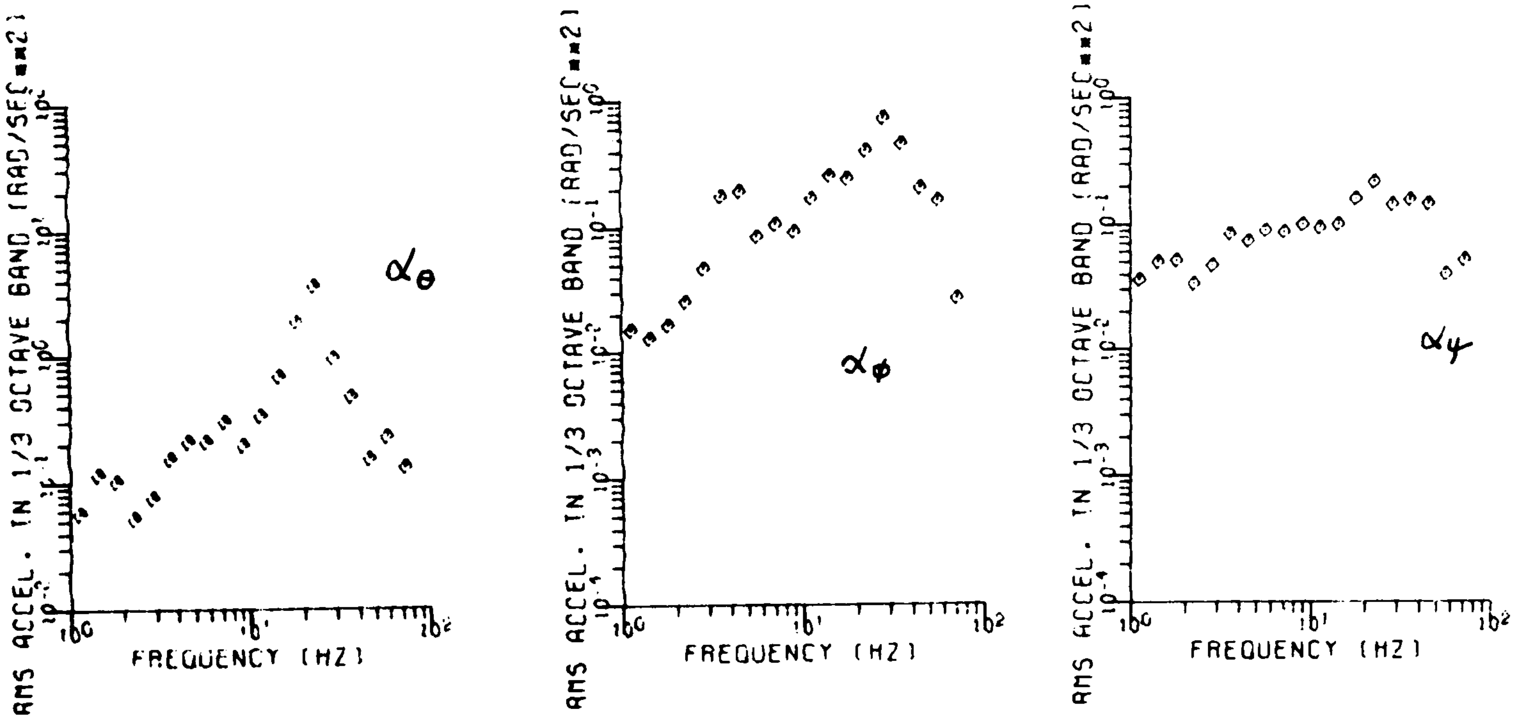

Figure E.22. 1/3 Octave Band Results α_θ, α_ϕ, α_ψ - Deceleration into Station C.

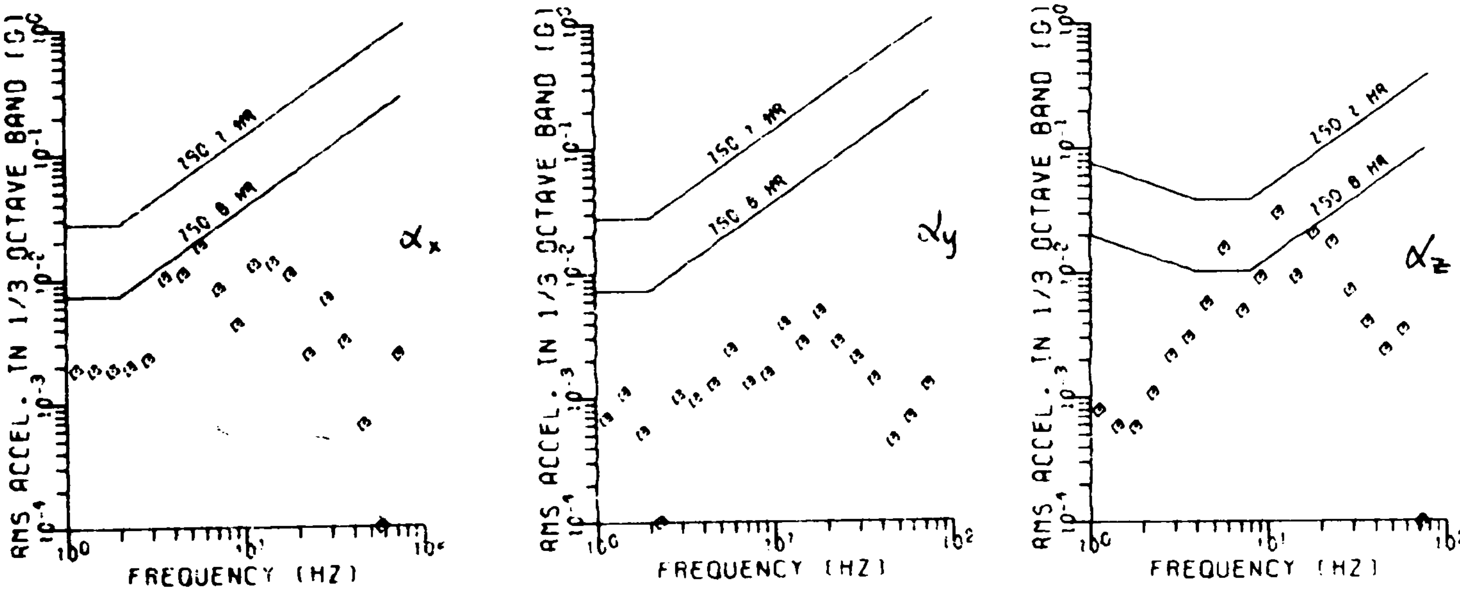

Figure E.23. 1/3 Octave Band Results a_x, a_y, a_z - Long Straight Section at Full Speed

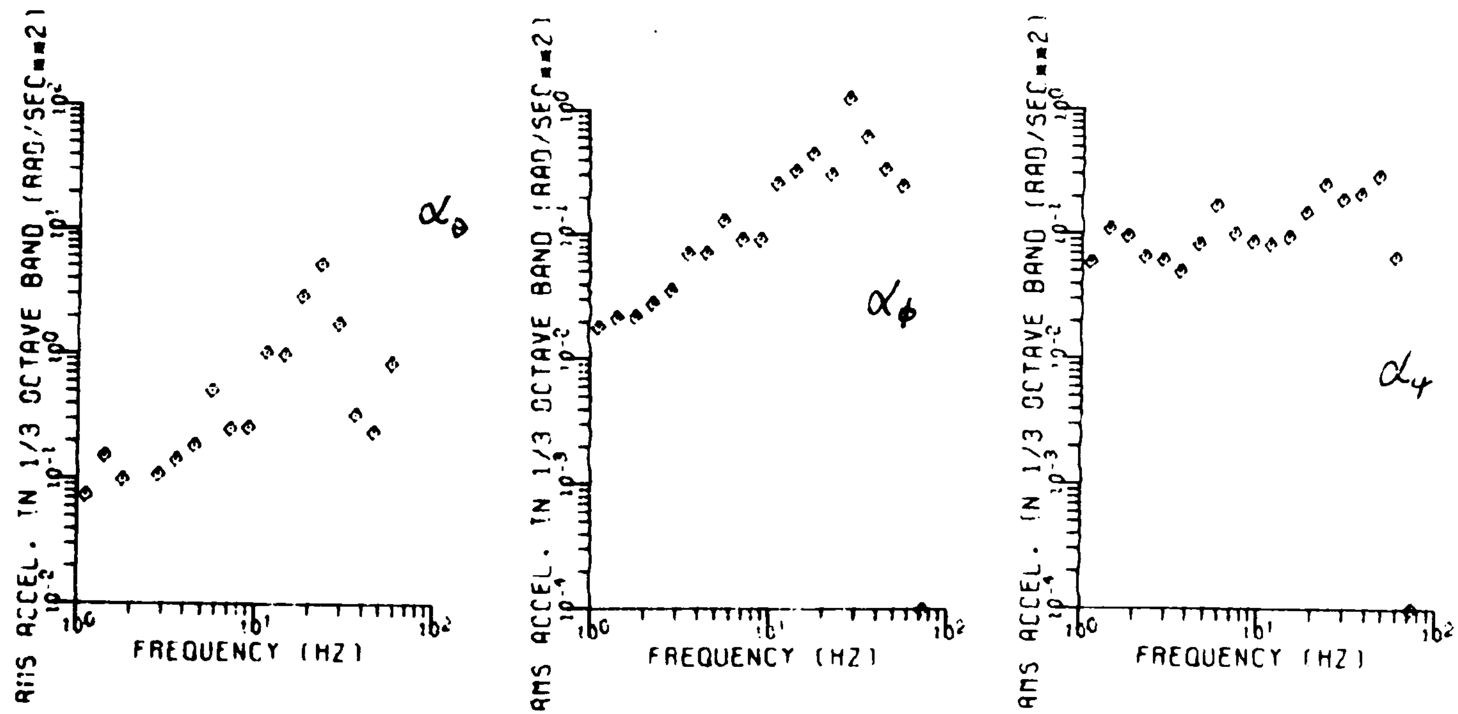

Figure E.24. **1/3 Uctave Band Reuslts α_θ, α_ϕ, α_ψ - Long Straight Section at Full Speed.**

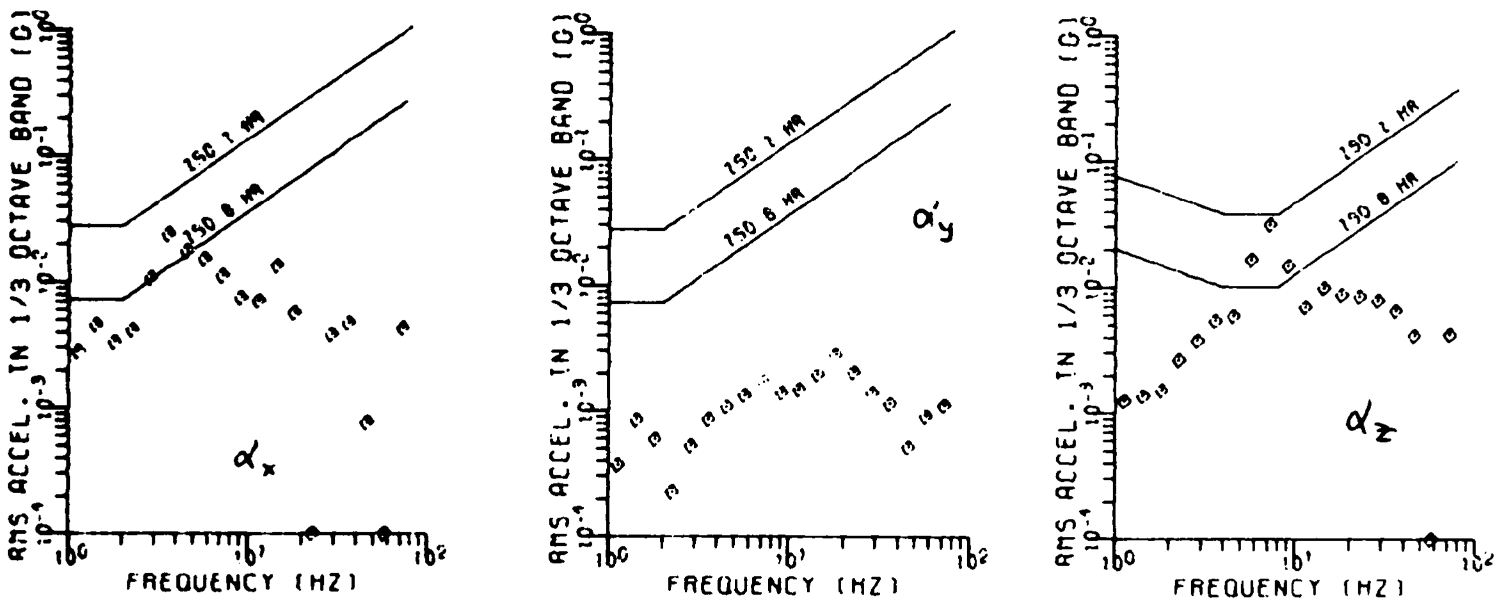

Figure E.25. 1/3 Octave Band Results α_x, α_y, α_z - Acceleration to Full Speed.

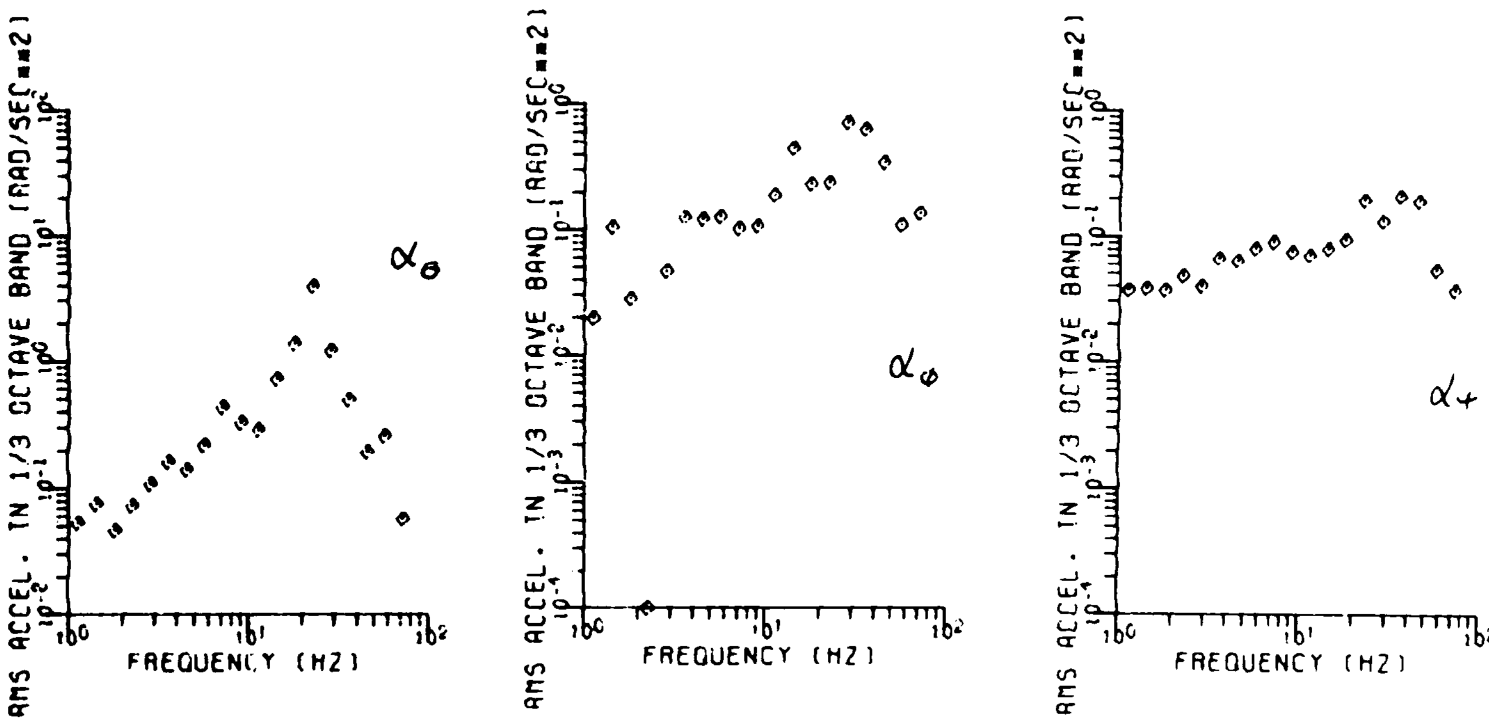

Figure E.26. 1/3 Octave Band Results α_θ, α_ϕ, α_ψ - Acceleration to Full Speed.

EFFECTS OF USING THE LINEAR INDUCTION MOTOR DRIVE

The experiment, as described previously, was repeated using another vehicle which had been modified by removing the two conventional drive motors and replacing them with two linear induction motor (L.I.M.) units. Figure E.27 shows a photograph of the L.I.M. driven vehicle. The motors were placed in line and mounted to the vehicle supporting yoke close to the bottom flange of the guideway. Because of the attractive force developed between the motor windings and the guideway lower flange, a set of spacing wheels are provided to limit the motor-guideway clearance to about 1/4 inch.

The vibration recordings, made in an identical fashion to those previously described, were again analyzed for spectral and one-third octave band content. Again, four classes of sections were isolated. Each of the cases (acceleration, deceleration, travel down the long straight section, travel in the curves) was isolated into records of 10-seconds duration and the analyses for each degree of freedom (a total of twenty four spectral curves) are given in Figures E.28-30. Figures E.40-51 give the one-third octave band results for the same cases. The figures are summarized in Table E-4.

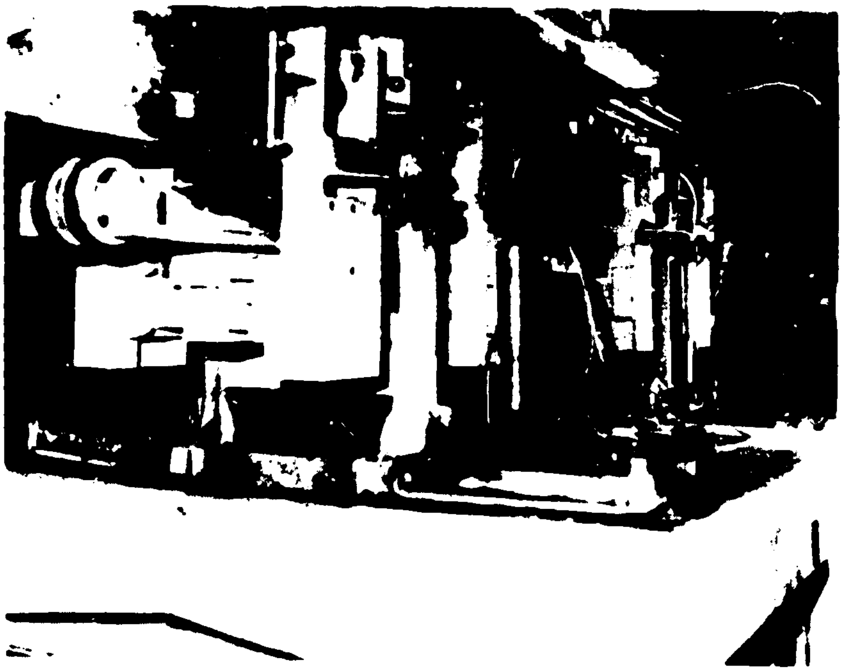

Figure E.27. Photograph Showing the L.I.M. Drive.

TABLE E-4. ORGANIZATION OF SPECTRAL PLOTS IN THE FIGURES (LIM VEHICLE)

Condition	P.S.D.	1/3 Octave Analysis
Sway in Curve	Figs. E.28 to E.30	Figs. E.40 to E.42
Deceleration into C	Figs. E.31 to E.33	Figs. E.40 to E.42
Long Straight Section	Figs. E.34 to E.36	Figs. E.46 to E.48
Acceleration to full speed from A	Figs. E.37 to E.39	Figs. E.49 to E.51

General Comments on the Frequency Content of the Ride

Based on an overview of the results, two outstanding features have been found. First, during the acceleration and deceleration periods, a fore-and-aft pulsation at about 4 Hz was found. Second, resonances at 15 Hz in the longitutinal direction and at 20 Hz in the transverse direction were observed. During the experiment, these components were noticed and by separate excitation it it was determined that these were structural modes in their respective directions. In terms of ride quality, the 4 Hz component would appear to be the most noticeable. Passenger sensitivity to components above 15 Hz is much less than for lower frequencies. It was noticed that the 15 Hz and 20 Hz components referred to above were also present with the conventional drive.

Summary of Ride Features as Compared to Long Straight Section Ride.

Firstly, with respect to the sway sections, the following comments can be made:

Sway Section;	α_x	virtually unchanged
	α_y	levels are higher for frequencies less than 4 Hz
	α_z	virtually unchanged
	α_θ	increased levels in the low frequency range
	α_ϕ	virtually unchanged
	α_ψ	higher levels in the low frequency range.

Secondly, with respect to the acceleration section.

Acceleration;	α_x	4 Hz component is enhanced
	α_y	little difference
	α_z	little difference
	α_θ	general increase in low frequency (0.1 Hz. to 4 Hz.)
	α_ϕ	4Hz. component stronger
	α_ψ	little change.

Thirdly, with respect to the deceleration section, a similar comparison can be made as for the acceleration case except that the αx and αy levels are much increased in the low frequency zone.

A general summary of root mean square values is given in Table V.

Also provided, in Table VI, is a summary of the I.S.O. weighted root mean square accelerations for the same conditions as in Table V. In Table VI only the translatory directions are used as the I.S.O. Guide (3) does not include a mechanism for assessing rotational components of motion.

TABLE E-5.

R.M.S. to 200Hz. for 6 degree of freedom motions.

	α_x	α_y	α_z	α_θ	α_ϕ	α_ψ	RATING
SWAY	0.037	0.011	0.035	8.73	0.923	0.684	3
DECELERATION	0.037	0.026	0.018	6.94	0.676	0.387	4
LONG STRAIGHT	0.038	0.008	0.032	6.64	0.881	0.599	3
ACCELERATION	0.056	0.008	0.027	6.58	0.911	0.513	4

NOTE: RATINGS.

1. Very Comfortable
2. Comfortable
3. Somewhat Comfortable
4. Neutral
5. Somewhat Uncomfortable
6. Uncomfortable
7. Very Uncomfortable

L.I.M. Vehicle

TABLE E-6.

I.S.O. Weighted R.M.S. Accelerations (g. units).

L.I.M. Vehicle.

CONDITION	X	Y	Z
SWAY	0.0149	0.0030	0.0239
DECELERATION	0.0211	0.0044	0.0056
STRAIGHT	0.0170	0.0024	0.0251
ACCELERATION	0.0356	0.0020	0.0216

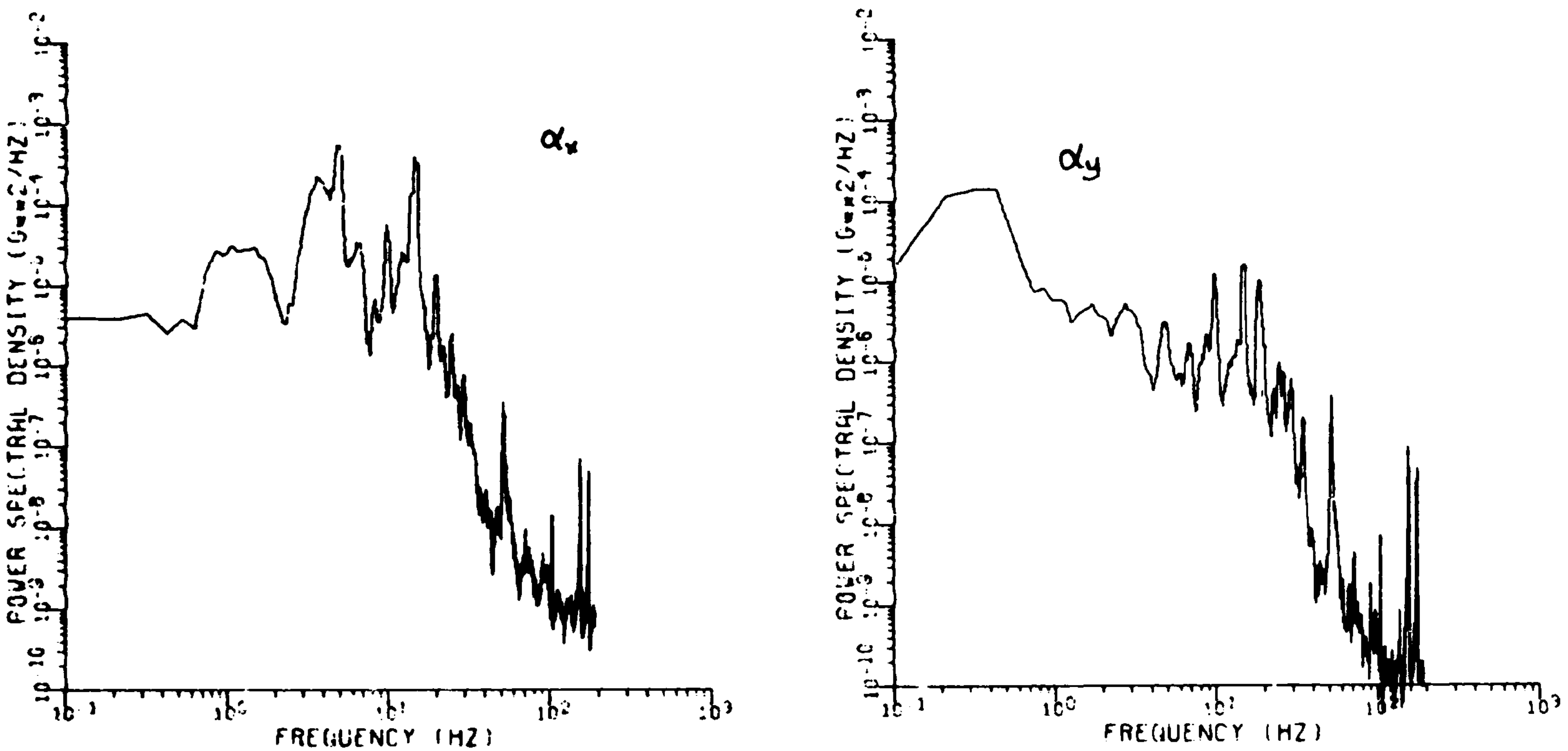

Figure E.28. Spectral Density α_x, α_y - Curve Section.

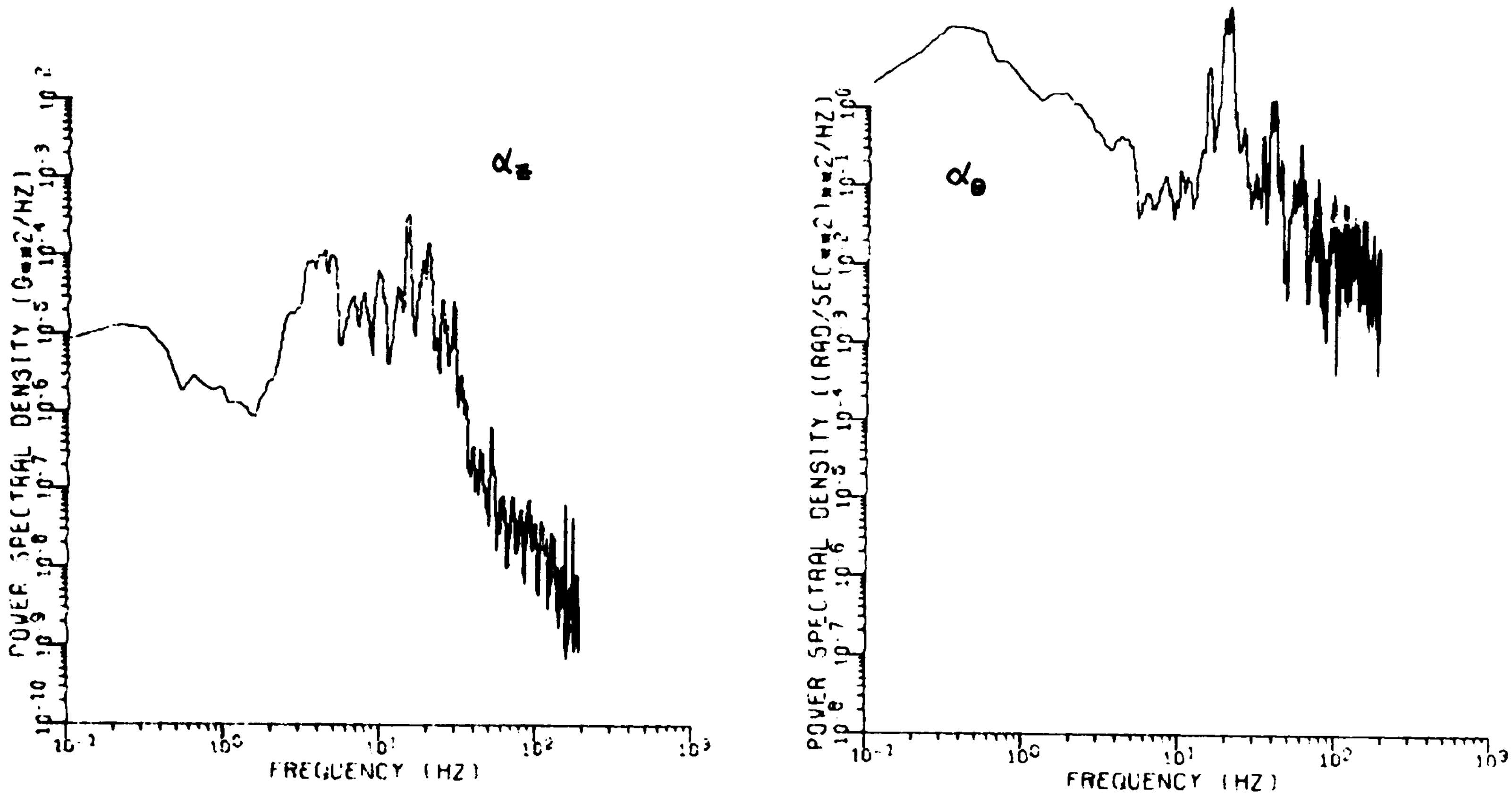

Figure E.29. Spectral Density α_z, α_θ - Curve Section.

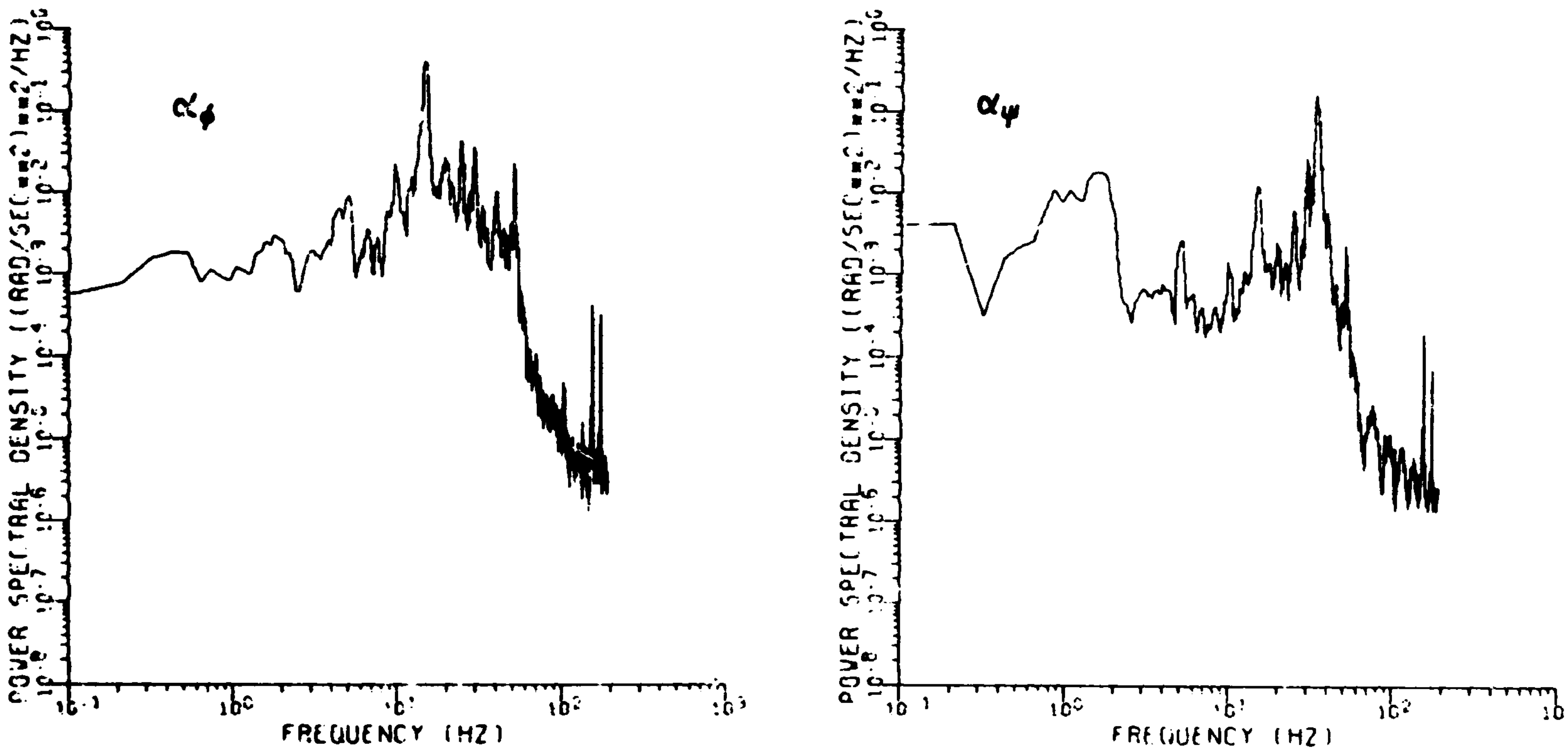

Figure E.30. Spectral Density α_ϕ, α_ψ - Curve Section.

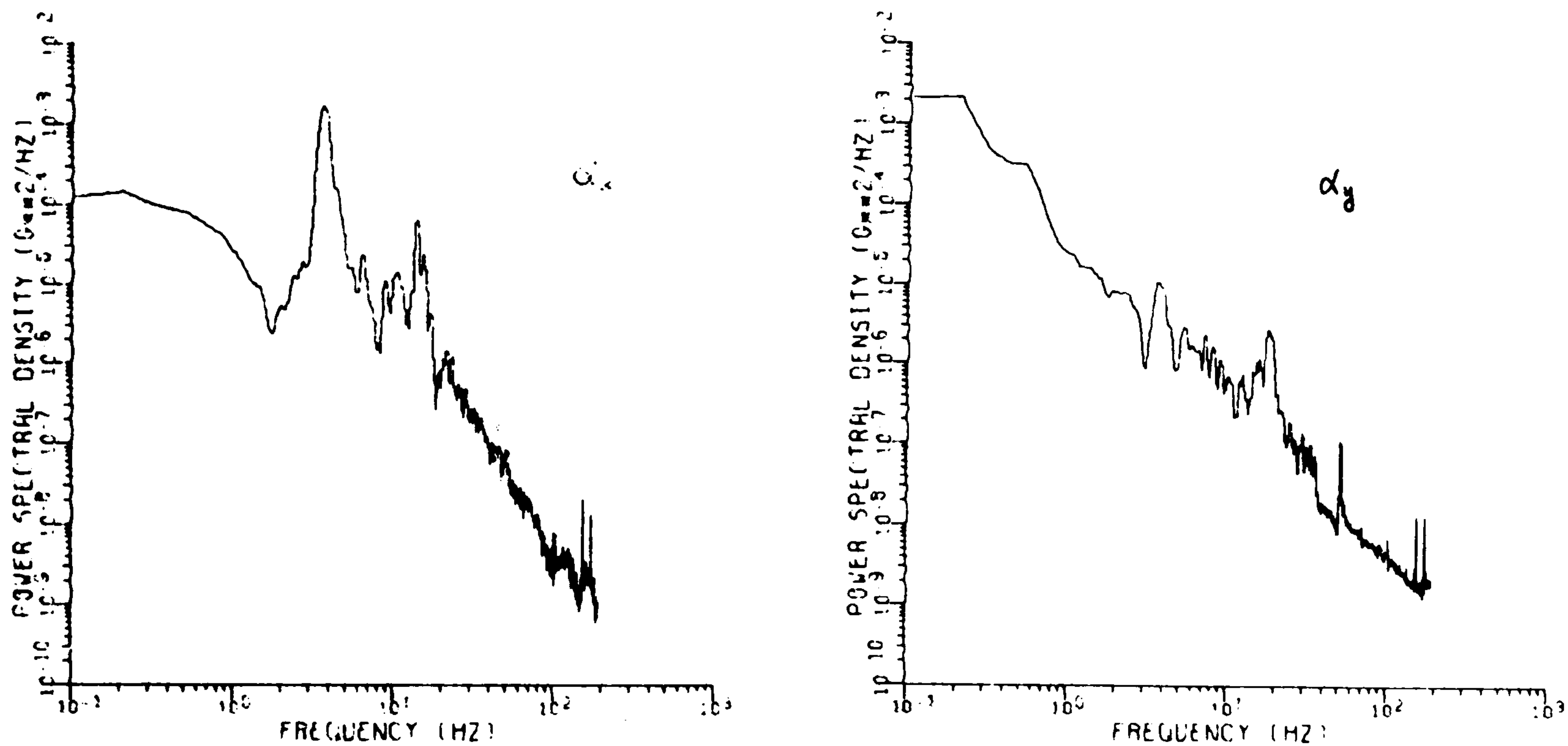

Figure E.31. Spectral Density α_x, α_y - Deceleration into Station C.

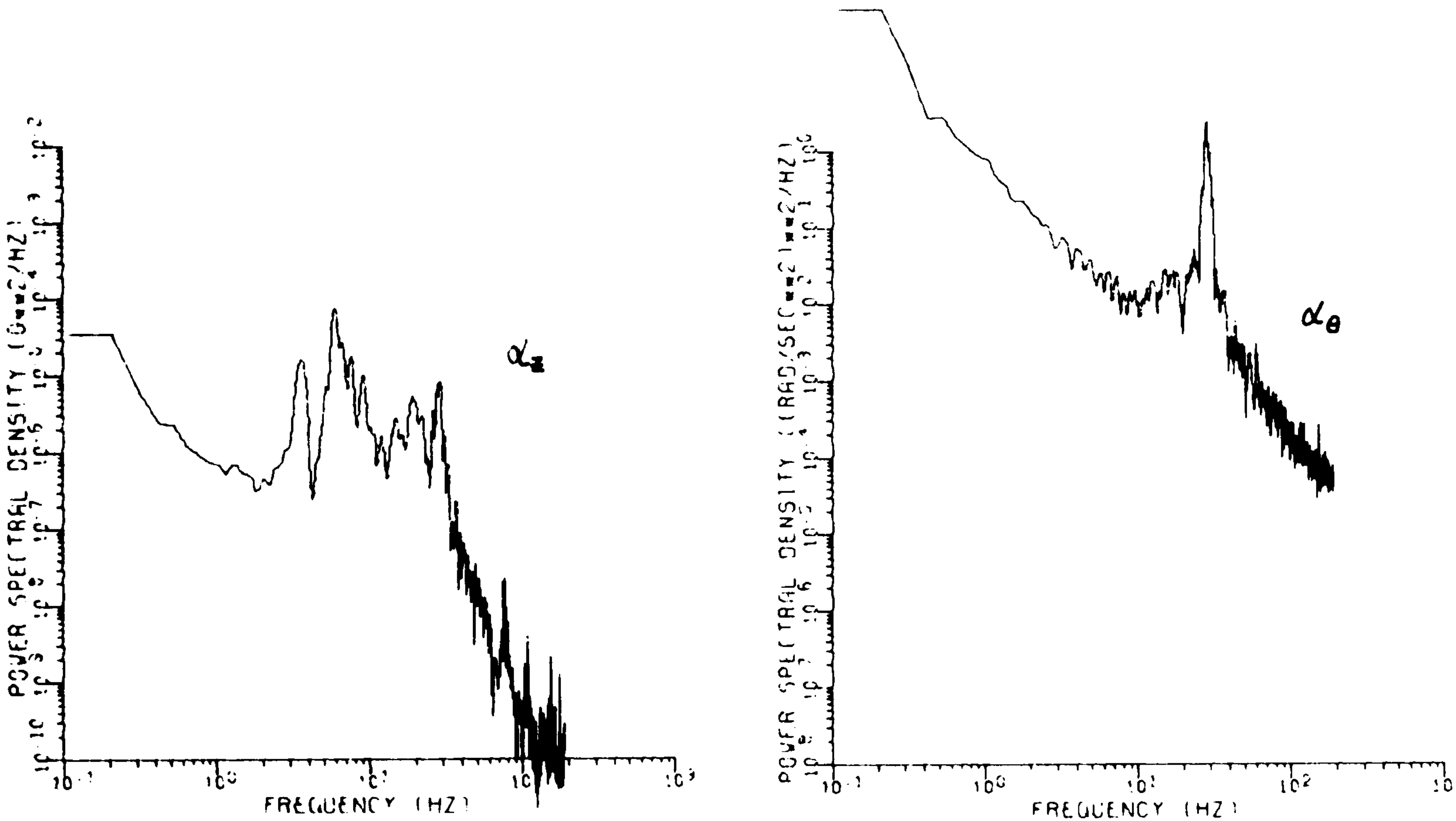

Figure E.32. Spectral Density α_z, α_θ - Deceleration into Station C.

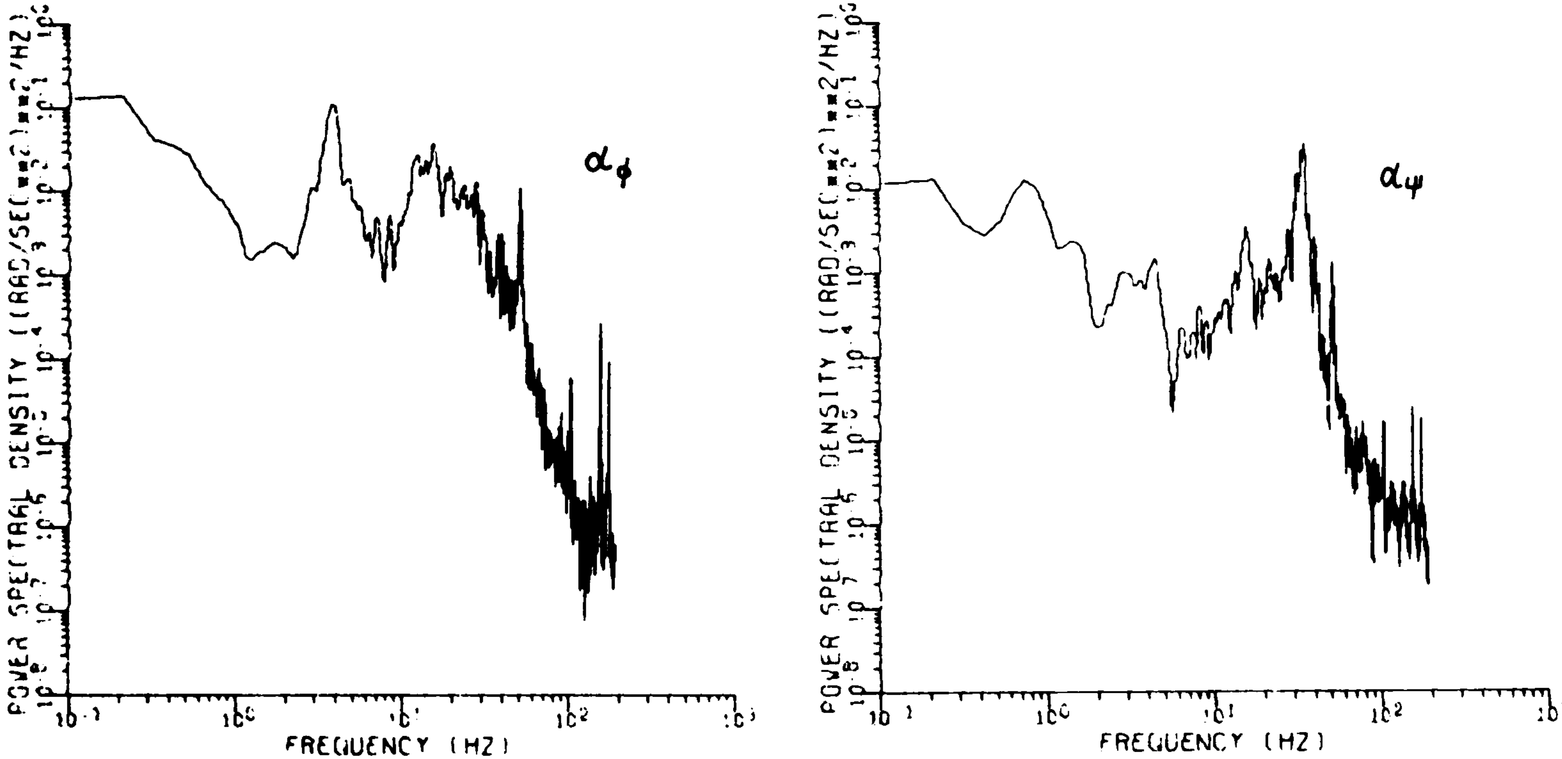

Figure E.33. Spectral Density α_ϕ, α_ψ - Deceleration into Station C.

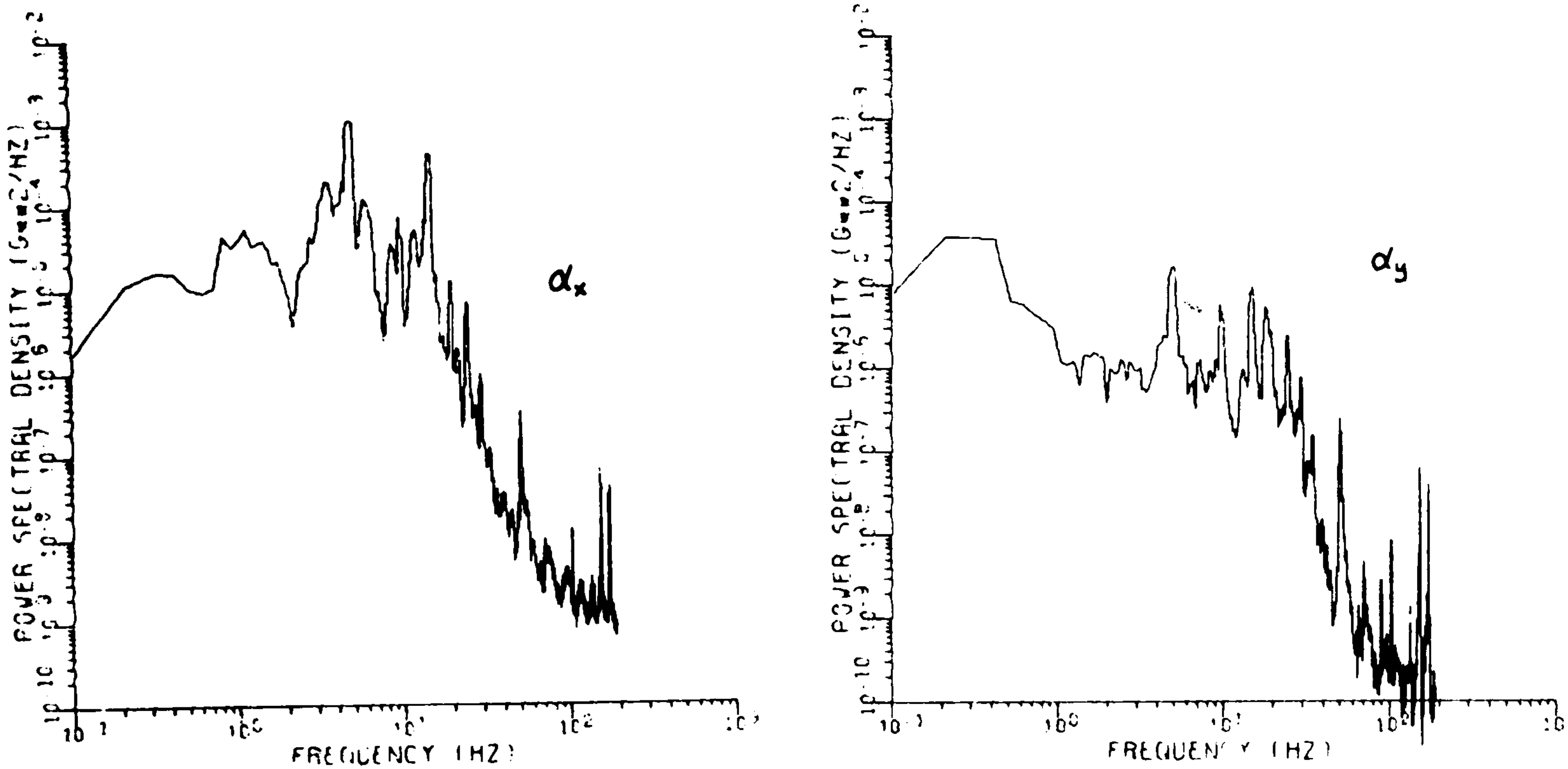

Figure E.34 Spectral Density α_x, α_y - Long Straight.

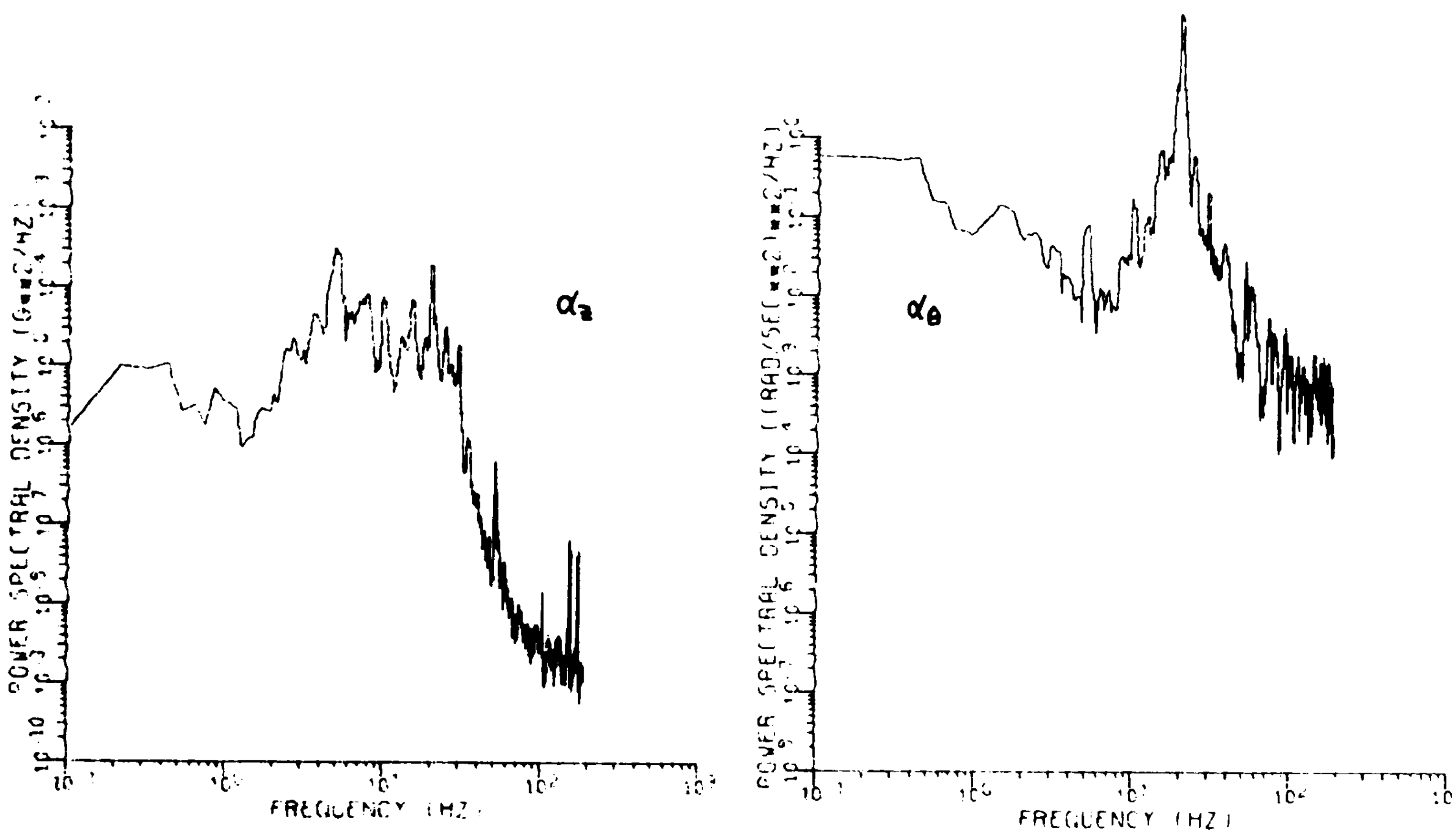

Figure E.35. Spectral Density α_z, α_θ - Long Straight.

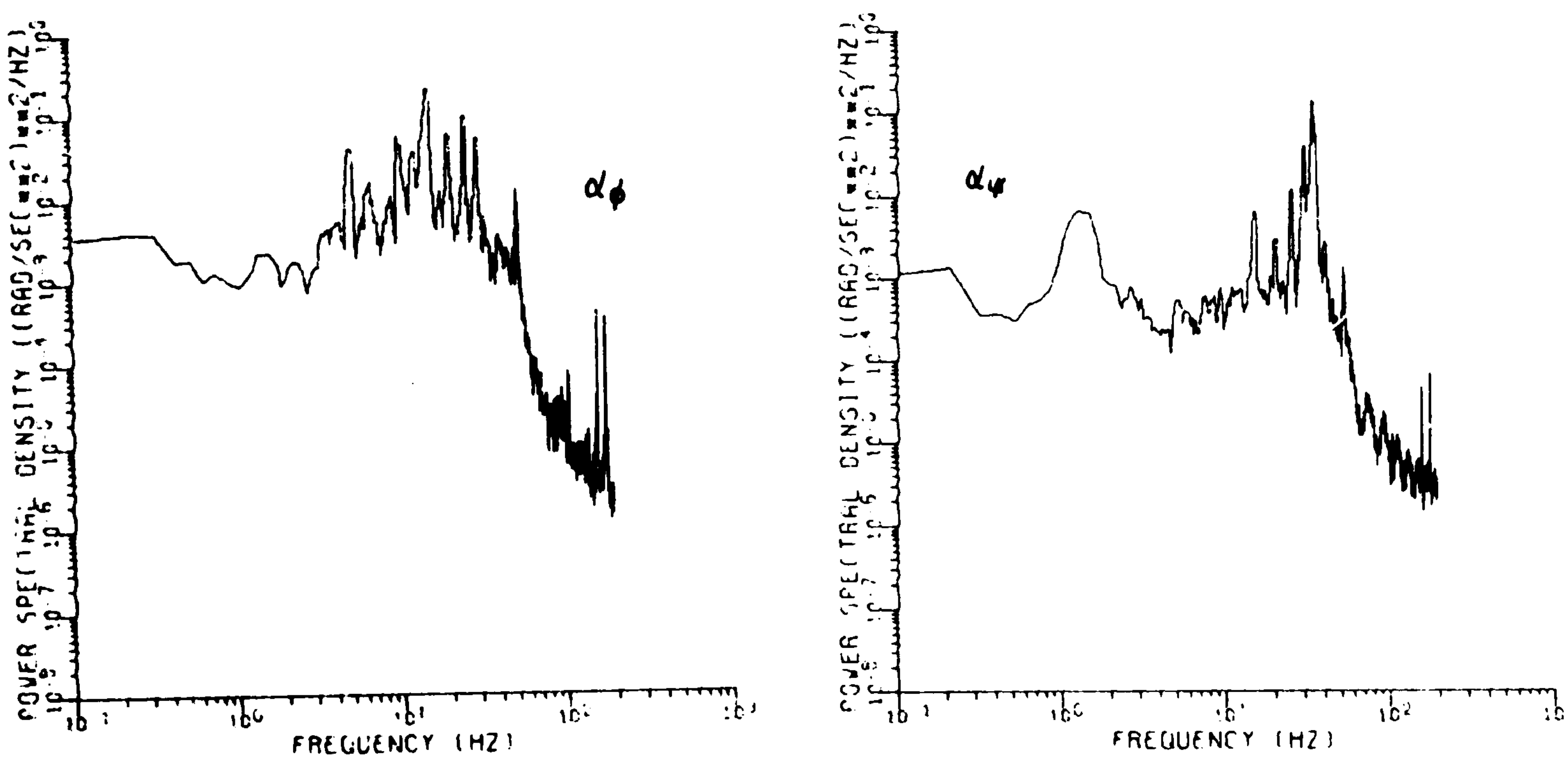

Figure E.36. Spectral Density α_ϕ, α_ψ - Long Straight.

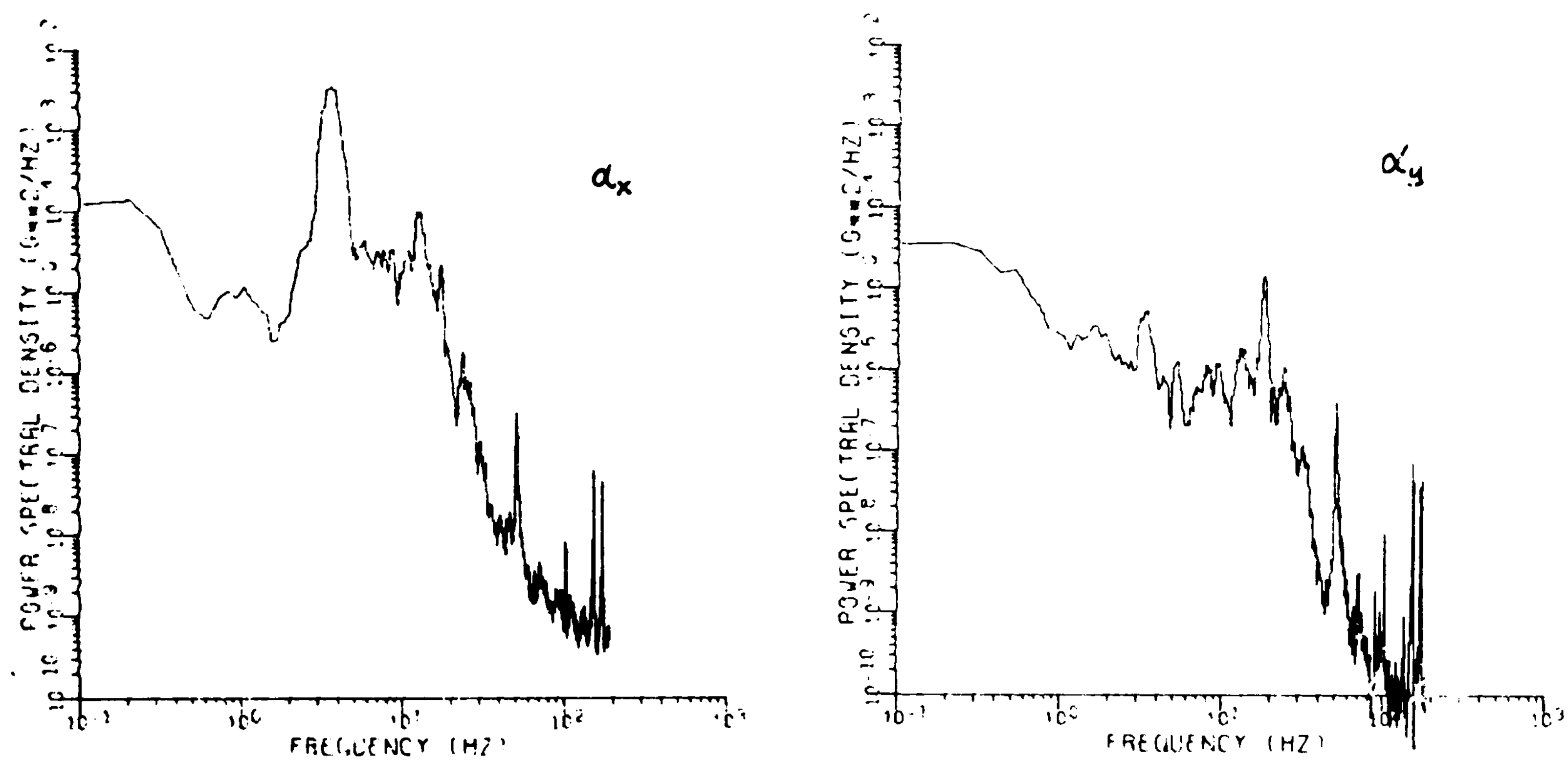

Figure E.37. Spectral Density α_x, α_y - Acceleration to Full Speed.

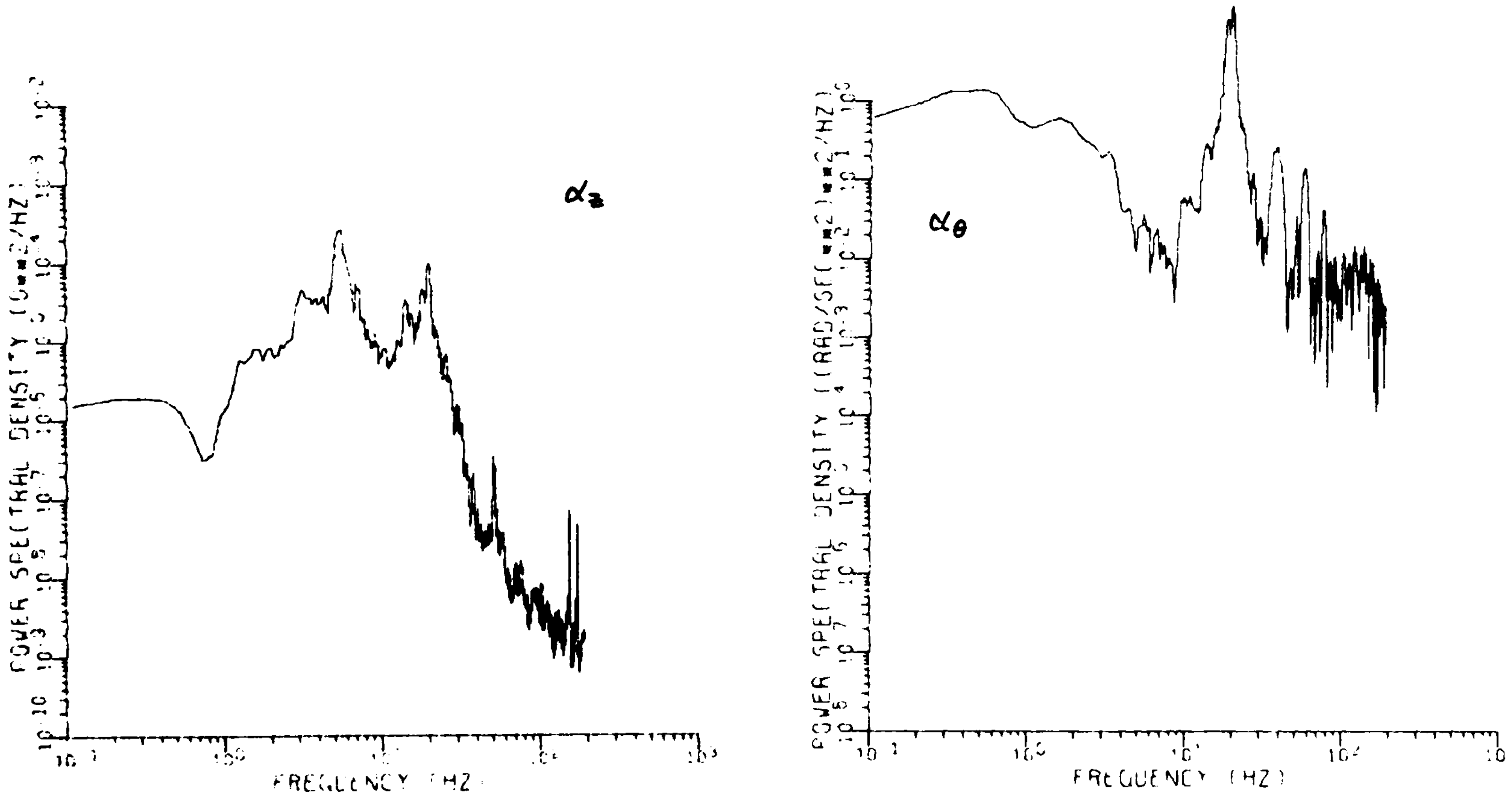

Figure E.38. Spectral Density α_z, α_θ - Acceleration to Full Speed.

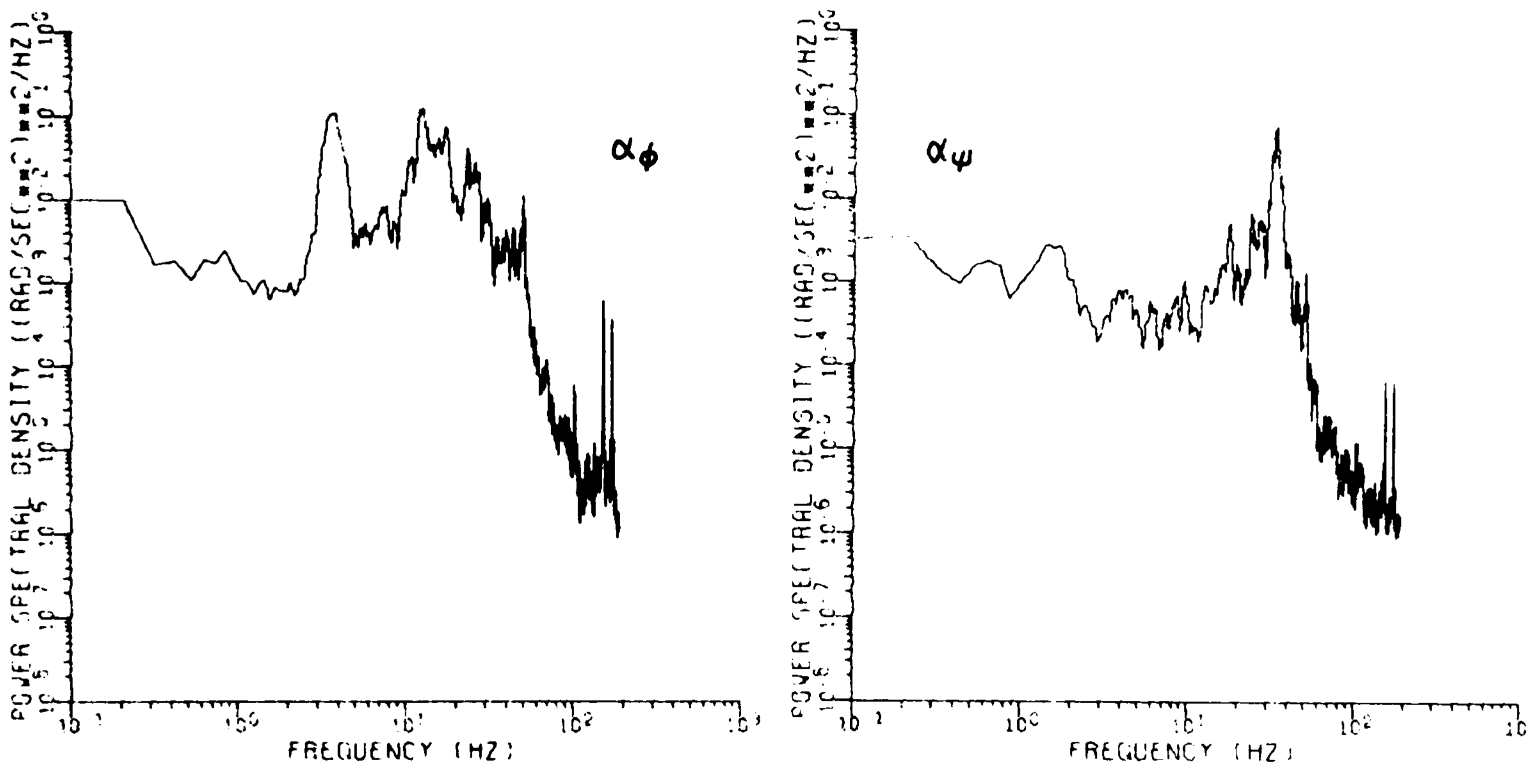

Figure E.39. Spectral Density α_ϕ, α_ψ - Acceleration to Full Speed.

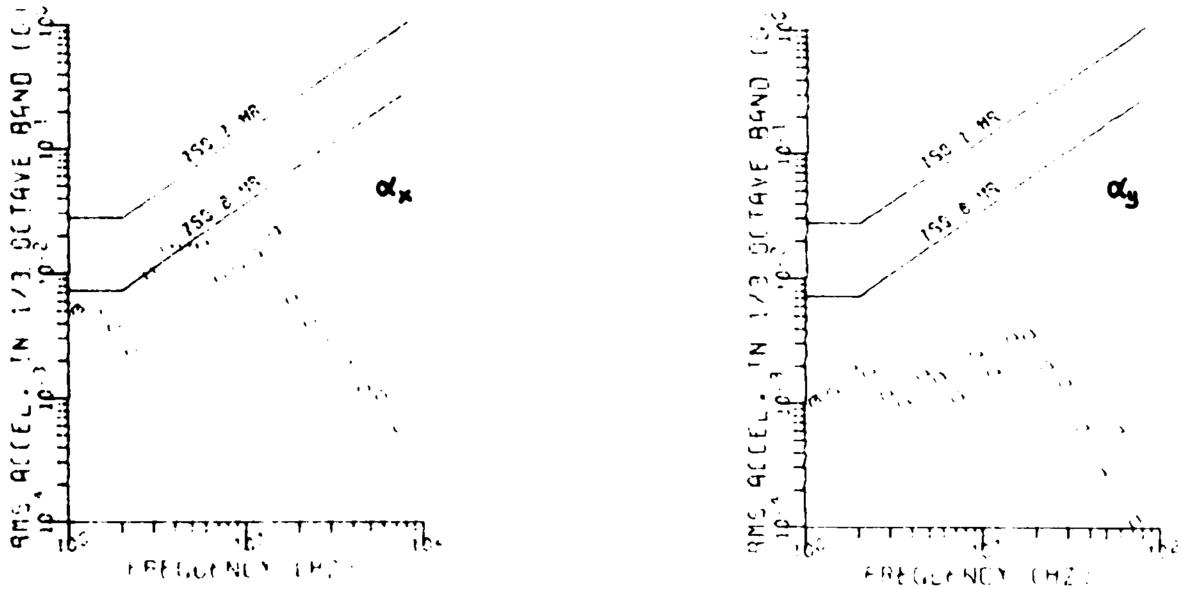

Figure E.40. 1/3 Oc+ave Band Results α_x, α_y - Curve Section.

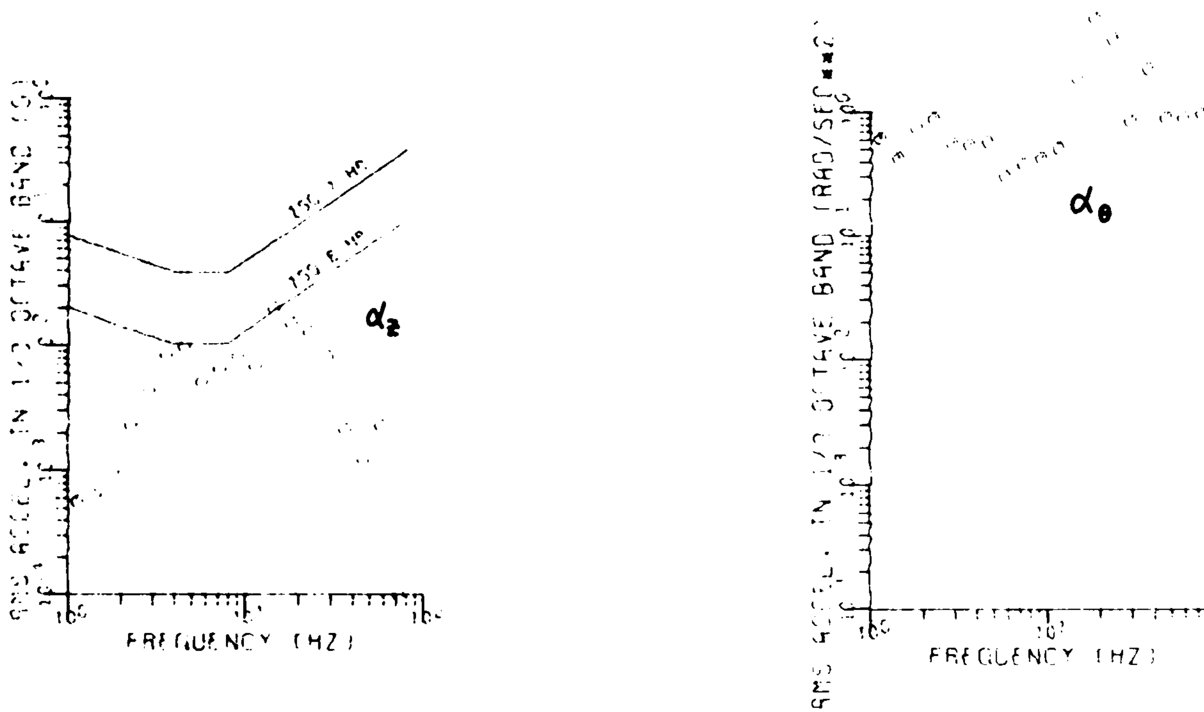

Figure E.41. 1/3 Octave Band Results α_z, α_θ - Curve Section.

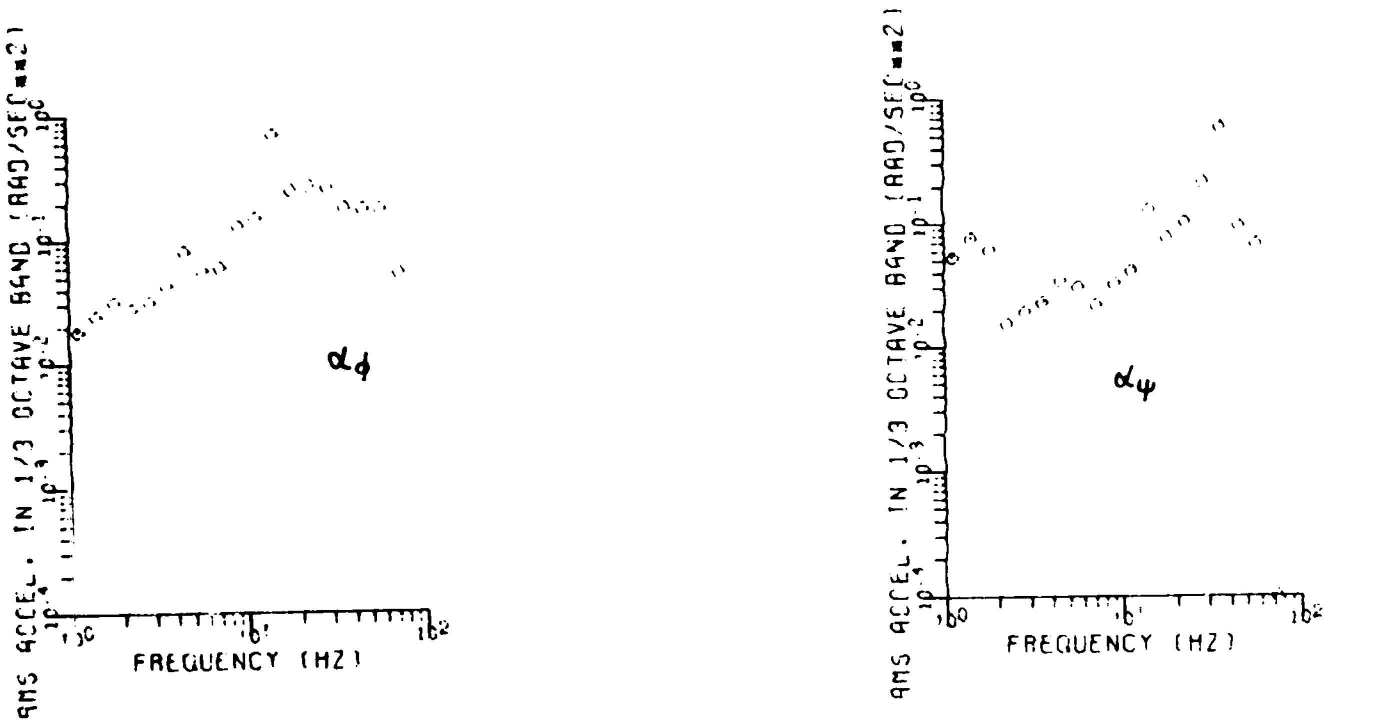

Figure E.42. 1/3 Octave Band Results α_ϕ, α_ψ · Curve Section.

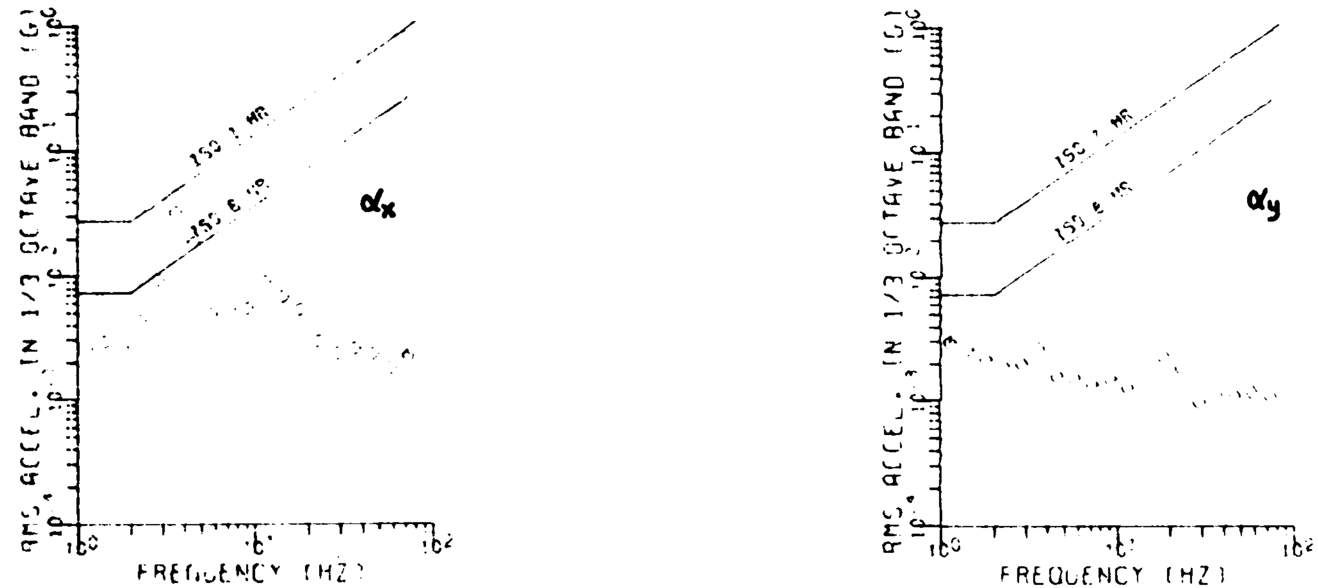

Figure E.43. 1/3 Octave Band Results α_x, α_y - Deceleration into Station C.

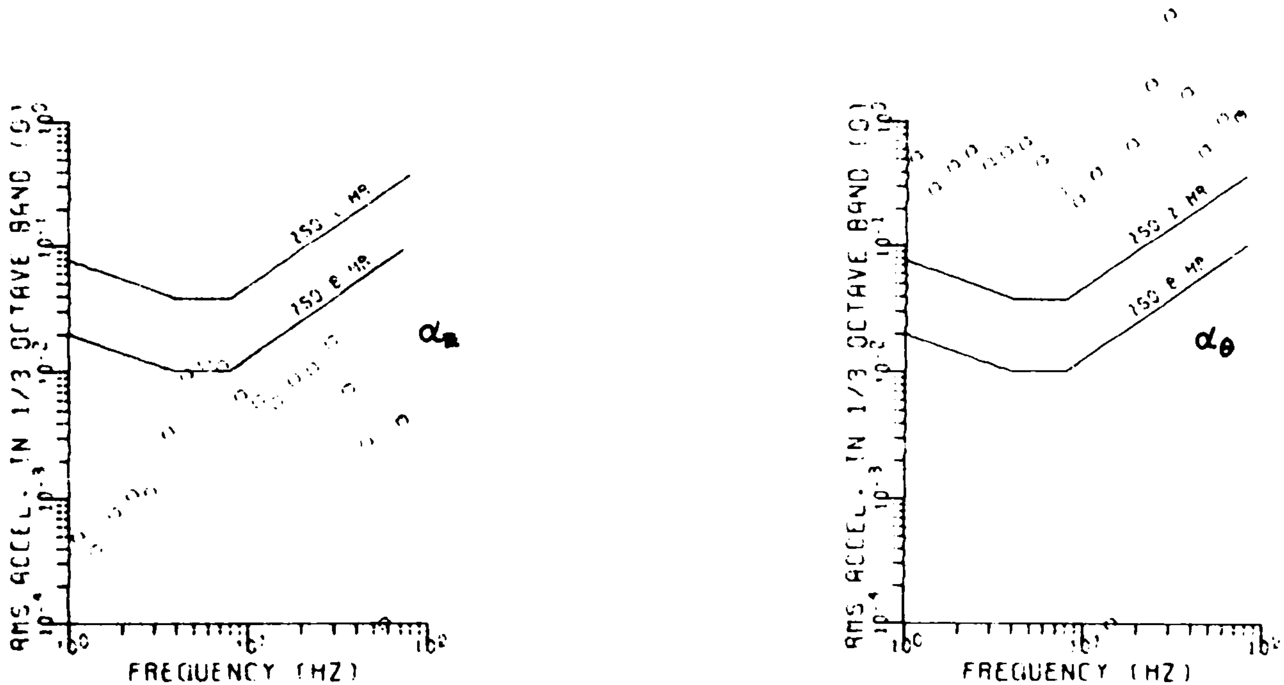

Figure E.44. 1/3 Octave Band Results α_z, α_θ - Deceleration into Station C

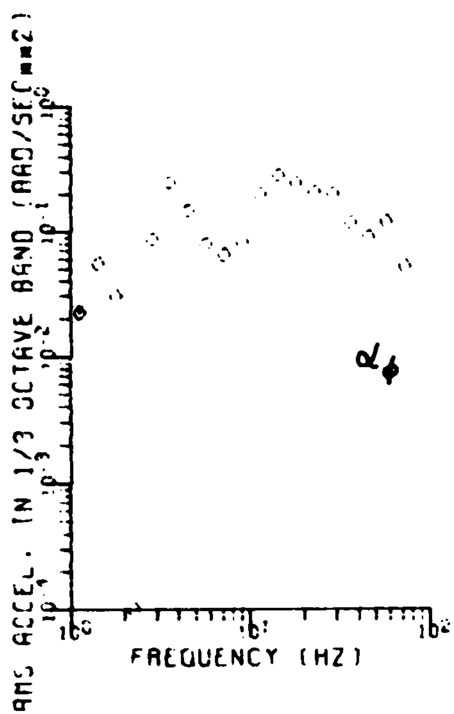

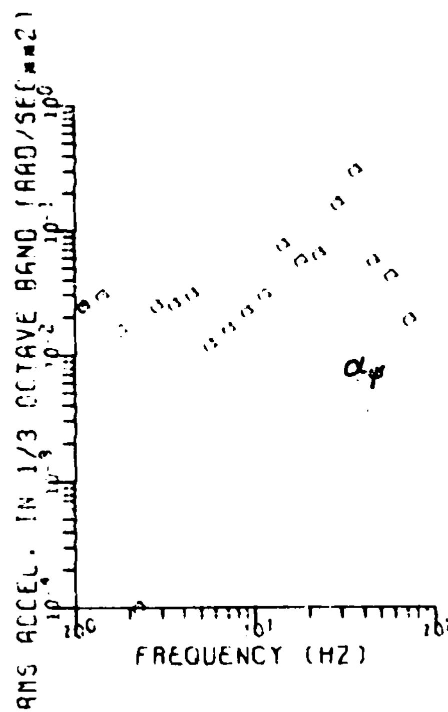

Figure E.45. 1/3 Octave Band Results α_ϕ, α_ψ - Deceleration into Station C.

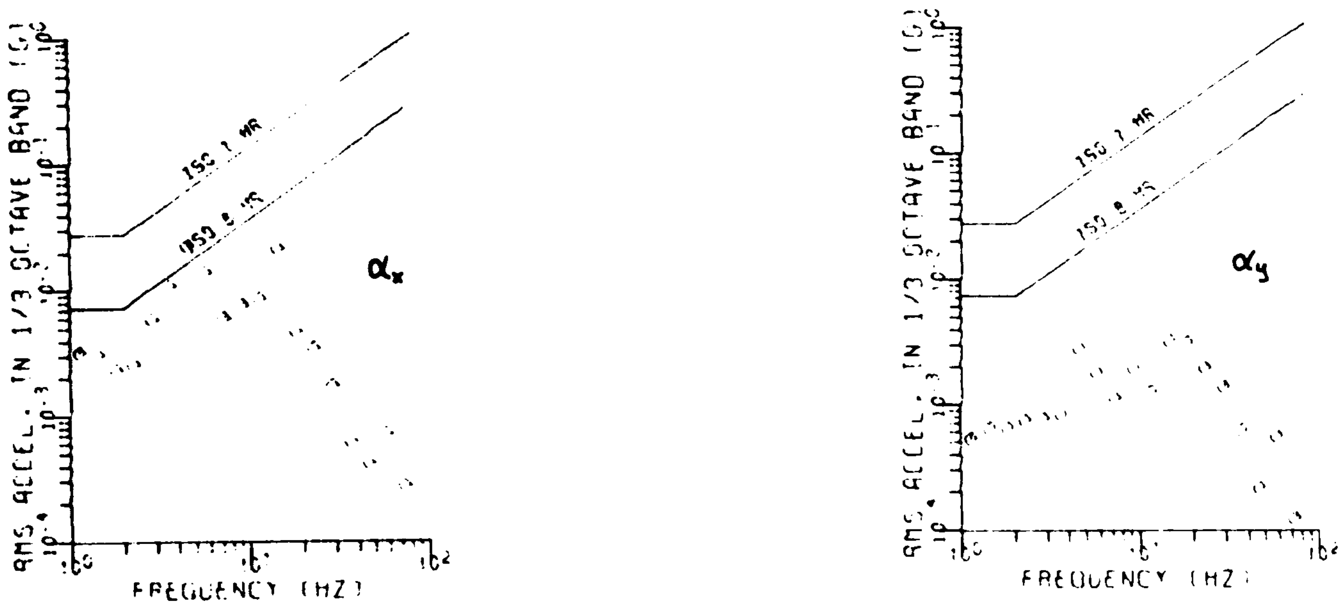

Figure E.46. 1/3 Octave Band Results a_x, a_y - Long Straight.

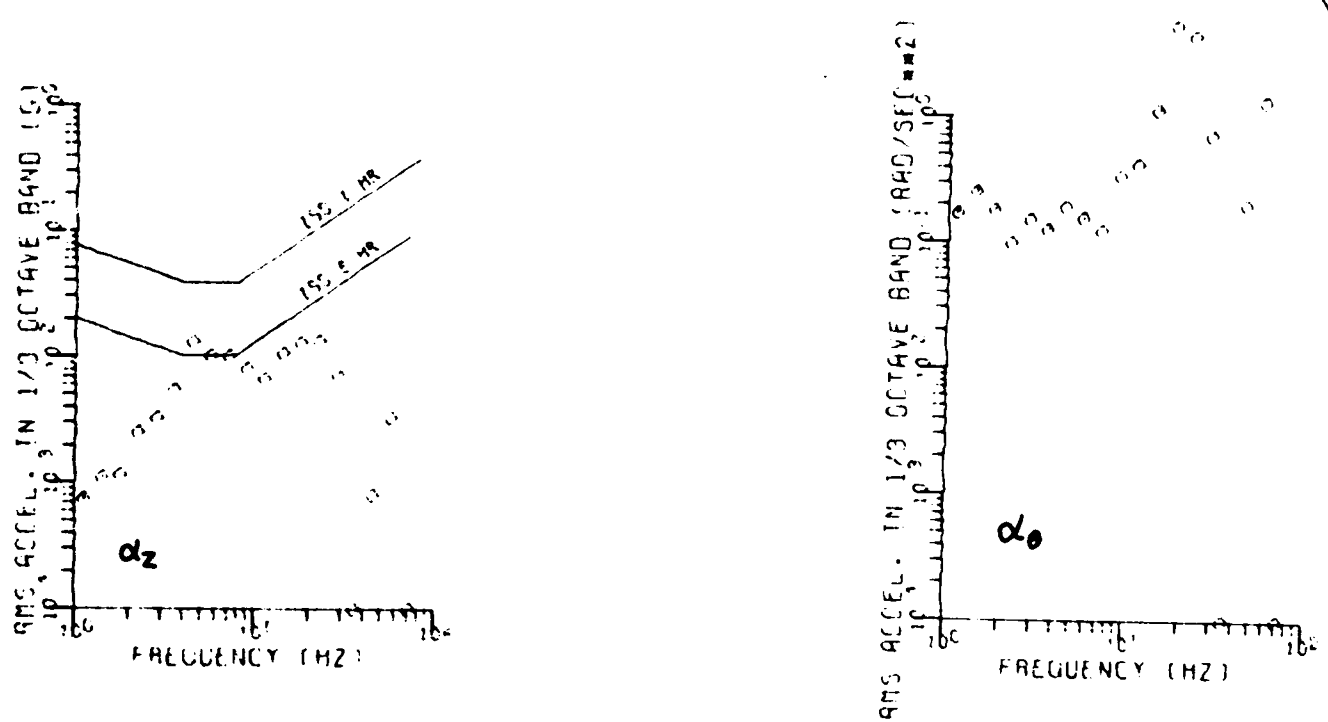

Figure E.47. 1/3 Octave Band Results α_z, α_θ - Long Straight.

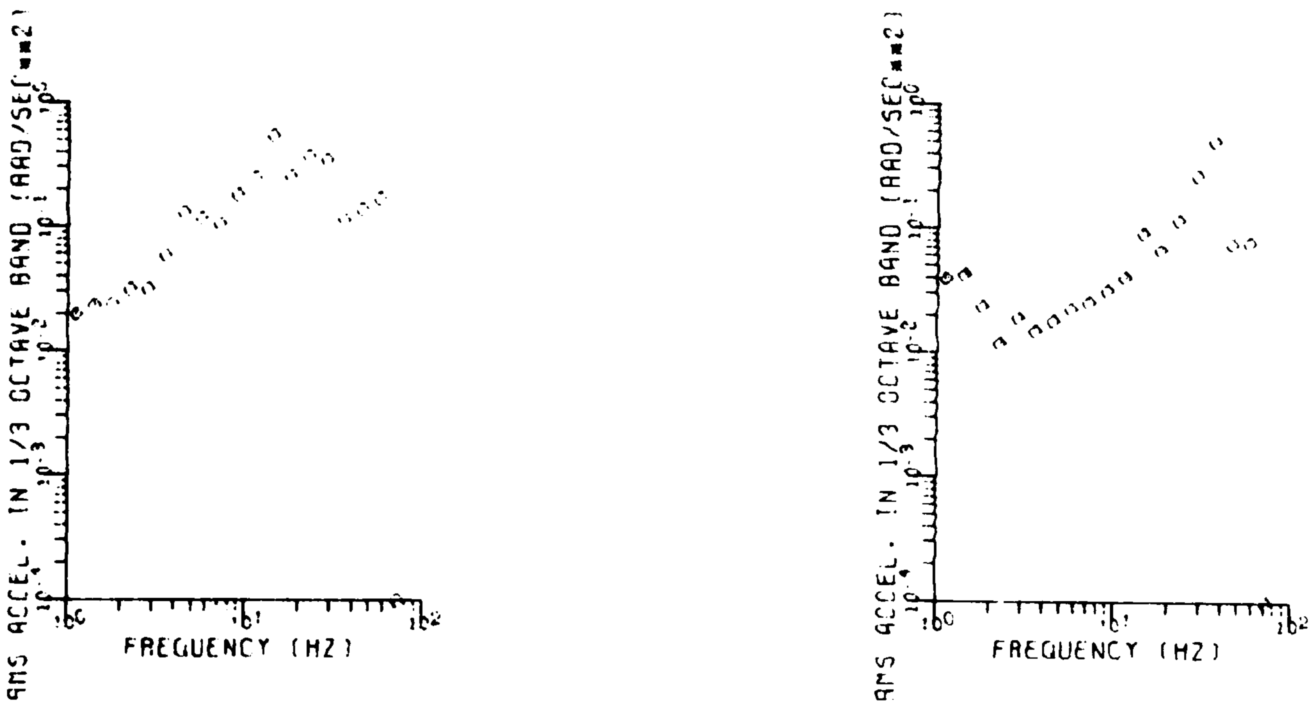

Figure E.48. 1/3 Octave Band Results α_ϕ, α_ψ - Long Straight.

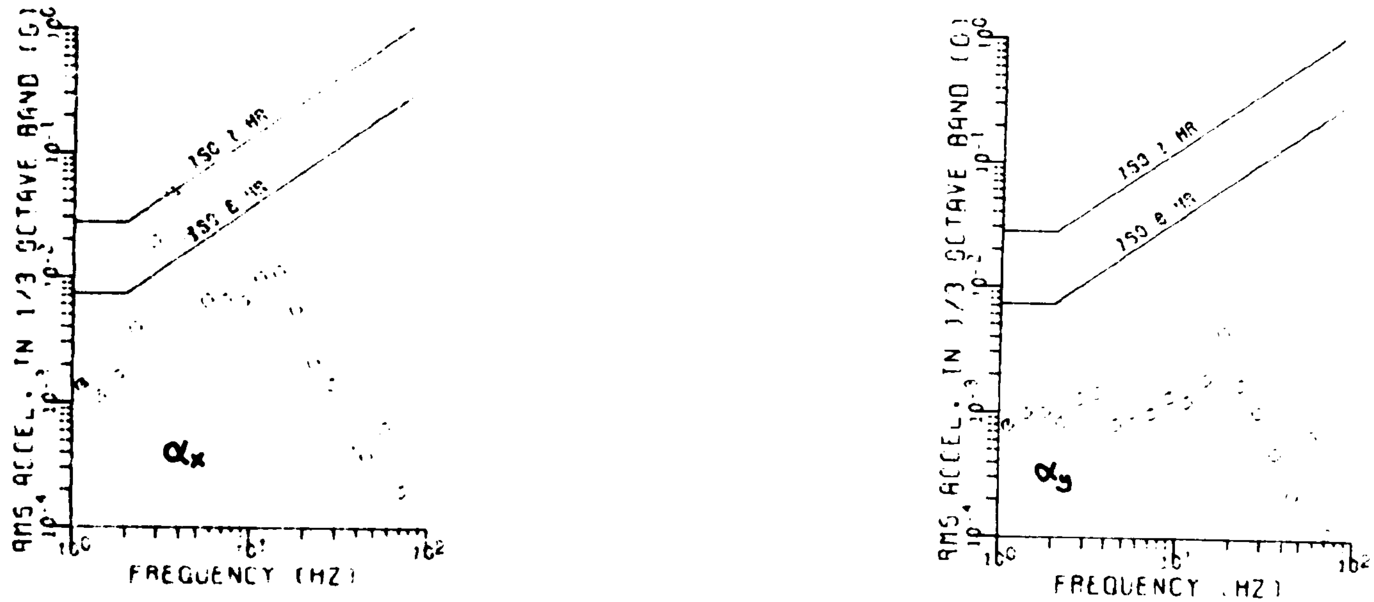

Figure E.49. 1/3 Octave Band Results a_x, a_y - Acceleration to Full Speed.

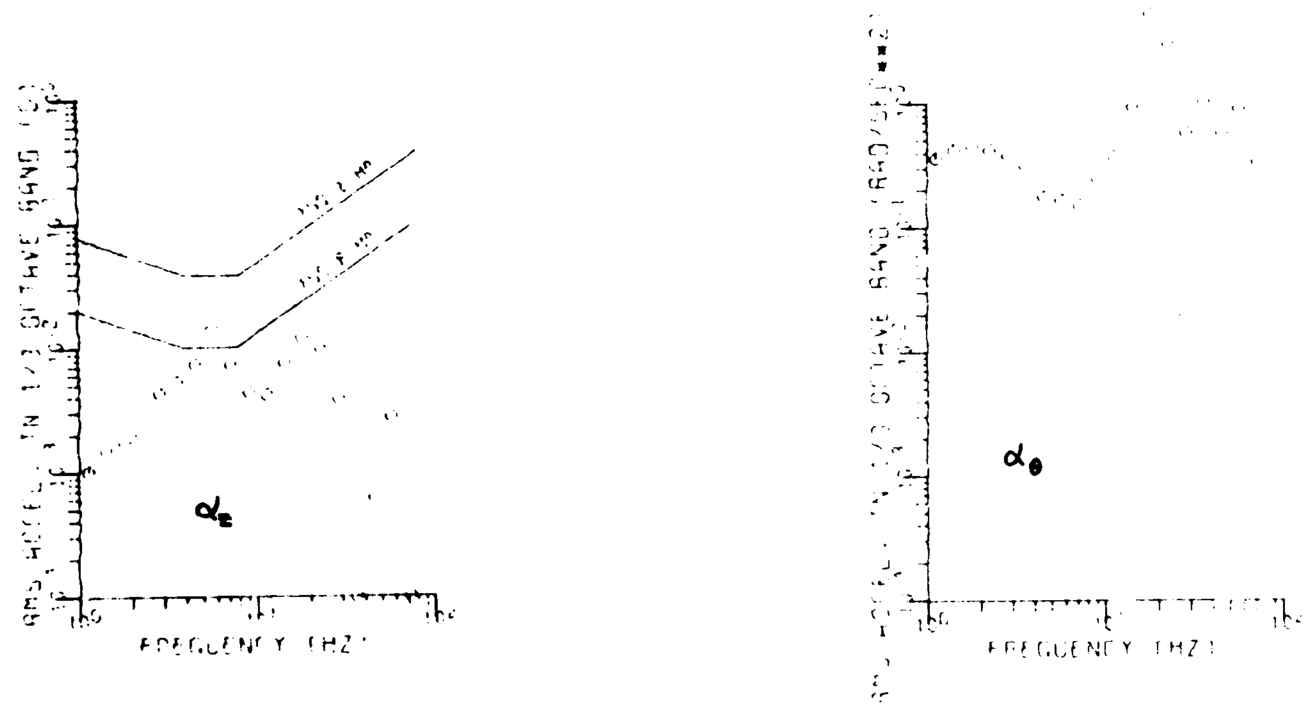

Figure E.50. 1/3 Octave Band Results α_z, α_θ - Acceleration to Full Speed.

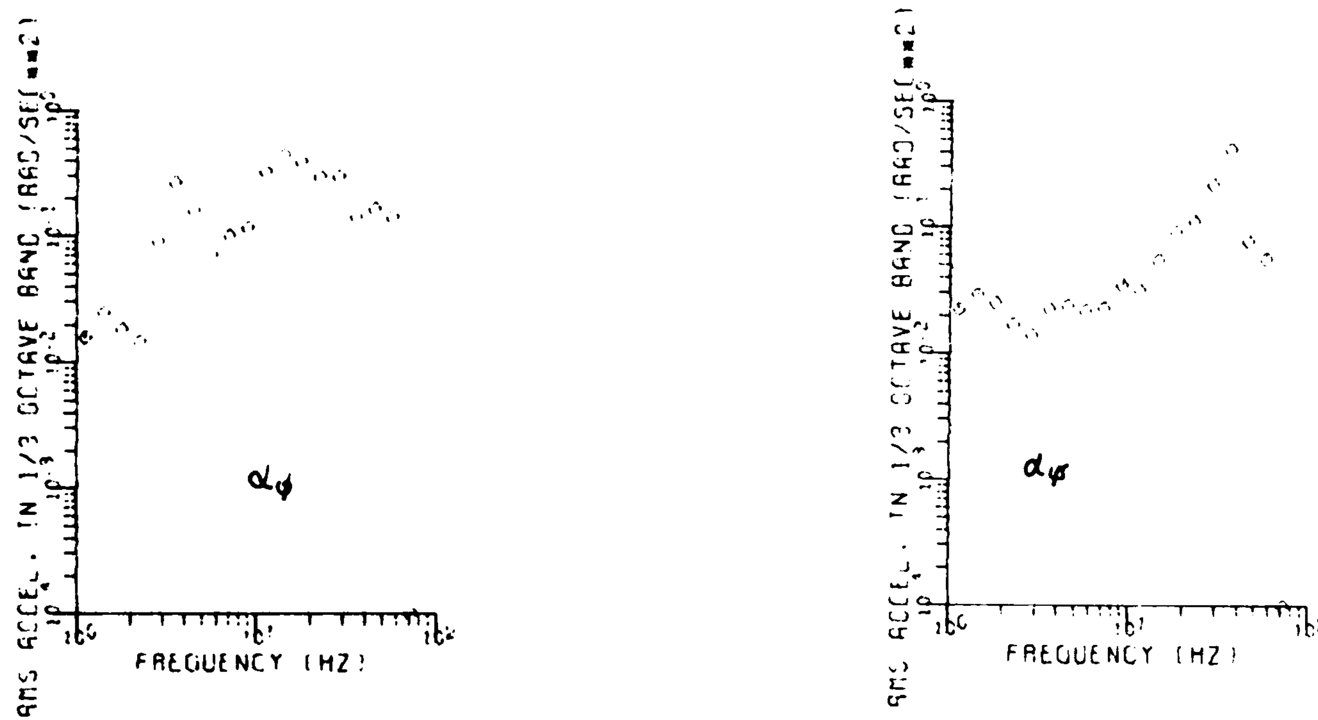

Figure E.51 **1/3 Octave Band Results** α_ϕ, α_ψ - Acceleration to Full Speed

COMPARISONS BETWEEN L.I.M. AND CONVENTIONAL VEHICLES

One of the important results of this study is to assess the improvement, if any, the L.I.M. motors have provided. In this section, the comparison will be done two ways, on the basis of spectra, and on the basis of root mean square values.

Spectra.

In the sway section the L.I.M. vehicle generally shows lower vibration levels in the low frequency range (0.1 to 10 Hz) for the X, Y, ϕ, and ψ coordinates. The vertical accelerations have not changed much. This would generally indicate a smoother ride in the curve sections. One possible reason could be that at high speed the attractive force developed in the motor may relieve some of the load on the wheels thereby reducing a prime source of excitation. This argument may not be conclusive since little difference was found between spectra for the long straight section. Levels were generally similar with the exception of the reduced levels in the yaw mode.

For the acceleration and deceleration cases, the 4 Hz frequency component is accentuated by the L.I.M. motor. In the transverse direction, the 15 Hz structural resonance was accentuated. These effects are thought to be due to the increased thrust force available with the L.I.M. motors.

R.M.S. Acceleration Levels.

Direct comparison can be made using Tables E-2 and E-5. The L.I.M. motor has clearly reduced the vibration levels in the sway section and also, with the exception of the longtitudinal and roll components, for travel down the long straight section.

For the acceleration case. the longitudinal accelerations have been increased slightly due to the enhancing of the 4 Hz component. Also larger levels are found in the transverse and roll accelerations. While these effects are noticable, the transverse accelerations in this instance are not large enough to cause a degrading of the ride quality.

A more direct comparison of the vehicles' ride quality is given in Table E-7 in which the data of Tables E-2 and E-5 are combined.

TABLE E-7. R.M.S. to 200Hz., Conventional and L.I.M. Vehicles Compared

CONDITION		α_x g's	α_y g's	α_z g's	α_θ	α_ϕ	α_ψ	RATING
SWAY	CONVENTIONAL	·0642	·0200	·0555	9·729	2·410	1·200	6
	L.I.M.	·0370	·0110	·0350	8·730	·9230	·684	3
DECELERATION	CONVENTIONAL	·0528	·0073	·0312	4·342	1·096	·4673	3
	L.I.M.	·0370	·0260	·0180	6·940	·6760	·3870	4
LONG STRAIGHT	CONVENTIONAL	·0344	·0092	·0464	5·447	1·575	·6162	5
	L.I.M.	·0380	·0080	·0320	6·640	·8810	·5590	3
ACCELERATION	CONVENTIONAL	·0463	·0064	·0456	4·488	1·262	·4562	4
	L.I.M.	·0560	·0080	·0270	6·580	·9110	·5130	4

REFERENCES

E-1 Catherines, J. J., Clevenson, S. A., Scholl, H. F., "A Method of Measuring and Analysis of Ride Vibrations of Transportation Systems". N.A.S.A. TN D-6785 May 1972.

E-2 Healey, A. J., Nathman, E., Smith, C. C. "An Analytical and Experimental Study of Automobile Dynamics with Random Roadway Inputs". Trans. A.A.M.E. Journal of Dynamic Systems Measurement and Control. 1977.

E-3 "Guide for the Evaluation of Human Exposure to Whole Body Vibration". International Organization for Standardization, I.S.O. 2631, 1972.

1500 copies

☆ U. S. GOVERNMENT PRINTING OFFICE: 1978--702-024--255